THE ROLE OF THE RHESUS MACAQUE (*MACACA MULATTA*) APOLIPOPROTEIN B MRNA-EDITING ENZYME CATALYTIC POLYPEPTIDE-LIKE 3 (APOBEC3) IN LENTIVIRAL REPLICATION AND PERSISTENCE

BY

Kimberly Patricia Schmitt

Submitted to the graduate degree program in Anatomy and Cell Biology and the Graduate Faculty of the University of Kansas in partial fulfillment of the requirements for the degree of Doctor of Philosophy

_____
Edward B. Stephens, Ph.D.
Chairperson

_____
Nancy Berman, Ph.D.

_____
Charlotte Vines, Ph.D.

_____
Michael Werle, Ph.D.

_____
Douglas Wright, Ph.D.

Date Defended: March 8, 2012

The Dissertation Committee for Kimberly P. Schmitt certifies that this is the approved version of the following thesis:

THE ROLE OF THE RHESUS MACAQUE (*MACACA MULATTA*) APOLIPOPROTEIN B MRNA-EDITING ENZYME CATALYTIC POLYPEPTIDE-LIKE 3 (APOBEC3) IN LENTIVIRAL REPLICATION AND PERSISTENCE

_____
Edward B. Stephens, Ph.D.
Chairperson

Date Approved: March 8, 2012

II. Abstract

SHIV infections in rhesus macaques have been used to extensively study accessory proteins of HIV-1 involved in pathogenesis as well as in vaccine development. All primate lentiviruses encode for a Vif (virion infectivity factor) protein, which is required for HIV-1 replication in primary $CD4^+$ T cells and macrophages. The Vif protein interacts with APOBEC3 (A3) proteins promoting their accelerated degradation by the 26S proteosome. Sequence analysis of Vif proteins from different lentiviruses revealed that there are two highly conserved domains in the carboxyl terminus that are required for recruitment of the of the Vif-CBF-β-Cul5/Elongin B/C/Rbx-1 E3 ubiquitin ligase complex. These domains are the viral BC box, SLQ(Y/F)LAL, and Zn^{2+} binding (H-X_5-C-X_{17-18}-C-X_{3-5}-H; HCCH) motifs. Previous cell culture studies have shown that the introduction of amino acid substitutions into the SLQ(Y/F)LA motif resulted in decreased binding of Vif to Elongin C, while substitutions into the HCCH motif prevented the interaction of Vif with Cullin 5. In this first study, we introduced two amino acid changes in the highly conserved SLQYLA domain (S147A, L148A; AAQYLA) of the SIV Vif protein in SHIV. *In vitro*, the resulting virus, $SHIV_{VifAAQYLA}$, replicated in A3G negative CEM-SS cells but failed to replicate in A3G positive CEM cells. We also showed that hA3G was incorporated into the virion. Following these *in vitro* studies, $SHIV_{VifAAQYLA}$ was inoculated into three rhesus macaques, which were followed for over six months to assess various viral and immunological factors throughout the duration of infection. All three macaques did not develop significant $CD4^+$ T cell loss over the course of infection, had plasma viral loads that were over 100-fold lower than macaques inoculated with parental $SHIV_{KU-1bMC33}$, and developed no

histological lesions in various lymphoid tissues, and developed immunoprecipitating antibodies. DNA and RT-PCR analysis revealed that only a select number of tissues were infected with virus, while sequence analysis of PBMC and select tissue DNA (at necropsy) showed that the site-directed changes were stable during the first three weeks after inoculation but thereafter the S147A amino acid sunstitution changed to a threonine in two of the three macaques. However, the L148A substitution remained stale in the *vif* amplified from the PBMC and select tissues at necropsy in all three macaques. Extensive sequence analysis of the *vif, vpu, nef*, and *env* genes revealed a increased number of G-to-A mutations in the genes amplified from macaques inoculated with SHIVVifAAQYLA. The majority of these mutations (>85%) were in the context of 5'-TC (minus strand) and not 3'-CC, suggesting that one or more of the rhesus A3 proteins may be responsible for the observed mutational patterns. To determine if infectious virus was present in the plasma at necropsy, plasma from the three macaques inoculated with $SHIV_{VifAAQYLA}$ were pooled and intravenously inoculated into a naïve macaque. This macaque maintained its levels of circulating CD4+ T cells throughout the duration of infection, maintained viral loads below the limits of detection, and did not produce immunoprecipitating antibodies. However, *gag* was present in the DNA and RNA isolated from PBMC throughout infection and in select tissues at necropsy. The results from this first study showed for the first time the importance of the SLYQLA domain *in vivo* in viral pathogenesis. It also showed that mutations in *vif* could lead to a persistent infection in rhesus macaques resulting in the accumulation of G-to-A substitutions in the viral genome.

In the second study, we used the SHIV/macaque model of infection to compare the replication and pathogenicity of SHIVs that express a Vif protein in which the entire SLQYLA ($SHIV_{Vif5A}$) or HCCH ($SHIV_{VifHCCH(-)}$) domains were substituted with alanine residues. Each virus was inoculated into three rhesus macaques where various viral and immunological parameters were followed for six months. Our *in vitro* results indicate that in the presence of these mutant Vif viruses, rhA3G is incorporated into the virion, stably expressed, restricts, and accumulates G-to-A substitutions (plus strand) in the *nef* gene of the mutated viral genomes. *In vivo*, all macaques maintained a stable level of circulating $CD4^+$ T cells, developed low viral burdens, maintained engineered mutations, yielded no histological lesions, and developed immunoprecipitating antibodies by 12 weeks post-inoculation. However, the production of viral RNA only persisted in macaques inoculated with $SHIV_{VifHCCH(-)}$. The analysis of *vif* sequences amplified from PBMC DNA between weeks 0-16 during $SHIV_{VifHCCH(-)}$ infection revealed an increased number of G-to-A substitutions that increased with time in two of the three macaques. Sequence analysis of *nef* and *vpu* from the small intestine (ileum), thymus, and the spleen showed G-to-A substitutions in *nef* genes isolated from macaques inoculated with $SHIV_{VifHCCH(-)}$. Macaques inoculated with $SHIV_{Vif5A}$ effectively controlled the virus three weeks post-inoculation and no viral sequences could be amplified from tissue DNA. These studies showed that the SLQYLA and HCCH domains are critical for viral pathogenesis *in vivo* and that there may exist APOBEC3 negative reservoirs in the rhesus macaque that allow for low levels of viral replication and persistence but not disease. Therefore, this study suggests that mutations targeted to one or more functional conserved domains within the Vif protein may limit viral replication and

generate an effective immune response leading to the “self-inactivation” of the virus by the activities of various APOBEC3 proteins resulting in a possible live-attenuated vaccine candidate.

The APOBEC3 family of restriction factors has been shown to inhibit certain retroviruses and retroelements. The APOBEC3 family in humans is comprised of seven cytidine deaminases (A3A, A3B, A3C, A3D, A3F, A3G, and A3H) that catalyze the deamination of cytidine to uracil on single-stranded DNA or RNA. While the human APOBEC3 repertoire has been extensively studied, the full complement of these proteins in the rhesus macaque remains unknown. Sequencing of the rhesus macaque genome has led to the identification of the rhesus homologues A3B, A3C, A3D, A3F, A3G, and A3H. Finally, we identified a human A3A (hA3A) homologue in the rhesus macaque (rhA3A) and presents evidence that both the human and rhesus *Apobec3* genes are orthologous. We show that rhA3A is highly expressed in activated $CD4^+$ T cells, widely expressed in both the visceral and central nervous system tissues of the rhesus macaque, and is degraded in the presence of the human immunodeficiency virus (HIV-1) and simian-human immunodeficiency virus (SHIV) genomes in a Vif-dependent manner. Our results also indicate that rhA3A reduced the level of infectious SHIVΔ*vif* by approximately 20-fold and HIV-1Δ*vif* by 3-fold. Human and monkey A3A amino acid sequences are 81% homologous and can be distinguished by a three amino acid indel located between residues 27-30. When these residues were deleted from rhA3A (rhA3AΔSVR), the antiviral activity of rhA3A was abolished suggesting that these residues are critical for lentivirus inhibition. Select APOBEC3 proteins are incorporated into the virion and can inhibit reverse transciption and/or

induce G-to-A hypermutation in nascent reverse transcripts in the next target cell. Previous studies revealed that rhA3G is incorporated into SHIVΔ*vif* virions and exerts its antiviral activity in target cells by an increase in cytidine deamination of newly synthesized minus-strand viral DNA from cytosines to uracils, leading to G-to-A substitutions (plus strand) in the viral genome. We were able to detect the incorporation of rhA3A into SHIVΔ*vif* and to a lesser extent in SHIV virions; however, we were unable to detect the incorporation of rhA3A into either HIV-1 or HIV-1Δ*vif* virions. Even though rhA3A is incorporated into SHIVΔ*vif* virions and potently restricts SHIVΔ*vif* similar to rhA3G, rhA3A produced an approximately 5-fold decrease in the number of G-to-A mutations compared to rhA3G. Unlike hA3A, rhA3A did not inhibit adeno-associated virus 2 (AAV-2) replication and L1 retrotransposition. This data suggests for the first time an evolutionary switch in primate A3A virus specificity and provides evidence that a primate A3A protein can inhibit lentiviral replication.

III. Acknowledgements

First, I would like to thank my mentor Dr. Edward Stephens, for all of your help and patience. Thank you for always encouraging me to work hard, to continually challenge myself, and for introducing me to the scientific world. I would also like to thank my committee members Dr. Charlotte Vines, Dr. Nancy Berman, Dr. Michael Werle, and Dr. Doug Wright for all of your support, guidance, and time to help me finish my graduate student career. I would also like to thank Dr. Brenda Rongish for your support, guidance, and helping to keep my on track while finishing my dissertation. I would also like to extend a thank you to the Anatomy and Cell Biology department for such a great atmosphere to complete my dissertation work.

A special thank you goes out to the Stephens' lab members: Sarah Hill, Autumn Ruiz, and Malinda Alagier. Sarah, you are an amazing person and you were an amazing help in creating experiments, bouncing around ideas, and just being there as continuous support system ("At least I figured it out"). You really helped me grow and develop as a scientist and truly are an amazing person and frient. Autumn, you are the best friend that anyone could ever want. Thank you from the bottom of my heart for supporting and encouraging me to stick through the difficult portions of graduate school. I truly wouldn't have had the drive and ambition to complete this degree without you by my side, whether it was dancing in the lab, movies, shopping, laughing, bottles of wine, etc. Thank you for all of your scientific advice, discussions, and positive outlook on science. You really are an amazing coworker, scientist, and friend.

Mom and Mike, none of this would have been possible without your support and love. Thank you for your courage, making me laugh, making me take much needed

vacations, and inspiring me to continually challenge myself to become a better person. I would not have been able to complete this degree without you. Thank you for always believing in me even when my belief in myself has waivered. Mom, thank you for coming down to visit and take care of me during difficult times. Without your support and helping me get through surgeries and physical limitations, I would have given up. Thank you for always being there to listen to my scientific accomplishments and failures and continually encouraging me to keep persuing my dreams. You and Mike are truly amazing and I couldn't have asked for more supportive and loving parents.

Grandma Jean, grandma Mary, and family, thank you so much for remembering me on holidays and providing encouraging cards and gifts during my graduate studies. It always brightened my day and was truly thoughtful, thank you.

Cash and Tango, my furry little companions, thank you for always making me smile at the end of the day. Thank you for your patience while I was writing this by not sitting on my computer to distract me and always making me feel welcome when I came home. I love you both.

IV. Dedication

Dedicated to those of us who have a special place in our hearts for viruses

Table of Contents

V. List of Figures

Chapter One: Introduction

VI. Chapter 1: Introduction

Epidemiology

The human immunodeficiency virus type 1 (HIV-1) is the causative agent of acquired immune deficiency syndrome (AIDS) (Barre-Sinoussi et al., 1983; Gallo et al., 1984). Since its discovery in 1981, the HIV-1 pandemic has killed more than 25 million people and infects about 0.6% of the world population (UNAIDS Report on the Global AIDS Epidemic, 2010; **Figure 1**). By the end of 2009, the Joint United Nations Program on HIV/AIDS (UNAIDS) reports that there are approximately 33.3 million people living with HIV-1, with 22.5 million of those infected individuals residing in Sub-Saharan Africa. During 2009, there were approximately 2.6 million newly acquired infections and 1.8 million AIDS-related deaths (UNAIDS Report, 2009). The high rate of viral replication, low fidelity of reverse transcription, and frequent recombination events leads to the genetic diversity of the HIV-1 species. While there is no known cure for HIV-1 infection, the introduction of highly active anti-retroviral therapy (HAART) in 1996 has led to long lasting viral suppression reducing both the morbidity and mortality of HIV-1 infection (Palella et al., 1998). However current drugs do not eradicate HIV-1 and factors such as resistance to antiretroviral therapy occurs due to the genetic diversity of HIV-1, limited treatment options in developing countries, non-compliance, inability to afford treatments, and drug toxicity contribute to continues virus spread. Further understanding of HIV-1 cell biology and pathogenesis will be required to expand drug discovery focusing on viral/host protein interactions or the identification of cellular

Figure 1. Global prevalence of HIV-1 infections according to the UNAIDS 2009 report on the global AIDS epidemic

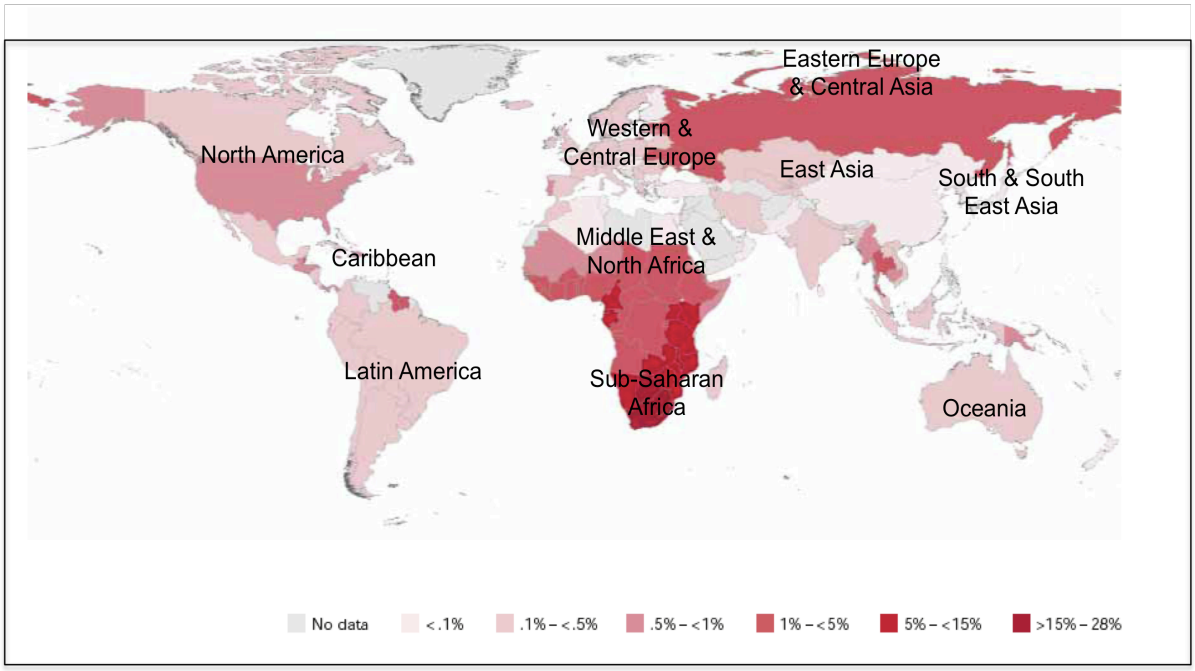

Adapted from UNAIDS 2009 Report on the Global AIDS Epidemic

targets conferring antiviral activity against HIV-1 thus making it possible to produce a safe and effective vaccines or antiviral treatments.

Classification

Simian and human immunodeficiency viruses (SIV, HIV-1, and HIV-2) are genetically related and classified in the Genus Lentivirus of the Family Retroviridae. Other members of the Genus Lentivirus include bovine immunodeficiency virus (BIV), equine infectious anemia virus (EIAV), feline immunodeficiency virus (FIV), caprine arthritis encephalitis virus (CAVE), and visna/maedi virus (MVV). Distinct SIVs has been isolated from more than 20 African nonhuman primate species, where there is extensive viremia in these monkeys without exaggerated immune response (Hahn et al., 2000; Rey-Cuille et al., 1998). Therefore, most of these particular isolates cause a nonpathogenic infection in their primary host (Hahn et al., 2000). However, several SIVs have been isolated from *Macaca nemestrina* (pig-tailed macaques; SIV_{MNE}) and the Asian macaque species *Macaca mulatta* (rhesus macaque; SIV_{MAC}). These viruses cause an AIDS-like disease in these macaques and arose from an initially infected rhesus macaque that was being housed with an infected sooty mangabey (Hahn et al., 2000)

The extensive genetic heterogenicity of HIV-1 is often classified by the lack of proofreading by the reverse transcriptase (RT), host selective pressures, rapid turnover of the virus *in vivo*, and recombination events that occur during replication (Ho et al., 1995; Michael et al., 1999; Op de Coul et al., 2001; Roberts et al., 1988;Temin et al., 1994). HIV-1 is classified into three phylogenic groups: group M (main), group O

(outlier), group N (non-M/O), and group P (Ayouba et al., 2000; Gurtler et al., 1994; Simon et al., 1998). Group P was recelty identified from two individuals originating from Cameroon (Ayouba et al., 2001; Plantier et al., 2009; Roques et al., 2004; Simon et al., 1998; Vallari et al., 2011). From phylogenetic data we can infer that HIV-1 group M and N originated by no fewer than three independent zoonotic cross-species transmission events of chimpanzee SIV (SIV_{CPZ}; *Pan troglodytes*) (Gao et al., 1999; Santiago et al., 2002). Group O and P are phylogenically related to SIV_{gor} (wild-living Western lowland gorillas, *Gorilla gorilla*), which was derived from an ancestor of a divergent SIV_{CPZ} lineage in chimpanzees (Keele et al., 2006; Plantier et al., 2009; Takehisa et al., 2009; Van Heuverswyn et al., 2006). Of the three main goups, group M is responsible for the HIV-1 pandemic and has evolved into nine distinct phylogenetic groups: A, B, C, D, F, G, H, J, and K (Hemelaar et al., 2006). Within a given subtype there are sub-subtypes that appear to be more genetically related. These would include the subtypes A, B, and F, which are further classified into sub-subtypes A1, A2, B, B', F1, F2, respectively (Gao et al., 2001; Triques et al., 2000). The phylogenetic subtypes are currently based on either the sequence analysis of the full-length viral genome or on nucleotide sequences from multiple subgenomic regions such as *gag, pol,* and *env*. Often multiple individuals become infected with two or more subtypes to produce intersubtype recombinant forms (Peeters et al., 2001; Robertson et al., 2000). When at least three epidemiologically unlinked individuals become infected with an identical recombinant virus that has been characterized by full-length genome sequencing, the virus can be characterized as a circulating recombinant form (CRF) (Peeters et al., 2001; Robertson et al., 2000). Currently, there are 43 CRFs, with the highest diversity occurring in West Africa (Los

Alamos National Laboratory database, 2009). CRFs can be linked to areas where the parental strains are co-circulating. This increases the probability that individuals will become infected with several different genetic forms ("superinfected") resulting in the generation of unique recombinant forms (URFs) (McCutchan et al., 2006). To date, 90% of the epidemic is comprised of four subtypes (A, B, C, and D) and two CRFs (CRF01_AE and CRF02_AG) (Gilbert et al., 2007). The global distribution of these subtypes and recombinants are in **Figure 2.**

HIV-2, while much less wide spread than HIV-1 is classified into eight phylogenetic groups, A-H (Hemelaar et al., 2011). Unlike HIV-1, HIV-2 is thought to have originated from zoonotic transmissions from the sooty mangabey (*Cerococebus atys*) due to phylogenic similarity in genomic structure (Sharp et al., 1995). It appears that seven independent transmissions from sooty mangabeys to humans occurred to result in the various HIV-2 subtypes (Chen et al., 1997; Gao et al., 1994; Yamaguchi et al., 2000).

Geographic Distribution

The size of the HIV-1 epidemic cause by group M, N, non-M/N varies considerably. HIV-1 group M is responsible for the majority of the global infections, approximently 33 million people. Unlike group M, group O is endemic West-Central Africa and Cameroon constituting only 1-5% of infections, group N has been found in a small group of people in Cameroon, and group P has only been identified in two individuals in Cameroon (Ayouba et al., 2001; Plantier et al., 2009; Roques et al., 2004; Simon et al., 1998; Vallari et al., 2011). On a global scale, the most prevalent group M

subtypes are A, B, and C. Subtype C infections account for almost 50% of all worldwide HIV-1 infections and are predominantly found in >80% of infections in southern Africa and India. Subtype A viruses are predominantly located in central and eastern Africa (Kenya, Uganda, Tanzania, and Rwanda) as well as the eastern Eurpoean countries formally known as the Solviet Union. The Subtype B viruses are mainly located in western and central Europe, the Americas, Austrailia, and in several countries of Southeast Asia, northern Africa. This subtype is also common in south african and russian homosexual men (Buonaguro et al., 2007). The relavence of CRFs in HIV-1 infection is increasingly on the rise accounting for approximently 18% of HIV-1 infections (Hemelaar et al., 2006; Osmanov et al., 2002). CFR01-AE and CRF02-AG represent the most prodomdinant CRFs from Southeast Asia and West/West Central Africa, respectively (**Figure 2**) (McCutchan et al., 1999; Montavon et al., 2000).

The HIV-2 is endemic primarily to West Africa, although there is recent spread to parts of Europe and the southwestern region of India. In Guinea-Bissau, there is prevalence up to 8-10% and Gambia is as high as 28% (Ghys et al., 1997; Langley et al., 1996; Poulsen et al., 1989; Wilkins et al., 1993). This is of concern because dual HIV-1 and HIV-2 infections are occurring more frequently in regions once considered endemic to HIV-2, which may lead to recombination events between the two viruses (Andersson et al., 1999; 2000; Ishikawa et al., 1998). The majority of HIV-2 infections are subtype A and predominant in Guinea-Bissau and Europe. To a lesser extent, HIV-2 subtype B is isolated predominantly from the eastern parts of west Africa and occassionally in Europe. More interestingly, the highest diversity of HIV-2

Figure 2. Global distribution and genetic diversity of the nine major subtypes and recombinants of HIV-1. The various colors indicate a total of ten different epidemic patterns that have been observed.

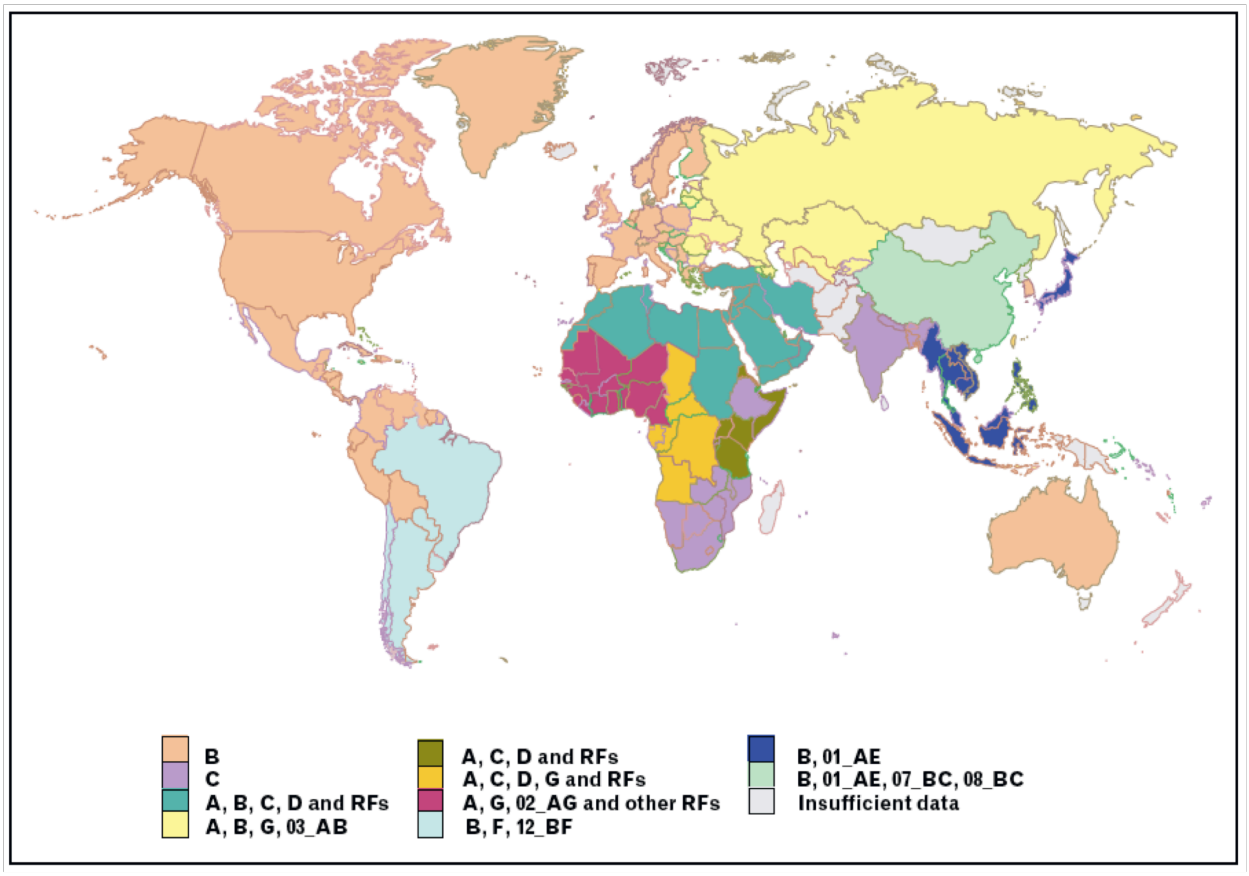

International AIDS Vaccine Initiative, 2009; Woodman and Williamson, 2009

subtypes (subtypes A, B, E, and F), ~0.02% of infections, have been isolated in Sierra Leone (Reeves et al., 2002).

Genomic Structure of Lentiviruses

HIV-1 encodes three structural and enzymatic polyproteins; Gag (group-specific antigen), Pol (polymerase), and Env (envelope), which are analogous to proteins commonly found in all retroviruses. Additionally, the HIV-1 genome encodes two regulatory proteins; Tat (transcriptional activator), Rev (regulator of virion), as well as four accessory proteins, Nef (negative factor), Vif (virion infectivity factor), Vpr (viral protein R), and Vpu (viral protein U) (Frankel and Young, 1998). In contrast to HIV-1, HIV-2 and SIV_{sm} phylogenetic lineages encode for an ortholog of HIV-1 Vpr known as Vpx (Viral protein X) (Goujon et al., 2007; Mailm et al., 2008; Sharova et al., 2008). Origianally, HIV-2 Vpr/Vpx was viewed as the functional counterpart of HIV-1 Vpr; however, more recent evidence shows that the targeted substrate and function of these proteins differs greatly (Gibbs et al., 1994; 1995; Goujon et al., 2007; 2008; Hirsch et al., 1998; Kawamura et al., 1994; Yu et al., 1991; Mahalingam et al., 2001; Mangeot et al., 2002; Ueno et al., 2003; Wolfrum et al., 2007). Furthermore, HIV-1, SIV chimpanzees (SIV_{CPZ}), and select monkeys in the *Cercopithecus* genus express a Vpu homologue. However, HIV-2 and the majority of SIV lineages do not encode for a *vpu* gene (Barlow et al., 2003; Beer et al., 1999; 2001; McCormick-Davis et al., 2000; Strebel et al., 1998). **Figure 3** illustrates the genomic structures of these members of the Genus Lentiviruses.

Viral Replication Cycle & Current HIV Therapeutic Targets

Using the envelope glycoprotein, gp120, HIV-1 initiates contact with the target cell by recognition of the CD4 recptor and then to a secondary chemokine coreceptor, CXCR4 or CCR5 (**Figure 4**) (Jakobsen et al., 2010). The CD4 receptor is a transmembrane glycoprotein expressed on the surface of T lymphocytes, T lymphocyte precursors in the bone marrow and thymus, monocytes, macrophages, dendritic cells, eosinophils, and microglial cells (Gorry and Ancuta, 2011). The high affinity binding of gp120 to CD4 tiggers a conformational change in gp120 that exposes the V3 loop region of gp120 that interacts with the secondary extracellular loop of the coreceptor. A gp120-bridging sheet is formed between specific domains of gp120 after the binding of CD4 interacts with the N-terminus of the coreceptor (Moore and Nara, 1991; Chesebro et al., 1992; Wyatt et al., 1992; Milich et al., 1993; Ross et al., 1998; Hoffman and Doms, 1999; Ogert et al., 2001; Cormier and Dragic, 2002; Hoffman et al., 2002; Nabatoc et al., 2004; Rizzuto et al., 1998; Sterjovski et al., 2010). The CD4-bound gp120 with coreceptor causes further conformational changes that expose the N-terminus of gp41, which contains a fusion peptide that inserts into the host cell membrane. This occurs through a gp41 ectodomain that forms an extended coiled coil conformation and a six-helix bundle structure. This promotes the juxaposition of the viral and host cell membrane, which is a stable structure allowing the fusion between

Figure 3. Schematic representation of the genomic structures from various members of the Lentiviridae subfamily: HIV-1, SIV_{CPZ}, HIV-2, SIV_{SM}, and SIV_{MAC}.

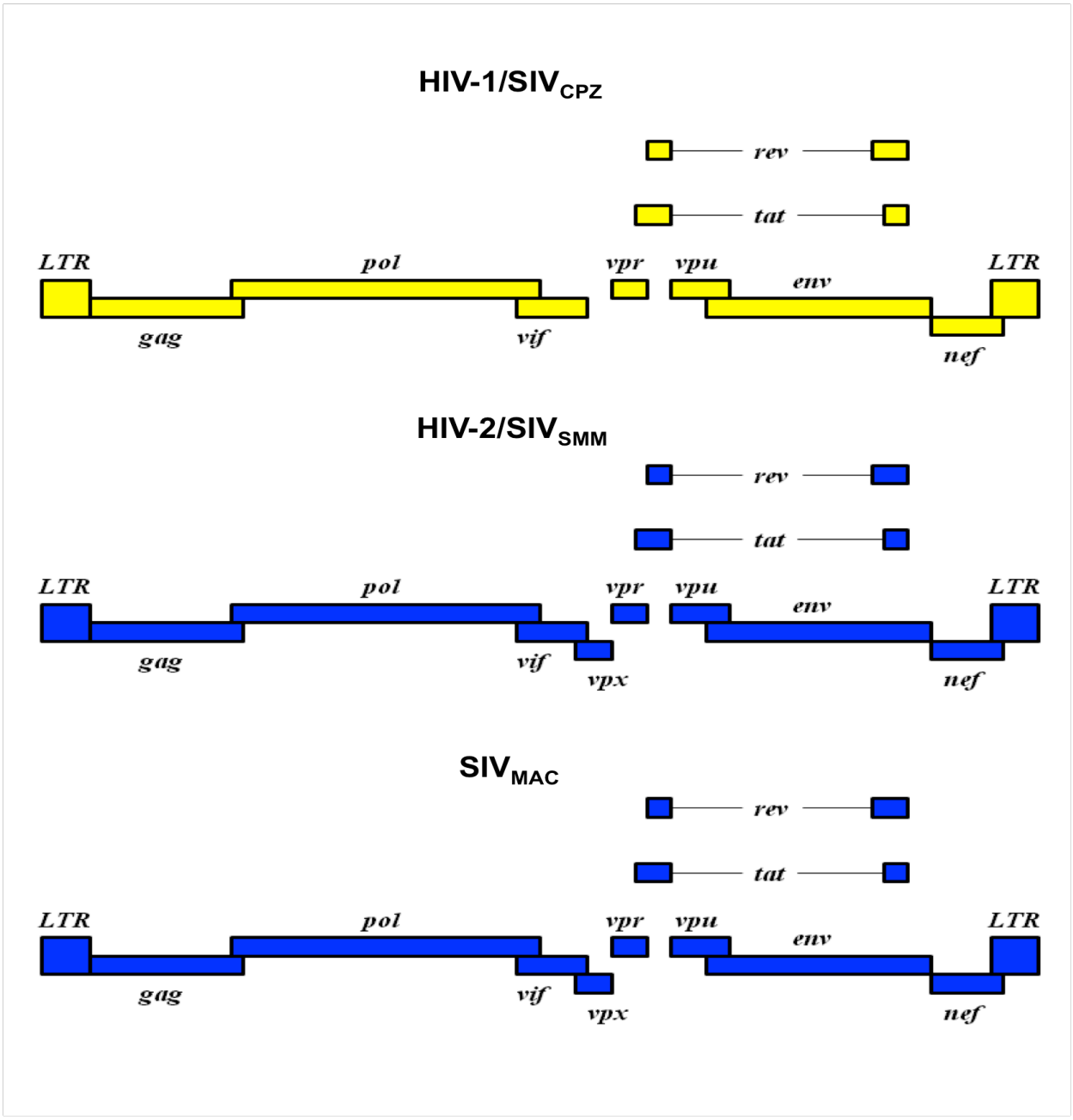
HIV-1/SIVCPZ
rev
tat
LTR
pol
vpr
vpu
env
LTR
gag
vif
nef
HIV-2/SIVSMM
rev
tat
LTR
pol
vpr
vpu
env
LTR
gag
vif
vpx
nef
SIVMAC
rev
tat
LTR
pol
vpr
vpu
env
LTR
gag
vif
vpx
nef

viral and cellular membranes resulting in a pore that allows for the release of the viral core into the host cell (Gorry and Ancuta, 2011; Helseth et al., 1991; Miller et al., 1993; Srinivas et al., 1992). There are a total of 12 different membrane proteins that have been identified as co-receptors for HIV-1. However, CXCR4 and CCR5 are the primary co-receptors for either T cell line tropic (T-tropic) or macrophage tropic (M-tropic) HIV-1 isolates, respectively (Berger et al., 1999; Deng et al., 1996; Deng et al., 1997; Doranz et al., 1996; Dragic et al., 1998; Feng et al., 1996; Gorry and Ancuta, 2011; Jakobsen et al., 2010; Liao et al., 1997). During the progression to the late stages of HIV-1 infection, 40-50% of infected individuals switch co-receptor specificity to either CXCR4 (X4 viruses) or to dual-tropic co-receptor specificity CCR5 and CXCR4 (R5/X4). The broadened cell tropism by co-receptor switching contributes to the development of a more rapid disease progression (Coetzer et al., 2008; Corry and Ancuta et al., 2011). Currently there are two anti-retrovirals that inhibit HIV-1 entry into target cells: one fusion inhibitor, enfuvirtide, and one CCR5 antagonist, maraviroc (De Clercq et al., 2009).

After the membranes fuse, the viral core is released into the cytoplasm of the cell (**Figure 4**). Viral uncoating is initiated with both cellular factors and the viral proteins MA, Nef, and Vif. The viral RNA genome is reverse transcribed using reverse transcriptase (RT) into a double stranded DNA copy of the viral genome (Hirsch and Curran, 1990; Harrich and Hooker, 2002). Correct regulation of the core uncoating is necessary for completion of the early stages during HIV-1 replication. TRIM5α exerts an anti-retroviral effect by targeting intact or partially uncoated viral cores (Forshey et al., 2005; Hatziiannou et al., 2004; Kar et al., 2008; Langelier et al., 2008; Sebastian

and Luban, 2005; Shi and Aiken, 2006; Stremlau et al., 2006). This block to replication occurs post-entry but pre-reverse transcription. TRIM5α inhibits replication by causing rapid and premature disassembly of the viral core and by recruiting cellular proteosomal degradation machinery (Anderson et al., 2006; Campbell et al., 2008; Rold and Aiken, 2008; Perron et al., 2007; Stremlau et al., 2006; Wu et al., 2006). This factor is species specific; for example, HIV-1 is not inhibited by human TRIM5α as efficiently as rhesus or owl monkey TRIM5α (Bieniasz, 2004; Hatziioannou et al., 2004; Keckesova et al., 2004; Luban, 2007; Nisole et al., 2005; Ozato et al., 2008; Perron et al., 2004; Stremlau et al., 2004; Towers, 2007; Yap et al., 2004). The reverse transcriptase (RT) is the target for three different classes of inhibitors: nucleoside RT inhibitors (NRTIs), nucleotide RT inhibitors (NtRTIs), and non-nucleoside RT inhibitors (NNRTIs). Both the NRTIs and NtRTIs interact with the substrate binding site of the RT and the NNRTIs interact with an allosteric site located a short distance away from the substrate binding site. The seven NRTIs approved for use today are zidovudine (AZT), didanosine (ddI), zalcitabine (ddC), stavudine (d4T), lamivudine (3TC), abacavir (ABC), and emtricitabine ((-) FTC). There is one NtRTI approved for use today, tenofovir, and our NNRTIs: nevirapine, delavirdine, efavirenz, and etravirine (De Clercq, 2009).

Following uncoating the reverse transcriptase, the formation of the preintegration complex occurs (PIC) (**Figure 4**). This complex contains the viral reverse transcribed double-stranded DNA, matrix protein (MA), integrase (IN), viral protein R (vpr), the central DNA flap, and several host proteins (Miller et al., 1997). The PIC complex must transverse the nuclear pore complex (NPC) of the nuclear membrane to be imported into the nucleus and integrate into the host genome (Zennou et al., 2000). The NPC

spans the nuclear membrane and provides an aqueous channel allowing the bi-directional transport of proteins up to approximently 60-kDa in size (Mattaj et al., 1998; Nigg et al., 1997; Weis et al., 1998). The translocation is completed using a class of proteins known as importins and exportins. These proteins engage import and export signals within the proteins that are being mediated for transport (Nigg et al., 1997; Weis et al., 1998). The exact mechanism of the PIC-associated proteins in nuclear transportion through the NPC is unknown. However, research has shown that there is a non-classical nuclear import signal buried in the catalytic domain of IN (Bouyac-Bertoia et al., 2001). Also, there is preliminary evidence suggesting that the transit involves the association of the PIC with microtubules (Hope, unpublished data). Furthermore, a central DNA flap, which is a triple-stranded intermediate, is created during reverse transcription. The central DNA flap acts as an import signal for the PIC (Hamm et al., 1990; Zennou et al., 2000). When this structure is mutated, the HIV-1 genomes accumulated at or just inside the nuclear envelope similar to an IN nuclear localization mutant (Zennou et al., 2000). While the PIC complex is still in the cytoplasm, the viral cDNA is primed for integration. The IN trims the 3' strand of the U3 and U5 LTRs of the viral cDNA and the ends of the viral genome in a process known as 3'-processing (3'-P). During this reaction, IN catalyzes an endonucleolytic cleavage at the 3' site of the conserved CA dinucleotide releasing a terminal GT dinucleotide. The CA-3'-hydroxyl ends generated provide nucleophile groups used for the strand transfer. The PIC complex migrates into the nucleus as described above, and IN catalyses the insertion of the two viral cDNA ends into the host chromosome (**Figure 4**). During strand transfer, the two 3'-hydroxyl ends ligate to the host chromosome with a five-base pair stagger

across the major groove DNA resulting in a two–base overhang on the viral cDNA 5'-end and a five-base pair single-stranded gap at each junction, which is repaired by host enzymes (Grandgenett, 2005; Holman and Coffin, 2005; Marcband et al., 2006; Marshall, et al., 2007; Van Maele and Debyser, 2005; Wu et al., 2005). There is only one integrase inhibitor available for clinical use, raltegravir. Raltegravir targets the strand transfer reaction. There is a similar drug now in Phase III trails that also inhibits strand transfer known as Elvitrgravir (De Chercq, 2009).

After the proviral DNA is integrated, cellular RNA polymerase II begins the first rounds of transcription of the proviral DNA. The RNA polymerase II binds cellular factors to the viral long terminal repeat (LTR) and transcription of basal amounts of Tat, Rev, and Nef begin (Jordan et al., 2001). The HIV-1 LTRs flank the viral DNA and the 3' LTR contains three distinct regions. These regions are the unique 3' region (U3), the repeated domain (R), and the unique 5' region (U5). These LTR enhancer/promoter sequences are required for the replication of HIV in T cell lines. The U3 region is further divided into three regions: the core promoter, enhancer, and modulatory regions (Fields et al., 2007). The LTR also has closely related *cis*-acting elements that allow for promotion of transcription by RNA polymerase II. These include the TATA boxes that bind transcription factor IID, three Sp1 binding sites, enhancers containing two NF-kB binding sites, modulatory regions that contain purine box arrays, and sites that bind the Ets family members (reviewed in Kilareski et al., 2009). During the initial stage of infection, only multiply spliced mRNAs of the regulatory proteins are expressed; Tat, Nef, and Rev. Once sufficient amounts Tat are expressed (**Figure 4**), Tat activates futher transcription of HIV-1 genes by binding the TAR element of the LTR and other

cellular transcription factors (Harrich et al, 1996; Harrich and Hooker, 2002). After sufficient amounts of Rev are expressed, Rev non-spliced and singly spliced mRNAs are produced and transported to the polysomes leading the production of other viral proteins; such as Gag, Pol, Env, Vpr, Vpu, and Vif, and genomic RNA (Pollard and Malim, 1998). Rev binds the Rev responsive element (RRE) found in singly spliced and unspliced viral RNA. This facilitates their transport through the nuclear membreane and into the cytoplasm (Sierra et al., 2005). The envelope glycoprotein precursr, gp160, is synthesized in the rough endoplasmic reticulum where high mannose moieties are added to the N-linked glycosylation sites (Asp-X-Ser/Thr). The proteins are then transported to the Golgi complex where the high mannose side chains are trimmed and complex carbohydrates are added. Additionally, the gp160 is cleaved by a host protease in the Golgi complex resulting in gp120 and the gp41 transmembrane protein. The gp120/gp41 complex proteins are transported by vescular trafficking to the cell plasma membrane, which together with two copies of the viral RNA and the Gag and Gag-Pol precursor proteins initiate assembly (Briggs et al., 2003; Derdowski et al., 2004; Sandefur et al., 2000; **Figure 4**). The Gag polyprotein precursor, $Pr55^{Gag}$, is essential for assembly and recruitment of components required for the formation of the virion by promoting interaction between various structural components, encapsidating the viral RNA, and associating with the envelope proteins to stimulate the budding process. $Pr55^{Gag}$ oligomerizes underneath the plasma membrane through protein-protein and protein-RNA interactions with the HIV-1 matrix (MA) protein facing and directly inserting into the lipid bilayer (Lee et al., 1999; Lee and Yu et al., 1998; Lingappa et al., 1997; Tritel and Resh, 2000). The budding of HIV-1 occurs by hijacking

the cellular endosomal sorting machinery (Bieniasz, 2006; Demirov and Freed, 2004; Morita and Sundquist, 2004). The p6 region of $Pr55^{Gag}$ binds to the ESCORT-1 (Endosomal Sorting Complex Required for Transport I) component Tsg101 or ALIX through the secondary assembly late domains PTAP and YPLTSL, repectively (Demirov et al., 2002; Gottlinger et al., 1991; Huang et al., 1995). ALIX binds and recruits the Snf7 subunit of ESCORT-III (McCullough et al., 2008). ESCORT-III excises the membrane neck between the viral particle and the plasma membrane. After the recruitment of all the necessary components of the virion, the immature viron buds from the plasma membrane containing the host lipid bilayer as its outer envelope (Freed, 2002; Ono and Freed, 2001). While T cells exclusively bud from the plasma membrane, HIV-1 vrions bud into vesicular structures in macrophages, which are subsequentally released at the cell surface. Gag is the only protein required to form and release virion-like particles (Gelderblom, 1991; Ono, 2009; Orenstein et al., 1998). Currently, there are no anti-retrovirals that target viron assembly and budding approved for clinical trials.

The immature particle buds from the plasma membrane and the viral protease (PR) proteolytically processes by cleaving the $Pr55^{Gag}$ and the Gag-Pol precursor ($Pr160^{Gag\text{-}Pol}$) yielding cleaved Gag and Pol proteins (Adamson and Freed, 2007; Vogt, 1996). During proteolytic cleavage the virion undergoes morphological changes resulting in a spherical particle with a dense core containing the genomic RNA (**Figure 5**) (Ganser et al., 1999; Yeager et al., 1998). Currently, there are ten protease inhibitors approved for clinical use. These include saquinavir, ritonavir, indinavir, nelfinavir, amprenavir, lopinavir, atazanavir, fosamprenavir, tipranavir, and darunvir (De Clercq et al., 2009).

Viral Proteins

All of the proteins encoded by HIV-1 contribute to producing optimal conditions for HIV-1 to replicate in the host cell as well as evade the host immune system resulting in productive infection. The HIV-1 genome is flanked by two long terminal repeats (LTR) regions that do not encode for any viral proteins but are necessary for integration into the host cell genome and for encoding promoter enhancer binding sites (5'LTR).

Gag

The *gag* gene is expressed as a 55-kDa polyprotein precursor Pr55 that is cleaved to produce the mature HIV-1 virion. These are the matrix (MA or p17), capsid (CA or p24), and nucleocapsid (NC or p7) proteins. Additionally, the proteolytic cleavage of Pr55 results in a C-terminal domain called p6 as well as two spacer proteins known as p1 and p2 (Henderson et al., 1992; Mervis et al., 1988). The MA protein is located at the N-terminal of Pr55 and remains associated with the lipid envelope of the mature virion. Its membrane association is dependent on an N-terminal myristic acid moiety (Bryant and Ratner, 1990; Gottlinger et al., 1989; Spearman et al., 1994). A charged N-proximal region contains a cluster of conserved basic residues that bind the acidic phospholipids in the host cell lipid bilayer (Yuan et al., 1993; Zhou et al., 1994). This charged N-proximal region is essential for stabilization of Pr55 to the membrane and for extracellular particle formation and virus replication. Interaction

Figure 4. HIV-1 replication. 1) Attachment and Entry; 2) Release into the cytoplasm and uncoating; 3) Reverse Transcription; 4) Integration; 5) Transcription of proviral DNA and full-length viral genome RNA; 6) Nuclear export; 7) Processing of viral proteins; 8) Processing of Env proteins; 9) Assembly; 10) Proteolytic cleavage

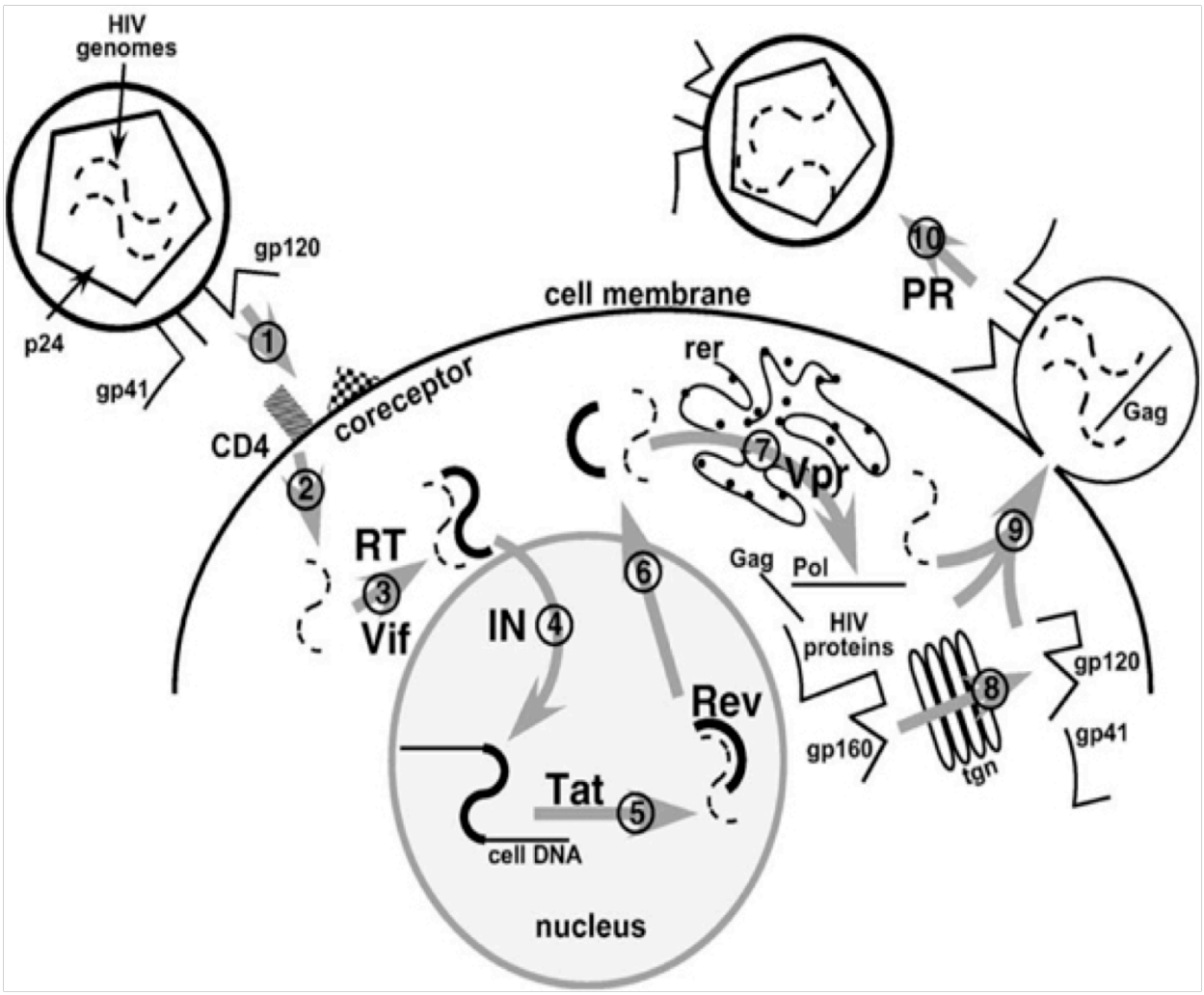
HIV genomes
gp120
p24
gp41
cell membrane
coreceptor
CD4
1
2
RT
3
Vif
IN 4
6
rer
7
Vpr
Gag
Pol
HIV proteins
9
10
PR
Gag
gp120
8
gp160
tgn
gp41
Rev
Tat
5
cell DNA
nucleus

NIH, 2007

Figure 5. Depiction of a mature HIV-1 virion

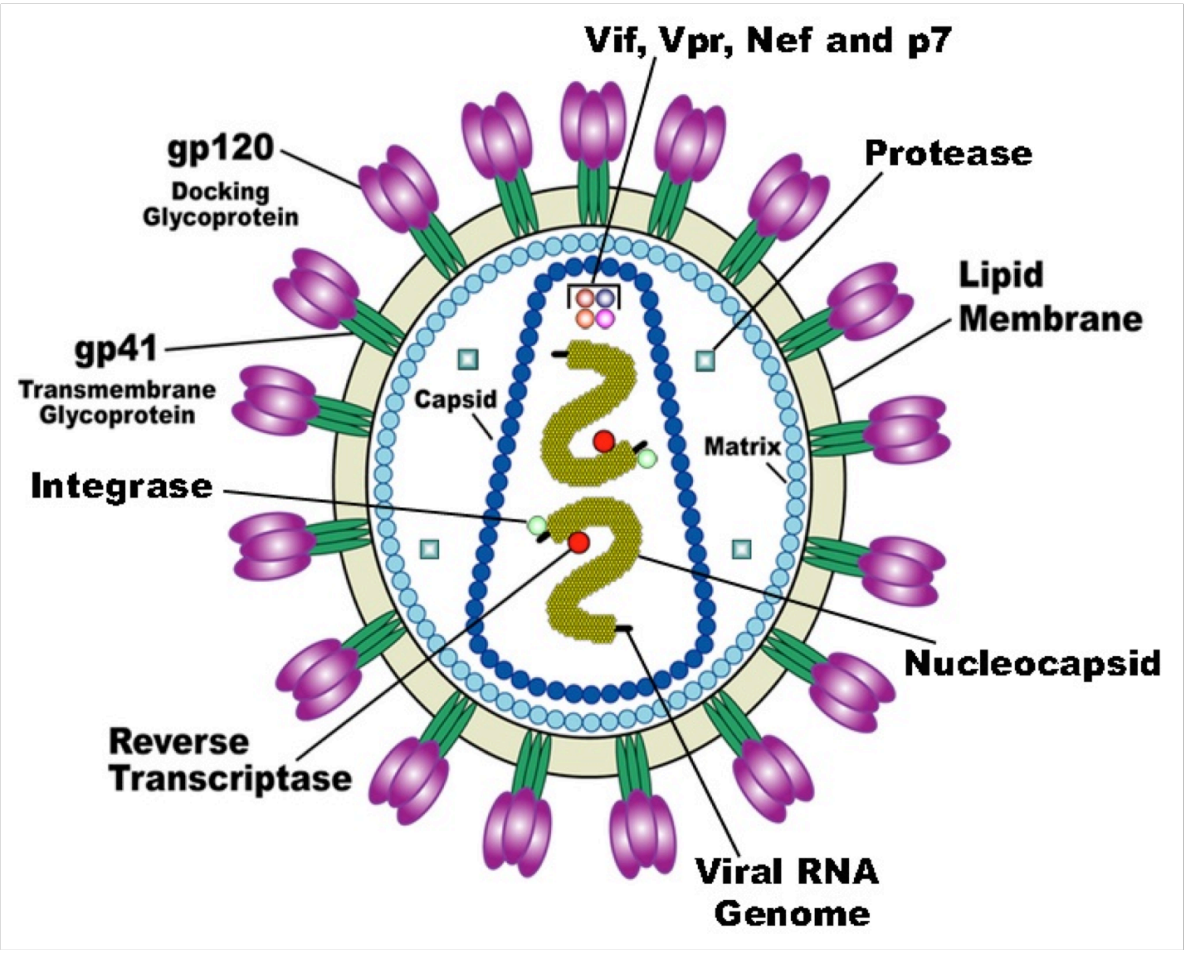

NIAD; Carl Henderson, 2007

between the MA and the acidic phospholipids enhance Gag membrane binding and contribute to Gag bringing the plasma membrane. A three-dimensional model structure shows that MA forms trimers with cationic charged faces resulting in Gag targeting to the anionic cytoplasmic leaflet of the plasma membrane (Hill et al., 1996; Matthews et al., 1995). An acidic phospholipid, PI(4, 5)P_2, specifically localizes to the cytoplasmic leaflet and binds to the conserved basic residue clusters on the MA proteins. This is most likely the reason Gag targets to the cytoplasmic leaflet of the plasma membrane (Chen et al., 2008; Ono et al., 2004; Saad et al., 2006). From recent studies it can be inferred that HIV-1 Gag specifically associates with raft-like microdomains in the plasma membrane (Lindwasser and Resh, 2001; Nguyen and Hildreth, 2000; Ono and Freed, 2001).

The myristylation site of Gag in the plasma membrane is generally sequestered. The insertion of this moiety into the plasma membrane is regulated by the CA protein. The CA is composed of two structurally independent, largely helical, domains: the N-terminal core and the C-terminal dimerization domain (Adamson et al., 2009; Ganser-Pornillos et al., 2008). Multimerization of the CA protein causes a conformational change in Gag allowing for the myristic acid to insert with high affinity into the plasma membrane (Saad et al., 2006). The N-terminal domain of CA also interacts with the human peptidyl-prolyl *cis-trans* isomerase cyclophilin A (CyPA) allowing it to be incorporated into the virion. CyPA is an intracellular receptor for the immunosuppressant cyclosporin A (CsA), which allows for optimum infectivity of HIV-1 (Franke et al., 1994; Luban et al., 1993; Handschumacher et al., 1984; Thali et al, 1994). CyPA virion incorporation stabilizes the virion and prevents human TRIM5α from

uncoating following infection (Sayah and Luban, 2004). Cleavage of CA-p2 boundry occurs late during virus maturation and is required to weaken the CA-CA interactions allowing the collapse of the spherical CA shell into a cone (Accola et al., 1998; Pettit et al., 1994; Wiegers et al., 1998).

The NC region of Pr55 contains two highly conserved copies of a CCHC-type zinc finger motif, which coordinates a zinc ion and is essential for virus replication (Aldovini and Young, 1990; Bess et al., 1992; Dorfman et al., 1993; Gorelick et al., 1993; Gorelick et al., 1990; Summers et al., 1992; Summers et al., 1990). These NC domains are also required for the packaging of the two copies of the genomic viral RNA into assembling virions (Berkowitz et al., 1996). The packaging signal (ψ) is located in the viral RNA 5' to the *gag* initiation codon. It is composed of four stem loop structures, which are required in *cis* for proper encapsidation of the viral RNA (Berkowitz et al., 1996).

Finally, the p6 domain is variable in both length and sequence. Both the PTAP (near the N-terminus) and LXXLF (Late assembly domain (L); near the C-terminus) motif are highly conserved and allow for the recruitment of the ESCORT-associated complexes. These motifs bind the ALIX (LXXLF) and TGS101 (PTAP) preventing the inward budding of vesicles into late endosomes and allow the virus to effectively bud from the plasma membrane (Bieniasz, 2006; Gottlinger et al., 1991; Huang et al., 1995; Ono and Freed, 2004; Rudner et al., 2005).

Pol

Pol is expressed from a 160-kDa Gag-pol precursor protein ($Pr160^{Gag\text{-}Pol}$). This protein is synthesized following a programmed -1 ribosomal framshift that occurs at a level of 5-10% of Gag Synthesis, ensuring a strict 20:1 ratio of Gag to Gag-Pol (Jacks et al., 1998). $Pr160^{Gag\text{-}Pol}$ is cleaved by the protease during maturation into the viral enzymatic proteins protease (PR), reverse transcriptase (RT), and integrase (IN). The relevent aspects of PR and IN are briefly described in the overview of viral replication.

The reverse transcriptase is a multifunctional enzyme with RNA-directed DNA polymerase, DNA-directed DNA polymerase, and ribonuclease H (RNase H) activities. The crystal structure of the RT and mapping of resistance mutations has been extensively studied and is beyond the scope of this dissertation. However, it is important to understand an overview of the reverse transcription process for this dissertation. The RT reverse transcribes the single-stranded RNA from the virion into double stranded DNA, which is then integrated as provirus into the host cell. The negative sense single-stranded DNA sysnthesis is initiated from the tRNALys.3 bound to the primer binding site (PBS) located on the single-stranded viral RNA genome 5' end. After primer binding, the RT proceeds to the RNA 5' terminus copying repeat (R) and the unique 5' (U5) sequences. The concomitant RNase H activity hydrolyzes the ensuing RNA/DNA hybrid, which allows the complementary R sequences at the termini of the genome promote transfer of nascent DNA to the RNA 3' terminus. This allows for continued DNA synthesis. Hydrolysis of the RNA/DNA replication intermediate continues, with the exception of the 3' and central polypurine tract (cPPT). The cPPT primes the positive strand and DNA-dependent synthesis up to eighteen nucleotides of the tRNA primer. This creates the complementary positive strand PBS sequence. Following synthesis,

the PPT and tRNA primers are excised and the PBS complementary promotes a second strand transfer event. This allows for bidirectional DNA synthesis creating a double-stranded proviral DNA flanked by the LTR sequences (reviewed in Götte et al., 2010). The lack of proofreading by the RT leads to 10- to 100- fold increase in errors. The processivity of RT is also very low and recombination of DNA during DNA synthesis occurs resulting in additional mutations in the HIV-1 genome. Therefore, the errors produced by the RT, while reverse transcribing the viral genome, allow the virus to quickly evolve and become resistant to antiretroviral treatment (Jonckheer et al., 2000).

Env

Env is synthesized as a polyprotein, gp160, precursor from a singly spliced bicistronic *vpu/env* mRNA on the rough endoplasmic reticulum (RER). This precursor is cleaved at an N-terminal ER sequence that targets Env to the RER. The signal sequence is then removed by cellular signal peptidases within the ER. The gp41 transmembrane domain prevents gp160 from being fully released into the lumen of the ER. The precursor is glycosylated with *N*- and *O*-linked oligosaccharide side chains (Allan et al., 1985; Leonard et al., 1990; Bernstein et al., 1994). This allows for oligomerization of gp160 into trimers and facilitating their trafficking to the Golgi complex where it acquires high-mannose oligosaccharide side chains and complex modifications in the *trans*-Golgi network (Earl et al., 1990; Earl et al., 1991; Pinter et al., 1989; Schawaller et al., 1989). This is to prevent the premature interaction of oligomerized gp160 with CD4 in the secretory pathway. Since gp120 binds to the CD4 receptor on susceptible cells, the viral accessory protein Vpu binds to CD4 to downregulate its

expression by targeting it to the proteosome for ubiquitin-mediated proteasomal degradation (Fujita et al., 1997; Margottin et al., 1998; Schubert et al., 1998). In the Golgi complex, gp160 is proteolytically cleaved by cellular furin to yield the mature surface glycoprotein gp120 and the transmembrane protein gp41. This cleavage is absolutely essential for viral infectivity. Following cleavage, three molecules of each gp120 and gp41 form a heterotrimeric HIV-1 glycoprotein spike. These glycoproteins remain associated through weak, noncovalent bonds, and are transported to the surface for incorporation into the budding virion (Egan et al., 1996; Rowell et al., 1995). Env is rapidly recycled to the endosome after it arrives at the plasma membrane. This leads to low maintenance on the cell surface, and helps HIV-1 evade the host immune system (Zhu et al., 2003). The expression of gp120/gp41 complexes on the cell suface of infected cells can cause fusion of two or more cells resulting in the formation of multinucleated giant cells called syncytia (Yao et al., 1993).

The gp120 protein contains discontinuous segments five variable (V1-V5) regions, five constant (C1-C5) regions, and eighteen cysteine residues. The CD4 receptor-binding site is formed from the conserved C1, C3, and C4 domains of gp120 (Lasky et al., 1987; Kowalski et al., 1987; Olshevsky et al., 1990). The V3 loop is important for both membrane fusion and co-receptor (CXCR4 and/or CCR5) specificity (Cann et al., 1992; Chesebro et al., 1991; Freed et al., 1991; Hwang et al., 1991; O'Brien et al., 1990; Shioda et al., 1991). The dominant epitopes are found on the V3 loop and are recognized by neutralizing antibodies of the host immue system (Fouchier et al., 1992; Pollakis et al., 2004; Shioda et al., 1994). After gp120 binds to CD4, gp120 undergoes a high degree of re-folding allowing the V3 loop to bind either CXCR4 or

CCR5 through either a strong negative or strong positive charge, respectively (Doms and Peiper, 1997; Kwong et al., 2000; Moulard et al., 2000; Sullivan et al., 1998). Further conformational changes occur dissociating gp120 from gp41. Then the gp41 transmembrane glycoprotein mediates fusion of the viral lipid envelop with the host cell membrane. The gp41 subunit is composed of three major domains; an extracellular domain (or ectodomain), transmembrane domain, and a C-terminal cytoplasmic domain. The gp41 protein anchors the viral envelope to the host cell membrane. The extracellular domain contains the major fusion determinants used to catalyze the fusion of the viral and host cell lipid bilayers during viral entry (Bosch et al., 1989; Freed et al., 1990; Freed et al., 1992).

Vif

Vif is a basic, cytoplasmic, 23-kDa phosphoprotein expressed late in the retroviral life cycle. This protein is highly conserved among all lentiviruses (except EIAV) and is essential for viral replication. Vif is translated from a single spliced viral mRNA, whose expression is dependent on Rev (Garret et al., 1991; Schwartz et al., 1991). Vif is part of the cytoplasmic ribonucleoprotein (RNP) complex and is packaged into viral particles at low levels. Packaging of Vif occurs through interactions with viral RNA, co-packaged cellular RNA, and the nucleocapsid domain of $Pr55^{Gag}$ (Kahn et al., 2001; Zhang et al., 2000; Dettenhofer et al., 2000; Huvent et al., 1998; Liu et al., 1995; Karczewski et al., 1996).

Vif is required for the production of infectious virus in a cell-type specific manner. In cells termed non-permissive, viruses lacking a functional *vif* gene are restricted in

their ability to replicate and produce infectious virus, when compared to wild type virus (Courcoul et al., 1995; Fan and Peden, 1992; Fouchier et al., 1996; Gaddis et al., 2003; Goncalves et al., 1996; Hoglund et al., 1994; Simm et al., 1995; Simon and Malim, 1996; Simon et al., 1998; Sova and Volsky, 1993; von Schwedler et al., 1993). This lead to the identification of the cellular restriction factor called aplolipoprotein B mRNA-editing catalytic polypeptide-like 3G (or APOBEC3G) (Sheehy et al., 2002). In the absence of Vif, APOBEC3G is encapsidated into the virion and exerts its effects on the next target cell. APOBEC3G induces massive cytidine deamination in the minus strand of viral DNA during reverse transcription producing an excessive number of G-to-A substitutions in the plus strand of DNA (Harris et al., 2003; Mangeat et al., 2003; Mariani et al., 2003; Suspene et al., 2004; Yu et al., 2004; Zhang et al., 2003). The G-to-A substitutions occur in a gradient throughout the viral genome. The most mutations are present in the Nef, and decrease towards the 5'UTR (Kijak et al., 2008; Koulinska et al., 2003; Suspene et al., 2006; 2004; Yu et al., 2004). However, Vif binds APOBEC3G and inhibits its packaging into the virion. The N-terminus of Vif binds APOBEC3G recruiting Cul5/EloB/C/Rbx-1 E2 ubiquitin ligase subsequently leading to the polyubiquitination and proteosomal degradation of APOBEC3G (Conticello et al., 2003; Kobayashi et al., 2005; Marin et al., 2003; Mehle et al., 2004; Sheehy et al., 2003; Stopak et al., 2003; Yu et al., 2003). Vif binds the E3 ubiquitin ligase complex through two highly conserved domains, ^{144}SLQ(Y/F)LA^{150} motif and the ^{108}Hx$_5$Cx$_{17\text{-}18}$Cx$_{3\text{-}5}$H^{139} domain. The ^{144}SLQ(Y/F)LA^{150} motif binds elongin C, while the ^{108}Hx$_5$Cx$_{17\text{-}18}$Cx$_{3\text{-}5}$H^{139} domain binds Cullin 5 (Luo et al., 2005; Mehle et al., 2004; 2006; Yu et al., 2004). This will be discussed in more depth below.

Nef

Nef is a small protein that is variable in length (between 200-215 amino acids) and devoid of enzymatic activity (O'Neill et al., 2006). This protein is myristoylated at the N-terminus, which is required for its expression at the plasma membrane. However, Nef is mainly localized to the paranuclear region of the infected cell with reduced expression at the plasma membrane. Nef serves as an adaptor protein to divert host cell proteins to amplify viral replication and is a major determinant of pathogenicity (Arold et al., 2001; Geyer et al., 2001; Laurent-Crawford and Hovanessian, 1992; Niederman and Ratner, 1992). *In vitro,* Nef has been determined to have four major functions: 1) downregulation of cell surface CD4 levels; 2) downregulation of cell surface major histocompatibility class I (MHCI) molecules; 3) mediation of cellular signaling and activation; 4) enhancement of viral particle infectivity by CD4 independent mechanisms (Aiken et al., 1996; 1997; 1998; Anderson et al., 1994; Arold et al., 2001; Aurora et al., 2000; Campbell et al., 2004; Chowers et al., 1994; Garcia et al., 1991; Greenburg et al., 1998; Lundquist et al., 2002; Luo et al., 1997; Mangasarian et al., 1997; Miller et al., 1994; Noviello et al., 2008; Pizzato et al., 2007; Renkema et al., 1999; Schwartz et al., 1996; Simmons et al., 2001; Wei et al., 2005; Wonderlich et al., 2008). Nef is defined as a pathogenic factor, because *nef*-deficient viruses result in lower viral burdens and severity of disease in both humans and nonhuman primates (Coleman et al., 2001; Greene et al., 2004).

The most extensively characterized function of Nef is the down-regulation of CD4 from the cell surface (Desrosiers et al., 1992; Garcia et al., 1991; Guy et al., 1987). This

involves the internalization of cell surface CD4 followed by the endosomal/lysosomal-mediated degradation. Nef binds the membrane proximal segment of the CD4 cytosolic domain and accumulates CD4 molecles into clathrin-coated pits at the cellular surface (Anderson et al., 1994; Garcia et al., 1991; Foti et al., 1997; Hua et al., 1997). A canonical dileucine motif (^{160}EXXXLL^{165}) and the two acidic residues in a structurally flexible loop that extends from amino acids 140 to 180, (^{174}(E/D)D^{175}) are required for Nef binding to adaptor protein 2 (AP-2) (Grzesiek et al., 1997; Lindwasser et al., 200). This binding facilitates the formation of clathrin-coated pits resulting in the internalization of CD4 from the cell surface and subsequent lysosomal degradation (Lindwasser et al., 2008).

Secondly, Nef allows infected cells to evade the destruction by cytotoxic T lymphocytes (CTLs) by inducing the downregulation of MHC-I molecules from the cell surface. Nef forms a ternary complex between the cytoplasmic tail of MHC-I and adaptor protein-1 (AP-1) (Noviello et al., 2008; Wonderlich et al., 2008)). AP-1 is a protein that directs proteins from the *trans*-Golgi network (TGN) to the endolysosomal pathways (Robinson and Bonifacino, 2001). MHC-I molecules are normally phosphorylated and transported to the plasma membrane for antigen presentation; however, the ternary complex activates a tyrosine-sorting signal in the cytoplasmic cytoplasmic tail of MHC-I. This allows the newly synthesized MHC-I molecules to be diverted from their transit to the plasma membrane to the lysosomes for degradation (Noviello et al., 2008; Roeth et al., 2006; Wonderlich et al., 2008). Nef also has been shown to increase the rate of MHC-I down-regulation from the plasma membrane by interacting with the phosphofurin acidic cluster sorting protein 1 and/or 2 (PACS-1/2)

(Atkins et al., 2008; Noviello et al., 2008; Wonderlich et al., 2008). However, much of this mechanism is still unknown. For example, we do not know how this process leads to activation of the endocytic pathway, and if Nef is blocking the recycling of MHC-I back to the plasma membrane, or if Nef delivers the MHCI molecules to the lysosome for degradation (Foster and Garcia, 2008).

Nef regulates cellular activation through several kinases such as Pak2 and Hck (Arora et al., 2000; Briggs et al., 2000; Renkema et al., 1999; Walker et al., 1987). Although controversial, supporting data suggested that Nef regulates the actin cytoskeleton rearrangment (Fackler et al., 1999; Janardhan et al., 2004; Renkema et al., 2001; Rauch et al., 2008). Nef forms a complex with Pak2 and induces its activation early in infection. P21 activated kinases (PAK) are effectors that link Rho GTPases to cytoskeleton rearrangement and nuclear signaling (Agopian et al., 2006; Kirchhoff et al., 2004; Pulkkinn et al., 2004; Rauch et al., 2008). Nef also activates the cellular myeloid lineage specific Src family of tyrosine kinase, Hck. This protein can bind to Nef in the absence of myristylation leading Nef to form dimer and trimers (Breuer et al., 2006). However, it is unknown how Nef dimerizes and activates Hck and how this activation enhances pathogenesis.

Single cycle infection assays are used to measure how Nef enhances infectivity (Campbell et al., 2004; Pizzato et al., 2007; Qi et al., 2007; Qi et al., 2008). From these assays there are currently three models on Nef enhances infection efficiency for HIV-1 virions without the down-regulation of the CD4 receptor. First, Campbell and colleagues showed that if the actin cytoskeleton in the target cell is disrupted the infectivity of the virus was able to overcome the *nef*-deficient virus (Campbell et al., 2004). This shows

that the expression of Nef in the producer cell is able to overcome the cytoskeleton barrier of infection. Secondly, Pizzato and colleagues suggested that an unknown cellular protein besides CD4 blocks the function of Env. Nef downregulates the unknown protein in the producer cell, thereby blocking its incorporation into the virion and enhancing viral infectivity (Pizzato et al., 2007). Finally, several studies have shown that Nef may protect the viral core from post-fusion degradation allowing reverse transcription to continue (Qi et al., 2007; Qi et al., 2008; Wei et al., 2005).

Vpr/Vpx

The HIV-2 and SIV primate lentiviruses encode for a *vpr* gene and a paraolog of *vpr* known as *vpx* gene, while HIV-1 only encodes for a *vpr* gene (Campbell et al., 1997). Both of these proteins are important for the transport of the pre-integration complex (PIC) into the nucleus and inducing cell cycle arrest at the G2/M phase of the cell cycle (Lang et al., 1993; Shimura et al., 1999). Both proteins have a supporting role during early infection and are selectively packaged into the virion. The incorporation occurs througha dileucine (LXXLF) motif in the p6 domain of the Gag precursor protein, $Pr55^{Gag}$ (Accola et al., 1999; Bachand et al., 1999; Kondo et al., 1995; Lu et al., 1995; Paxton et al, 1993; Selig et al., 1999). In addition, Vpr can regulate apoptosis and transactivate the viral promoter (Le Rouzic and Benichou, 2005; Planelles and Benichou, 2010). However, Vpx is essential for viral growth in monocyte-derived macrophages (MDMs) and primary T lymphocytes, nuclear import of viral DNA, and is critical for reverse transcription in monocyte-derived dendritic and non-dividing cells by

promoting the accumulation of full-length DNA (Fletcher et al., 1996; Fujita et al., 2008; Goujon et al., 2007; Srivastava et al., 2008).

Vpr induces cell cycle arrest at the G_2-to-M transition by activation of ataxia telangietasia-mutated and Rad-3-related kinase (ATR), which is a sensor for replication stress (Roshal et al., 2003). Vpr also associates with damaged DNA-specific binding proteins 1 (DDB1) and Cullin 4-associated factor (DCAF)-1 (Angers et al., 2006; He et al., 2006; Higa et al., 2006; Jin et al., 2006). This recruits the $Cul4A^{DDB1}$ E3 ligase, which is involved in genome stability, DNA replication, and cell cycle arrest by activation of the G_2 checkpoint (DeHart and Planelles, 2008; Huang and Chen, 2008). Prolonged G2 cell cycle arrest may attribute to Vpr-induced apoptosis; therefore, Vpr-induced cytopathicity in macrophages could be due to the absence of ATR signaling (Zimmerman et al., 2006). Also, Vpr inhibits T cell proliferation and modulates immune responses through interaction with proteins like the glucocorticoid receptor (Ayyayoo et al., 1997). One of the immune modulatory functions of Vpr is to cause a dysregulation in selective co-stimmulatory molecules and cytokines in moncytes, macrophages, and dendritic cells (Granelli-Piperno et al., 2004; M et al., 2000; Majumder et al., 2005; Mirani et al., 2002; Muthumani et al., 2004; Smed-Sorensen et al., 2004).

The Vpr protein is present at the start of the replication cycle. Vpr-deficient HIV-1 shows a significant replication defect in primary macrophages, but not in T cells or laboratory cell lines (Balliet et al., 1994; Connor et al., 1995). Vpr has been shown to enhance HIV-1 transcription in monocytic cells (Varin et al., 2005). This is due to a nuclear localization signal on Vpr that interacts with proteins associcated with the HIV-1 PIC, such as human uracil-DNA glycosylase (hCGI), nucleoporin, importin alpha, and

exporin 1 (Bergamaschi et al., 2009; Chen et al., 2004; Jacquot et al., 2007; Nitahara-Kasahara et al., 2007; Sherman et al., 2003). Vpr is not essential for HIV-1 infection of macrophages, but depending on the lineage of SIV, is required for replication (Bergamaschi et al., 2009; Campbell et al., 1997; Fletcher et al., 1996; Ueno et al., 2003). This shows that the *vpr* genes have significantly diverged and that the importance of Vpr in macrophage infection differs between lentiviral lineages.

So far, Vpx is not implicated in cell cylce arrest and does not contain a nuclear localization signal to import the PIC complex into the nucleus (Fletcher et al., 1996; Kappes et al., 1993). However, Vpx has been shown to be essential for SIVmac infection of monocytes and monocyte-derived dendritic cells (Gibs et al., 1995; Goujon et al., 2007; 2008; Wolfrum et al., 2007). In pig-tailed macaques inoculated with SIVsmPBjΔ*vpx*, the effect of Vpx deletion was dramatic on viral pathogenicity. These macaques displayed delayed kinetics in viral replication and delayed disease manifestations (Gibbs et al., 1995; Hirsch et al., 1998). Vpx does not minic Vpr as was previously suggested, because Vpx is required for infecting monocytes, non-diving macrophages, and monocyte-derived dendritic cells (Gibs et al., 1995; Goujon et al., 2007; 2008; Wolfrum et al., 2007). Deletion of *vpr* in these viruses, does not affect the requirement for Vpx in HIV-2/SIV infection (Gramberg et al., 2009; Kappes et al., 1993). However, similar to Vpr, Vpx uses the DCAF1 unbiquitin ligase to remove cellular restriction factors present in macrophages and dendritic cells (Kappes et al., 1993; Sharova et al., 2008; Srivastava et al., 2008). While the ubiquitin ligase machinery has been identified, the restriction factor degraded is still unknown.

Tat/Rev

Tat is a transactivator protein that contributes to trans-activation of viral and cellular genes (Ju et al., 2009; Mahlknecht et al., 2008; Nekhai et al., 2007). The HIV-1 Tat protein is synthesized during the early and late stages of viral replication and is variable in length of 86-104 amino acids. There are five functional domains in Tat, which include the N-terminus, the cysteine-rich region, the core, the basic, and the C-terminal domains. Also, there is a region known as the protein transduction domain that contains a rich-lysine and arginine region that allows Tat to cross the cell membrane. (Morris et al., 2001) The extracellular form of Tat is efficient in cell membrane transduction, is released into the microenvironment by productively infected cells and, taken up by target cells in the surrounding environment (Ferrari et al., 2003; Zheng et al., 2005). Tat has several functions such as chromatin remodeling, phosphorylation of RNA polymerase II that is involved in the transcription of full-length viral mRNAs, transactivation of viral genes, and binding to nascent leader RNA known as trans-activation responsive element RNA (TAR) (Ammosova et al., 2006; Richman et al., 2009; Wong et al., 2005; Yedavalli et al., 2003). Post-integration of the viral genome, the expression of the viral genome is controlled by the enhancer and promoter elements located in the (LTR) located at the 5' end of the integrated genome (Rohr et al., 2003). To relieve the LTR, Tat interacts with several chromatin modifying complexes and histone modifying enzymes. For example, Tat recruits histone acetyltransferases (HATs) such as CREB-binding protein (CBP/p300) complex to acetylate the nucleosomes on the HIV-1 promoter region relieving LTR repression. This allows RNA polymerase II to efficiently transcribe viral genes (Deng et al., 2000; 2001; Pumfry et al.,

2003). By Tat changing the conformation of CBP/p300, the CBP/p300 complex is better able to bind the basal transcription factors such as the TATA-binding protein and transcription factor IIB (Dang et al., 2000; 2001). In the absence of Tat or cellular activation signals, abortive short viral mRNA transcripts are produced due to the reduced efficiency with which RNA polymerase II binds the HIV-1 promoter (Pagans et al., 2005; Williams et al., 2006). However, when Tat binds the TAR stem loop structure located at the 5' end of all initiated viral transcripts, the P-TEFb complex composed of cellular cyclin T1 and CDK9 proteins is recruited (Williams et al., 2006). This complex phosphorylates serine residues in the C-terminal domain (CTD) of RNA polymerase II leading to the synthesis of full-length HIV transcripts (Williams et al., 2006; Zhou et al., 2003). Tat also induces the phosphorylation of additional transcription factors including Sp1, CREB, the alpha subunit of eukaryotic initiation factor 2 (eIF2α), and NF-κB (Demarchi et al., 1998; Li et al., 2005; Rossi et al., 2006; Zauli et al., 2001).

Tat has been shown to modulate the expression level of other cellular proteins such as cytokines, CCR5, IL-2, and CD25, while down regulating cellular proteins such as MHC I (Matsui et al., 1996; Mayol et al., 2007; Stettner et al., 2009; Zheng et al., 2005). Since Tat can be taken up by uninfected target cells, Tat is able up regulate cellular genes to induce additional effects such as the induction of apoptosis and immunosuppression (Bennasser and Bahraoui, 2002; Gupta et al., 2008; Ju et al., 2009; Poggi and Zocci, 2006; Zheng et al., 2005). Tat can cross the blood brain barrier (BBB) and transverse cells such as neurons causing neurotoxicity, induce the release of tumor necrosis factor-α (TNF-α) from macrophages and astrocytes, IL-6 from astrocytes, and IL-1β from monocytes, causing apoptosis, which may provide an

explanation for the neurodegenerative effects of HIV-1 (Chang et al., 1997a; Chen et al., 1997; Nath et al., 1999; Cheng et al., 1998; Magnuson et al., 1995; Song et al., 2003). Tat also interacts with both non-polymerized subunits of microtubules and polymerized microtubules leading to the mitochondrial induction of apoptosis (de Mareuil et al., 2005; Giacca et al., 2005; Vendeville et al., 2004). Due to this neuronal cytoskeleton rearrangement, neuropathogenesis associated with HIV-1 infection may occur (Drewes et al, 1998).

Following integration of the provirus into the host-cell genome, the late phase of viral replication begins with transcription of the integrated proviral DNA and subsequent splicing and trafficking of viral RNAs (Grewe and Überla, 2010; Freed et al., 2001). Transcription from the LTR leads to the generation of unspliced incompletely spliced, and multiply spliced RNAs. These major types of viral transcripts are 1) full length unspliced transcript encoding the $Pr55^{Gag}$ and $Pr160^{GagPol}$ precursors and the full length HIV-1 ~9-kb RNA genome; 2) singly spliced RNAs that encode for Vif, Vpr, Vpu, and Nef proteins; 3) multiply spliced RNAs that encode for Tat, Rev, and Nef proteins. Rev is a 116 amino acid protein that allows mammalian cells to overcome the highly selective nuclear export of unspliced or partially spliced mRNAs (Cullen et al., 1998). The function of the Rev protein is mediated by two distinct domains: 1) an arginine-rich sequence that functions as both a nuclear localization signal (NLS) and an RNA-binding domain (RBD); and 2) a leucine-rich sequence located between amino acid residues 75 to 85 that contains the nuclear export signal (NES) (Böhnlein et al., 1991; Daly et al., 1989; Fischer et al., 1995; Hope et al., 1990; 1991; Kubota et al., 1989; Malim et al., 1989; Malim and Cullen, 1991; Malim et al., 1991; Mermer et al., 1990; Meyer et al.,

1996; Neville et al., 1997; Venkatesh et al., 1990; Weichselbraun et al., 1992; Wen et al., 1995; Zapp et al., 1991; Zapp and Green, 1989). During the early stage of infection, HIV-1 full-length RNAs are expressed in the nucleus and gradually spliced to completion. These spliced RNAs are exported from the nucleus using the cellular mRNA export pathway and lead to the synthesis of Tat, Nef, and Rev. Following translation, Tat and Rev are transported back into the nucleus using nuclear localization signals (NLS) to assist in viral transcription. After enough Rev protein is expressed, nuclear export of both partially and unspliced transcripts occurs leading to the translation of all viral proteins (Cullen, 1998).

Rev function is mediated by binding a *cis*-acting viral RNA stem-loop structure located in the *env* gene known as the Rev response element (RRE) (Malim et al., 1989). This interaction induces multimerization of Rev molecules to the RRE. Ran-GTP bound exportin 1 binds to the NES of Rev forming a complex required for the docking and translocation through the nuclear pore into the cytoplasm (Fornerod et al., 1997; Neville et al., 1997; Stade et al., 1997). Once the complex is translocated to the cytoplasm, the hydrolysis of Ran-GFP to Ran-GDP occurs inducing the release Rev from the complex. In the cytoplasm, Rev then binds importin-β and translocates back into the nucleus. Following translocation to the nucleus, the importin-β/Rev complex interacts with Ran-GTP and disassembles to release Rev back into the nucleus (Henderson et a., 1997; Palmeri et al., 1998).

Vpu

Vpu is an 81 amino acid type I integral membrane protein. Amino acid residues 1-27 constitute the N-terminal membrane anchor followed by 54 residues that extend into the cytoplasm. The cytoplasmic component consists of a highly conserved region spanning amino acid residues 47-58 that contain a pair of serine residues that are consitutively phosphorylated by casein kinase II (Schubert et al., 1994; Tiganos et al., 1998). The cytoplasmic domain of Vpu contains two α-helical structures comprised of amino acid residues 35-50 and 58-70 separated by a flexible segment containing two conserved serine residues that are phosphorylated (Federau et al., 1996; Henklein et al., 1993; Kochendoerfer et al., 2004; Wittlich et al., 2009; Wray et al., 1995; Zheng et al., 2003). HIV-1 infected cells show that Vpu interacts with several host factors such as CD4, β-TrCP, and BST-2. Also, homo-oligomerization of Vpu creates a pentameric complex to form cation-selective membrane pores (Ewart et al., 1996; Grice et al., 1997; Kruger and Fischer, 2009; 2010; Park et al., 2003; Schubert et al., 1996).

One function of Vpu is to induce the degradation of CD4. The Env precursor gp160 blocks the trafficking of newly synthesized CD4 by binding and forming stable complexes that are retained in the endoplasmic reticulum (ER) (Bour et al., 1991; Crise et al., 1990; Jabbar and Nayak, 1990). The cytoplasmic domain of Vpu interacts with the cytoplasmic domain of CD4 complexed with Env in the ER to target CD4 for proteosomal degradation (Bour et al., 1995; Margottin et al., 1996). The two-conserved serine residues at amino acid positions 52 and 56 in the cytoplasmic domain of Vpu are phosphorylated and interact with the WD repeats of human beta Transducin-repeat Containing Protein (β-TrCP) (Margottin et al., 1998; Neer et al., 1994). Human β-TrCP contains seven C-terminal WD repeats to mediate protein-protein interaction and an F-

box domain that acts to connect target proteins to the ubiquitin-dependent proteolytic pathway (Bai et al., 1996; Neer et al., 1994).

A second function of Vpu is the regulation of virus release from HIV-1 infected cells (Strebel et al., 1988; Terwilliger et al., 1989). There have been a number of different models that propose the regulation of virus release by Vpu. First, virus release is regulated by the Vpu-associated ion channel activity. When the transmembrane domain of Vpu is scrambled, the ion channel activity is inhibited resulting in the impairment of Vpu to regulate virus release but not CD4 degradation (Schubert et al., 1996). Secondly, Vpu may form heter-oligomeric complexes that interfere with the activity of TASK-1, a cellular ion channel (Hsu et al., 2004). In the third model, the dependence on Vpu for virus release is cell-type specific (Varthakavi et al., 2003). In addition to TASK-1, other host factors, such as BST-2, have been identified that are associated with inhibited virus reelase (Neil et al., 2008; Van Damme et al., 2008). BST-2 is a 180 amino acid type II transmembrane protein that was originally identified as a membrane protein in terminally differentiated human B cells of patients with multiple myeloma (Goto et al., 1994; Ohtomo et al., 1999; Ishikawa et al., 1995). This protein consists of an N-terminal transmembrane domain and a C-terminal glycosylphosphatidylinositol (GPI) anchor that allows BST-2 to associate with lipid rafts at the cell surface and on internal membranes such as the Trans-Golgi Network (TGN) (Dube et al., 2009; Kupzig et al., 2003; Masuyama et al., 2009). The ectodomain of BST-2 can form stable cysteine-linked dimmers that are critical for the inhibition of HIV-1 release (Andrew et al., 2009; Perez-Caballero et al., 2009). However, BST-2 positive cells that are infected with HIV-1ΔVpu accumulate virions at the cell surface. The BST-

2 N-terminal transmembrane domain and its C-terminal GPI anchor tethers together fully detached virions to the producer cell (Neil et al., 2008). In wild type virus, BST-2 is redistributed from the plasma membrane into early endosomes through clathrin-mediated endocytosis (Habermann et al., 2010; Neil et al., 2006; Mitchell et al., 2009; Rollason et al., 2007). Vpu interacts with BST-2 in endosomes and the TGN to downregulate BST-2 from the cell surface increasing virus release (Douglas et al., 2009; Dube et al., 2009; Habermann et al., 2010; Le Tortorex and Neil, 2009; Mitchell et al., 2009; Miyagi et al., 2009; Neil et al., 2008; Pardieu et al., 2010; Rollason et al., 2007; Sato et al., 2009; Schindler et al., 2010; Van Damme et al., 2008).

Pathogenesis

HIV-1 is transmitted through sexual contact and by direct blood-to-blood contact. The blood-to-blood contact includes intravenous drug users, occupational accidental needle sticks, transfusions, and vertical mother-to-child perinatal transmission (Curran et al., 1988; Parazzini et al., 1995). HIV-1 is the etiological agent of AIDS and results in a depletion of helper $CD4^+$ T lymphocytes resulting in the loss of immune competence (Stevenson et al., 2003). The slow continuous depletion of CD4+ lymphocytes during the infection results in damaged immune defense leading to the susceptibility to opportunistic infections that eventually leads to death. The exact mechanism for the depletion of $CD4^+$ lymphocytes is still unknown. There are two working hypothesis to identify the mechanism by which HIV causes disease. In the first hypothesis, it is thought that HIV causes a major depletion of $CD4^+$ T lymphocytes by direct infection

and apoptosis. The second hypothesis considers that HIV infection is indirectly impairing cell function by a possible aberrant reaction of the immune response to the infection (Stevenson et al., 2003). A deeper understanding of viral replication, host response, reservoirs, and viral pathogenicity will help identify answers to these unanswered questions.

HIV infection can be divided into three phases: acute primary infection, asymptomatic infection, and symptomatic infection and AIDS (Coffin et al., 1995). During the acute phase of infection, ~50% of the patients remain asymptomatic, while ~50% develop flu-like symptoms such as as fever, headache, sore muscles and joints, stomachache, swollen lymph glands, and/or rash, during the first four weeks of infection. During primary infection viral loads in the peripheral blood are high and the virus disseminates to many lymphoid and non-lymphoid tissues (Piatak et al., 1993). Following the acute phase, the asymptomatic carrier state begins and lasts between 10 to 12 years in an untreated typical progressor patient. During this stage, viral replication remains steady and there is a gradual decline in the number of circulating $CD4^+$ T cells. Virus is persistently replicating in the primary and secondary lymph nodes and there is a rapid turn over of plasma virions and CD4+ T lymphocytes (Embertson et al., 1993; Pantaleo et al., 1993; Ho et al., 1995; Wei et al., 1995). This stage is also known as clinical latency. Eventually, the continuous damage to the immune system results in an increase in viral loads and life-threatening AIDS-defining diseases emerge (Sierra et al., 2005). When infected individuals establish clinical AIDS, the circulating $CD4^+$ T lymphocytes decline to below 200 cells per microliter and/or the patient acquires an

AIDS-defining illness such as opportunistic infection(s), cancer(s), and/or HIV-related enecephalopathy (Coffin et al., 1995).

Between 5-10% of patients are classified as rapid progressors and develop AIDS within 3-4 years following infection with HIV-1. These patients do not develop clinical latency, but continue to exhibit high viral loads and display a rapid decrease in the level of circulating $CD4^+$ T lymphocytes (Arens et al., 1993; Bollinger et al., 1996; Demarest et al., 2001). There are HIV-1 patients that exhibit high viral loads initially during primary infection and then continue to present with low viral burdens for an extended period of infection. These individuals represent ~5% of the patients infected and are termed long-term non-progressors (LTNP). The level of circulating CD4+ T lymphocytes remains stable in these patients, and these individuals remain asymptomatic. These patients also display a strong qualitative and quantitative HIV-1 specific cytotoxic T-lymphocyte (CTL) response (Migueles et al., 2002). LTNP may result due to host/cellular restriction factors, attenuated HIV-1 due to mutations in *nef* (Δ*nef*), or genetic polymorphisms that impair or abrogate expression of coreceptor proteins (CCR5Δ32) (Coffin et al., 1995; Deacon et al., 1995; Kirchhoff et al., 1995).

Additionally, HIV-1 invades the central nervous system early during infection and can cause persistent infection of the brain and inflammation (Shapshak et al., 2011). This infection can result in neurodegenerative disease known as neuroAIDS. The severity of this disease can range from asymptomatic neurocognitive impairment (ANI), in a mild neurocognitive disorder (MND), or be full-blown HIV-associated dementia (HAD) in infected patients (Antinori et al., 2007; Shapshak et al., 2011). These HIV-associated neurocognitive disorders (HAND) are influenced by host and viral

characteristics, co-morbid factors, substance abuse, and HARRT therapy (Bhaskaran et al., 2008). HAND is thought to occur by HIV-1 infected macrophages/monocytes transversing the tight junctions of the cerebral endothelial cells (CECs) of the blood brain barrier (BBB). Once past the BBB, the monocytes differentiate into macrophages/microglia cells (Shapshak et al., 2011). HIV-1 activates these macrophages/microglia and astrocyte cells causing the production of pro-inflammatory cytokines resulting in neuronal toxicity (Borjabad et al., 2009; Kaul et al., 2001; Minagar et al., 2004; Shapshak et al., 2004). Unfortunately, few anti-retroviral drugs treat neuroAIDS effectively because they are unable to penetrate the BBB. However, there are studies underway working to search for a way to either deliver a therapeutic drug to bypass the BBB or to create new therapeutics to treat these conditions (Shapshak et al., 2011).

Endogenous Retroelements

Genomic structural variations (SVs) are common in the human genome and occur through insertions, deletions, inversions, duplications, and translocations. Due to their mobility, abundance, and high sequence identity, transposable elements (TEs) are usually involved in creating genomic SVs (Konkel et al., 2010). Retrotransposons are TEs that use an RNA intermediate, are reverse transcribed, and move within the genome through a copy-and-paste mechanism (Batzer et al., 2002; Ostertag et al., 2001). Based on the presence or absence of long terminal repeats (LTRs), retrotransposons can be divided into two groups: non-LTR retrotransposons or LTR-retrotransposons (Konkel et al., 2010). Besides the non-LTR elements listed, there

are inactive old non-LTR retrotransposons encompassing approximently 6% of the human genome (Lander et al., 2001). LTR retrotransposons are the endogenous retroviruses and comprise approximently 8% of the human genome. However, there are no active LTR retrotransposones in the human genome today (Lander et al, 2001; Mills et al., 2007).

Non-LTR retrotransposons are comprised of three different families: long interspersed nuclear elements 1 (LINE1 or L1), *Alu* elements (a short interspersed element or SINE), and SVA (named after composite parts; SINE-R, VNTR (variable number of tandem repeats) (Cordaux et al., 2009; Belancio et al., 2008; Batzer et al., 2002; Bennett et al., 2008; Lander et al., 2001). L1s comprise about 17% (>500,000 copies) of the human genome and display evidence of ongoing activity for over the past 160 million years (Lander et al., 2001). Most L1 insertions are retrotranspositionally incompetent due to truncations and debilitating mutations; therefore, only ~80 to 100 retrotrasnposition competent L1s have been identified in the human genome (Brouha et al., 2003; Lander et al., 2001). L1s are known as autonomous retrotransposons that are currently mobilizing and at full-length are approximently 6-kb (Lander et al., 2001; Swergold et al., 1990). The element consists of a 5'UTR containing an internal RNA polymerase II (RNAPII) promoter, two open reading frams (ORF 1 and ORF 2), and a 3'UTR containing a polyadenylation signal ending with an oligo(dA)-rich tail of variable length (Figure 6) (Babushok et al., 2007; Swergold et al., 1990). ORF1 encodes for a protein involved in RNA binding and ORF2 encodes for a protein that contains both endonuclease and reverse transcriptase activity (Feng et al., 1996; Jurka et al., 1997; Martin et al., 2003; Mathias et al., 1991).

L1 retrotransposition duplication begins with RNA polymerase II transcription of the *L1* gene locus from an internal promoter (Figure 6). Initiation of transcription occurs at the 5' end of the L1 element and the internal promoter generates autonomous duplicate copies at multiple locations in the genome (Lavie et al., 2004; Swergold et al., 1990). L1 RNA is then exported to the cytoplasm where ORF1 and ORF2 are translated. ORF1 and ORF2 bind the L1 RNA transcript in a *cis* fashion and produce a ribonucleoprotein (RNP) complex that is transported back into the nucleus by an unknown mechanism (Lavie et al., 2004; Swergold et al., 1990; Wei et al., 2001). The integration of L1 into the genome occurs through a process referred to as target-primed reverse transcription (TPRT) (Cost et al., 2002; Feng et al., 1996; Moran et al., 1996). The L1 endonuclease cleaves the first strand of target DNA, at 5'-TTTTAA-3' consensus sites (Jurka et al., 1997). The free 3' hydroxyl generated by the DNA nick is used to prime the reverse transcription of L1 RNA by the L1 reverse transcriptase. The second strand of the target DNA is cleaved and used to prime second strand synthesis by unidentified mechanisms. It is thought that host repair systems are involved (Beauregard et al., 2008; Gasior et al., 2006; Gilbert et al., 2005; Ichiyanagi et al., 2007; Zingler et al., 2005). Since there are frequent staggered breaks in the host DNA at the insertion site, the retrotransposon is flanked by short stretches of host DNA between 6-20 base pairs in length and is referred to as target site duplications (TSD) (Feng et al., 1996; Szak et al., 2002). A variation of TPRT can also occur call "twin priming." When inversions are formed, the second strand of DNA is cleaved during reverse transcription of the first strand. The 3'OH of the second strand acts as a primer for the reverse transcription on the L1 RNA and the resolution of this second cDNA produces the

inversion (Kriegs et al., 2007; Bejerano et al., 2006). Furthermore, it is thought that *Alu* and SVA retrotransposition occurs through the TPRT process using the L1 reverse trasncriptase machinery. However, most of this process has remained elusive (Dewannieux et al., 2003; Ostertag et al., 2003; Wang et al., 2005).

There are greater than 1 million *Alu* copies in the human genome, making this element the most successful TE in the human genome. This element is non-autonomous and relies on the enzymatic machinery of L1 to complete retrotransposition (Wei et al., 2001; Weiner et al., 1986). *Alu* elements are approximently 300 base pairs long and is dimeric in structure. This element is formed by the fusion of two monomers originally derived from the *7SL* RNA gene (Kriegs et al., 2007). The two monomers of *Alu* are divided by an A-rich linker. The 5' region contains an internal RNA polymerase III, while the 3' region contains a polyadenylation signal ending with an oligo(dA)-rich tail of a variable length (Figure 6) (Babushok et al., 2007; Swergold et al., 1990). There is no termination signal for the RNA polymerase III, so the transcripts extend into the downstream flanking sequences until a terminator can be found (Comeaux et al., 2009; Shaikh et al., 1997).

SVA elements are less characterized with approximently 3,000 copies existing in the human genome (Ostertag et al., 2003; Wang et al., 2005). This element is non-autonomous and requires the enzymatic machinery of the L1 retrotransposon. Similar to L1 elements, SVA elements are often truncated and terminate in a polyadenylation signal followed by a polyA tail (Ostertag et al., 2003; Wang et al., 2005). SVA elements are approximently 2-kb in length and are composed of a hexamer repeat region, an *Alu*

Figure 6. Schematic representation of the non-LTR retrotransposon structure. (A) The L1 element consists of a 5'UTR, two open reading frames (ORF1 and ORF2), and a 3'UTR. The 5'UTR contains an internal RNA polymerase II promoter (gray box). The element ends with a oligo(dA)-rich tail (AAA) preceded by a polyadenylation signal (pA). (B) The *Alu* element consists of two related monomers separated by an A-rich linker (consensus sequence A_5TACA_6). The left monomer consists of A and B boxes (gray boxes). These boxes are transcriptional promoters for RNA polymerase III. The 3' end of the element contains an oligo(dA)-rich tail (AAA) that can be up to 100 base pairs long. (C) The SVA element (from 5' to 3') consists of a $(CCTCT)_n$ hexamer repeat region, an *Alu*-like domain containing two antisense *Alu* fragments with additional sequences of unknown origin, a 35-50 base pair (VNTR) region derived from envelope polyprotein (*env*), and the 3'LTR of the human endogenous retrovirus (HERV)-K10. The 3' end of this element is an oligo(dA)-rich tail preceded by a polyadenylation signal similar to that observed in (A). All three elements are flanked with target site duplications (not shown) that are generated post integration.

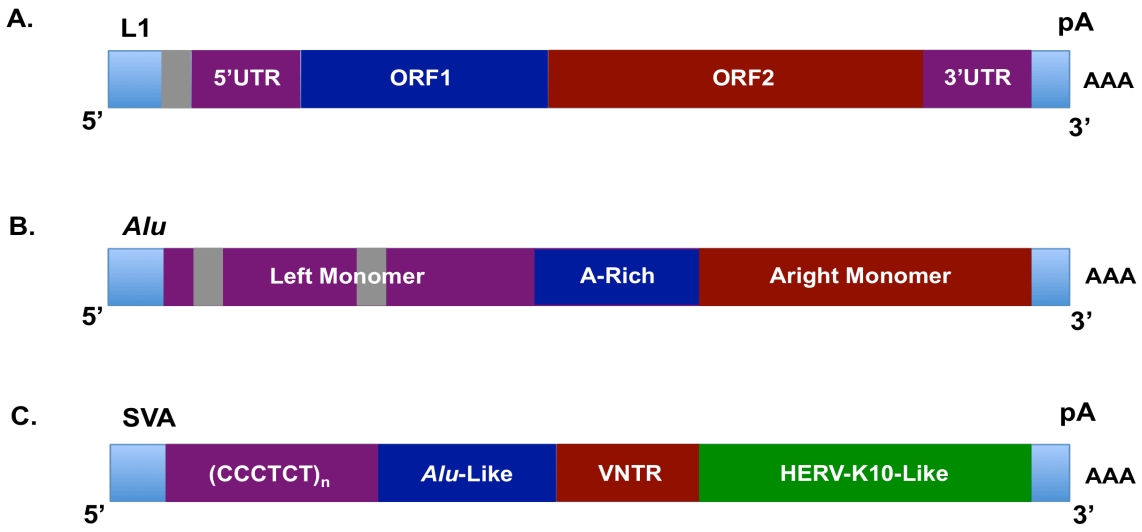

Adapted from Cordaux et al., 2009

like region, a VNTR (variable number of tandem repeats), a HERV-K10-like region, and a polyadenylation signal ending with a oligo(dA)-rich tail of variable length (Figure 6) (Ostertag et al., 2003; Wang et al., 2005). However, there is no internal promoter suggesting that promoter activity comes from flanking regions and that the element may be transcribed by RNA polymerase II (Ostertag et al., 2003; Wang et al., 2005).

LTR retrotransposons are very similar to exogenous retroviruses in structure. They contain two LTR's at the 5' and 3' end of the element, slighty overlapping ORFs for *gag*, protease, and a *pol* gene, which encodes for the reverse transcriptase, endonuclease, integrase, and ribonuclease H (Kazazian et al., 2004; Voytas et al., 2002). LTR elements either lack or encode for a remnant of an *env* gene. Retrotransposition reverse transcription is essentially like retroviral reverse transcription, and the LTR retrotransposon RNA is made within the cytoplasm (Voytak et al., 2002). Some examples of LTR retrotransposons that are responsible for the majority of insertions are yeast Ty1 elements (*Saccharomyces cerevisiae*), IAP elements (intracisternal A-particles), MusD ETns (early transposons, and MaLR elements (mammalian LTR-retrotransposons). Most of these mobile elements are found in mice and are not present in humans, are essentially defective, and the reverse transcriptase source is still unknown (Kazazian et al., 2004k). However, IAPs and MusD elements are still highly mobile in the mouse genome (Maksakova et al., 2006). It is important to note that unlike human, endogenous retroelements in the mouse genome are 5-fold more abundant than in the human genome (Maksakova et al., 2006). In the human genome, although none of the HERVs are currently active, sequences can be recovered and reconstructed to study (Lee et al., 2007).

Disruption of coding or regulatory sequences due to deleterious insertions can occur due to non-LTR retrotransposons (Belancio et al., 2008a; Callinan et al., 2006; Chen et al., 2005; Deininger et al., 1999). This can ultimately disrupt splice sites and cause exon skipping altering gene expression and increase the risk of certain diseases like cancer (Belancio et al., 2008b; Belancio et al., 2009; Chen et al., 2008; Chen et al., 2006; Han et al., 2005; Landry et al., 2001; Perepelitsa-Belancio et al., 2003; Sobczak et al., 2002). Recent research has shown that a family of cytidine deaminases, APOBEC3 (apolipoprotein B mRNA-editing enzyme catalytic- polypeptide like 3), are capable of either introducing mutations into retroelement DNA or inhibiting retrotransposition in the absence of editing (Chen et al., 2006; Esnault et al., 2005). This is due to these retroelements undergoing a reverse transcription process analogous to exogenous retroviruses like HIV-1. These APOBEC3 proteins exude dual inhibitory effects on these endogenous retroviruses such as decreasing the number of transposed cDNA copies and extensive editing of the transposed copies (Esnault et al., 2005; Esnault et al., 2006). This material will be discussed in more detail later in the Introduction.

SHIV/Macaque Model of Infection

Simian-human immunodeficiency virus (SHIV) is a chimeric virus consisting of HIV-1 *tat, rev, vpu, and env* genes in the genetic background of pathogenic $SIV_{mac}239$ (Figure 7). The pathogenic SHIV model has allowed researchers to study the role of specific genes in HIV-1 using the SHIV/macaque model of infection. Using this model, HIV-1 pathogenesis can be studied using non-human primates to evaluate mutations in

Figure 7. Schematic representation of SHIV. $SIV_{mac}239$ genes are encoded in blue and HIV-1 genes are encoded in yellow.

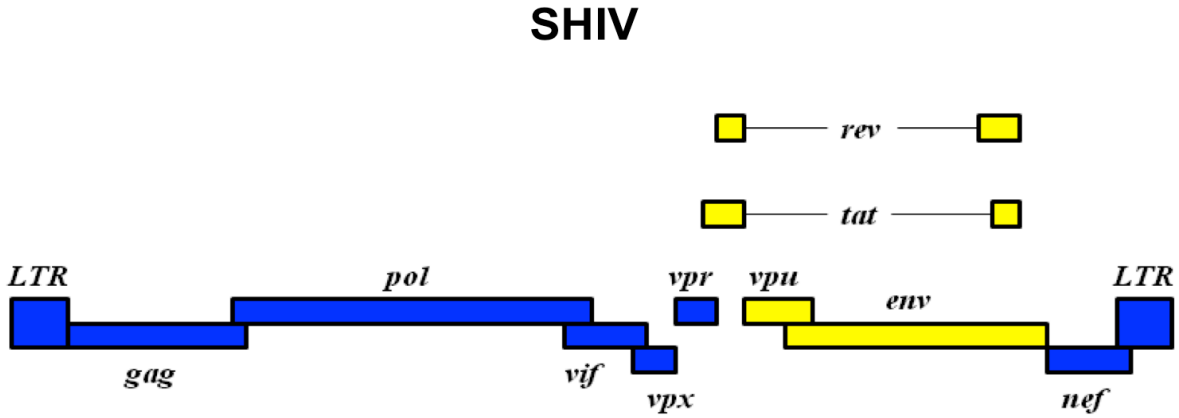
SHIV
rev
tat
LTR
pol
vpr
vpu
env
LTR
gag
vif
vpx
nef

HIV-1 *env* and *vpu* within the context of viral transmission, pathogenesis, and immune responses. SHIVs are known to cause AIDS and productive central nervous system (CNS) infection in rhesus macaques (Joag et al., 1997; Raghavan et al., 1997). Originally, the SHIV constructed (SHIV-4) was able to infect both rhesus and pig-tailed macaques and cause a persistent infection. However, these macaques did not develop a loss in circulating $CD4^+$ T lymphocytes and did not develop an AIDS-like disease. SHIV-4 was passaged through a series of rhesus and pig-tailed macaques yielding pathogenic variants that developed a rapid loss of circulating $CD4^+$ T lymphocytes, replicated to extremely high titers, and showed severe lymphoid depletion. Within eight months to a year, these macaques developed AIDS, neurological and end-stage renal disease. Also, SHIV contains unique structural motifs in gp160 of HIV-1, which allows SHIV to use the co-receptor CXCR4 similar to HIV-1 infection in humans (Joag et al., 1997; Karlsson et al., 1997; Liu et al., 1999; Shibata et al., 1997). Our laboratory uses the pathogenic SHIV variants $SHIV_{KU\text{-}1bMC33}$ and $SHIV_{KU\text{-}2MC4}$, which have been shown to cause a rapid loss of CD4+ T lymphocytes eventually resulting in the development of AIDS six to eight months post-infection (Liu et al., 1999; Narayan et al., 1999; McCormick-Davis et al., 2000a).

HIV-1 Vif Phenotype

The Vif protein is highly conserved among all lentiviruses, except for equine infectious anemia virus (EIAV), and is necessary for the production of infectious virus from $CD4^+$ T cells and macrophages (Fisher et al., 1987; Strebel et al., 1987). Viruses lacking a functional *vif* gene fail to mount a spreading infection in cells termed

"nonpermissive." These nonpermissive cells include $CD4^+$ T cells, macrophages, and some T cell leukemia lines, such as H9, HuT78, C8166, and MT2 cells (Gabuzda et al., 1992; Sova et al., 1993; von Schwedler et al., 1993). These nonpermissive cells support the normal production of HIV-1Δ*vif* virions, but are unable to productively infect the next target cell (Gabuzda et al., 1992; Sova et al., 1993; von Schwedler et al., 1993). Conversely, Vif is dispensable for the production of infectious virus from cells termed "permissive (Gabuzda et al., 1992; von Schwedler et al., 1993)." These permissive cells include T cell lines, such as Jurkat, SupT1, and CEM-SS cells, as well as nonhematopoietic cell lines, such as, HeLa, 293T, and COS cells (Gabuzda et al., 1992; Sova et al., 1993; von Schwedler et al., 1993). This particular "Vif phenotype" was found to be producer cell dependent, because experiments showed that transcomplementation of Vif in the producer cell was successful in rescuing viral infectivity (Strebel et al., 1987; von Schwedler et al., 1993). However, expression of Vif in the target cell had no effect (Strebel et al., 1987). Therefore, it was proposed that either Vif overcomes the effect of a negative factor in the nonpermissive cells or that permissive cells may express a host factor that influences viral infectivity.

Identification of a Vif Sensitive Anti-HIV-1 Factor

Using subtractive hybridization techniques, Sheehy and colleagues showed that nonpermissive cells produced an endogenous inhibitor, *CEM15* or *Apobec3G*, which prevented the infectious spread of HIV-1 in the absence of Vif (Sheehy et al., 2002). CEM-SS (nonpermissive) cells pseudotyped with VSV-G (vesicular stomatitis virus envelope protein) were infected with HIV-1Δ*vif*Δ*env* and incubated with CEM

(permissive) cells expressing HIV-1 Env (Sheehy et al., 2002). Heterokaryons formed due to the fusion of CD4/CXCR4 receptors present on both nonpermissive and permissive cells. When progeny virions (HIV-1Δ*vif*) were incubated with CEM-SS cells, no spreading infection resulted and HIV-1Δ*vif* replication was inhibited (Madani et al., 1998; Simon et al, 1998; Sheehy et al., 2002). However, when the Vif protein was re-introduced into the virus, spreading infection resulted and the inhibition was relieved. Then using subtractive cloning, cDNA from the permissive (CEM) cell line was subtracted from the nonpermissive (CEM-SS) cell line to identify the cDNA clone *CEM15*. This Vif-sensitive antiviral cytidine deaminase is now known as APOBEC3G (apolipoprotein B mRNA-editing enzyme, catalytic polypeptide-like 3G, or hA3G). To validate its identity, cDNA from hA3G was transfected into permissive cells, and hA3G was sufficient to convert these cells into a permissive state without affecting the number of virions released (Sheehy et al., 2002).

APOBEC Family of Cytidine Deaminases

The APOBEC family of cytidine deaminases in human consists of activation-induced deaminase (AID), APOBEC1, APOBEC2, APOBEC3A-H, and APOBEC4 (Conticello et al., 2005; Jarmuz et al., 2002; OhAinle et al., 2006; Rogozin et al., 2005). These tissue restricted cytidine deaminases exhibit either RNA editing and/or DNA mutating activity by hydrolytic deamination of dC to dU (Harris et al., 2002; Teng et al., 1993). The gene for AID is located on human chromosome 12 and is important for humoral immune and required in activated germinal center B cells during antibody affinity maturation (Muramatsu et al., 2000). AID introduces dC to dU mutations in

single-stranded DNA substrates of specific sequence hotspots on the VDJ region of the immunoglobulin gene (Ig) by initiating somatic hypermutation (Bransteitter et al., 2003; Langlois et al., 2005; Neuberger et al., 2003; Pham et al., 2003). Hypermutation of the Ig gene enhances the affinity with which the antibody binds to and neutralizes antigens. AID also initiates class switch recombination, enabling the expression of various antibody isotypes by deamination events that lead to DNA double-stranded breaks required for the switching of constant regions of the Ig gene (Schrader et al., 2009). Individuals who lack a functional AID suffer from severe recurrent inflammatory and autoimmune disorders, whereas individuals who have abnormal AID function suffer various large B cell lymphomas and non-Hodgkin's lymphomas (Alce et al., 2004; Luo et al., 2004; Revy et al., 2000; Svarovskaia et al., 2004).

APOBEC1 (Apo1) is also located in tandem with AID on human chromosome 12 and is primarily expressed in gastrointestinal tissue with a well-characterized role in lipid metabolism (Powell et al., 1987; Rogozin et al., 2005; Teng et al., 1993). Apo1 is the central component of an RNA editosome complex that deaminates the cytidine-6,666 in apolipoprotein B (apoB) mRNA producing two isoforms of the apoB protein (Powell et al., 1987; Rogozin et al., 2005; Teng et al., 1993). The full-length apoB100 protein mediates the transport of endogenously produced triglycerides and cholesterol in the blood (Powell et al., 1987; Yamanaka et al., 1995), and the truncated apoB48 protein regulates the absorption and transport of exogenous dietary lipids from the intestines to the tissues (Yamanaka et al., 1995). Apo1 is the most extensively studied APOBEC protein and the only APOBEC protein that requires RNA as its substrate. Over

expression of Apo1 in transgenic rabbits and mice led to both liver dysplasia and hepatocellular carcinomas (Yamanaka et al., 1995).

APOBEC2 (Apo2) is located on human chromosome 6 and is expressed specifically in skeletal muscle and heart (Jarmuz et al., 2002; Prochnow et al., 2007). Apo2 has proved to be the most enigmatic APOBEC to characterize given that its enzymatic activity is unrelated to its paralogs (Anant et al., 2001; Harris et al., 2002; Liao et al., 1999; Miki et al., 2005). Similar to Apo2, APOBEC4 (Apo4), which is located on human chromosome 1, is very poorly understood. Apo4 is primarily expressed in the testes, has low sequence similarity to the other AID/APOBEC proteins, and its function is unknown (Rogozin et al., 2005; Conticello et al., 2007). The ancestry of Apo4 reveals possible connections to tRNA-editing enzymes that may provide clues as to the origin of the APOBEC family of cytidine deaminases (Conticello et al., 2007).

APOBEC3 (A3) genes are unique to mammals and were first identified as paralogs to Apo1 (Jarmuz et al., 2002). There are a total of seven *A3* genes in humans, four in felines, six in horse, two to three in artiodactyls, and a single gene in the mouse (Bogerd et al., 2008; Conticello et al., 2005; Conticello et al., 2008; LaRue et al., 2008; Munk et al., 2008). All seven *A3* genes in humans are tandemly arrayed on chromosome 22 and arose through gene duplication of a single-copy primordial gene (Conticello et al., 2008; Jarmuz et al., 2002). These include APOBEC3A (A3A), APOBEC3B (A3B), APOBEC3C (A3C), APOBEC3D (A3D), APOBEC3F (A3F), APOBEC3G (A3G), and APOBEC3H (A3H) (Jarmuz et al., 2002). The *A3* genes in humans demonstrate a high degree of polymorphic variation; for example, *Apobec3H*, which suggests that these genes are under strong selective pressure (Munk et al.,

2008; OhAinle et al., 2006; OhAinle et al., 2008; Sawyer et al., 2004; Takeda et al., 2008; Zhang et al., 2004). The A3 family of cytidine deaminases play an important role in the innate host immune response to inhibit a wide range of retroviruses, retrotransposons, hepadnaviruses, papillomavirus, foamy viruses, and parvoviruses (Abe et al., 2009; Baumert et al., 2007; Bonvin and Greeve, 2007; Bonvin et al., 2006; Chen et al., 2006; Henry et al., 2009; Jarmuz et al., 2002; Köck and Blum et al., 2008; Mahieux et al., 2005; Narvaiza et al., 2009; Noguchi et al., 2007; Paprotka et al., 2010; Sheehy et al., 2002; Strebel et al., 2005; Turelli et al., 2004; Vartanian et al., 2008; Zhang et al., 2008). However, the majority of the research on A3 proteins has been on A3G and A3F, which display the most potent antiviral activity against HIV-1 and SIV.

Structural Characteristics of APOBEC Cytidine Deaminases

All APOBEC cytidine deaminase family members contain a short α-helical domain followed by a catalytic domain (CD), a short linker peptide, and a pseudocatalytic domain (PCD) (Jarmuz et al., 2002). Each catalytic domain is characterized by a highly conserved sequence required for cytidine deamination, C/H-X-E-X_{23-28}-P-C-X_{2-4}-C. The histidine and cysteine residues coordinate Zn^{2+}, while the critical glutamate residue is involved in the proton shuttle (Betts et al., 1994; Iwatani et al., 2006; Jarmuz et al., 2002; Wedekind et al., 2003; Xie et al., 2004). The catalytic domain of A3 proteins undergo the hydrolytic deamination at the C4 position of 2'-deoxycytidine using the conserved amino acids described above. The 2'-deoxycytidine is converted to 2'-deoxyuridine in the presence of water due to the removal of an amine group (Figure 8) (Rada et al., 2002). While there is no high-resolution crystal structure,

several structural studies of the C-terminal cytidine deaminase domain (CDA; residues 198-384) of A3G and the single domain of Apo2 have shown that the CDA core consists of five β strands flanked by α-helices on either side and appropriate connecting loops (Chen et al., 2008; Furukawa et al., 2009; Harjes et al., 2009; Holden et al., 2008; Prochnow et al., 2007; Zhang et al., 2007).

The members of the APOBEC family of cytidine deaminases contain either one or two CDA domains. Apo1, AID, Apo2, A3A, A3C, A3H, and Apo4 contain only one CDA, while A3B, A3D, A3F, and A3G contain two CDAs (Figure 8). The APOBEC proteins containing two CDAs, usually only have one domain that is catalytically active and required for species specificity, while the other CDA is involved in nucleic acid binding/sequence specificity, subcellular localization, and virion incorporation (Bogerd et al., 2007; Hache et al, 2005; Iwatani et al., 2006; Jonsson et al., 2006; Opi et al., 2006; Navarro et al., 2005; Newman et al., 2005). However, A3B is an exception because one report found both CDAs to be catalytically active (Bogerd et al., 2007).

Figure 8. APOBEC family of cytidine deaminases. A) APOBEC family members contain wither one or two CDA domain. The APOBEC proteins are aligned by their catalytically active CDA domain, depicted in purple, or their catalytically inactive CDA domain, depicted in red. The specific APOBEC protein is shown on the left and the consensus sequence is shown at the bottom. B) During deamination the 2'-deoxycytidine is converted 20 2'-deoxyuridine as a result of the removal of an amine group in the presence of water.

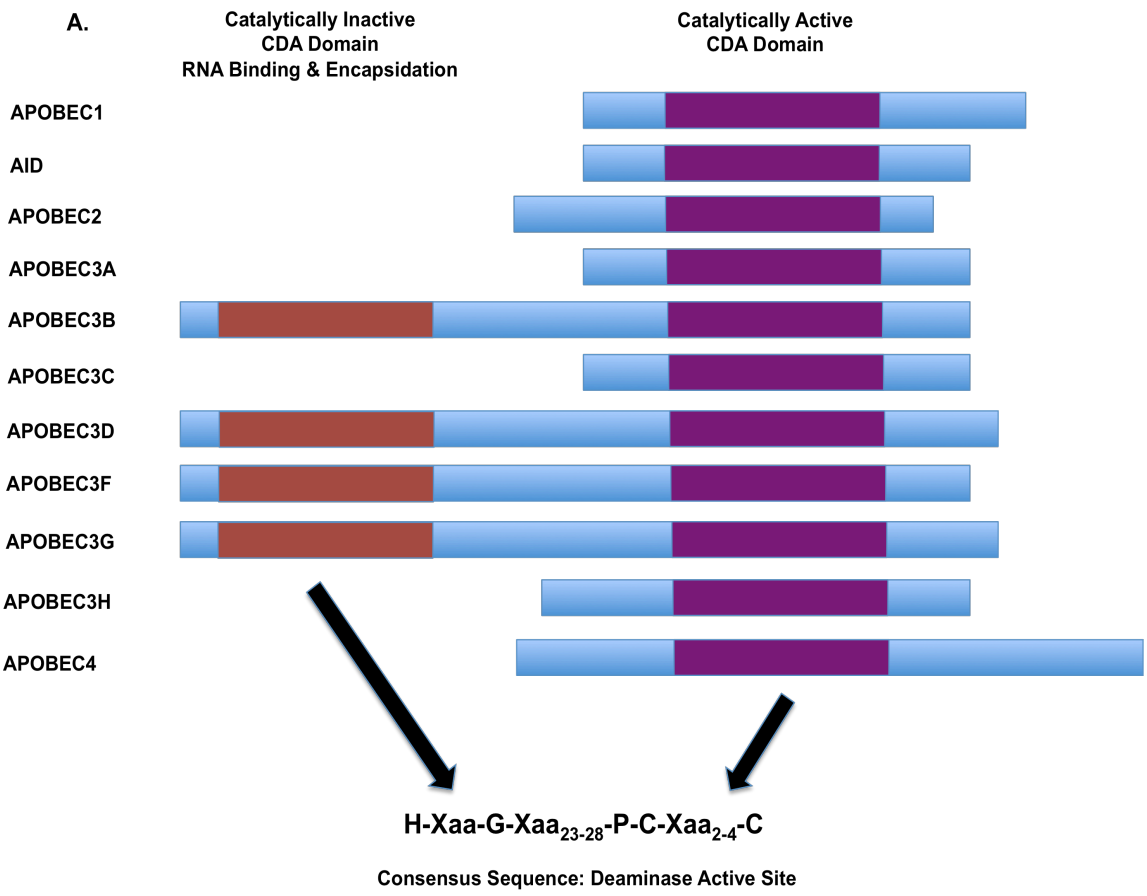
A.
Catalytically Inactive
CDA Domain
RNA Binding & Encapsidation
Catalytically Active
CDA Domain
APOBEC1
AID
APOBEC2
APOBEC3A
APOBEC3B
APOBEC3C
APOBEC3D
APOBEC3F
APOBEC3G
APOBEC3H
APOBEC4
H-Xaa-G-Xaa23-28-P-C-Xaa2-4-C
Consensus Sequence: Deaminase Active Site

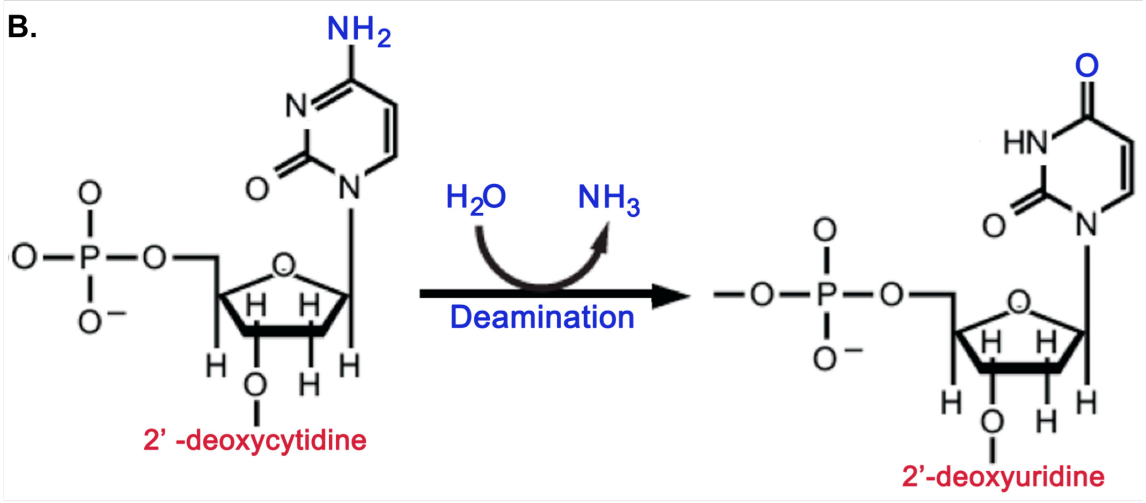
B.
NH2
N
O
N
O
O
P
O
O
O−
O
H
H
H
O
H
H
2' -deoxycytidine
H2O
NH3
Deamination
O
HN
O
N
O
P
O
O
O−
O
H
H
H
O
H
H
2'-deoxyuridine

The N-terminus of double CDA A3 proteins mediate RNA binding, while the C-terminus mediates sequence specific cytidine deamination of single-stranded DNA (Friew et al., 2009; Gooch and Cullen et al., 2008; Hache et al., 2005; Iwatani et al., 2006; Li et al., 2004; Navarro et al., 2005). When mutations are introduced into the N-terminus of A3G (residues 124-127), the RNA-binding properties of A3G are impaired and A3G is no longer incorporated into budding virions (Burnett and Spearman, 2007; Huthoff et al., 2009; Huthoff and Malim, 2007; Navarro et al., 2005). The double CDA A3 proteins are also capable of both homo- and heter-oligomerization, forming higher order multimers in cells that are stabilized by RNA (Bennett et al., 2008; Burnett et al., 2007; Friew et al., 2009; Jarmuz et al., 2002; Navarro et al., 2005). For example, APOBEC3G forms homo-multimers, which do not appear to be essential for its catalytic activity or virion incorporation, but allow A3G to be form multi-protein complexes of high molecular mass (HMM) (Opi et al., 2006).

Since the deamination sequence is organized in a modular fashion at the APOBEC3 locus, the CDA domains are also characterized as either single or double Z-domain proteins (Jarmuz et al., 2002; Liddament et al., 2004). These Z-domains fall into three phylogenetic clusters depending on the conserved amino acid variations within the zinc-binding motif. These clusters are designated as type Z1, Z2, or Z3. This nomenclature is very useful in comparing cross-species and modeling the evolutionary history of the APOBEC family (Conticello et al., 2005; LaRue et al., 2008).

Mechanism of Antiviral Activity by APOBEC3 Proteins

In nonpermissive cells (such as activated PBMC), HIV-1ΔVif effectively incorporates approximately 7 (± 4) molecules of A3G (Xu et al., 2007). The A3G molecules are then effectively introduced into the target cell during the next round of infection and are sufficient to inhibit HIV-1 replication (Soros et al., 2007; Xu et al., 2007). In order for successful incorporation to occur, A3G directly interacts with the N-terminal region of the nucleocapsid protein (NC) of the Gag polyprotein and viral genomic RNA (Luo et al., 2004; Schafer et al., 2004; Svarovskaia et al., 2004; Zennou et al., 2004). Once inside the virion, A3G resides in the viral core, bound to the ribonucleoprotein (RNP) complex containing the viral genomic RNA, NC, integrase (IN), and Vpr proteins (Soros et al., 2007). Recently, a studied showed the importance of amino acids Y124 and W127 of A3G in facilitating RNA binding and lipid raft association. This study also showed that A3G associates with both lipid rafts and the genomic viral RNA to be effectively incorporated into the budding virion (Khan et al., 2009).

Following infection of the target cell, the minus strand of DNA is synthesized, and the RNA template is degraded by RNase H activity of the reverse transcriptase, which exposes the minus strand of DNA making it susceptible to A3G mediated degradation (Suspene et al., 2004; Yu et al., 2004). A3G then binds the single stranded DNA randomly and processively "slides or jumps" for 100 nucleotides before it begins deamination in a predominantly 3' to 5' manner (Chelico et al., 2006). The deamination by A3G produces excessive dC-to-dU substitutions in the minus strand of DNA (Figure 9) (Suspene et al., 2004; Yu et al., 2004). The mutated minus strand of DNA can be destroyed by two DNA base-excision repair enzymes: uracil DNA glycosylase 2 (UDG2)

or apurinic-apyrimidinic endonuclease (Schrofelbauer et al., 2005). For example, the UNG recognizes and excises the cDNA uracils, leaving an abasic site. This abasic site is cleaved by an endonucease such as APEX1, which would cleave the cDNA backbone (Harris et al., 2003a; 2003b; Yang et al., 2007). These processes can lead to either strand breakage and impaired plus strand DNA synthesis or destruction of the minus strand of DNA (Figure 9) (Harris et al., 2003; Lecossier et al., 2003; Mangeat et al., 2003; Zhang et al., 2003). However, further studies are needed to clarify the potential mechanisms by which viral cDNA is processed and degraded following A3G mediated deamination. The few minus strands of DNA that are not degraded are synthesized into plus strand DNA where the dU promotes the misincorporation of dA resulting in G-to-A mutation (Harris et al., 2003; Mangeat et al., 2003; Mariani et al., 2003; Zhang et al., 2003). If these G-to-A substitutions exceed 10% of the dG residues in the viral genome, a phenomenon called hypermutation has occurred (Bishop et al., 2004; Harris et al., 2003; Suspene et al., 2004; Yu et al., 2004). These G-to-A substitutions occur throughout the viral genome and have been shown to produce a gradient from 3' to 5' in the minus strand of DNA (Kahn et al., 2007; Suspene et al., 2006). A gradient of hypermutation occurs depending on the length of time that the minus strand of remains single stranded. This is predominantly from 3' to 5', with the most G-to-A substitutions residing in the Env (envelope) and Nef regions and then decreasing towards the 5' UTR (Kijack et al, 2008; Koulinska et al., 2003; Suspene et al., 2004, Suspene et al., 2006; Yu et al., 2004). Hypermutation can negate HIV-1 infectivity by leading to alteration in the viral open reading frames, the incorporation of termination codons in viral genes, impairments in plus-strand synthesis, and defects in

Figure 9. The antiviral activities of human A3G incorporated into HIV-1Δ*vif* virions. HA3G present in the cytoplasm of cells infected with HIV-1Δ*vif* is readily incorporated into budding virions. Following infection of the next target cell, hA3G is available to exert its antiviral effects on HIV-1 replication. These inhibitory effects on HIV-1 replication can be deaminase-dependent and/or deaminase-independent. 1) HA3G bound to viral RNA can physically impede the reverse transcriptase on the viral RNA template, thus resulting in a decrease in the number of reverse transcripts (deaminase-independent). This form of inhibition is usually incomplete and minus-stranded viral DNA is generated acting as a target for the deaminase-dependent hA3G inhibition. 2) Extensive deamination of the minus-strand of viral DNA occurs halting HIV-1 replication by either an accumulation of dG-to-dA mutations in the subsequently synthesized plus-strand of viral DNA or because the minus-strand of DNA is destroyed by uracil DNA glycosylase (UDG) and apurinic-apyrimidinic endonuclease (deaminase-dependent). 3) Also, defects in the $tRNA^{Lys3}$ primer cleavage can lead to the formation of viral DNA with aberrant ends. This prevents the integration of the double-stranded viral DNA into the chromosome. Figure adapted from Chiu and Greene, 2008.

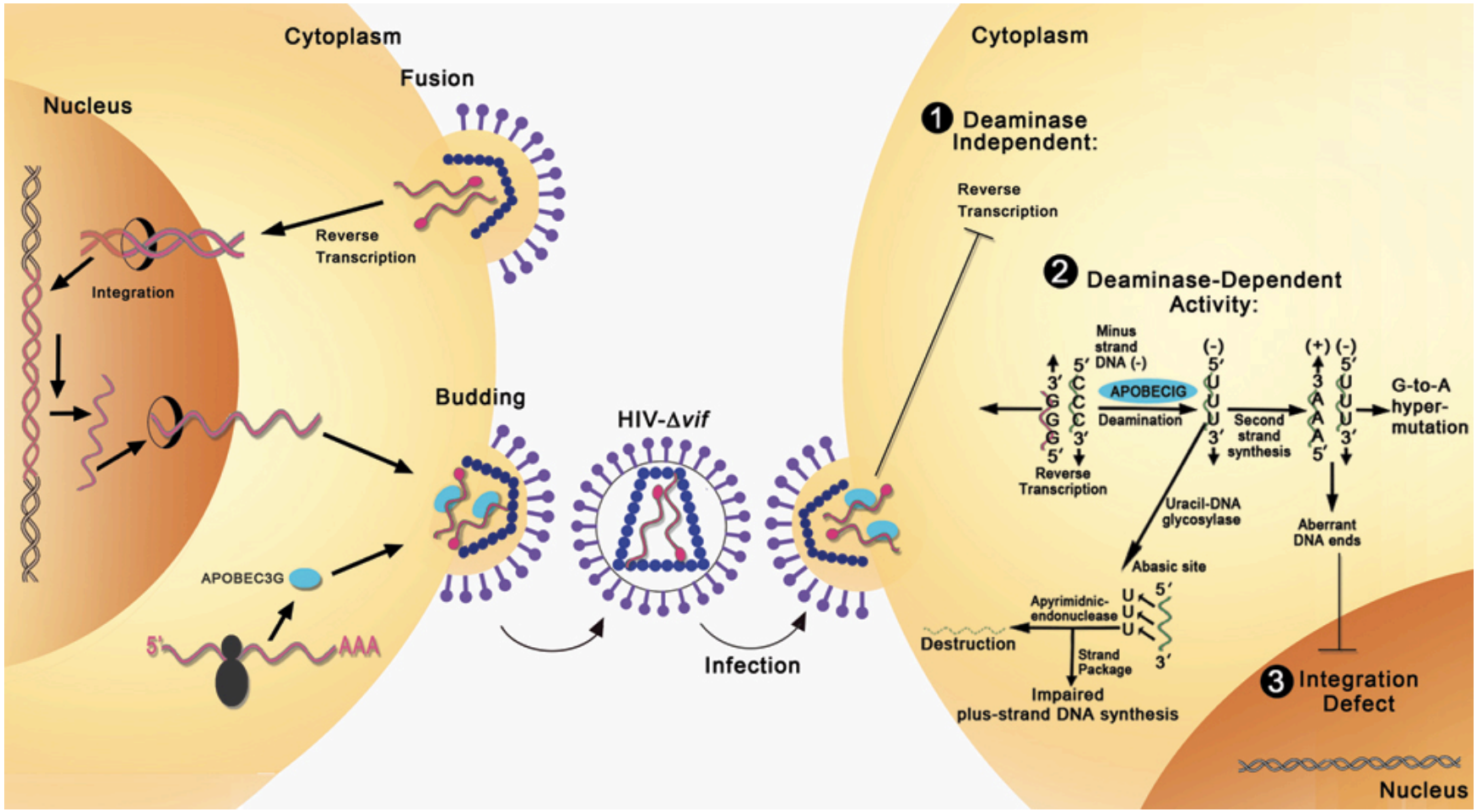
Cytoplasm
Fusion
Nucleus
Reverse
Transcription
Integration
Budding
HIV-Δvif
APOBEC3G
5'
AAA
Infection
Cytoplasm
1 Deaminase
Independent:
Reverse
Transcription
2 Deaminase-Dependent
Activity:
Minus
strand
DNA (-)
APOBECIG
Deamination
Second
strand
synthesis
G-to-A
hyper-
mutation
Reverse
Transcription
Uracil-DNA
glycosylase
Aberrant
DNA ends
Abasic site
Apyrimidnic-
endonuclease
Destruction
Strand
Package
Impaired
plus-strand DNA synthesis
3 Integration
Defect
Nucleus

integration (Figure 9) (Chiu et al., 2008). This editing activity has strong antiretroviral effects and has been shown to block the replication of HIV-1, SIV, EIAV, and murine leukemia virus (MLV) (Delebecque et al., 2006; Harris et al., 2003; Mangeat et al., 2003; Mariani et al., 2003; Russell et al., 2005).

A3 proteins leave a distinct footprint of the sequence context in which they typically mutate minus sense strand viral cDNA. Since multiple A3 proteins are expressed *in vivo*, the sequence context helps assess which viral substrate is required for deamination. For example, A3G preferentially mutates cytidine residues in the context of 5'-CC-3' (minus strand) or 5'-GG-3' (plus strand); whereas other A3 proteins most often mutate thymidine residues resulting in 5'-TC-3' (minus strand) or 5'-GA-3' (plus strand) (Bishop et al., 2004; Harris et al., 2003; Liddament et al., 2004; Mangeat et al., 2003; Wiegand et al., 2004; Yu et al., 2004; Zhang et al., 2003; Zheng et al., 2004). Also, by assessing these sequence contexts one can determine hypermutation hotspots or determine how hypermutation can be lethal to the virus. For example, in the presence of A3G, a UGG codon encodes for a tryptophan and may be susceptible to the creation of either a UAG or even a UAA stop codon (Watts et al., 2009). Depending on the base pair next in the sequence, an AUG start codon could be replaced with a wobble base ablating the initiating methionines required for protein translation. This extensive mutation also has the ability to disrupt HIV-1 secondary RNA structures that are essential for the regulation of gene expression (Watts et al., 2009).

It is important to note that a high frequency of G-to-A mutations were evident in HIV-1 sequences from patients before the discovery of A3 proteins (Janini et al., 2001; Vartanian et al., 1991; Vartanian et al., 1994). These early studies showed that the

preferential sequence of the mutations for HIV-1 infected patients were in the context of 5'-GA-3' (plus strand) and to a lesser extent 5'-GG-3' (plus strand) (Liddament et al., 2004). However, it remains unknown which A3 protein is responsible for these reported mutations (Gandhi et al., 2008; Ulenga et al., 2008). So far, hypermutation does not appear to correlate with viral loads based off a cohort study of Senegalese female sex workers. However, this study did find that the level of hypermutation is directly correlated to level of A3G mRNA expression. This study found that patients with a lower viral set point have significantly higher levels of A3G mRNA (Ulenga et al., 2008). However, there is conflicting data on this topic. Another study involving 28 Kenyan women showed no correlation between hypermutation and viral load or CD4+ T cell counts (Piantadosi et al., 2009). Further studies are needed with larger cohorts to correlate indicators with both hypermutation and the expression of A3 proteins. Since hypermutation is common *in vivo*, A3 proteins through hypermutation may be aiding in the evolution of HIV-1 drug-resistance (Berkhout et al., 2004; Haché et al., 2006; Pillai et al., 2008). However, the data to support this topic is limited.

Even though the antiviral activity of A3 proteins mainly relies on the cytidine deaminase activity, A3 proteins have also been shown to wield antiviral activity independent of cytidine deamination. When mutations in the catalytic domain of A3G are introduced, deaminase activity is prevented but the mutants continue to exert antiviral activity against HIV-1 by reducing infectivity and the amount of HIV-1 cDNA produced in the target cell (Navarro et al., 2005; Newman et al., 2005). A3G has deaminase-independent functions that interfere with primer tRNA annealing, primer tRNA progression, minus- and plus- strand transfer, and DNA elongation (Anderson and

Hope, 2008; Bishop et al., 2006; Guo et al., 2006; 2007; 2009; Holmes et al., 2007; Iwatani et al., 2007; Li et al., 2007; Luo et al., 2007; Mangeat et al., 2003; Mariani et al., 2003; Mbisa et al., 2007). A3G contained a docking site for the C-terminus of HIV-1 integrase, which interferes with the preintegration complex (PIC) structure. This inhibits the nuclear import of the PIC complex and impairs the integration of proviral DNA (Luo et al., 2007).

A3 proteins have also been implicated in using deaminase independent functions to inhibit the replication of in retroviruses such as human T cell leukemia virus type-1 (HTLV-1), hepatitis B virus (HBV), papillomaviruses and parvoviruses (Abe et al., 2009; Baumert et al., 2007; Bonvin and Greeve, 2007; Bonvin et al., 2006; Chen et al., 2006; Henry et al., 2009; Jarmuz et al., 2002; Köck and Blum, 2008; Mahieux et al., 2005; Narvaiza et al., 2009; Noguchi et al., 2007; Paprotka et al., 2010; Rosler et al., 2004; Sasada et al., 2005; Sheehy et al., 2002; Turelli et al., 2004; Vartanian et al., 2008; Zhang et al., 2008). For example, human A3G is incorporated into HTLV-1 virions and exerts an antiviral effect. No hypermutation is observed and it appears that A3G interferes with virus maturation through a deaminase-independent mechanism (Sasada et al., 2005). HBV contains a reverse transcriptase that is required for the pregenomic RNA intermediates in the cytoplasm of cells producing virus. Human A3G inhibits HBV through a deaminase-independent mechanism during the early steps of viral reverse transcription and strand elongation inhibiting viral pregenome packaging (Nguyen et al., 2007; Rosler et al., 2004; Turelli et al., 2004; Zhang et al., 2008). Human A3A inhibits the replication of parvovirus adeno-associated virus (AAV) and the autonomous parvovirus minute virus of mice (MVM) (Narvaiza et al., 2009). Both AAV and MVM are

single-stranded DNA viruses that do not contain a reverse transcriptase or any RNA substrates. However, hA3A inhibits the replication of both these viruses through a direct interaction with viral DNA or the replication machinery. Mutants that lack deaminase activity still retain the ability to inhibit these viruses through deaminase-independent functions (Chen et al., 2006; Narvaiza et al., 2009). Also, in the absence of hypermutation, A3A displays inhibitory activity against LINE-1 (long-interspersed nuclear element-1) and other retroelements (Bogerd et al., 2006a, 2006b; Hulme et al., 2007; Niewiadomska et al., 2007; Muckenfuss et al., 2006).

Antiviral Activity of the APOBEC3 Family of Cytidine Deaminases

In general, the evidence indicates that among activated Th1 $CD4^+$ T cells, the expression of A3G and A3F are increased (Vetter et al., 2009). This increase in expression results in an increase of A3G/F incorporation into virions and an overall lower infectivity of target cells (Koning et al., 2009). This was found in most A3 proteins with the exception of A3A and to a lesser extent A3B in primary $CD4^+$ T cells (Koning et al., 2009). IFN-α and to a lesser extent IFN-γ treatment also result in a higher expression of A3 proteins and an increased resistance to HIV-1 infection (Peng et al., 2007). IFN-α has been found to increase the expression of A3 proteins and to a greater extent A3A in macrophages. However A3B and A3C are possible exceptions to increased expression by IFN-α because they are part of the normal IFN response (Koning et al., 2009). Immature dendritic cells are resistant to HIV-1 infection due to an increased expression in A3G and A3F; however, as dendritic cells mature, the high

expression levels of these proteins are reduced (Pion et al., 2006). More work is still needed focusing on the expression of various A3 proteins by IFN.

APOBEC3G has been extensively described above; therefore, this section will mainly focus on the other six members (A3A, A3B, A3B, A3D, A3F, and A3H) of the A3 subfamily of single-stranded DNA cytidine deaminases. Compiled data regarding the inhibition of HIV-1, $SIV_{mac}239$, LTR retroelements, non-LTR retroelements, hepatitis B virus, or adeno-associated virus by various human A3 proteins is listed in Table I and Table II, respectively. Of these A3 proteins, hA3B, hA3D, hA3G, and hA3F, have been shown to inhibit the replication of HIV-1Δ*vif*, while hA3B, hA3C, hA3D, hA3G, and hA3F, have been shown to restrict $SIV_{mac}239$Δ*vif* (Dang et al., 2006; 2008; Doehle et al., 2005; Mariani et al., 2003; Wiegand et al., 2004; Yang et al., 2007; Yu et al., 2004a; 2004b; Zennou and Bieniasz, 2006; Zheng et al., 2004). Currently, more is becoming known about the rhesus A3 proteins. It is known that HIV-1Δ*vif* can be inhibited by rhA3G, rhA3F, rhA3B, and to a lesser extent rhA3H and rhA3D, while $SIV_{mac}239$Δ*vif* has been shown to be restricted by rhA3B, rhA3D, rhA3F, rhA3G, and rhA3H (Virgen and Haziioannou, 2007; Zennou and Bieniasz, 2006).

APOBEC3A

Human APOBEC3A (hA3A) is expressed in the keratinocytes, spleen, small intestine, PBLs (neutrophils, primary monocytes such as macrophages and dendritic cells), bone marrow, and lungs (Refsland et al., 2010; Thielen et al., 2010). A3A is localized in both the cytoplasm and the nucleus and contains a single cytidine deaminase catalytic domain (Table I) (Goila-Gaur et al., 2007; Hultquist et al., 2011).

This A3 protein does not have antiviral activity against either HIV-1 or HIV-1Δ*vif* (Bogerd et al., 2006; Goila-Gaur et al., 2007). When A3A is knocked down in monocytes, the susceptibility of the monocytes to HIV-1 infection increases and the spread of R5-tropic HIV-1 viruses are augmented (Berger et al., 2011; Peng et al., 2007). It is thought that this antiviral effect occurs because a large pool of hA3A exists in the target cells, that decreases the viral DNA accumulation (Berger et al., 2011). A3A is packaged into virions even in the presence of a functional Vif but does not associate with the viral nucleoprotein complex (NPC). However, when constructed into a chimeric protein with A3G, where the N-terminus of A3G was fused to A3A, the A3G-A3A chimera was packaged into the HIV-1Δ*vif* virions by associating with the viral NPC, displayed cytoplasmic localization similar to A3G, and restored its inhibitory effects on HIV-1Δ*vif* (Goila-Gaur et al., 2007). The target specificity sequence for hA3A has been identified as 5'-TC (minus strand) (Bulliard et al., 2011; Thielen et al., 2010). Overexpression of A3A *in vitro* results in increased dC-to-dU (minus strand) mutations in the human papillomavirus (HPV) genome; however it is still unknown as to whether hA3A displays deaminase-dependent restriction against hepatitis B virus (HBV) (Vartanian et al., 2008).

Another important feature of hA3A is its ability to restrict foreign DNA, which can enter cells through multiple exogenous sources. Recent research shows that the detection of foreign DNA and upregulation of IFN-α in phagocytes results in the degradation of foreign DNA by hA3A through cytidine deamination and a uracil-excision mechanism (Stenglein et al., 2010). While monocyte and *in vitro* cell culture genomic

DNA is unaffected, approximately 97% of cytidines in detected foreign DNA are deaminated (Stenglein et al., 2010).

A3A can block endogenous LTR-retrotransposons such as IAP and MusD as well as non-LTR retroelements such as L1 and *Alu* (Table II) (Bogerd et al., 2006; Chen et al., 2006). In A3A expressing cells, adeno-associated virus (AAV) producer cell replicating genomes are inhibited (Chen et al., 2006). Twelve residues (amino acids H29, K30, N57, K60, R69, F75, W98, R128, Y130, D131, E217, and P247) have been identified at the core of A3A antiviral activity and are involved in the restriction of LINE-1, AAV, and gene expression from foreign plasmid DNA. It is thought that these residues are responsible for forming the polynucleotide-accommodating groove of hA3A. If these residues are mutated the inhibition of LINE-1, AAV, and the restriction of foreign DNA is prevented by deaminase-independent mechanisms (Bulliard et al., 2011; Chen et al., 2006; Madsen et al., 1999; Melo et al., 1998; Moran et al., 1996). These mutants defective in editing lead to the accumulation of LINE-1 reverse transcripts, increasing level of viral replicative intermediates, and the expression of genes on foreign DNA (Bulliard et al., 2011; Chen et al., 2006).

Viral protein X (Vpx) has been shown to bind hA3A (Berger et al., 2010). Vpx is uniquely encoded in human immunodeficiency virus type 2 (HIV-2) and simian immunodeficiency virus (SIV_{mac}/SIV_{sm}) (Horton et al., 1994; Wolfrum et al., 2007). This protein is crucial for *in vitro* infection of human macrophages and dendritic cells, but dispensable for infection of primary lymphocytes and laboratory cell lines (Cheng et al., 2008; Fletcher et al., 1996; Sharova et al., 2008; Wolfrum et al., 2007). SIV_{mac} Vpx has been shown to partially bind and degrade hA3A during the early stages of infection

promoting the replication of SIV_{mac}. If a single-point mutation in Vpx at the histidine in amino acid position 82 is substituted for an alanine, Vpx is no longer able to bind and suppress hA3A abrogating the infection of monocytes (Berger et al., 2010; Berger et al., 2011). Another study fused viral protein R (Vpr) to hA3A to convert hA3A into an inhibitor of viral replication. The Vpr protein of HIV-1 is needed to cause cell cycle arrest at the G2-to-M transition phase and to import the preintegration complexes (PIC) into the nucleus of cells (He et al., 1995; Jowett et al., 1995; Re et al., 1995; Rogel et al., 1995). The constructed fusion protein, Vpr.A3A chimera, was readily incorporated into the viral core and potently restricted both HIV-1 and SIVmac in the presence of Vif (Aguiar et al., 2008).

APOBEC3B

Human APOBEC3B (hA3B) is expressed in the peripheral blood leukocytes, bone marrow, lung, and stem cells (Refsland et al., 2010). A3B is not Vif sensitive and inhibits both HIV-1 and $SIV_{mac}239$ in the presence of Vif, Table I (Bishop et al., 2004; Doehle et al., 2005; Yu et al., 2004). A3B contains two CDAs, as described above. Proteins that contain at double CDA display a separation of function between the domains. For example, the N-terminal CDA is responsible for viral-RNA binding and is required for encapsidation, while the C-terminal CDA determines DNA deaminase activity and substrate specificity (Bishop et al., 2004; Haché et al., 2005; Iwatani et al.,

Table I. Summary of both the expression and restriction profile by human APOBEC3 Proteins. All references for this table are listed in the text.

Human	Expression Profile	Subcellular Localization	HIV-1	HIV-1 ΔVif	SIVmac	SIVmac ΔVif
APOBEC3A	Keratinocytes, spleen, small intestine, PBLs, bone marrow, lung	Cytoplasm & Nucleus	No	No	No	Yes
APOBEC3B	Keratinocytes, colon, small intestine, testis, ovaries, stem cells, PBLs, bone marrow, lung	Nuclear	Yes	Yes	Yes	Yes
APOBEC3C	PBLs, thymus, spleen, lymph node, testis, ovary, small intestine, colon, liver, pancreas, heat, lung, adipose tissue	Cytoplasm & Nucleus	No	Weak	No	Yes
APOBEC3D	PBLs, thymus, spleen, lymph node, ovary, liver, lung, adipose	Cytoplasm & Nucleus	No	Yes	No	Yes
APOBEC3F	PBLs, thymus, spleen, lymph node, testis, ovary, uterus, brain, lung, colon, liver, kidney, pancreas	Cytoplasm	No	Yes	No	Yes
APOBE3G	PBLs, thymus, spleen, lymph node, testis, ovary, uterus, brain, lung, small intestine, colon, liver, kidney, pancreas	Cytoplasm	No	Yes	No	Yes
APOBEC3H	PBLs, thymus, testis, ovary, brain, small intestine, colon, keratinocytes	Cytoplasm & Nucleus	No	Select Variants	No	No

Table II. Summary of the restriction profile of LTR retorelements, non-LTR retroelements, and other viruses by human APOBEC3 Proteins. All references used in this table can be found in the text.

Human	IAP	MusD	Ty1	L1	*Alu*	HBV	AAV	HPV
APOBEC3A	Yes	Yes	?	Yes	Yes	?	Yes	Yes
APOBEC3B	Yes	Yes	?	Yes	Yes	Moderate	No	Yes
APOBEC3C	Yes	Yes	Yes	Moderate	Moderate	Yes	No	Yes
APOBEC3D	?	?	?	No	?	?	?	?
APOBEC3F	Yes	Yes	Yes	Yes	?	Yes	No	Yes
APOBE3G	Yes	Yes	Yes	No	Yes	Yes	No	Yes
APOBEC3H	?	?	?	Yes, only stably expressed HapII	Yes, only stably expressed HapII	Yes, only stably expressed HapII	?	Yes, only stably expressed HapII

2006; Liddament et al., 2004; Navarro et al., 2005; Newman et al., 2005; Wiegand et al., 2004). However, the C-terminal CDA of A3B is catalytically dominant and determines sequence specificity (5'-TC, minus strand), but the N-terminal CDA also elicits deaminase activity that is capable of mutating the viral genome (Bogerd et al., 2008). Human A3B has also been found to inihibit both LTR and non-LTR retroelements (Table II) (Boderg et al., 2006; Chen et al., 2006; Esnault et al., 2005; Musckenfuss et al., 2006; Stenglein et al., 2006). Mouse LTR retrotransposons, IAP and MusD elements are strongly inhibited by hA3B (Bogerd et al., 2006; Chen et al., 2006; Esnault et al., 2005). Secondly, hA3B strongly inhibits non-LTR retorelements such as LI and Alu (Bogerd et al., 2006; Chen et al., 2006; Muckenfuss et al., 2006; Stenglein et al., 2006). Using CDA mutants that lack deaminase activity, A3B still effectively inhibits L1 retrotransposition by approximently 75% (Wissing et al., 2011). This may occur due to a highly homologous region in the CDA that directly interacts with L1 ORF2 (Turelli et al., 2004). A3B is predominantly localized to the nucleus, and in overexpression experiments performed in HeLa cells the nuclear localization of A3B is not essential for A3B to inhibit L1 retrotransposition (Hultquist et al., 2011; Pak et al., 2011). Finally, in cotransfected hepatoma cell lines, hA3B used deaminase-independent functions to interfere with the replication of HBV (Okeoma et al., 2007). This is due to hA3B having two splice variants in the human liver, which are both expressed, but only the longer variant is capable to inhibit HBV (Bonvin et al., 2006).

Interestingly, a small ~4-kb deletion in A3B is found in some patients with breast cancer (Komatsu et al., 2008). Also, some patients display homozygous deletions of A3B, which can be associated with malignant tissues (Iskow et al., 2010). There is also a common deletion polymorphism in the Oceanic population where 29.5 kb of genomic sequence spanning from the fifth exon of A3A to the eighth exon of A3B. While A3B is deleted, A3A is produced and is a functional-full length A3A fusion protein with the 3'UTR of A3B (Kidd et al., 2007). At this time, it is unknown if this fusion protein is functional, restricts L1 retrotransposition, or what the potential role of this protein could be.

APOBEC3C

Human APOBEC3C (hA3C) is insensitive to IFN and expressed in the PBLs, thymus, spleen, lymph node, testis, ovary, small intestine, colon, liver, pancreas, heart, lung, and adipose tissue (Table I) (Refsland et al., 2010). A3C contains one CDA and is localized to both the cytoplasm and the nucleus (Hultquist et al., 2011). In contrast to A3B, the deaminase activity of A3C is poorly active against its sequence specific target, 5'-TC (minus strand), and requires dimerization to exert its antiviral effect (Stauch et al., 2009; Yu et al., 2004). This A3 protein has potent antiviral activity against $SIV_{mac}239$ and to a much lesser extent HIV-1Δ*vif* (Yu et al., 2004) (Table I). Even though A3C is efficiently incorporated into the virions of these viruses, very few G-to-A (plus strand) mutations result (Yu et al., 2004). If the N-terminal region (amino acid residues 2-47, before the CDA) of hA3C is deleted, than hA3C is insensitive to HIV-1 or SIVagm (African green monkey) Vif (Zhang et al., 2008). This indicates that this region contains

an important determinant required for Vif-induced degradation. When residue E106, located after the CDA, is mutated, hA3C is no longer sensitive to HIV-1 Vif (Smith et al., 2010). Also, the amino acid residue E289 in hA3C has been shown to be critical for HIV-1 Vif mediated degradation (Smith et al., 2010).

When hA3C is overexpressed *in vitro* cell culture, hA3C mildly inhibits Non-LTR Retroelements such as L1 and Alu (Bogerd et al., 2006; Muckenfuss et al., 2006; Stenglein et al., 2006). In contrast, hA3C effectively inhibits LTR retroelements such as IAP and MusD (Bogerd et al., 2006; Chen et al., 2006; Esnault et al., 2005) (Table II). In tissue culture, hA3C overexpression can reduce herpes simplex virus 1 (HSV-1) and Epstein-Barr herpesvirus (EBV) viral titers, decrease the particle/plaque forming unit ratio by approximately 10-fold, and hypermutate genomes (Suspène et al., 2011a). Human A3C has also been shown to mutate transfected human papillomavirus (HPV) and edit mitochondrial DNA (mtDNA) (Suspène et al., 2011b; Vartanian et al., 2008). Excessive hypermutation of the hepatitis B virus (HBV) genome has also been reported (Baumert et al., 2007; Köck et al., 2008).

APOBEC3D

Human APOBEC3D (hA3D; formally known as APOBEC3DE) is expressed in the PBLs, thymus, spleen, lymph node, ovary, liver, lung, adipose tissue, and more extensively than hA3F in nonpermissive cells (Dang et al., 2006; Refsland et al., 2010). This A3 protein is localized similar to A3C in both the cytoplasm and nucleus but contains two CDAs (Hultquist et al., 2011). HA3D inhibits the replication of both HIV-1Δ*vif* and SIVmac239Δ*vif* (Table I) (Dang et al., 2006). This A3 protein is efficiently

incorporated into virions in the absence of Vif, which resulted in excessive G-to-A hypermutation. A3D introduces 5'-CC, 5'-TC, and 5'-GC (minus strand shown) mutations into newly synthesized viral minus-strand DNA (Dang et al., 2006). Using a GST-hA3D pull down assay in cells expressed with hA3G and hA3F, hA3D formed heteromultimers with both A3G and A3F which may enhance the antiretroviral effect (Dang et al., 2006; Wiegand et al., 2004). Very little is known about the inhibition of hA3D on other viruses, LTR retrotransposons, or non-LTR retrotransposons. Therefore, more studies are needed to determine the extent to which hA3D exerts its antiviral activities.

APOBEC3F

Human APOBEC3F (hA3F) is expressed in the PBLs, thymus, spleen, lymph node, testis, ovary, uterus, brain, lung, colon, kidney, and pancreas (Refsland et al., 2010). The cellular localization of hA3F is cytoplasmic (Table I) (Hultquist et al., 2011). HA3F is the second most potent inhibitor of HIV-1Δ*vif*, but is produced at lower levels in natural target cells of HIV-1, is partially resistant to Vif, and is less potent than hA3G (Koning et al., 2009; Liddament et al., 2004; Simon et al., 2005; Xu et al., 2004; Wiegand et al., 2004; Zennou and Bieniasz, 2006). Mutations in binding domain of Vif that prevent interaction with hA3G increase the sensitivity of Vif to hA3F (Russell et al., 2009). This protein has two catalytically active cytidine deaminase domains; however, unlike A3G, the deaminase activity in the C-terminal CDA is not required for inhibition of HIV-1Δ*vif*. Catalytically inactive mutants of A3F are just as potent inhibitors of viral infectivity causing reductions in the accumulation of viral reverse transcripts (Holmes et

al., 2007). Therefore, A3F-mediated inhibition of HIV-1Δ*vif* infectivity primarily occurs through a deaminase-independent mechanism (Holmes et al., 2007).

A3F has been isolated from purified HBV capsids and can inhibit the replication of HBV in the absence of hypermutation (Noguchi et al., 2005; Rosler et al., 2005; Suspene et al., 2005; Wiegand et al., 2004). However, using 3D-PCR, G-to-A hypermutated HBV genomes (context 5'-TC, minus strand) have been found in the serum of patients with chronic HBV at low frequencies (Haché et al., 2005; Suspene et al., 2005). Furthermore, A3F has been shown to inhibit both LTR retroelements such as IAP, MusD, and Ty1 (Boderd et al., 2006; Chen et al., 2006; Dutko et al., 2005; Schumacher et al., 2005). This A3 protein is also a potent inhibitor of L1 retrotransposition in the absence of hypermutation (Table II) (Muckenfuss et al., 2006; Stenglein et al., 2006).

APOBEC3H

Human APOBEC3H (hA3H) is expressed in the PBLs, thymus, testis, ovary, brain, small intestine, colon, and keratinocytes (Table I) (Refsland et al., 2010). This A3 protein has cytonuclear localization and is poorly expressed *in vivo* (Doehle et al., 2005; Hultquist et al., 2011; Kidd et al., 2007). A3H contains one cytidine deaminase catalytic domain (CDA); therefore, A3H lacks the second CDA that mediates RNA binding, homodimerization, and virion incorporation (Gooch et al., 2008; Navarro et al., 2005). However, the CDA of hA3H can inihibit the replication of both non-LTR retrotransposons such as L1 and *Alu* (Holmes et al., 2007; OhAinle et al., 2008). Interestingly, hA3H has been reported to hypermutate the genomes of both HBV and HPV (Table II) (Lecossier

et al., 2003). Thus far, h*A3H* is composed of five single nucleotide polymorphisms (SNP) (amino acid residues N15Δ, R18L, G105R, K121D, and E178D) and seven haplotypes (I-VII) (Harari et al., 2008; Wang et al., 2011). These various SNP mutations are readily found as variations in the different haplotypes. *A3H* mRNA can be detected; however, the protein expression of A3H has not been observed (Li et al., 2010; OhAinle et al., 2006). The reason for an absence of protein expression can be explained by a premature termination codon (PTC) in the fifth exon of the human *A3H* gene. If the PTC is repaired, high levels of hA3H protein are observed in cell culture (Dang et al., 2008). When the N15Δ or G105R mutations are present, there is a dramatic decrease in the expression of *A3H* (OhAinle et al., 2008). Only haplotype II (hapII) of hA3H, which does not have the N15Δ and/or G105R mutations, can be stably expressed. Hap II was originally identified as being the most common haplotype among the African-American population (OhAinle et al., 2008). More recently, Hap V was detected frequently in African-American, Caribbean, and Chinese populations whereas Hap VII was identified in only Euorpean Caucasian populations (Wang et al., 2011). Both hap V and hap VII have been shown to incorporate into HIV-1 virions using the ^{112}YYXW^{115} motif instead of the CDA like various other A3 proteins such as hA3G. Also, both of these haplotypes inhibit HIV-1 replication. However, it appears that all the various haplotypes of human A3H are resistant to HIV-1 Vif; therefore, further research needs to be conducted to determine the antiviral activites of hA3H on HIV-1 replciation (Wang et al., 2011).

Humans, chimpanzees, and the rhesus macaque (*Macaca mulatta*) have undergone extensive positive selection and locus expansion, but appear to share similar locus architectures. While the A3 proteins in humans have been excessively studied,

less is known about the A3 proteins in the rhesus macaque (*macaca mulata*). Rhesus A3B, C, D, F, G, and H have been identified, while rhA3A has yet to be identified (Hultquist et al., 2011; Virgen et al., 2007). RhA3D, rhA3F rhA3G, and rhA3H all contribute to the antiviral restriction of HIV-1Δ*vif* and are targeted for degradation by SIVmac239 (Hultquist et al., 2011, Virgen et al., 2007; Zennou and Bieniasz, 2006). These homologous A3 proteins of both human and the rhesus macaque have comparable steady-state localization as well as both HIV-1 and SIV_{mac} restriction abilities such as hypermutation in the absence of Vif (Hultquist et al., 2011; Virgen et al., 2007). However, futher studies will be needed to identify rhA3A, assess the expression patterns of these proteins *in vivo*, and determine their significance in the rhesus macaque.

Vif-APOBEC3 Paradigm

Vif reduces the encapsidation of A3G into virions by 99% either directly inhibiting the incorporation of A3G or more importantly by depleting the cellular stores of A3G (Kao et al., 2003; Mariani et al., 2003; Marin et al., 2003; Mehle et al., 2004; Sheehy et al., 2003; Stopak et al., 2003). This ensures that the progeny virions will be highly infectious. Vif uses multiple protein-protein interactions to ensure that the antiviral effects of A3G are inhibited. The N-terminus of Vif is required for interaction with genomic RNA and to bind/interact with various regions of the A3 proteins, which will be discussed in detail below, while the C-terminus of Vif is essential to recruiting an active E3-ubiquitin ligase complex.

Sequence analysis from different lentiviral Vif proteins display several highly conserved domains in the C-terminus of Vif that are required for the assembly of the Vif-CBF-β-Cullin 5/Elongin B/Elongin C/ Nedd8/Ring box-1 E3 ubiquitin ligase complex. Vif accomplishes this by binding A3 and then a substrate recognition subunit of the Cul5/EloB/C complex targeting A3 for polyubiquitination and subsequent degradation by the 26S proteosome (Figures 10 and 11**)** (Conticello et al., 2003; Jäger et al., 2011; Marin et al., 2003; Sheehy et al., 2003; Stopak et al., 2003; Yu et al., 2003; Yu et al., 2004). These domains in HIV-1 Vif are the ^{108}HCCH^{139} motif, ^{144}SLQ(Y/F)LA^{150} domain, E^{88}WRRKK^{93} and the P^{161}PLP^{164} domain.

The highly conserved zinc binding domain of HIV-1 Vif is referred to as the HCCH domain and is located between amino acid residues (108-139) (Figure 12). The ^{108}H-X_5-C—X_{17-18}-C-X_{3-5}-H^{139} domain is indispensable for Vif function and thought to maintain a structural conformation of Histines and cysteines flanked by hydrophobic residues that coordinate zinc to form the Cul 5 binding site (Luo et al., 2005; Mehle et al., 2006; Xiao et al., 2006; Xiao et al., 2007). Zinc binding to the HCCH motif is both specific and reversible producing conformational changes leading to protein aggregate formation (Paul et al., 2006). These high order protein assemblies alter protein conformation to expose possible protein-protein interaction sites (Giri and Maynard, 2009; Paul et al., 2006). Upon further investigation using fluorescence and CD spectroscopy, the binding of the HCCH domain to zinc confirmed that zinc binding increases tertiary packing supporting the theory that zinc binding and protein conformation are coupled tightly (34). Chelation of zinc by cell-permeable *N, N, N′, N′*-tetrakis-(2-pyridylmethyl)ethylenediamine (TPEN) results in the loss of Vif function

Figure 10. Proteosomal degradation of human A3G by HIV-1 Vif. 1) HIV-1 Vif binds to hA3G and recruits the E3 ubiquitin ligase complex leading to the ubiquitination and subsequent proteosomal degradation of hA3G. 2) HIV-1 Vif can impair the translation of hA3G mRNA. 3) HIV-1 Vif can physically bind hA3G excluding it from the virion and sequestering hA3G away from the sites of viral assembly. Figure adapted from Chiu and Greene, 2008.

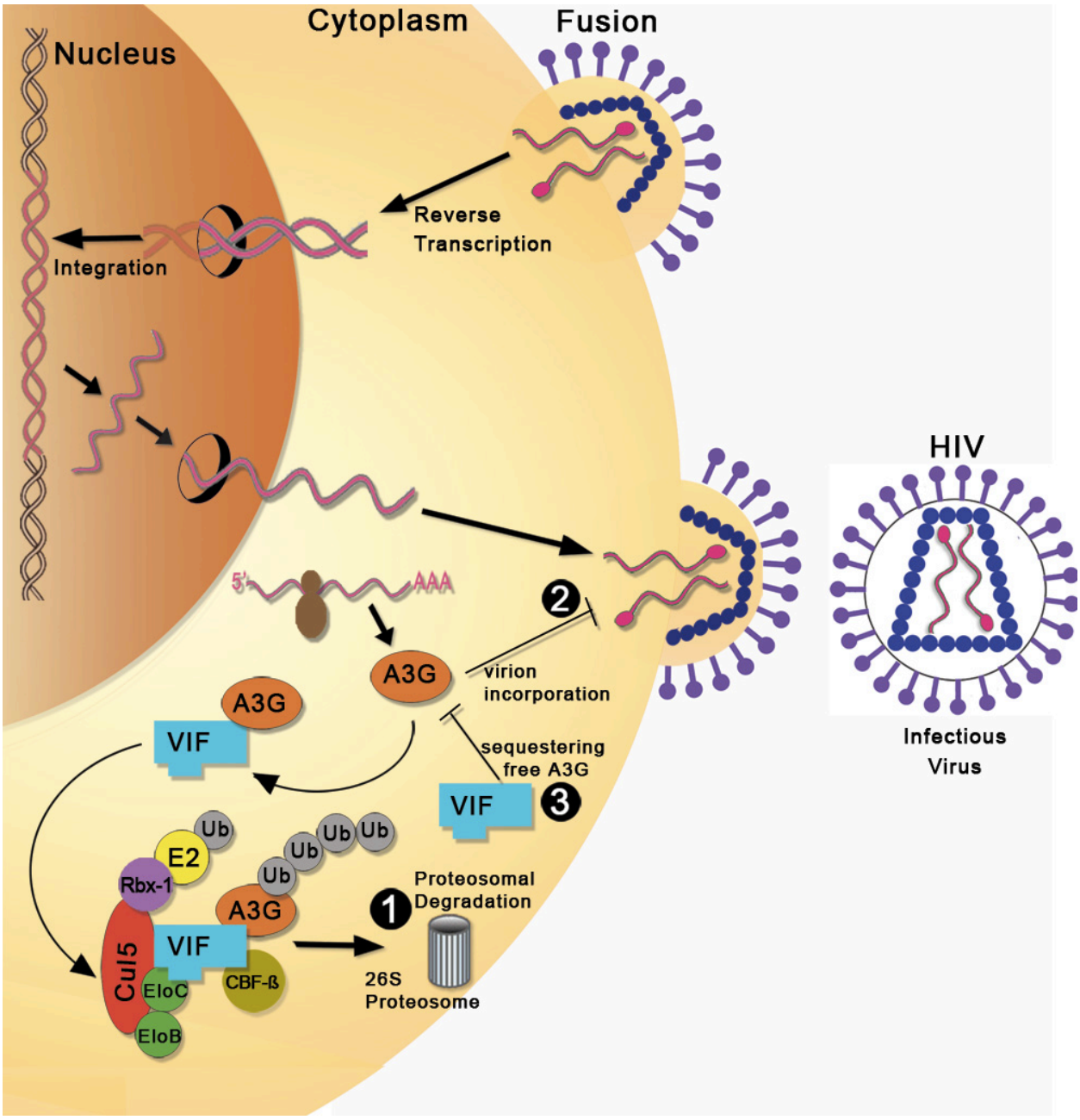
Cytoplasm
Fusion
Nucleus
Reverse
Transcription
Integration
HIV
5'
AAA
2
A3G
virion
incorporation
A3G
VIF
sequestering
free A3G
VIF
3
Infectious
Virus
Ub
E2
Rbx-1
Ub
Ub
Ub
Ub
A3G
1
Proteosomal
Degradation
Cul5
VIF
EloC
CBF-ß
EloB
26S
Proteosome

Figure 11. Vif induced polyubiquitination of A3G through the recruitment of the CBF-β-Cul5-EloB/C-Rbx 1 E3 ubiquitin ligase complex and the specific amino acid motifs that mediate protein-protein interactions.

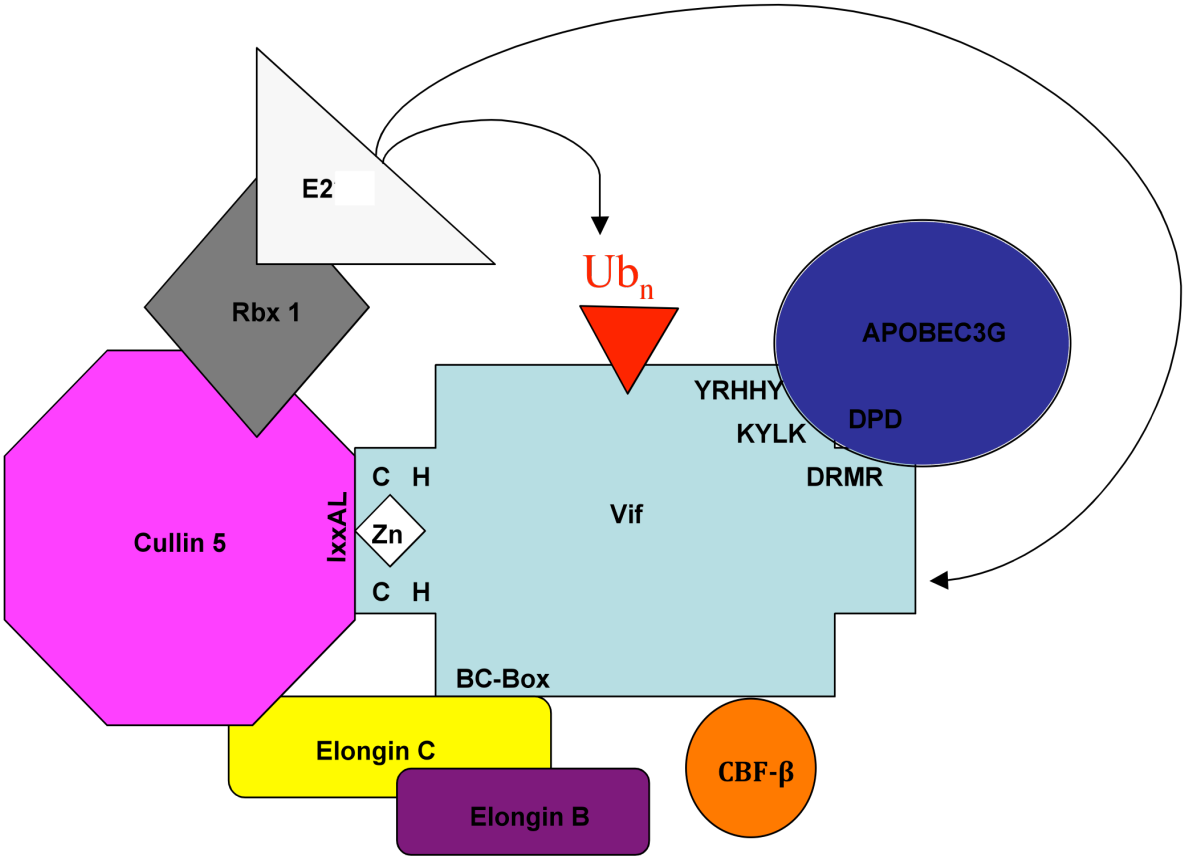

Adapted from Mailm et al., 2009

Figure 12. The HCCH and BC box domains of Vif are highly conserved in primate lentiviruses. The HCCH domain is indicated in orange and the BC box domain is depicted in blue.

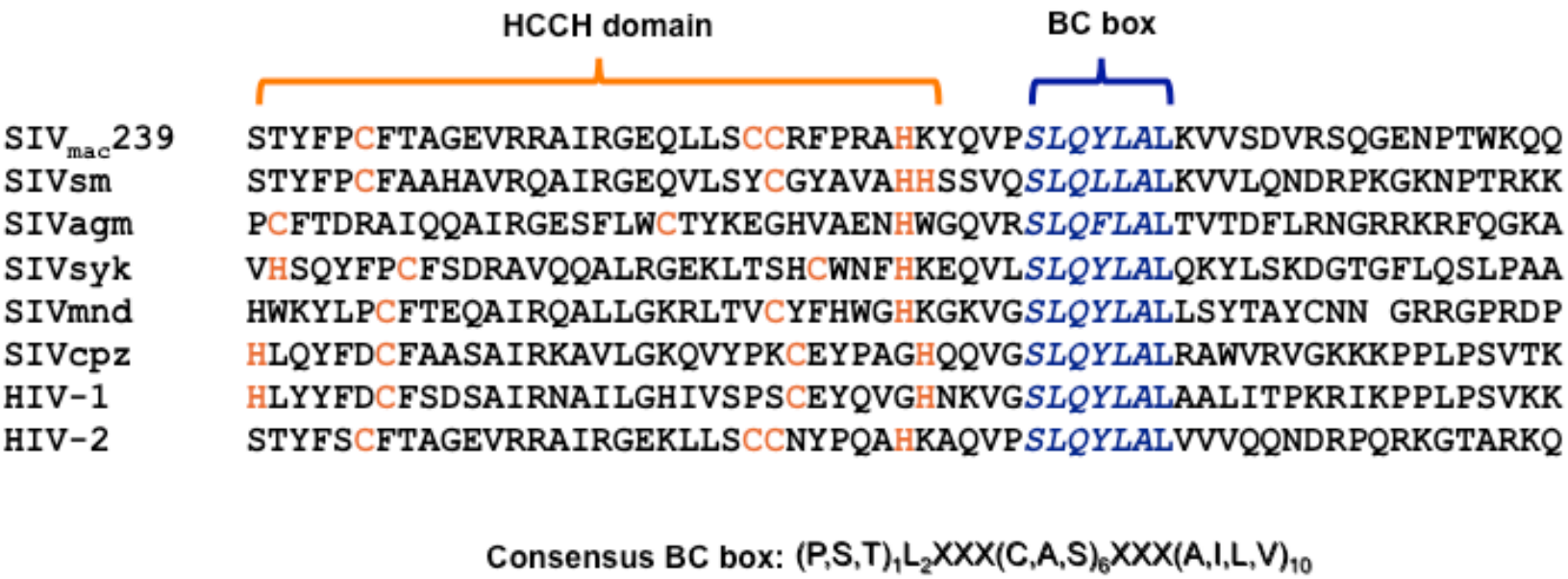
HCCH domain
BC box
SIV$_{mac}$239 STYFPCFTAGEVRRAIRGEQLLSCCRFPRAHKYQVPSLQYLALKVVSDVRSQGENPTWKQQ
SIVsm STYFPCFAAHAVRQAIRGEQVLSYCGYAVAHHSSVQSLQLLALKVVLQNDRPKGKNPTRKK
SIVagm PCFTDRAIQQAIRGESFLWCTYKEGHVAENHWGQVRSLQFLALTVTDFLRNGRRKRFQGKA
SIVsyk VHSQYFPCFSDRAVQQALRGEKLTSHCWNFHKEQVLSLQYLALQKYLSKDGTGFLQSLPAA
SIVmnd HWKYLPCFTEQAIRQALLGKRLTVCYFHWGHKGKVGSLQYLALLSYTAYCNN GRRGPRDP
SIVcpz HLQYFDCFAASAIRKAVLGKQVYPKCEYPAGHQQVGSLQYLALRAWVRVGKKKPPLPSVTK
HIV-1 HLYYFDCFSDSAIRNAILGHIVSPSCEYQVGHNKVGSLQYLALAALITPKRIKPPLPSVKK
HIV-2 STYFSCFTAGEVRRAIRGEKLLSCCNYPQAHKAQVPSLQYLALVVVQQNDRPQRKGTARKQ
Consensus BC box: (P,S,T)$_1$L$_2$XXX(C,A,S)$_6$XXX(A,I,L,V)$_{10}$

leading to an increase in antiviral activity by A3G (Xiao et al., 2007). Mutation of either cysteine residue or spacing within the HCCH motif results in the inability of Vif to target A3G for proteosomal degradation (Paul et al., 2007; Xiao et al., 2006). This is due to a conformational change in the HCCH motif that prevents the exposure of possible protein-protein interaction sites (Giri and Maynard, 2009; Paul et al., 2006). Upon further investigation using fluorescence and CD spectroscopy, the binding of the HCCH domain to zinc confirmed that zinc binding increases tertiary packing supporting the theory that zinc binding and protein conformation are coupled tightly (34). Chelation of zinc by cell-permeable *N, N, N′, N′*-tetrakis-(2-pyridylmethyl)ethylenediamine (TPEN) results in the loss of Vif function leading to an increase in antiviral activity by A3G (Xiao et al., 2007). Mutation of either cysteine residue or spacing within the HCCH motif results in the inability of Vif to target A3G for proteosomal degradation (Paul et al., 2007; Xiao et al., 2006). Therefore, it would be interesting to see how mutations in the HCCH domain affect HIV-1 pathogenesis *in vivo*.

Another highly conserved domain crucial for the function of Vif is the ^{144}SLQ(Y/F)LA^{150} motif which binds the cullin adapter protein EloBC through a BC-box motif (Figure 12) (Yu et al., 2003). The BC-box of the suppressors of cytokine signaling (SOCS) proteins is a loop helix motif with the consensus sequence ((A/P/T/S)$_1$L$_2$xxx(C/A/S)$_6$xxx(A/V/L/I)$_{10}$) that also exists in other cellular proteins known to interact with EloBC (Kamura et al., 1998). The serine at amino acid position 144 is regulated by phosphorylation thus negatively regulating the binding of Vif to EloC. If this serine is mutated to an alanine, phosphorylation is prevented, but this mutant still efficiently depletes cellular stores of A3G. However, the virions that are produced are

severely reduced in infectivity (Mehle et al., 2004). While Vif binds EloBC heterodimer with high affinity, it does not fit the consensus sequence perfectly. The BC-box of Vif is unstructured in its unbound state; however, this motif binds EloC through two α-helicies and becomes structured. Once EloC is bound, the $P^{161}PLP^{164}$ domain (described below) interacts with the amino acid residues 101-104 of EloB (Bergeron et al., 2010). These two binding steps are essential for the Vif-EloBC interaction and recruit the E3 ligase. If either EloB or C are deleted or mutated, the Vif-EloBC interaction is lost (Mehle et al., 2004; Yu et al., 2001; Yu et al., 2003). More studies are needed to look at the *in vivo* pathogenesis by making site-directed mutations in the SLQ(Y/F)LA domain of Vif.

The central hydrophobic domain $E^{88}WRRKK^{93}$ and the conserved $P^{161}PLP^{164}$ domain of HIV-1 Vif are important for the steady-state levels of Vif and for interactions with tyrosine kinases (Donahue et al., 2008; Fujita et al., 2003; 2004). Mutation of either of these sites results in decreased Vif-Vif multimerization, dimished Vif expression, reduced A3G binding, and a loss of viral infectivity (Fujita et al., 2003; 2004; Kataropoulou et al., 2009; Yang et al., 2001; Yang et al., 2003). Furthermore, if the PPLP motif is mutated or deleted, HIV-1 in the presence of Vif is unable to exclude A3G from the virion. This dominant negative effect leads to a decrease in virion infectivity (Walker et al., 2010). Although the role of the PPLP domain not completely clear, it has been shown that the PPLP domain may help promote the dimerization of VIf in the absence of Cul 5, that it directly interacts with Cul 5, and that it is essential for Vif function (Simon et al., 1999; Yang et al., 2001; Yang et al., 2003).

Structural Determinants of Vif that Interact with APOBEC3

As disscussed above, HIV-1 and HIV-2 were transmitted to humans by different zoonotic transmission events (Sharp et al., 2001). Briefly, SIVcpz (chimpanzee, *Pan troglodytes)* was the precursor for HIV-1 and SIVsm (sooty mangabey, *Cerocebus)* was the source of HIV-2, which are both related but very distinct SIVs that naturally infect nonhuman primates (Sharp et al., 2001). These zoonotic infections seem to occur when the host cell does not strongly resist lentiviral infection with post-entry restriction factors, such as TRIM5α or A3G (Cullen et al., 2006; Stremlau et al., 2004). The Vif-A3G interaction is an important factor in species-specificity between HIV and various SIVs. Zoonotic infections only persist when the lentiviral Vif protein can bind to and induce the degradation of A3G (Cullen et al., 2006; Mariani et al., 2003). For example, HIV-1 and SIVcpz Vif can bind and degrade human A3G but not African green monkey A3G rendering humans resistant to infection by SIVagm. On the contrary, SIVagm cannot bind and degrade HIV-1 or SIVcpz Vif (Cullen et al., 2006; Mariani et al., 2003). The direct interaction between A3G and Vif are dependent on amino acids 128-130 in A3G (Huthoff and Malim, 2007; Russell et al., 2009). Previous research has determined that species-specificity is determined by a single amino acid in human A3G, D128, and Africa green monkey A3G, K128 (Bogerd et al., 2004; Mangeat et al., 2004; Schrofelbauer et al., 2004; Xu et al., 2004) and amino acids 14-17 on HIV-1 Vif (Schrofelbauer et al., 2006). In human A3G if the aspartic acid is replaced with a lysine, hA3G becomes sensitive to SIVagm Vif and insensitive to HIV-1 Vif (Bogerd et al., 2004; Mangeat et al., 2004; Schrofelbauer et al., 2004; Xu et al., 2004). Also, if the $D^{14}RMR^{17}$ motif in HIV-1 Vif is replaced with either the $S^{14}ERQ^{17}$ or $S^{14}EMQ^{17}$ residues

in SIVagm VIf, the HIV-1 Vif protein is now able to interact with both A3G from African green monkeys and rhesus macaques (Schrofelbauer et al., 2006). These species-specific limitations of Vif form a means to prevent or minimize the number of successful zoonotic transmissions of various primate lentiviruses.

Regions implicated ability of Vif to bind and interact with A3 proteins have been mapped to the N-terminal region of HIV-1 Vif (Figure 13). The amino acid residues involved are arranged in a non-linear fashion thereby indicating that multiple surfaces are involved in this interaction. The exact binding domain in HIV-1 Vif consists of several discontinuous subdomains (Goila-Gaur et al., 2008, Marin et al., 2003; Mehle et al., 2007; Russell et al., 2007; Russell et al., 2009; Schrofelbauer et al., 2006; Simon et al., 2005; Tian et al., 2006). For example, using site-directed mutagenesis, hydrophilic motifs ^{40}YRHHY^{44} and ^{23}SLVK^{26} were found to be essential for the restriction of A3G or A3G and A3F, respectively (Chen et al., 2009; Dang et al., 2009; Marin et al., 2003; Russell et al., 2007; Russell et al., 2009; Yamashita et al., 2008; Zhang et al., 2008) The hydrophobic patch, ^{69}YWxL^{72} was shown to suppress A3G, A3F, and A3B and the ^{55}VxIPLx$_4$L^{64} motif is important for binding A3G (Walker 18, 50; He et al., 2008; Pery al., 2009). These residues 55-72 are sufficient alone for A3G binding and the charged residues in this region (R56, R61, and R63) are dispensable for A3G degradation (He et al., 2008; Mehle et al., 2007). The ^{12}QVDRMR^{17} motif is important for interaction with A3F and A3C (Mehle et al., 2007; Russell et al., 2007). The ^{81}LGxGxxIxW^{89} domain has been found to bind and regulate both A3G and A3F neutralizing activities. The L81 and G82 regulates the binding of Vif to A3F, while G84, I87, and W89 regulate interaction with both A3G and A3F (Dang et al., 2010). Both the ^{74}TGERxW^{79} and

^{171}EDRWN^{175} domains specifically bind and neutralize A3F (Dang et al., 2010; Russell et al., 2007).

Although there is only approximately 50% homology between HIV-1 Vif and $SIV_{mac}239$, very few domains in the N-terminus of HIV-1 Vif are partially conserved in $SIV_{mac}239$ Vif (Dang et al., 2009; He et al., 2008; Pery et al., 2009). These domains are listed in Figure 13. Identifying these domains on SIVmac239 Vif is essential for using the rhesus macaque as a model to study viral pathogenesis. Even though the interaction surfaces on Vif are structurally complicated, it is important to understand and identify these domains to determine the mechanism by which Vif recognizes A3 proteins.

APOBEC3 and Vif as Therapeutic Targets

Since a protective vaccine is not available, the Merck vaccine trial proved unsuccessful, and the resistance to HARRT therapy occurs, we need new and more effective antiviral drugs for the management of HIV-1 infection (Barouch et al., 2008; Robb et al., 2008). Some scientists are now looking into using the Vif-A3 protein interactions as targets for antiviral drug development. This is possible because several studies have implied that interference with the Vif-A3 interaction strongly suppress HIV-1 viral replication in nonpermisive cells (Gabuzda et al., 1992; Fisher et al., 1987; Strebel et al., 1987; von Schwedler et al., 1993).

In order to use APOBEC3 proteins as therapeutics, the significant quantities of APOBEC3 needs to be incorporated/packaged into the HIV-1 virion. Using this

Figure 13. The domains of HIV-1 and $SIV_{mac}239$ Vif that have been implicated in binding A3 proteins. Shown are representations of both the N-terminus of HIV-1 (top) and $SIV_{mac}239$ (bottom) Vif from amino acids 1 to 174 as indicated below the protein. Labeled in the boxes are specific amino acid motifs that are required to interact with the designated A3 proteins listed above the proteins.

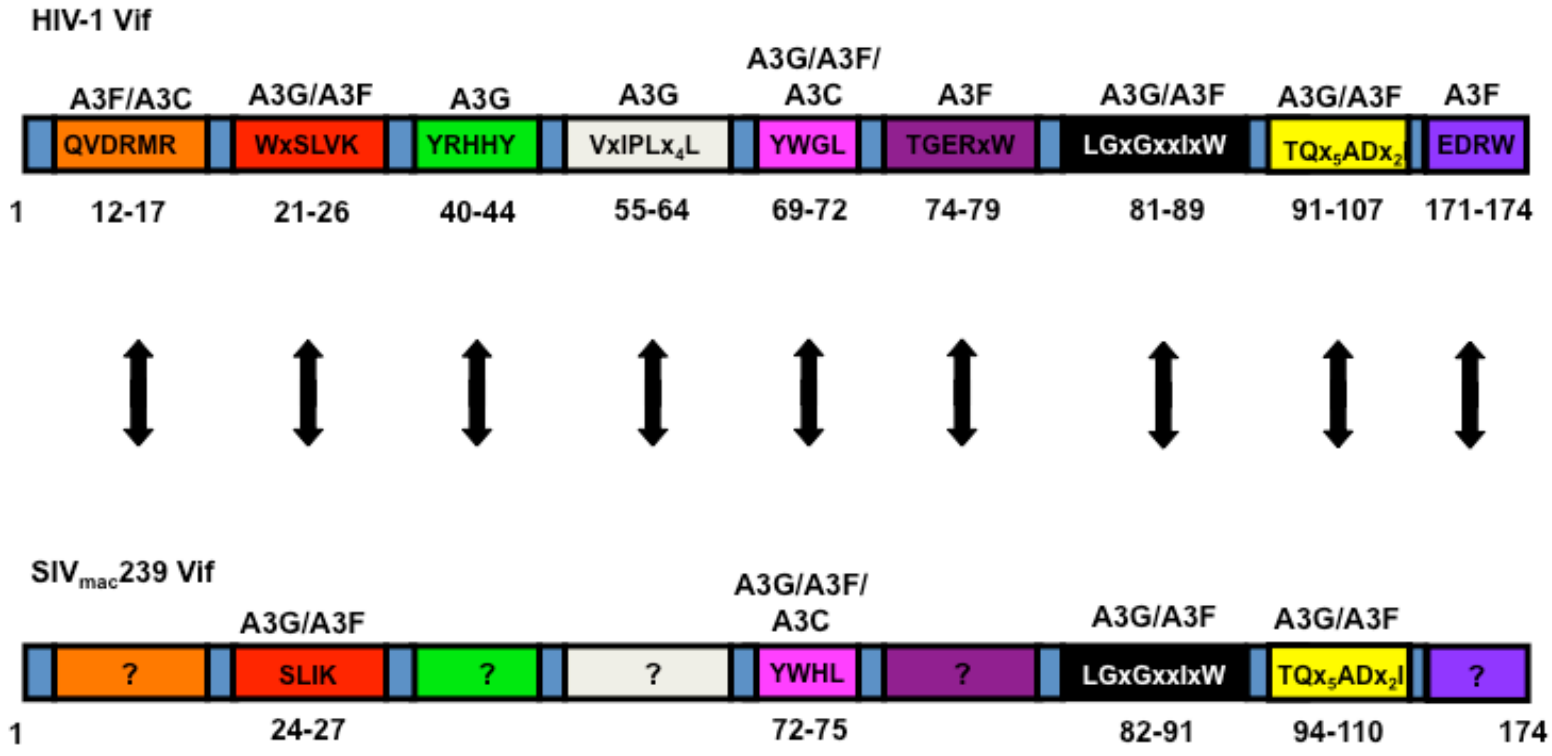
HIV-1 Vif
A3F/A3C
A3G/A3F
A3G
A3G
A3G/A3F/ A3C
A3F
A3G/A3F
A3G/A3F
A3F
QVDRMR
WxSLVK
YRHHY
VxIPLx4L
YWGL
TGERxW
LGxGxxIxW
TQx5ADx2I
EDRW
1
12-17
21-26
40-44
55-64
69-72
74-79
81-89
91-107
171-174
SIVmac239 Vif
A3G/A3F
A3G/A3F/ A3C
A3G/A3F
A3G/A3F
?
SLIK
?
?
YWHL
?
LGxGxxIxW
TQx5ADx2I
?
1
24-27
72-75
82-91
94-110
174

scenario, even HIV-1 virions would contain increased amounts of A3 effectively overwhelming the normal Vif function thus preventing the genomic RNA from becoming a replication-competent provirus in the target cell (Albin et al., 2010; Jern et al., 2009; Mulder et al., 2008). The amount of risk associated with increasing A3G expression and causing mutagenic activity would need to be smaller than the ability of A3G to exert its antiviral activities. In order to increase encapsidation of A3G into HIV-1 virions and prevent the degradation of A3G, two different approaches can be employed: 1.) Directly increasing incorporation of A3G by increasing the expression of A3G, or 2.) Indirectly increasing A3G incorporation by preventing proteosomal degradation of A3G (Albin et al., 2010).

In order to directly increase the expression of A3G thus increasing the incorporation, IFN-α treatment is possible. Induction of A3 proteins in macrophages by IFN-α treatment is effective in restricting the infectivity of HIV-1 (Peng et al., 2006). By doing this, we may be able to selectively increase A3G expression and aid the immune system in controlling HIV-1 infection. This treatment could also enhance other small molecules that occur naturally to aid the immune system or inhibit viral replication. However, IFN-α treatment induces many non-specific cellular effects making it difficult to rule out the A3 antiviral activity. Another side effect of this treatment could also be the hypermutation of the human genome because A3 expression levels would overwhelm the cellular regulatory mechanisms leading to the development of certain cancers (Harris et al., 2002; Yamanaka et al., 1995).

Another direct approach could also be to selectively target A3 proteins to the viral core in HIV-1 virions. For example; if A3G is fused to a fragment of Vpr, A3G is

efficiently incorporated into HIV-1 virions in the presence of Vif (Aguiar et al., 2008). Also, fusing A3A to Vpr resulted in enhanced antiviral activity in the target cell. This is important because normally A3A does not restrict HIV-1 or reach the viral core; however, when fused to Vpr, the A3A-Vpr protein is specifically targeted to the viral core and potently restricts HIV-1 (Aguiar et al., 2008).

An indirect approach would be to increase incorporation of the A3 protein and to prevent its proteosomal degradation. For example, in one study a membrane-permeable zinc chelator, TPEN was used to prevent the formation of the E3 ubiquitin ligase by inhibiting the Vif-Cullin 5 binding thus preventing the degradation of A3G (Xiao et al., 2007). However, TPEN *in vitro* has been shown to induce apoptosis in human cells by inhibiting other cellular functions, which would make this chelator undesirable (Martin et al., 1991; Cao et al., 2005). Also, proline-rich peptides containing the PPLP motif have been used to prevent the oligomerization of Vif in nonpermissive cells and inhibit the replication of HIV-1 (Miller et al., 2007; Yang et al., 2003). Peptide inhibitors, such as these, provide useful information on protein-protein interactions, but are not desirable as antiviral drugs due to their low stability and poor bioavailability (Adessi et al., 2002).

In order to indirectly increase incorporation of A3 proteins into HIV-1 virions, the interacting domains of both Vif and A3 need to be elucidated. Currently, *in vitro* Vif-A3G binding assays are underway using a fluorescence resonance energy transfer (FRET) assay to measure the interactions between GST-Vif and a biotinylated A3G peptide. High-throughput screening is being used to identify potential candidate molecules that may target the Vif-A3G interaction (Mehle et al., 2007).

Another indirect approach may be to create a molecule that directly binds A3 and inhibits the binding of HIV-1 Vif (Harris et al., 2004). Also, it could be theoretically possible to create a molecule that could be used to inhibit the interaction of HIV-1 Vif with either A3 proteins or the proteosomal machinery. For example, RN-18 (containing a 2-(4-nitophenylthio-*N*-phenylbenzamide) moiety) is a small-molecule antagonist of HIV-1 Vif that inhibits the interaction between A3-Vif (Nathans et al., 2008). RN-18 increases the expression levels of A3G, A3F, A3C as well as the incorporation of A3G into the virion, but it does not affect the binding of HIV-1 Vif to A3G or A3F. The inhibitor does increase the proteosomal degradation of Vif in the presence of A3G, A3F, or A3C. Also, RN-18 did not display cytotoxic effects at a concentration of 50-100 μM (Nathans et al., 2008). However, this inhibitor is a recent development and is not yet ready for clinical trials. While there has been promising success in designing small molecule inhibitors, more research is needed to visualize the structural interaction between A3 and Vif to design efficient interaction inhibitors.

The final approach may be the use of gene therapy. However, further advances in both safety and efficacy of both cell therapy and gene delivery must be overcome. As mentioned above, the Vif-A3 interaction is species-specific. If human A3G aspartate 128 is substituted with the lysine found in both the rhesus macaque and the African green monkey A3G, the human A3G would become resistant to Vif-mediated proteosomal degradation (Mariani et al., 2003). The human D128K A3G mutation would protect hA3G from binding HIV-1 Vif (Bogerd et al., 2004; Huthoff et al., 2007; Li et al., 2008; Mangeat et al., 2004; Schröfelbauer et al., 2004). Theoretically this would lead to increased packaging of A3G into the HIV-1 virion by preventing its interaction

with Vif thus leading to the restriction of HIV-1. To date, there are no known occurrences of this allele circulating in the human population; therefore, therapeutic gene delivery would be necessary. Another method would be to fuse A3G to ubiquitin-associated domain 2 (UBA2), a stabilization signal known to protect proteins from proteosomal degradation (Li et al., 2008). This fusion only has a partial effect on restriction of HIV-1 and is only partially restricted to Vif-mediated degradation (Li et al., 2008). This modifcation along with others may someday provide a tactic in engineering T cells to be resistant to HIV-1 infection.

Goals of the study

All primate lentiviruses encode for a Vif protein, which is necessary for HIV-1 replication in primary $CD4^+$ T cells and macrophages (Fan and Peden, 1992; Gabuzda et al., 1992; Blanc et al., 1993; Sakai et al., 1993; von Schwedler et al., 1993; Borman et al., 1995). The Vif protein interacts with apolipoprotein B mRNA-editing enzyme catalytic peptide-like 3 (APOBEC3; A3) proteins promoting their accelerated degradation by the 26S proteosome (Sheehy et al., 2002). Sequence analysis of Vif proteins from different lentiviruses revealed that there are two highly conserved domains in the carboxyl terminus that are required for the recruitment of the Vif-CBF-β-Cul5/Elongin B/C/Rbx-1 E3 ubiquitin ligase complex (Hultquist et al., 2012; Luo et al., 2005; Mehle et al., 2004; 2006; Yu et al., 2004). These domains are the viral BC box, SLQ(Y/F)LA, and the Zn^{2+} (H-X_5-C-X_{17-18}-C-X_{3-5}-H; HCCH) binding domains. Previous cell culture studies have shown that the introduction of amino acid substitutions in the SLQ(Y/F)LA motif resulted in decreased binding of Vif to Elongin C, while substitutions

in the HCCH domain prevented interactions with Cullin 5 in the Vif-CBF-β-Cul5/Elongin B/C/Rbx-1 E3 ubiquitin ligase complex (Luo et al., 2005; Mehle et al., 2004a; 2004b; 2006; Stopak et al., 2003; Yu et al., 2203; 2004).

In our first study we were interested in determining the importance of the highly conserved SLQYLA motif in viral pathogenesis using the SHIV/macaque model of infection. Two amino acid substitutions were introduced into the SLQYLA (AAQYLA) domain of the SIV Vif protein. Prior to our rhesus macaque study, the resulting virus, $SHIV_{VifAAQYLA}$, was assessed in both non-permissive (CEM) and permissive (CEM-SS) cells to examine the replication of these mutant viruses relative to parental SHIV. We found that, while $SHIV_{VifAAQYLA}$ replicated with similar kinetics to $SHIV_{KU\text{-}1bMC33}$ in CEM-SS cells, it did not replicate in CEM cells. We were also interested in determining if human A3G is incorporated into $SHIV_{VifAAQYLA}$ and showed that human A3G was readily incorporated into $SHIV_{VifAAQYLA}$ virions but not $SHIV_{KU\text{-}1bMC33}$. To assess the replication and persistence of $SHIV_{VifAAQYLA}$ *in vivo*, $SHIV_{VifAAQYLA}$ was inoculated into three rhesus macaques where various viral and immunological parameters were followed for six months. All three macaques inoculated with $SHIV_{VifAAQYLA}$ developed a transient decrease in circulating CD4+ T cells one week post-inoculation that rebounded to pre-inoculation levels by four weeks post-inoculation. These macaques also had plasma viral loads that were 100-fold lower than macaques inoculated with $SHIV_{KU\text{-}1bMC33}$, developed no histological lesions in lymphoid tissues, and had a decreased distribution of replicating virus in visceral tissues. The engineered Vif mutations were stable during the first three weeks post-inoculation, but by four weeks post-inoculation the S147A amino acid substitution changed to a threonine in two of the three macaques. At

necropsy, plasma was analyzed for the presence of immunoprecipitating antibodies, and all three macaques developed immunoprecipitating antibodies although one macaque developed significantly less. Sequence analysis of *vif, vpu, env,* and *nef* from the thymus, mesenteric, axillary, and inguinal lymph nodes, revealed an increased amount of G-to-A substitutions in the dinucleotide context of 5'-TC (minus strand) in these genes amplified from macaques inoculated with $SHIV_{VifAAQYLA}$. To determine if pathogenic virus was present in plasma from macaques inoculated with $SHIV_{VifAAQYLA}$ at the time of necropsy, plasma was pooled from two of the three macaques and inoculated into a naïve macaque (macaque I95). Macaque I95 was assessed for various viral parameters such as circulating $CD4^+$ T cell levels, virus burden, imuunoprecipitating antibodies, and the detection of replicating virus in both PBMC and visceral tissues. We showed that this macaque maintained circulating CD4+ T cell levels, no viral loads, and no immunoprecipitating antibodies. Viral DNA sequences (the *gag* gene) could be detected in PBMC through out the duration of infection; however, viral RNA sequences could not. At necropsy, viral DNA and RNA could be detected in the liver, kidney, spleen, tonsil, axillary lymph node, and small intestine (ileum). This study indicated that a certain level of infectious viral replication was occurring in macaques inoculated with $SHIV_{VifAAQYLA}$ and that the pooled plasma contained only low levels of infectious virus that was efficiently controlled by macaque I95.

In our second study we used the SHIV/macaque model of infection to compare the replication and pathogenicity of SHIVs that express a Vif protein in which the entire SLQYLA ($SHIV_{Vif5A}$) or HCCH ($SHIV_{VifHCCH(-)}$) domains were substituted with alanine

residues. We were interested in extending our previous studies to determine if these highly conserved domains were critical to Vif function *in vivo*. Prior to our rhesus macaque study, we were interested in determining whether $SHIV_{Vif5A}$ and $SHIV_{VifHCCH(-)}$ were effectively inhibited by rhesus A3G/F. We performed assays to examine the replication of these mutants in both non-permissive (C8166, PBMC) and permissive (SupT1) cells. We also determined if $SHIV_{Vif5A}$ and $SHIV_{VifHCCH(-)}$ in the presence of rhesus A3G/F incorporated into virions, remained stably expressed in cells, restricted virus replication, and if these viruses were capable of introducing significant G-to-A substitutions into the *nef* gene of the SHIV genome *in vitro*. We found that both $SHIV_{Vif5A}$ and $SHIV_{VifHCCH(-)}$ did not replicate in non-permissive cells but replicated efficiently in permissive cells. We also showed that rhesus A3G/F was readily incorporated into $SHIV_{Vif5A}$ and $SHIV_{VifHCCH(-)}$ virions, remained stably expressed in the cell, severely restricted viral replication, and induced a significant number of G-to-A substitutions in *nef* similar to $SHIV_{VifStop}$ (SHIV expressing a Vif protein with two stop codons introduced at amino acid residues 28 and 29). To assess the replication and persistence of these viruses *in vivo*, each virus was inoculated into three rhesus macaques where various viral and immunological parameters were followed for six months. All macaques maintained a stable level of circulating $CD4^+$ T cells, low viral burdens, maintained engineered mutations, yielded no histological lesions, and developed immunoprecipitating antibodies by 12 weeks post-inoculation. However, the production of viral RNA only persisted in macaques inoculated with $SHIV_{VifHCCH(-)}$. Sequence analysis of *nef* and *vpu* from the small intestine (ileum), thymus, and the spleen showed extensive G-to-A substitutions in *nef* genes isolated from macaques

inoculated with $SHIV_{VifHCCH(-)}$. Macaques inoculated with $SHIV_{Vif5A}$ effectively controlled the virus three weeks post-inoculation and no viral sequences could be amplified from tissue DNA. These studies showed that the SLQYLA and HCCH domains are critical for viral pathogenesis *in vivo* and that there may exist APOBEC3 negative reservoirs in the rhesus macaque that allow for low levels of viral replication and persistence but not disease. Therefore, from these first two studies we inferred that mutations targeted to one or more functional conserved domains within the Vif protein may limit viral replication and generate an effective immune response leading to the "self-inactivation" of the virus by the activities of various APOBEC3 proteins resulting in a possible live-attenuated vaccine candidate.

While the human APOBEC3 repertoire has been extensively studied, the full complement of these proteins in the rhesus macaque remains unknown. Sequencing of the rhesus macaque genome has led to the identification of the rhesus homologues A3B, A3C, A3D, A3F, A3G, and A3H. In the final study, we were interested in identifying and characterizing the human A3A (hA3A) homologue in the rhesus macaque (rhA3A). Using cDNA from Concanavalin-A-activated rhesus macaque PBMCs, we were able to detect and clone rhesus A3A. Using the cloned rhesus A3A sequence we were able to determine that both the human and rhesus *Apobec3* genes are orthologous. We show that rhA3A is highly expressed in activated $CD4^+$ T cells, widely expressed in both the visceral and central nervous system tissues of the rhesus macaque, maintains nucleocytoplasmic localization, does not inhibit virus release, does not restrict foreign DNA, and is degraded in the presence of the human immunodeficiency virus (HIV-1) and simian-human immunodeficiency virus (SHIV)

genomes in a Vif-dependent manner. Our results also indicate that rhA3A reduced the level of infectious SHIVΔ*vif* by approximately 20-fold and HIV-1Δ*vif* by 3-fold. Human and monkey A3A amino acid sequences are 81% homologous and can be distinguished by a three amino acid indel (insertion and/or deletion) located between residues 27-30. When these residues were deleted from rhA3A (rhA3AΔSVR), the antiviral activity of rhA3A was abolished suggesting that these residues are critical for lentivirus inhibition. Select APOBEC3 proteins are incorporated into the virion and can inhibit reverse transcription and/or induce G-to-A hypermutation in nascent reverse transcripts in the next target cell. Previous studies revealed that rhA3G is incorporated into SHIVΔ*vif* virions and exerts its antiviral activity in target cells by an increase in cytidine deamination of newly synthesized minus-strand viral DNA from cytosines to uracils, leading to G-to-A substitutions (plus strand) in the viral genome. We were able to detect the incorporation of rhA3A into SHIVΔ*vif* and to a lesser extent in SHIV virions; however, we were unable to detect the incorporation of rhA3A into either HIV-1 or HIV-1Δ*vif* virions. Even though rhA3A is incorporated into SHIVΔ*vif* virions and potently restricts SHIVΔ*vif* similar to rhA3G, rhA3A produced an approximately 5-fold decrease in the number of G-to-A mutations compared to rhA3G. Since previous research showed that human A3A inhibits the replication of adeno-associated virus 2 (AAV-2), intracisternal A particles (IAP), and long interspersed nuclear element 1 (L1), we were interested in determining if rhesus A3A could inhibit AAV-2 replication and L1 retrotransposition (Bogerd et al., 2006a; 2006b; Chen et al., 2006; Muckenfuss et al., 2006). We found that rhesus A3A could not inhibit AAV-2 replication or L1 retrotransposition. The data from this study suggests for the first time that a primate

A3A protein can inhibit lentiviral replication but not AAV-2 replication or L1 retrotransposition.

VI. Chapter Two: Mutations in the SLQYLA Motif of Vif in the Simian-Human Virus Results in a Less Pathogenic Virus in Rhesus Macaques

Abstract

The simian-human immunodeficiency virus (SHIV)/macaque model for human immunodeficiency virus type 1 (HIV-1) has become a useful tool to assess the role of accessory genes like virion infectivity factor (Vif), in lentiviral pathogenesis. In this study, we introduced two amino acid changes in the highly conserved SLQYLA domain (to AAQYLA) of the SIV Vif protein. The resulting virus $SHIV_{VifAAQYLA}$, was used to infect three macaques, which were followed for over six months. Plasma viral loads and circulating $CD4^+$ T cell levels were assessed during the course of infection. The three macaques inoculated with $SHIV_{VifAAQYLA}$ did not develop significant $CD4^+$ T cell loss over the course of their infection, had plasma viral loads that were over 100-fold lower than macaques inoculated with parental $SHIV_{KU\text{-}1bMC33}$, and developed no histological lesions in lymphoid tissues. DNA and RT-PCR analysis revealed that only a select number of tissues were infected with this virus. Sequence analysis indicates that the site-directed changes were stable during the first three weeks after inoculation but thereafter the S147A amino acid substitution changed to a threonine in two of the three macaques. However, the L148A substitution remained stable in the *vif* amplified from the PBMC of all three macaques. Sequence analysis of *vif, vpu, env,* and *nef* genes revealed G-to-A substitutions in the genes amplified from macaques inoculated with $SHIV_{VifAAQYLA}$, which were higher than in a macaque inoculated with parental $SHIV_{KU\text{-}1bMC33}$. We found that the majority (>85%) of the G-to-A substitutions were in the context of 5'-TC (minus

strand) and not 5'-CC, suggestive that one or more the rhesus APOBEC3 proteins may be responsible for the observed mutational patterns. Finally, macaques inoculated with $SHIV_{VifAAQYLA}$ developed immunoprecipitating antibody responses against the virus. The results from this study provide the first *in vivo* evidence of the importance of the conserved SLQYLA domain in viral pathogenesis and show that targeted mutations in *vif* can lead to a persistent infection with G-to-A (plus strand) changes accumulating in the viral genome.

Introduction

Human immunodeficiency virus type 1 (HIV-1) as well as other lentiviruses encode for a Vif protein, which has been shown to be essential for HIV-1 replication in certain cell types. The Vif protein of HIV-1 was first shown to interact with apolipoprotein B mRNA editing enzyme catalytic polypeptide-like 3G (APOBEC3G; hA3G) (Sheehy et al., 2002). This protein was found to be incorporated into the virus and provide cells with an innate intracellular anti-retroviral activity that is associated with hypermutation of the viral genome through cytidine deamination (Harris et al., 2003; Lecossier et al., 2003; Mangeat et al., 2003; Zhang et al., 2003). This hA3G-induced cytidine deamination results in cytidine to uridine changes during minus strand DNA synthesis triggering the DNA repair pathways that lead to the degradation of viral transcripts (Harris et al., 2003; Mangeat et al., 2003; Mariani et al., 2003; Yu et al., 2004; Zhang et al., 2003). Several groups subsequently showed that the Vif protein can prevent hypermutation by binding to hA3G and targeting this protein for degradation via the proteasome (Conticello et al., 2003; Kao et al., 2004; Mariani et al., 2003; Marin et

al., 2003; Mehle et al., 2004; Sheehy et al., 2003; Stopak et al., 2003; Yu et al., 2003; 2004). In addition to A3G, humans have six other A3 genes: hA3A, hA3B, hA3C, hA3DE, hA3F, and hA3H (Jarmuz et al., 2002). The members of this family either have one (hA3A, hA3C, and hA3H) or two (hA3B, hA3DE, hA3F and hA3G) Zn^{+2} coordinating deaminase domains organized as H-x_1-E-x_{25-31}-C-x_{2-4}-C (with x being a non-conserved position) (Chiu and Greene, 2008). Other APOBEC3 family members such as hA3B, hA3DE, hA3F, and hA3H have also been shown to also inhibit the replication of HIV-1Δ*vif* (Dang et al., 2007; Doehle et al., 2005; Wiegand et al., 2004; Yang et al., 2007; Yu et al., 2004; Zheng et al., 2004). Moreover, SIV_{mac}239Δ*vif* is potently restricted by hA3G, hA3F, and hA3H and to a lesser extent by hA3B, hA3C, and hA3DE (Dang et al., 2007; 2008; Mariani et al., 2003; Virgen et al., 2007; Yu et al., 2004). While fewer studies have been performed on the APOBEC3 family proteins from macaques, two studies have shown that rhesus macaque A3G and A3F inhibit the replication of SIV_{mac}Δ*vif* (Zennou et al., 2006; Virgen et al., 2007).

As mentioned, previous studies have shown that Vif inhibits the antiviral activity of APOBEC3 proteins by targeting A3 proteins for proteosomal degradation through a CBF-β-Vif-Cul5/ElonginB/C/Rbx-1 E3-dependent ubiquitin ligase (Jäger et al., 2011; Kobayashi et al., 2005; Mehle et al., 2004; Shao et al., 2010; Stanley et al., 2008; Yu et al., 2004). Vif binds the Cullin 5 complex through a highly conserved BC-box region known as the ^{144}SLQ(Y/F)LA^{149} domain (Yu et al., 2003). The BC-box of Vif is a loop-helix motif with a consensus sequence ($(A/P/T/S)_1L_2xxx(C/A/S)_6xxx(A/V/L/I)_{10}$) that has also been identified in other cellular proteins that are known to interact with elongin B/C (Kamura et al., 2004; Luo et al., 2005). Through this motif, Vif has a high affinity for

elongin B/C (Mehle et al., 2004). Mutation or deletion of the SLQ(Y/F)LA motif disrupts the proteosomal targeting and degradation of A3 proteins, and prevents the production of infectious HIV-1 virions (Kobayashi et al., 2005; Mehle et al., 2004a; 2004b; Shao et al., 2010; Simon et al., 1999; Stanley et al., 2008; Yu et al., 2004). While this domain has been extensively studied *in vitro*, no studies have assessed the role of this domain using a non-human primate model of HIV-1 pathogenesis.

In this study, we constructed a simian-human immunodeficiency virus (SHIV) with amino acid changes in the highly conserved SLQYLA ($SHIV_{VifAAQYLA}$) domain and assessed it for pathogenesis in macaques. Mutation of this motif resulted in lower viral loads, stabilization of circulating $CD4^+$ T cell levels, immunoprecipitating antibodies, and the accumulation of G-to-A substitutions in secondary lymphoid tissues. Our results show for the first time that the SLQYLA domain has determinants that contribute to the pathogenicity of SHIV in macaques and that mutations in this particular domain result in the accumulation of G-to-A mutations in the viral genome.

Results

Replication of $SHIV_{VifAAQYLA}$ in APOBEC3G (A3G) positive and negative cell lines

We performed assays to examine the replication of parental $SHIV_{KU\text{-}1bMC33}$ and $SHIV_{VifAAQYLA}$ in A3G/F positive (CEM) and negative (CEM-SS) cell lines. Cells were infected with each of the two viruses and the levels of p27 Gag released into the culture medium were quantified using a commercial antigen capture assay. $SHIV_{VifAAQYLA}$ replication in CEM-SS cells with similar kinetics to $SHIV_{KU\text{-}1bMC33}$ (Figure 14A).

However, $SHIV_{VifAAQYLA}$ released less than 0.5% p27 compared to the parental $SHIV_{KU-1bMC33}$ in CEM cells (Figure 14B).

Human APOBEC3G is incorporated into $SHIV_{VifAAQYLA}$ virions

Since $SHIV_{VifAAQYLA}$ released significantly less p27 than $SHIV_{KU-1bMC33}$ in CEM (A3G/F positive) cells, we determined if human A3G was incorporated into maturing virus particles leading to the restriction of $SHIV_{VifAAQYLA}$ replication. 293 cells were transfected with HA-hA3G and the complete genomes of either $SHIV_{VifAAQYLA}$ or $SHIV_{KU-1bMC33}$. At 48 hours post-transfection, the culture medium was collected, clarified, and the virus partially purified and concentrated by ultracentrifugation. The amount of p27 was determined and a western blot was run to detect for the presence or absence of hA3G. The results shown in Figure 15 indicate that hA3G was incorporated into $SHIV_{VifAAQYLA}$ virus particles but excluded from $SHIV_{KU-1bMC33}$.

Disease in macaques inoculated with $SHIV_{VifAAQYLA}$

We inoculated three macaques with $SHIV_{VifAAQYLA}$ (RAK10, RCS10, and RPL10). These macaques developed a transient decrease in the level of circulating $CD4^+$ T cells at one week post-inoculation (Figure 16B). However, by four weeks post-inoculation the level of circulating $CD4^+$ T cells rebounded to near pre-inoculation levels (Figure 16B). These macaques maintained high levels of circulating $CD4^+$ T cells throughout the course of their infection. All three macaques were euthanized at 28 weeks post-inoculation. At necropsy, macaques inoculated with

Figure 14. Replication of $SHIV_{KU\text{-}1bMC33}$ and $SHIV_{VifAAQYLA}$ in APOBEC3G positive (CEM) and negative (CEM-SS) cell lines. CEM and CEM-SS cells were inoculated with equal amounts of each virus and levels of p27 in the culture supernatants determined at various time points post-inoculation. (Panel A) Replication of $SHIV_{KU\text{-}1bMC33}$ and $SHIV_{VifAAQYLA}$ in CEM-SS cells. (Panel B) $SHIV_{KU\text{-}1bMC33}$ and $SHIV_{VifAAQYLA}$ in CEM cells. (⬮) $SHIV_{KU\text{-}1bMC33}$; (■) $SHIV_{VifAAQYLA}$.

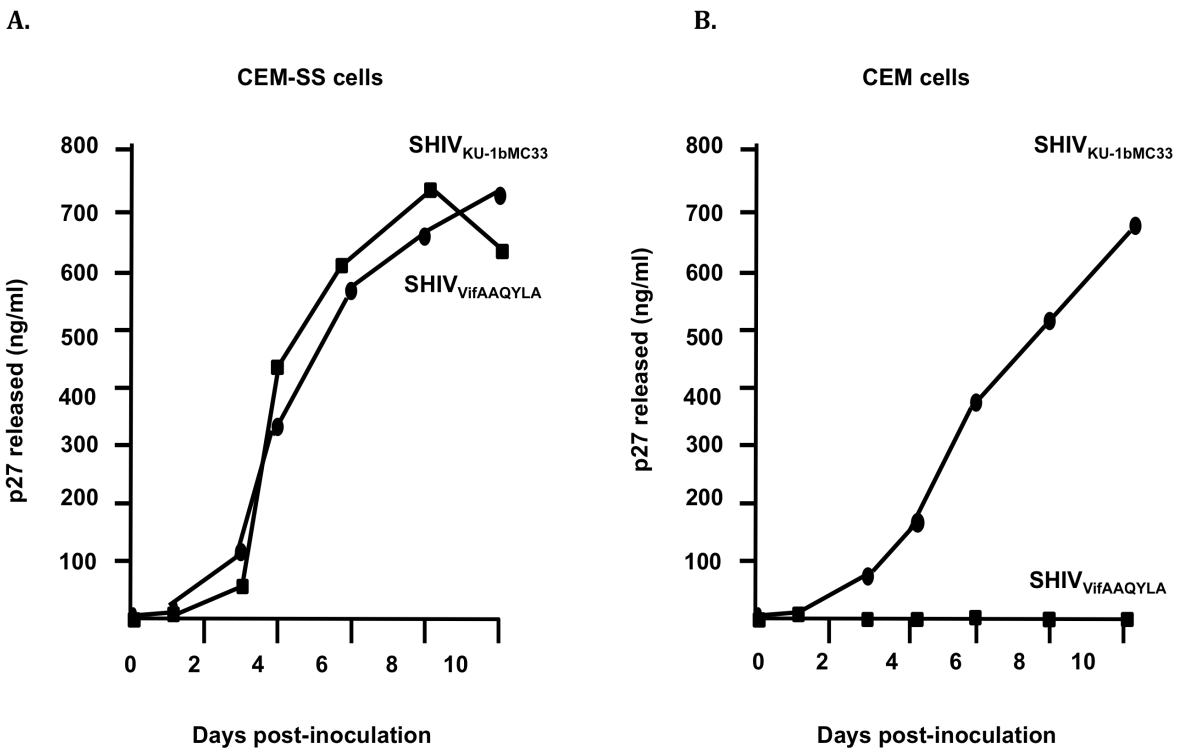
A.
CEM-SS cells
p27 released (ng/ml)
800
700
600
500
400
300
200
100
0
2
4
6
8
10
Days post-inoculation
SHIV KU-1bMC33
SHIV VifAAQYLA
B.
CEM cells
p27 released (ng/ml)
800
700
600
500
400
300
200
100
0
2
4
6
8
10
Days post-inoculation
SHIV KU-1bMC33
SHIV VifAAQYLA

Figure 15. Human APOBEC3G is incorporated into $SHIV_{VifAAQYLA}$ virions. 293 cells were transfected with a plasmid that expresses the genome of either $SHIV_{KU-1bMC33}$ or $SHIV_{VifAAQYLA}$ and a vector expressing HA-hA3G. At 48 hours, the culture medium was collected, clarified, and concentrated by ultracentrifugation through a 20/60% sucrose (w/v) gradient. Equivalent levels of p27 from each sample was resuspended in 2x sample reducing buffer, boiled, and proteins separated by SDS-PAGE. The presence of hA3G was detected by Western blot using an antibody directed against the HA-tag. Lane 1. Human A3G protein in pelleted supernatant from cells transfected with empty vectors. Lane 2-4. Human A3G detected in virus from cells transfected with the vector expressing hA3G and $SHIV_{KU-1bMC33}$ (Lane 2), $SHIV_{VifAAQYLA}$ (Lane 3), or the positive control SHIVΔVif (Lane 4).

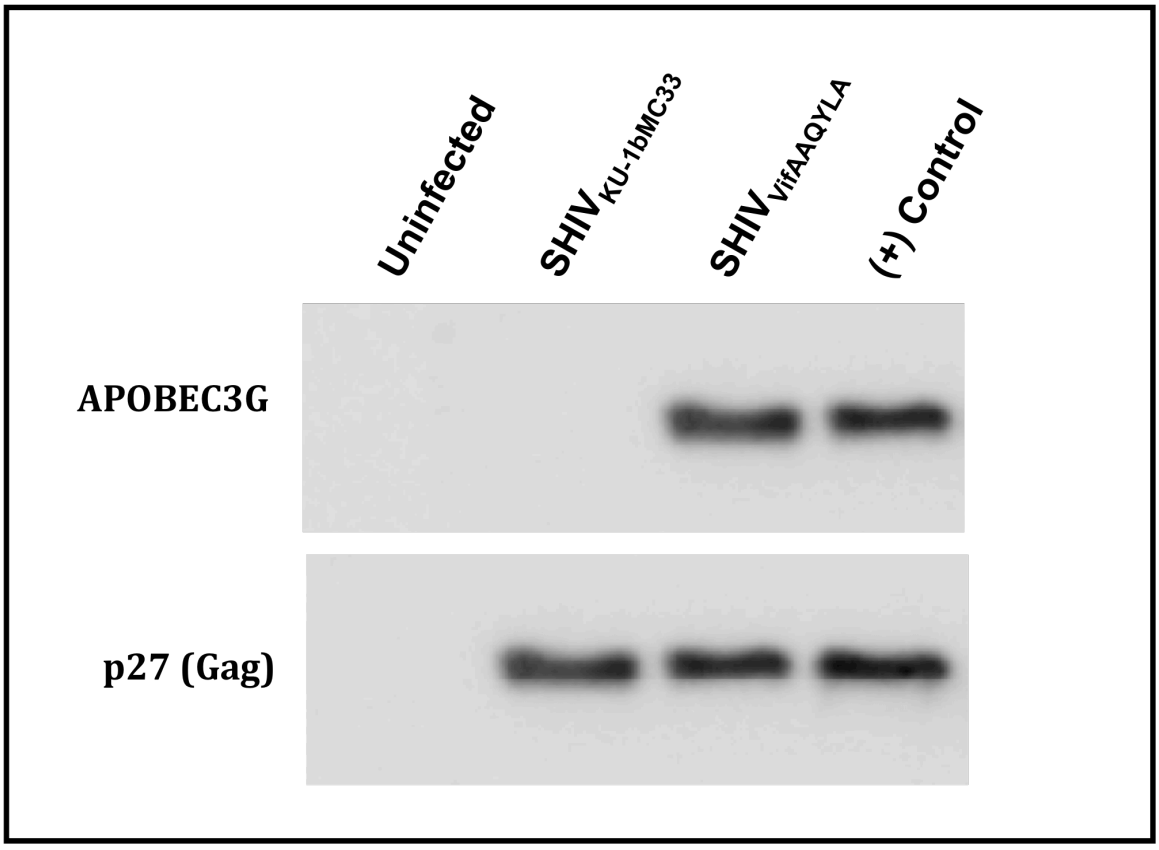
Uninfected
SHIV KU-1bMC33
SHIV VifAAQYLA
(+) Control
APOBEC3G
p27 (Gag)

Figure 16. Circulating $CD4^+$ T cell levels in macaques inoculated with $SHIV_{KU-1bMC33}$ and $SHIV_{VifAAQYLA}$. (Panel A) The levels of circulating $CD4^+$ T cells in five macaques inoculated with $SHIV_{KU-1bMC33}$ (2000, ● ; CM4G, ■ ; CM4K, ▲ ; RRH10, ▼). (Panel B) The levels of circulating CD4+ T cells in three macaques inoculated with $SHIV_{VifAAQYLA}$ (RAK10, ● ; RCS10, ◆; RPL10, ▲).

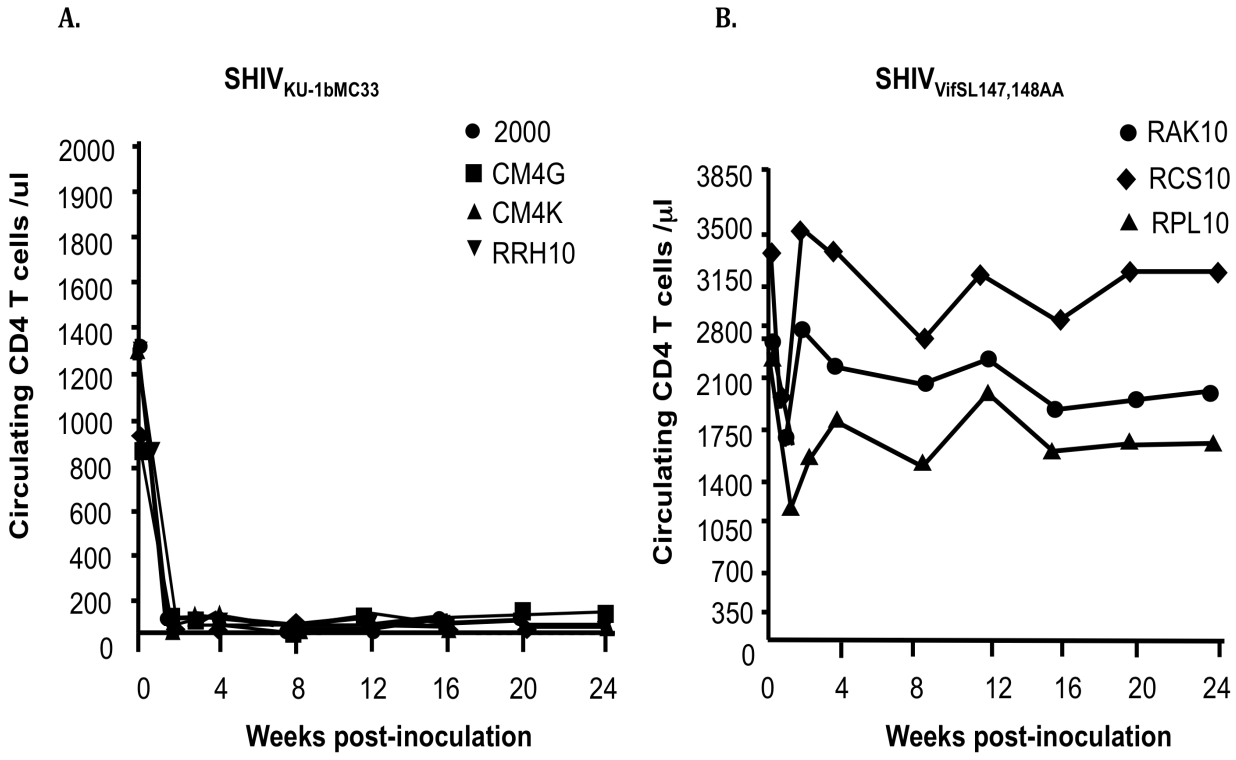
A.
SHIV KU-1bMC33
2000
CM4G
CM4K
RRH10
Circulating CD4 T cells /ul
2000
1900
1800
1600
1400
1200
1000
800
600
400
200
0
0
4
8
12
16
20
24
Weeks post-inoculation
B.
SHIV VifSL147,148AA
RAK10
RCS10
RPL10
Circulating CD4 T cells /µl
3850
3500
3150
2800
2100
1750
1400
1050
700
350
0
0
4
8
12
16
20
24
Weeks post-inoculation

$SHIV_{VifAAQYLA}$ had circulating $CD4^+$ T cell counts of 2427, 1656, and 3021, respectively. This contrasts with macaques inoculated with $SHIV_{KU\text{-}1bMC33}$ (Figure 16A). Analysis of plasma viral loads in macaques inoculated with $SHIV_{VifAAQYLA}$ revealed that during the early peak (1 to 3 weeks) of viremia, the mean load was 8.52×10^4 copies per ml (Figure 17A), approximately 100-fold less than macaques inoculated with parental $SHIV_{KU\text{-}1bMC33}$ (Figure 17B). Following the first month of infection, the plasma viral loads in macaque RPL10 declined faster than macaques RAK10 and RCS10 (Figure 17A).

Stability of the *vif* gene mutations during the course of infection and at necropsy

We assessed the stability of the engineered mutations in the *vif* gene during the course of infection. DNA was extracted from PBMC samples at various times post-inoculation and from lymphoid tissues at necropsy. The *vif* sequences were amplified, directly sequenced and compared to the input *vif* sequence of $SHIV_{VifAAQYLA}$. The *vif* mutations were stable from one to three weeks post-inoculation for all three $SHIV_{VifAAQYLA}$ infected macaques (Figure 18). However, four weeks post-inoculation the S147A amino acid substitution changed to a threonine in two of the macaques, RPL10 and RAK10. Interestingly, this amino acid substitution was mediated by a G-to-A mutation. DNA from lymphoid organs obtained at necropsy from RAK10 and RPL10 also showed the A147T mutation whereas macaque RCS10 maintained the S147A amino acid substitution (Figure 18). The L148A substitution was found to be stable during the course of infection for all three macaques and in the lymphoid organs analyzed at necropsy. There were no mutations in this region of *vif* from RRH10, which was inoculated with $SHIV_{KU\text{-}1bMC33}$ (Figure 18).

Figure 17. Plasma viral loads in macaques inoculated with $SHIV_{VifAAQYLA}$ and $SHIV_{KU\text{-}1bMC33}$. (Panel A) Plasma viral loads in three macaques inoculated with $SHIV_{VifAAQYLA}$ (RAK10, ● ; RCS10, ◆ ; RPL10, ▲). (Panel B) Plasma viral loads in four macaques (2000, ● ; CEM4G, ■ ; CEM4K, ▲ ; and RRH10, ▼) following inoculation with $SHIV_{KU\text{-}1bMC33}$.

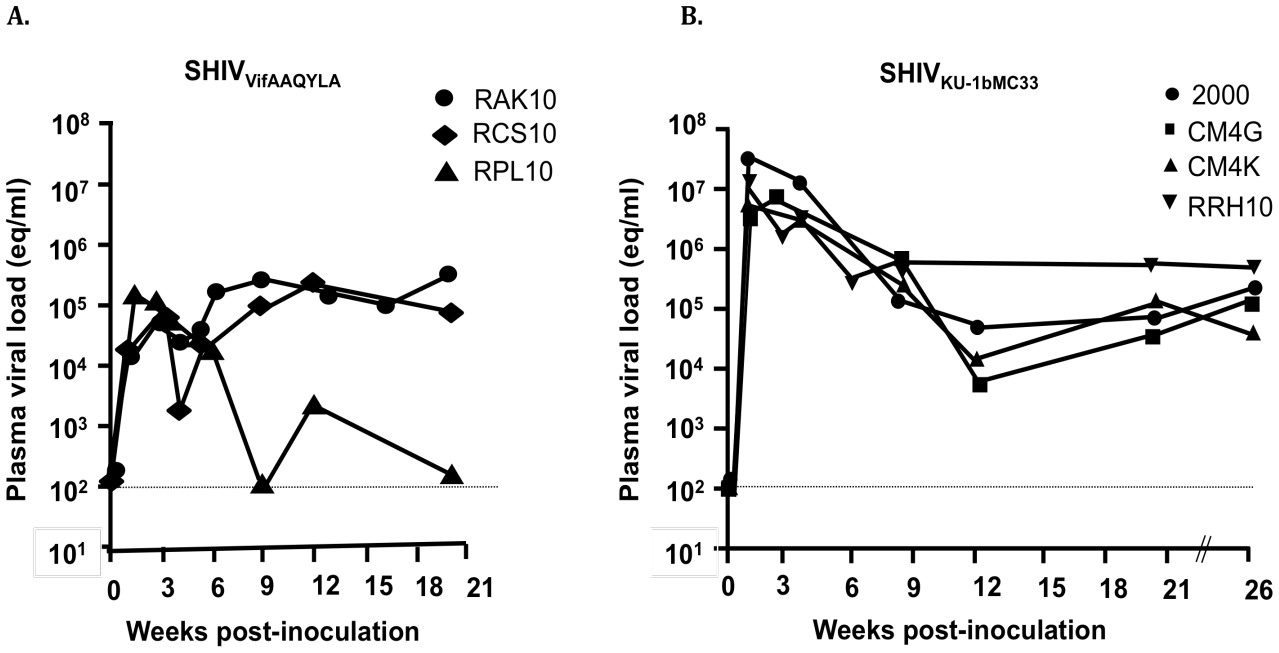
A.
SHIV VifAAQYLA
RAK10
RCS10
RPL10
Plasma viral load (eq/ml)
10^8
10^7
10^6
10^5
10^4
10^3
10^2
10^1
0 3 6 9 12 15 18 21
Weeks post-inoculation
B.
SHIV KU-1bMC33
2000
CM4G
CM4K
RRH10
Plasma viral load (eq/ml)
10^8
10^7
10^6
10^5
10^4
10^3
10^2
10^1
0 3 6 9 12 15 18 21 26
Weeks post-inoculation

Figure 18. Analysis of the *vif* gene for the stability of the engineered mutations. DNA was isolated from PBMC at 1, 3, 4, 8, 12, and 28 weeks post-inoculation and from lymphoid tissues (thymus, mesenteric lymph node and inguinal lymph node) at necropsy. The *vif* gene was amplified and directly sequence. Shown at the top are the sequences for both parental $SHIV_{KU\text{-}1bMC33}$ and $SHIV_{VifAAQYLA}$. Amino acids depicted in red indicate the A147T mutation and the amino acids shown in blue indicate the maintained S147A amino acid substitution.

	S	L	Q	Y	L	A
$SHIV_{KU-1bMC33}$	**147-**AGCCTACAGTACTTAGCA **– 152**					
$SHIV_{VifAAQYLA}$	A	A	Q	Y	L	A
Macaque RAK10						
PBMC/week 1	A	A	Q	Y	L	A
PBMC/week 3	A	A	Q	Y	L	A
PBMC/week 4	T	A	Q	Y	L	A
PBMC/week 8	T	A	Q	Y	L	A
PBMC/week 12	T	A	Q	Y	L	A
PBMC/Necropsy	T					
Thymus	T	A	Q	Y	L	A
Mesenteric LN	A	A	Q	Y	L	A
Ing. LN	T	A	Q	Y	L	A
Macaque RCS10						
PBMC/week 1	A	A	Q	Y	L	A
PBMC/week 3	A	A	Q	Y	L	A
PBMC/week 4	A	A	Q	Y	L	A
PBMC/week 8	A	A	Q	Y	L	A
PBMC/week 12	A	A	Q	Y	L	A
Thymus	A	A	Q	Y	L	A
Mesenteric LN	A	A	Q	Y	L	A
Ing. LN	A	A	Q	Y	L	A
Macaque RCS10						
PBMC/week 1	A	A	Q	Y	L	A
PBMC/week 3	A	A	Q	Y	L	A
PBMC/week 4	T	A	Q	Y	L	A
PBMC/week 8	T	A	Q	Y	L	A
PBMC/week 12	T	A	Q	Y	L	A
Thymus	T	A	Q	Y	L	A
Mesenteric LN	T	A	Q	Y	L	A
Ing. LN	T	A	Q	Y	L	A

Macaques inoculated with $SHIV_{VifAAQYLA}$ developed antibody responses against SHIV

At necropsy, we analyzed the plasma for the presence of immunoprecipitating antibodies against $SHIV_{KU\text{-}1bMC33}$. All three macaques developed immunoprecipitating antibody responses against $SHIV_{KU\text{-}1bMC33}$, although macaque RCS10 developed significantly lower antibody response compared to the other two macaques (Figure 19). In contrast, a macaque inoculated with parental $SHIV_{KU\text{-}1bMC33}$ (RRH10) did not develop antibodies to the virus, which is common for macaques that develop severe $CD4^+$ T cell loss during the acute phase (<4 weeks) following inoculation with pathogenic X4 SHIV (Figure 19).

Histological examination of tissues

Tissues from macaques were examined for the presence of histological lesions consistent with pathogenic X4 SHIV infection (Stephens et al., 2002). Histological examination of tissues from macaque RRH10, which was inoculated with $SHIV_{KU\text{-}1bMC33}$, revealed severe lymphoid depletion in both the thymus and lymph nodes and mild lymphoid depletion in the spleen (Figure 20). The lymphoid depletion observed in the macaques is consistent of that observed following inoculation with the parental $SHIV_{KU\text{-}1bMC33}$ (Stephens et al., 2002). The macaques inoculated with $SHIV_{VifAAQYLA}$ did not exhibit lesions in any of the 13 visceral organs and CNS. Micrographs of sections from the thymus, mesenteric lymph node, and spleen from macaque RAK10 are shown along with micrographs of histological sections from an uninfected macaque in Figure 20.

Figure 19. Macaques inoculated with $SHIV_{VifAAQYLA}$ developed antibody responses against SHIV. C8166 cells were inoculated with $SHIV_{KU\text{-}1bMC33}$ for 5 days, starved in methionine/cysteine-free media and radiolabeled overnight with ^{35}S-methionine/cysteine. The culture medium was harvested and used in immunoprecipitation reactions with plasma from RAK10, RCS10, RPL10 and RRH10 as described in the Experimental Methods. The immunoprecipitates were washed with 1x RIPA buffer, boiled in 2x sample reducing buffer and proteins separated on 10% SDS-PAGE gels. (Lane 1) SHIV proteins immunoprecipitated using supernatant from an uninfected culture. (Lane 2) SHIV proteins immunoprecipitated from a positive control plasma sample. (Lane 3) SHIV proteins immunoprecipitated using RAK10 plasma. (Lane 4) SHIV proteins immunoprecipitated using RCS10 plasma. (Lane 5). SHIV proteins immunoprecipitated using RPL10 plasma. (Lane 6) SHIV proteins immunoprecipitated using RRH10 plasma. The molecular weight standards are displayed on the left and specific SHIV proteins are shown on the right.

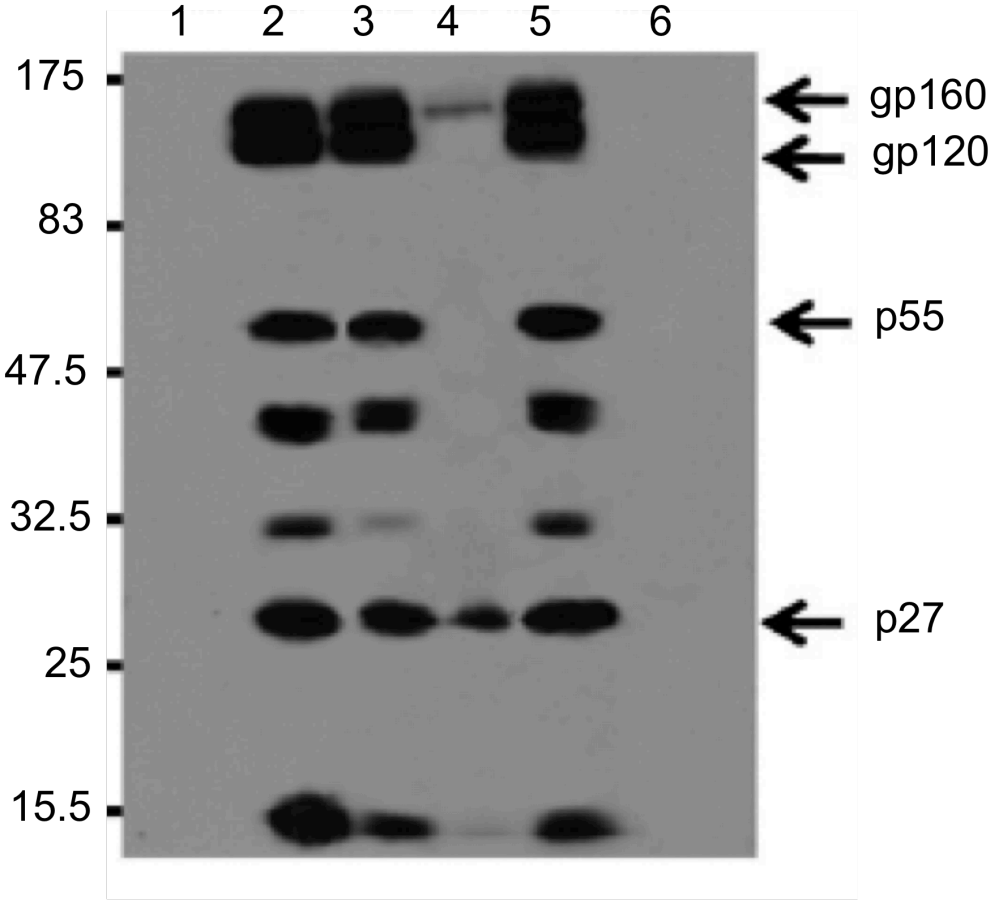
1
2
3
4
5
6
175
83
47.5
32.5
25
15.5
gp160
gp120
p55
p27

Figure 20. Histopathology associated with $SHIV_{VifAAQYLA}$ infection of macaques. Hematoxylin and eosin stains of section from the thymus (A-C), mesenteric lymph node (Panels D-F) and spleen (Panels G-I) from a $SHIV_{VifAAQYLA}$ inoculated macaque RAK10 (Panels A, D, and G), an uninfected macaque (Panels B, E and H) and a $SHIV_{KU\text{-}1bMC33}$ infected macaque RRH10 (Panels C, F, and I).

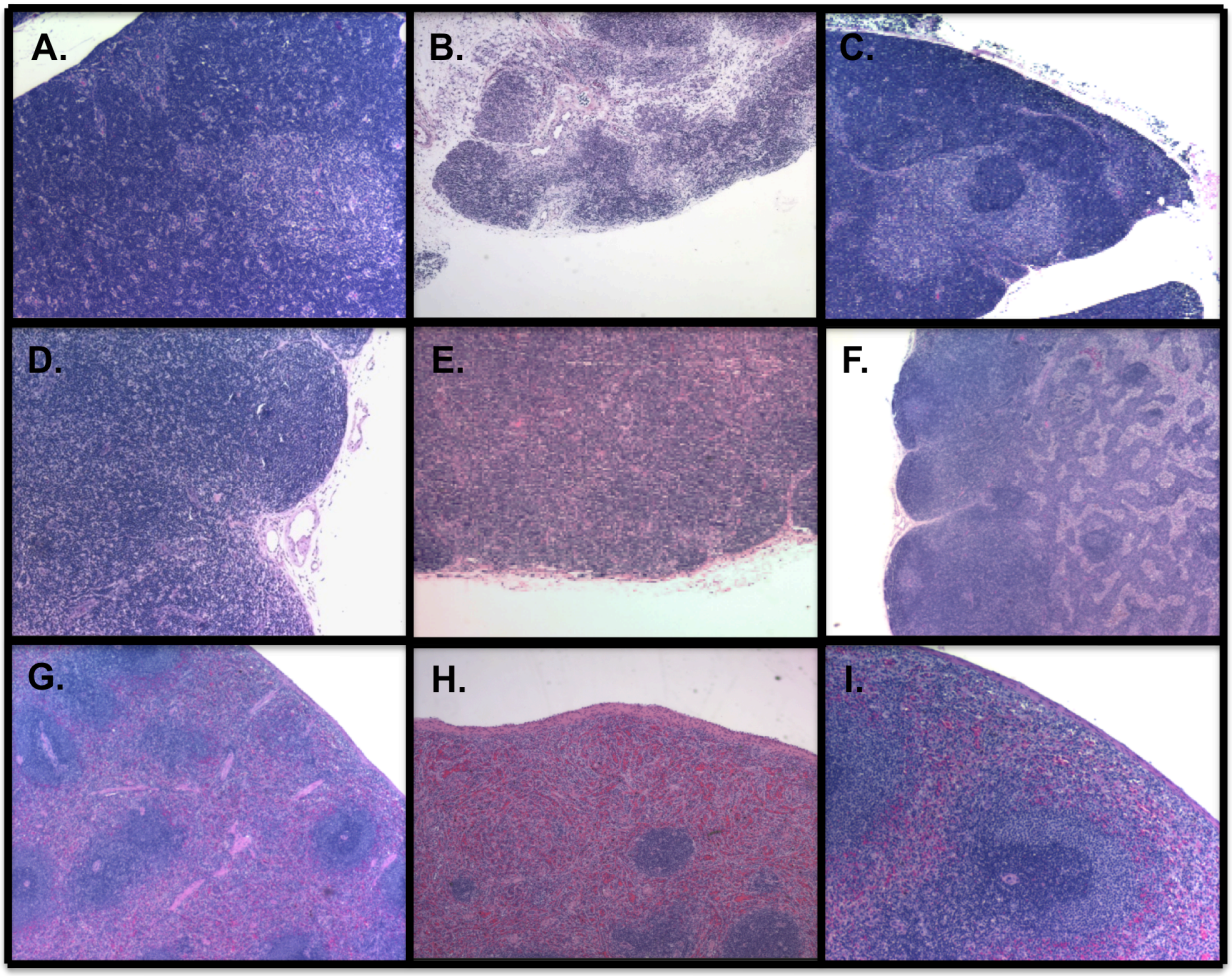
A.
B.
C.
D.
E.
F.
G.
H.
I.

Macaques inoculated with $SHIV_{VifAAQYLA}$ had decreased tissue distribution of replicating virus

Since the plasma viral loads were decreased in comparison to macaques inoculated with parental $SHIV_{KU\text{-}1bMC33}$, we were interested in determining if this effect was due to the infection of select cell populations in one or more organs, which may not express rhesus A3G. First, we analyzed DNA isolated from 13 visceral organs from $SHIV_{VifAAQYLA}$ macaques for the presence of viral *gag* sequences by nested DNA PCR. We found that 12 of the 13 visceral organs from a $SHIV_{KU\text{-}1bMC33}$ inoculated macaque (RRH10) were positive for viral *gag* sequences in DNA samples (Figure 21). For macaques inoculated with $SHIV_{VifAAQYLA}$, we found that 6 of the 13, 8 of the 13, and 12 of the 13 organs from macaques RAK10, RCS10 and RPL10, respectively, were positive for viral *gag* sequences by nested DNA PCR (Figure 21). The majority of the organs that were *gag* positive were lymphoid organs. We next assessed RNA isolated from these tissues for the presence of viral *gag* RNA sequences using RT-PCR. The results of this analysis are shown in Figure 22. We found that 5 of 13, 6 of 13, and 9 of 13 visceral organs from macaques RAK10, RCS10 and RPL10 were positive for viral *gag* RNA sequences, respectively. A macaque inoculated with $SHIV_{KU\text{-}1bMC33}$ (RRH10) had 11 of the 13 organs positive for the presence of *gag* RNA sequences. Taken together, these results indicate that the $SHIV_{VifAAQYLA}$ infection was less widespread in 2 or the 3 macaques compared to a macaque inoculated with parental $SHIV_{KU\text{-}1bMC33}$.

Figure 21. Macaques inoculated with $SHIV_{VifAAQYLA}$ had a decreased tissue distribution of proviral DNA. DNA was isolated from different organs as indicated at necropsy and amplified using nested DNA PCR and oligonucleotides specific for *gag*. Samples were run on a 1.5% agarose gel, stained with ethidium bromide, and photographed. Shown are the results of the nested DNA PCR reaction using DNA from macaques RRH10 (Panel A), RAK10 (Panel B), RCS10 (Panel C) and RPL10 (Panel D). The tissues DNAs analyzed are noted above each lane and the 100 base pair marker is indicated on the right. The positive control was *gag* amplified from lymph node tissue obtained from macaque 50O that died of neuroAIDS (McCormick-Davis et al., 2000) and the negative control was spleen tissue DNA from an uninfected macaque.

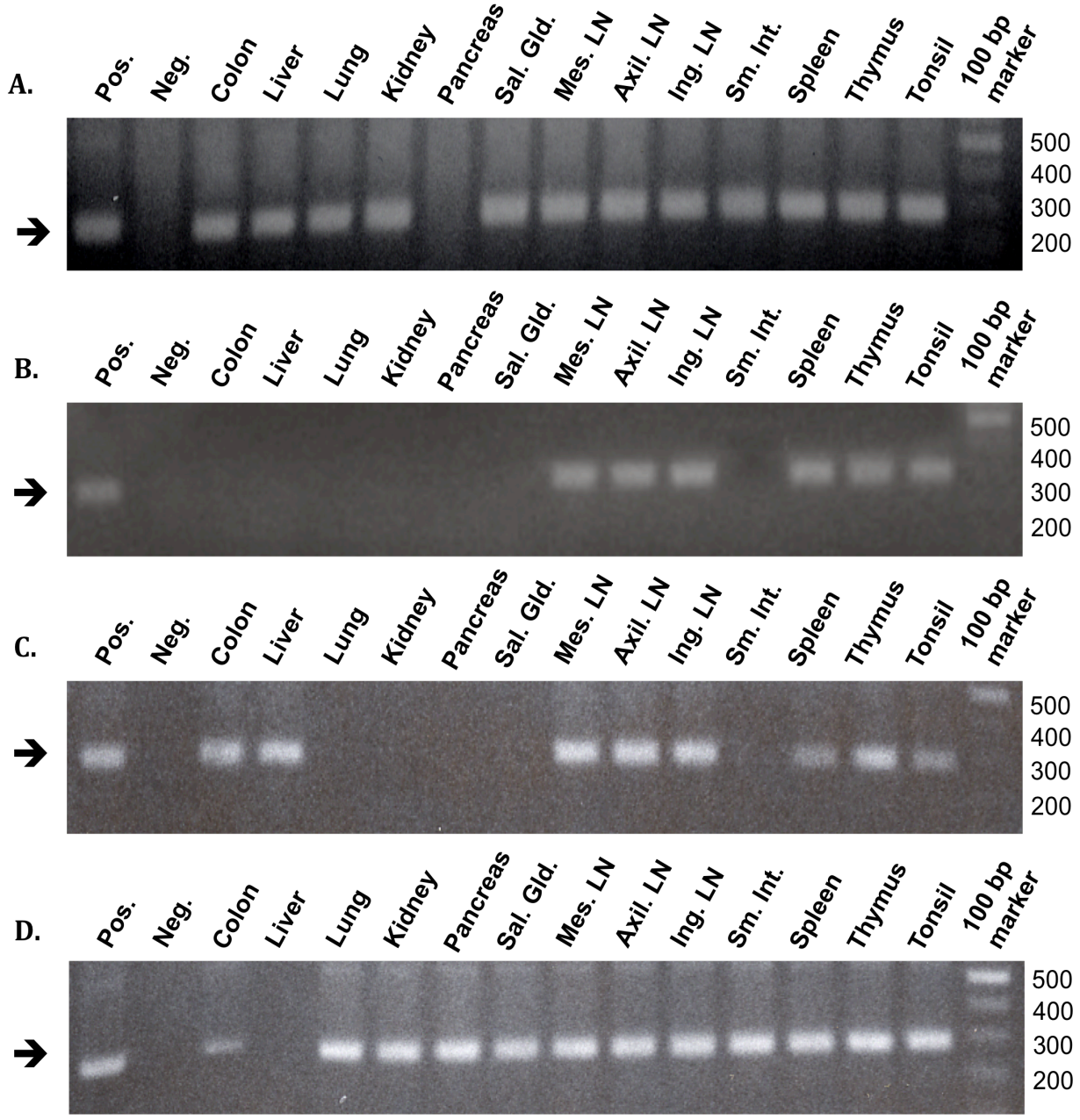
A.
Pos.
Neg.
Colon
Liver
Lung
Kidney
Pancreas
Sal. Gld.
Mes. LN
Axil. LN
Ing. LN
Sm. Int.
Spleen
Thymus
Tonsil
100 bp marker
500
400
300
200
B.
Pos.
Neg.
Colon
Liver
Lung
Kidney
Pancreas
Sal. Gld.
Mes. LN
Axil. LN
Ing. LN
Sm. Int.
Spleen
Thymus
Tonsil
100 bp marker
500
400
300
200
C.
Pos.
Neg.
Colon
Liver
Lung
Kidney
Pancreas
Sal. Gld.
Mes. LN
Axil. LN
Ing. LN
Sm. Int.
Spleen
Thymus
Tonsil
100 bp marker
500
400
300
200
D.
Pos.
Neg.
Colon
Liver
Lung
Kidney
Pancreas
Sal. Gld.
Mes. LN
Axil. LN
Ing. LN
Sm. Int.
Spleen
Thymus
Tonsil
100 bp marker
500
400
300
200

Figure 22. Macaques inoculated with $SHIV_{VifAAQYLA}$ had a decreased tissue distribution of viral RNA. RNA was isolated from 13 different visceral organs obtained at necropsy. The RNA was DNase I treated to remove residual DNA and used in a nested RT-PCR reaction with oligonucleotides specific for *gag*. Samples were run on a 1.5% agarose gel, stained with ethidium bromide and photographed. The results are shown as follows: Macaques RRH10 (Panel A), RAK10 (Panel B), RCS10 (Panel C) and RPL10 (Panel D). The tissue RNAs analyzed are noted above each lane. The positive control was amplified from lymph node tissue obtained from macaque 50O that died of neuroAIDS (McCormick-Davis et al., 2000). The negative control was spleen RNA isolated from an uninfected macaque. The 100 bp marker is indicated on the right.

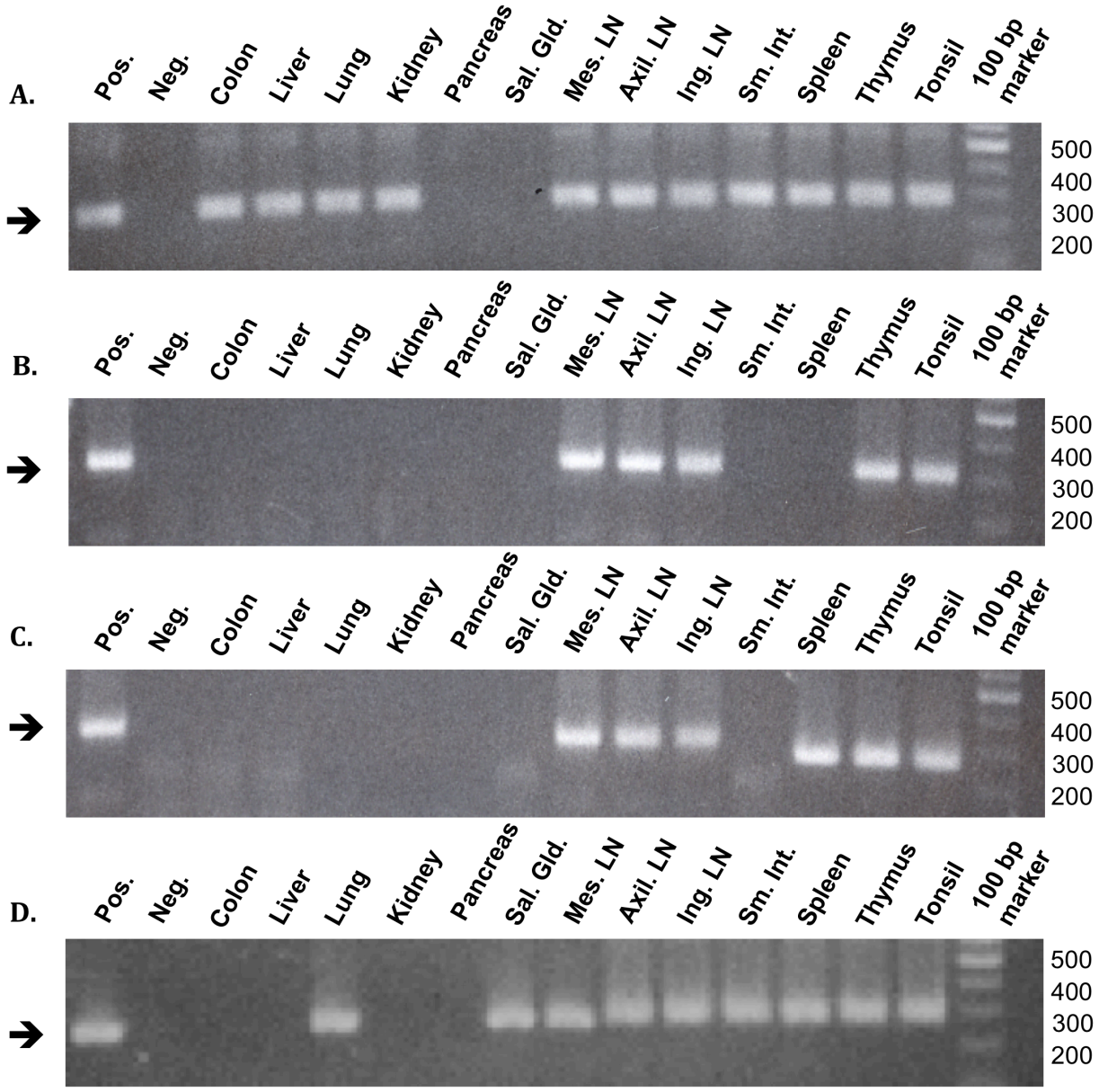
A.
Pos.
Neg.
Colon
Liver
Lung
Kidney
Pancreas
Sal. Gld.
Mes. LN
Axil. LN
Ing. LN
Sm. Int.
Spleen
Thymus
Tonsil
100 bp marker
500
400
300
200
B.
Pos.
Neg.
Colon
Liver
Lung
Kidney
Pancreas
Sal. Gld.
Mes. LN
Axil. LN
Ing. LN
Sm. Int.
Spleen
Thymus
Tonsil
100 bp marker
500
400
300
200
C.
Pos.
Neg.
Colon
Liver
Lung
Kidney
Pancreas
Sal. Gld.
Mes. LN
Axil. LN
Ing. LN
Sm. Int.
Spleen
Thymus
Tonsil
100 bp marker
500
400
300
200
D.
Pos.
Neg.
Colon
Liver
Lung
Kidney
Pancreas
Sal. Gld.
Mes. LN
Axil. LN
Ing. LN
Sm. Int.
Spleen
Thymus
Tonsil
100 bp marker
500
400
300
200

Sequence changes in *vif, vpu, env* and *nef* in primary and secondary lymphoid organs at necropsy

Previous research has shown that HIV-1Δ*vif* incorporates select A3 proteins into viral particles leading to cytosine deamination in the minus strand during DNA synthesis (Sheehy et al., 2002; Bishop et al., 2004). Hypermutation in HIV-1 reverse transcripts display a high frequency of G-to-A substitutions in the plus strand of DNA resulting in inhibition of virus replication (Harris et al., 2003; Mangeat et al., 2003; Zhang et al., 2003). We examined the extent of G-to-A mutations in viral DNA amplified from one primary lymphoid organ (thymus) and several secondary lymphoid organs (mesenteric, axillary, and inguinal lymph nodes) from three macaques inoculated with $SHIV_{VifAAQYLA}$ and one macaque inoculated with $SHIV_{KU\text{-}1bMC33}$ (RRH10). We analyzed sequences from the *vif, vpu, env,* and *nef* genes. The results of the sequence analysis are shown in Table III. These analyses showed that: a) with the exception of *env*, the thymus consistently had the lowest percentage of G-to-A substitutions; b) not all lymphoid organs had significant G-to-A substitutions; and c) greater than 85% of the G-to-A mutations were in the context of T<u>C</u> and not C<u>C</u>. The sequence of *vpu* amplified from the lymphoid tissues of macaque RPL10 is shown as an example in Figure 23. Macaque RRH10 had the fewest G-to-A substitutions in all of the lymphoid organs, which is similar to other macaques inoculated with $SHIV_{KU\text{-}1bMC33}$ (unpublished observations). The percentage of mutations was approximately <0.2-0.41% of the nucleotides analyzed for macaque RRH10. The highest percentage of G-to-A substitutions was found in the *nef* gene of macaque RCS10 inoculated with $SHIV_{VifAAQYLA}$ (5.0%).

Table III. Results of viral DNA sequence analysis from visceral tissues at necropsy

Macaque/ gene	Tissue			
	Thymus	MLN	ALN	ILN
RRH10				
vif	1/466 (0.21%)[a]	1/466 (0.21%)	1/466 (0.21%)	1/466 (0.21%)
vpu	2/246 (0.0%)	1/246 (0.4%)	1/246 (0.4%)	1/246 (0.4%)
env	2/490 (0.41%)	0/490 (0.0%)	0/480 (0.0%)	0/480 (0/0%)
nef	1/400 (0.25%)	1/400 (0.25%)	2/400 (0.50%)	0/400 (0.0%)
RAK10				
vif	0/466 (0.00%)	16/466 (3.4%)	7/400 (1.50%)	1/466 (0.21%)
vpu	1/246 (0.4%)	4/246 (0.4%)	4/246 (1.63%)	4/246 (1.63%)
env	12/490 (2.44%)	10/490 (2.04%)	12/490 (2.44%)	10/490 (2.04%)
nef	2/400 (0.50%)	1/400 (0.25%)	17/400 (4.25%)	1/400 (0.25%)
RCS10				
vif	0/466 (0.0%)	1/466 (0.21%)	8/466 (3.25%)	1/466 (0.21%)
vpu	1/246 (0.4%)	1/246 (0.4%)	4/246 (1.62%)	2/246 (0.8%)
env	10/490 (2.04%)	8/490 (1.63%)	10/490 (2.04%)	12/490 (2.44%)
nef	1/400 (0.25%)	20/400 (5.00%)	2/400 (0.5%)	1/400 (0.25%)
RPL10				
vif	3/466 (0.64%)	6/466 (1.28%)	9/466 (1.93%)	8/466 (1.72%)
vpu	3/246 (1.2%)	6/246 (2.4%)	9/246 (3.70%)	8/246 (3.3%)
env	9/490 (1.83%)	8/490 (1.63%)	8/490 (1.63%)	8/490 (1.63%)
nef	1/400 (0.25%)	2/400 (0.5%)	6/400 (1.25%)	4/400 (1.0%)

The ratio of the number of G-to-A nucleotide substitutions/number of bases sequenced is shown.

[a] The percentage of G-to-A substitutions are in parentheses.

Figure 23. Sequence of the *vpu* gene amplified from lymphoid tissues of macaque RPL10. Shown on the top line is the input sequence of *vpu* from $SHIV_{KU\text{-}1bMC33}$. The (.) represents identity with the nucleotide sequence shown above. The underlined sequences represent the context in which the G-to-A substitutions occurred.

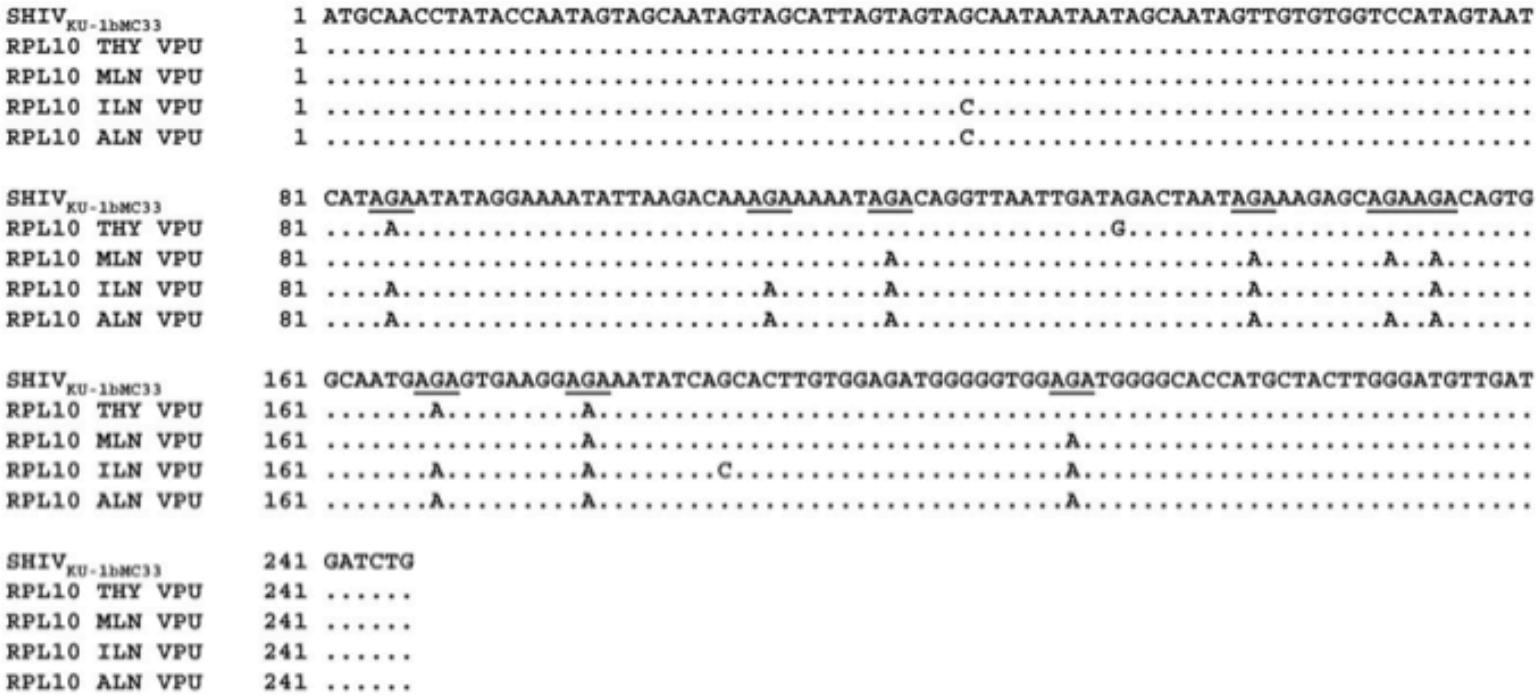
SHIV KU-1bMC33 1 ATGCAACCTATACCAATAGTAGCAATAGTAGCATTAGTAGTAGCAATAATAATAGCAATAGTTGTGTGGTCCATAGTAAT
RPL10 THY VPU 1 .....
RPL10 MLN VPU 1 .....
RPL10 ILN VPU 1 .....C.....
RPL10 ALN VPU 1 .....C.....
SHIV KU-1bMC33 81 CATAGAATATAGGAAAATATTAAGACAAAGAAAAATAGACAGGTTAATTGATAGACTAATAGAAAGAGCAGAAGACAGTG
RPL10 THY VPU 81 ....A.....G.....
RPL10 MLN VPU 81 .....A.....A.....A..A.....
RPL10 ILN VPU 81 ....A.....A.....A.....A.....A.....
RPL10 ALN VPU 81 ....A.....A.....A.....A.....A..A.....
SHIV KU-1bMC33 161 GCAATGAGAGTGAAGGAGAAATATCAGCACTTGTGGAGATGGGGGTGGAGATGGGGCACCATGCTACTTGGGATGTTGAT
RPL10 THY VPU 161 .....A.....A.....
RPL10 MLN VPU 161 .....A.....A.....
RPL10 ILN VPU 161 .....A.....A.....C.....A.....
RPL10 ALN VPU 161 .....A.....A.....A.....
SHIV KU-1bMC33 241 GATCTG
RPL10 THY VPU 241 .....
RPL10 MLN VPU 241 .....
RPL10 ILN VPU 241 .....
RPL10 ALN VPU 241 .....

Pooled plasma from two macaques inoculated with $SHIV_{VifAAQYLA}$ contained low levels of infectious virus when transfused into a naïve macaque

In order to determine if infectious virus was present in plasma that was not detected in our infectivity assays, plasma from macaques RAK10 and RPL10 was pooled and intravenously inoculated into a naïve macaque, I95. We were able to detect viral *gag* sequences in DNA isolated from PBMC at 0, 1, 2, 3, 4, 5, 6, and 20 weeks post-inoculation (Figure 25). We also assessed plasmas from macaque I95 for viral loads using real-time PCR from weeks 0 to 20. We were unable to detect viral burdens in macaque I95. The level of circulating $CD4^+$ T cells did not decrease from the pre-inoculation levels (Figure 24). We were unable to detect antibodies in the plasma from this macaque at week 9 (data not shown). At 20 weeks post-inoculation, macaque I95 was sacrificed. DNA was isolated from PBMC at various time points throughout the duration of infections and from 10 visceral organs and used in a nested PCR to detect viral *gag* sequences. Viral *gag* sequences were amplified from all 10 visceral organs examined (Figure 26). We also isolated RNA from the same organs for use in RT-PCR to detect viral *gag* RNA sequences. The viral RNA was detected in six organs (liver, kidney, axillary lymph node, small intestine (ileum), spleen, and tonsil) (Figure 27). This indicates that some level of viral replication was ongoing although we were unable to isolate infectious virus on CEM-SS and SupT1 cells (data not shown). Taken together, these results indicate that pooled plasma contained only low levels of infectious virus that were controlled by the immune system of macaque I95.

Figure 24. Viral loads and circulating $CD4^+$ T cell levels in macaque I95 that was intravenously inoculated with pooled plasma from macaques RAK10 and RPL10 obtained at necropsy. Blood was obtained at 0 (just prior to inoculation), 1, 2, 3, 4, 5, 6 and 20 weeks after inoculation. Results of the real-time PCR for viral *gag* sequences from plasma samples (▲ ; scale to left) and circulating $CD4^+$ T cell levels (● ; scale to right).

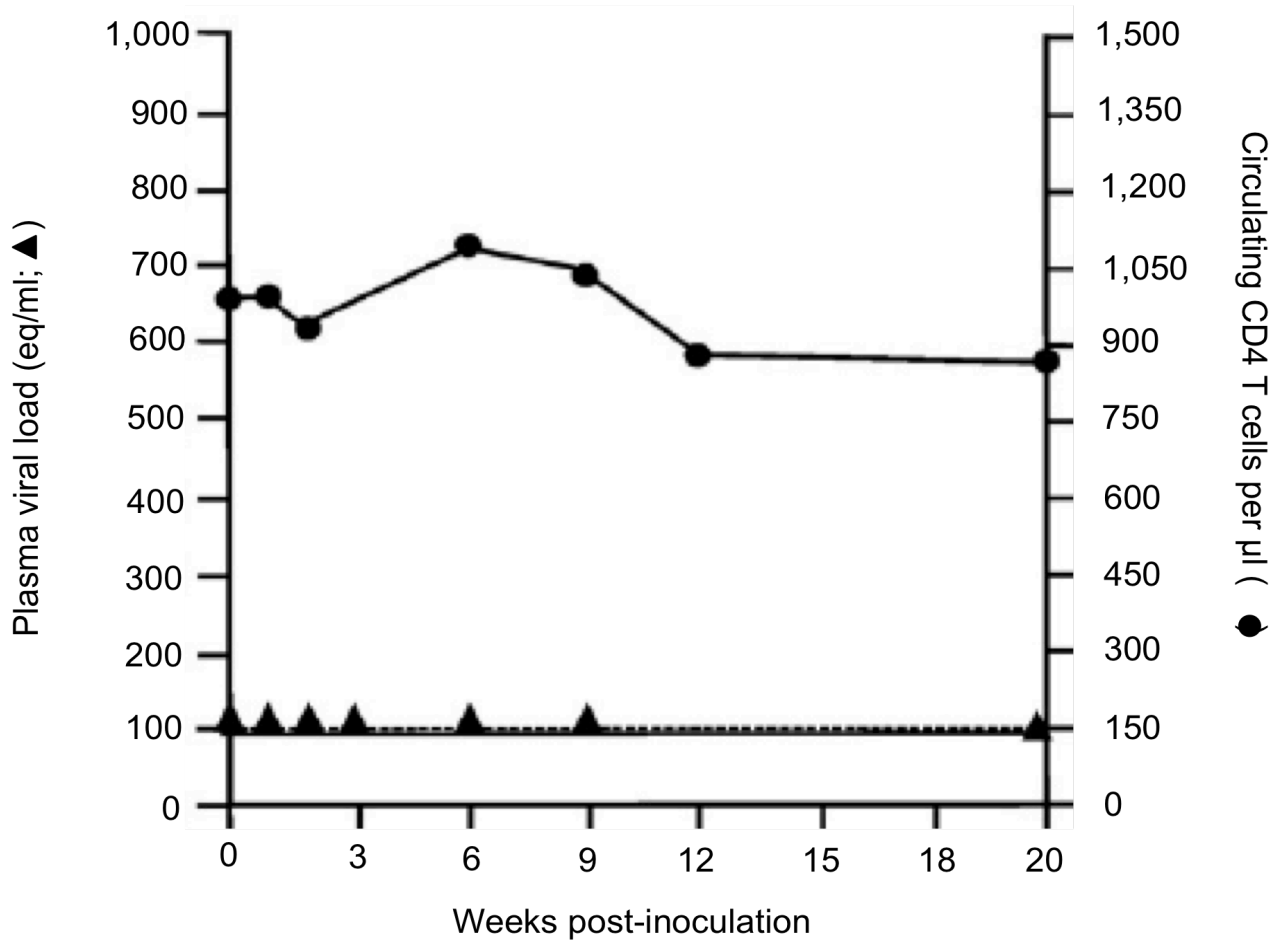
Plasma viral load (eq/ml; ▲)
1,000
900
800
700
600
500
400
300
200
100
0
1,500
1,350
1,200
1,050
900
750
600
450
300
150
0
Circulating CD4 T cells per µl (
0
3
6
9
12
15
18
20
Weeks post-inoculation

Figure 25. Presence of viral DNA sequences in PBMC from macaque 195. PBMC were purified over Ficoll-Hypaque gradients and total cellular DNA was isolated. DNA was used in a nested DNA PCR for viral *gag*. (Lane 1) 100 base pair marker. (Lane 2) Positive control, week 1 PBMC DNA from macaque RRH10 (inoculated with $SHIV_{KU\text{-}1bMC33}$. (Lane 3-10) Represent *gag* sequences amplified from PBMC isolated from I95 at 0, 1, 2, 3, 4, 5, 6, and 20 weeks post-inoculation, respectively.

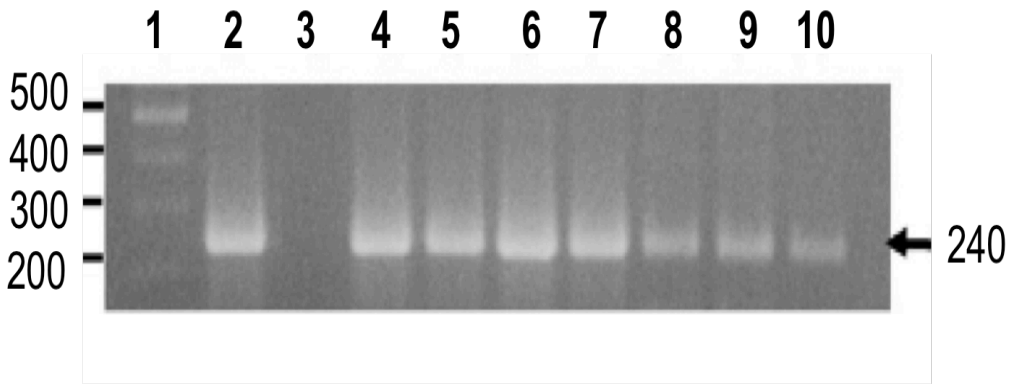
1 2 3 4 5 6 7 8 9 10
500
400
300
200
240

Figure 26. Distribution of viral DNA *gag* sequences in tissues from macaque I95. At necropsy tissues were harvested, DNA isolated and a nested PCR for *gag* run. (Lane 1) Positive control, lymph node tissue DNA from macaque 50O that died of neuroAIDS (McCormick-Davis et al., 2000). (Lane 2) Negative control, spleen tissue DNA from an uninfected macaque. (Lane 3) Liver. (Lane 4) Lung. (Lane 5) Kidney. (Lane 6) Mesenteric lymph node. (Lane 7) Axillary lymph node. (Lane 8) Ingunial lymph node. (Lane 9) Small intestine (ileum). (Lane 10) Spleen. (Lane 11) Thymus. (Lane 12) Tonsil. (Lane 13) 100 base pair marker.

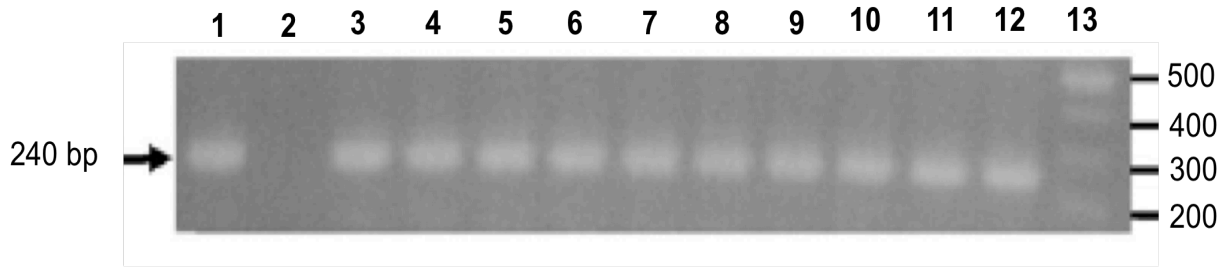
1
2
3
4
5
6
7
8
9
10
11
12
13
240 bp
500
400
300
200

Figure 27. Distribution of viral RNA gag sequences in tissues from macaque I95. At necropsy, tissues were harvested for total RNA and a nested RT-PCR for *gag* was run. (Lane 1) 100 base pair marker. (Lane 2) Positive control, lymph node tissue RNA from macaque 50O that died of neuroAIDS (McCormick-Davis et al., 2000). (Lane 3) Negative control, spleen tissue DNA from an uninfected macaque. (Lane 4) Liver. (Lane 5) Lung. (Lane 6) Kidney. (Lane 7) Mesenteric lymph node. (Lane 8) Axillary lymph node. (Lane 9) Inguinal lymph node. (Lane 10) Small intestine (ileum). (Lane 11) Spleen. (Lane 12) Thymus. (Lane 13) Tonsil.

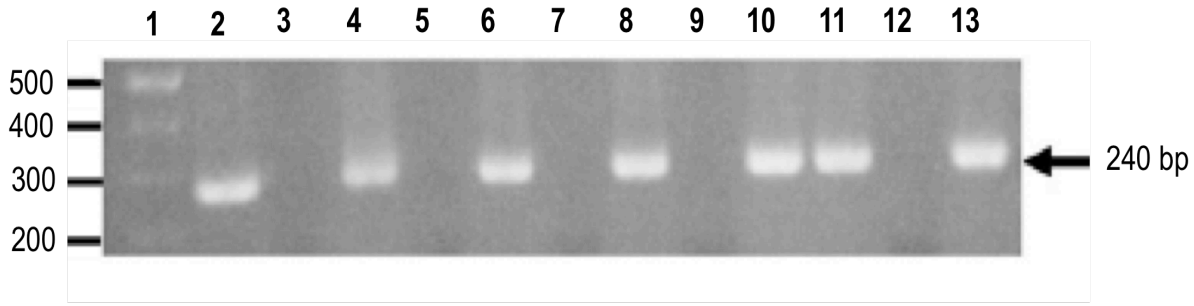
1
2
3
4
5
6
7
8
9
10
11
12
13
500
400
300
200
240 bp

Discussion

The results presented in this publication are the first to evaluate the role of domain-specific mutations in the BC box domain of the *vif* gene using a non-human primate model of HIV-1/AIDS. Previous studies have shown that the BC box domain of HIV-1 Vif (SLQYLALAAL) interacts with elongin C, which contains the consensus sequence $(A, P, S, T)_1L_2xxx(C, A, S)_6xxx(A, I, L, V)_{10}$ with the leucine at position 2 being invariant (Luo et al., 2005; Mehle et al., 2004). The invariant leucine at position 2 of the BC box domain is critical because mutation of this amino acid to an alanine prevents the interaction between Vif and elongin C preventing assembly of the E3 ubiquitin Ligase complex (Kobayashi et al., 2005; Yu et al., 2003; Yu et al., 2004a, 2004b, 2004c). Since the S147 and L148 amino acid residues of the SLQYLALAAL domain are highly conserved among primate lentivirus Vif proteins, we chose to mutate these amino acid residues to alanine residues. The results from this study indicate that macaques inoculated with $SHIV_{VifAAQYLA}$ developed no significant loss of circulating $CD4^+$ T cells and had a 100-fold lower plasma viral loads during the acute phase of infection, when compared to macaques inoculated with $SHIV_{KU\text{-}1bMC33}$. Additionally, our analyses revealed fewer tissues positive for viral *gag* DNA and RNA sequences in 2 of the 3 macaques inoculated with $SHIV_{VifAAQYLA}$, suggesting that $SHIV_{VifAAQYLA}$ was controlled by the host. This could be due to the presence of susceptible cells expressing one or more of the A3 proteins that could restrict a virus containing mutations such as these. The presence of plasma viral loads in these macaques indicates that virus may have persisted in populations of cells that either did not express A3 proteins or expressed these proteins at very low levels.

Thus, a major question that emerged was, “Are the viruses produced from these cellular reservoirs infectious, replication competent viruses?” In order to detect small amounts of virus that we were unable to see in our infectious centers assay (data not shown), we inoculated a naïve macaque, I95, with plasma pooled from 2 of the 3 macaques inoculated with $SHIV_{VifAAQYLA}$. Macaque I95 revealed the presence of virus in PBMCs between weeks 1 to 20 and in 10 tissues (liver, lung, kidney, mesenteric lymph node, axillary lymph node, inguinal lymph node, ileum, spleen, thymus, and tonsil) examined at necropsy, although the plasma viral loads were below the limits of detection (Figure 25). These results suggested that plasma from the $SHIV_{VifAAQYLA}$ inoculated macaques had infectious virus, but the macaques readily controlled the virus.

While none of the three macaques inoculated with $SHIV_{VifAAQYLA}$ exhibited histological lesions, there were two incongruent observations. First, macaque RPL10 had the lowest viral loads but also had the most widespread visceral tissue distribution of viral *gag* sequences. While the reason for this result is unclear, it could be explained by a greater viral distribution during the early stage of infection. Second, macaques RCS10 developed less immunoprecipitating antibodies compared with macaques RAK10 and RPL10. Although the answer to this question is currently unknown, if could relate to the inability of RCS10 to select for the A147T amino acid substitution. Perhaps the A147T substitution permitted more replication in macaques RAK10 and RPL10 providing a better antigenic stimulus. It should also be noted that $SHIV_{VifTAQYLA}$ from RAK10 and RPL10 could not be isolated. Therefore, we do not know if a virus with the ^{146}TAQYLALAAL^{155} motif is capable of causing CD4+ T cell loss, histological lesions or high viral burdens.

Our sequence analysis indicated that not all viral genes amplified from the lymphoid tissues contained G-to-A substitutions above background levels. For the three macaques inoculated with $SHIV_{VifAAQYLA}$, a total of four lymph tissues (thymus, mesenteric, axillary, and inguinal lymph nodes) and four viral genes (*vif, vpu, env,* and *nef*) were assessed (Table III). Approximately half (25) of the 48 sequences contained G-to-A substitutions that were above 1.2% with the majority of the substitutions being in the context of 5'-TC. Potential reasons for this may include that the aliquot of tissue examined may have contained archived virus from the initial round of infection, the viruses amplified were from a cell type that did not express A3G, or that the domain-specific mutations may have crippled but not completely abolished the antiviral activity of Vif. Alternatively, it is possible that both deaminase-dependent and deaminase-independent mechanisms of restriction may be present to decrease the replication of $SHIV_{VifAAQYLA}$ in macaques. The context of the G-to-A substitutions identified in viral sequences can provide insight into which A3 members are involved in cytidine deamination. For instance, human A3G is known to cause cytidine deamination with a base preference of 5'-CC, while A3F, A3H and A3A have a preference for 5'-TC (Beale et al., 2004; Langolis et al., 2005; Liddament et al., 2004; Thielen et al., 2010). However, A3D has a preference for 5'-T/A-T/A-C-G/T and A3B and A3C favor both 5'-TC and 5'-CC (Dang et al., 2007; Doehle et al., 2005; Yu et al., 2004). This indicates that most likely an A3 protein other than A3G is causing the majority of the mutations we observed.

Attenuated viruses have been used to prevent many viral diseases in humans (smallpox, poliovirus, measles, mumps, rubella, chickenpox etc.). It is known that live,

attenuated virus vaccines generally result in better immune responses (both humoral and cell mediated) that are longer lived when compared to killed virus vaccines. However, the major drawback of attenuated virus vaccines is that live viruses are genetic elements and replication can introduce mutations that result in reversion of the attenuated phenotype to a pathogenic phenotype. The prime example of this is the live attenuated poliovirus vaccine (Kew et al., 2005). The major concern for the use of attenuated lentiviruses has been that it involved the removal of "non-essential" viral genes such as *vpr*, *vpx*, *nef* or *vpu*, which could allow for low level virus replication and the accumulation of compensatory mutations in other gene and potentially a reversion to a pathogenic phenotype. The work by Daniel and colleagues (1992) showed that deletion of the *nef* from the pathogenic $SIV_{mac}239$ resulted in an attenuated virus that resisted challenge against pathogenic parental virus. However, the hope that an attenuated vaccine approach was soon diminished by the studies showing that inoculation of a $SIV_{mac}239$ derivative with deletions in *vpr*, *nef* and the negative regulatory element (NRE) could cause AIDS in neonatal macaques (Baba et al., 1995). This was followed with a study showing that the same virus could cause disease in both neonatal and adult macaques (Baba et al., 1999). Despite these setbacks, the vaccines against SIV (or HIV-1) infection that have shown the most promise have been those that have deleted or inactivated one or more genes of the virus (Koff et al., 2006). In contrast to Vpr, Vpx, Vpu and Nef, the Vif protein is required for replication in $CD4^+$ T cells and macrophages, the two major cell populations that HIV-1 infects productively (Chiu and Greene, 2008). This suggests that mutations that target one or more conserved (and functional) domains within Vif may permit limited replication and

generation of effective immune responses against the virus prior to “self inactivation” through the activities of various APOBEC3 family members and may represent a novel means to attenuate lentiviruses for candidate vaccines.

Experimental Methods

Cells, Plasmids, and Viruses

The CEM and CEM-SS lymphocyte cell lines obtained from the NIH AIDS Research and Reagents Program were used for the production of viral stocks, the measure of infectivity and the cytopathicity of the viruses used in this study (Salter et al., 1985; Foley et al., 1965; Nara et al., 1987; Nara et al., 1988). CEM, CEM-SS, and C8166 cell lines were maintained in RPMI-1640 supplemented with 10 mM Hepes buffer pH 7.3, 10% fetal bovine serum (R10FBS), 5 μg/mL gentamicin, and 1% penicillin/streptomycin. The derivation of $SHIV_{KU\text{-}1bMC33}$ has been previously described (McCormick-Davis et al., 2000; Stephens et al., 2002).

Proviral DNA Plasmid Construction

For the construction of $SHIV_{VifAAQYLA}$, a PacI/SphI fragment (nucleotides 4609 to 5901) from the p5’SHIV-4 was subcloned into the pGEM3Zf (+) vector. The serine at amino acid position 147 of Vif was substituted to an alanine using oligonucleotides (only sense strand shown) 5’-AAGTACCAGGTACCAGCCCTACAGTACTTA-3’ and the Quick-Change Mutagenesis Kit (Stratagene) according to the manufacturer’s instructions. The resulting plasmid, pGEM3Zf (+)-PacI/SphI Vif_{AAQYLA}, was used to

change the leucine at amino acid position 148 of Vif to an alanine using oligonucleotides (sense strand shown) 5'-ACCAGGTACCAGCCGCACAGTACTTAGCAC-3' and the Quick-Change Mutagenesis Kit (Stratagene) according to the manufacturer's instructions. The resulting plasmid, pGEM3Zf (+)-Vif_{AAQYLA}, was purified and digested with PacI/SphI. The isolated fragment was purified and subcloned into p5'SHIV-4 to generate p5'$SHIV_{VifAAQYLA}$. The proviral plasmid DNA was sequenced to determine if the desired mutations were introduced as expected. To generate virus, p5'$SHIV_{VifAAQYLA}$ and p3'SHIV were digested with SphI and the two plasmids were ligated together with T4 DNA Ligase (Promega). The resulting ligation was transfected into CEM-SS cells as previously described (Stephens et al., 2002; Hout et al., 2005; 2006). Stocks of $SHIV_{KU-1bMC33}$ and $SHIV_{VifAAQYLA}$ were harvested, tittered onto CEM-SS cells to determine the $TCID_{50}$/mL and stored at -86°C.

Replication of $SHIV_{VifAAQYLA}$ in both non-permissive and permissive cell lines

The replication of $SHIV_{VifAAQYLA}$ was assessed in CEM (A3G/F positive) and CEM-SS (A3G/F negative) cell lines. One million cells were infected with equivalent levels (50 ng) of parental $SHIV_{KU-1bMC33}$ or $SHIV_{VifAAQYLA}$ for 4 h at 37°C. The cells were centrifuged and washed 3 times to remove the inoculum and incubated in fresh medium at 37°C for 9 days. Aliquots of culture supernatants were obtained at 0, 1, 3, 5, 7 and 9 days post-inoculation. The level of p27 was assessed using a commercially available p27 antigen capture assay kits (Zeptometrix).

Virion Incorporation Assay

Plasmids containing the genomes of viruses $SHIV_{KU\text{-}1bMC33}$ and $SHIV_{VifAAQYLA}$ were co-transfected with human HA-APOBEC3G (HA-hA3G) into 293 cells using polyethylenimine transfection reagent (PEI; ExGen-500, Fermentas) along with a plasmid expressing HA-hA3G. At 48 hours, virus containing supernatants were harvested and clarified by low speed centrifugation. The clarified supernatant was then subjected to ultracentrifugation to pellet the virus (SW41 rotor 247,000 xg, 1 h). The pellet was resuspended in 1x PBS (137 mM NaCl, 2.7 mM KCl, 10 mM $Na_2HPO_4 \cdot 2H_2O$, 1.76 mM KH_2PO_4; pH 7.4). An aliquot was saved to determine the p27 content by a commercially available antigen capture assay (Zeptometrix). The remaining sample was boiled in 2x sample reducing buffer (125 mM Tris pH 6.8, 4% SDS, 10% glycerol, 0.006% bromophenol blue, 1% β-mercaptoethanol) and boiled for 5 minutes. Equivalent amounts of p27 were loaded on a 12% SDS-PAGE gel and transferred to PVDF membrane. HA-hA3G proteins were detected by Western blotting using an antibody directed against the HA tag (HA-probe, Santa Cruz) of HA3G. The blot was stripped in 1x stripping buffer (62.5 mM Tris-HCl, pH6.8 and 2% SDS in 1x PBS, pH 7.4) and reprobed using a rabbit polyclonal antibody specific for p27.

Macaques analyzed in this study

Five 1-1.5 year old pig-tailed macaques (*Macaca nemestrina:* 2000; CM4G; CM4K; RRH10) were intravenously inoculated with 1 ml of undiluted $SHIV_{KU\text{-}1bMC33}$ containing 10^4 $TCID_{50}$ per ml (titered in CEM cells). Three additional pig-tailed macaques (RPL10; RCS10; RAK10) were inoculated with 10^4 $TCID_{50}$ $SHIV_{VifAAQYLA}$ (tittered in CEM-SS cells). Twenty-four weeks post-inoculation, 2 ml of plasma was

pooled from macaques RPL10 and RAK10 and used to inoculate a naïve macaque, I95. The animals were all housed in the AAALAC-approved animal facility at the University of Kansas Medical Center. Blood was collected weekly for the first 4 weeks, then at 2-week intervals for the next month, and thereafter at monthly intervals.

Circulating $CD4^+$ T cells

The levels of circulating CD4+ T cells was assessed at 0, 1, 2, 3, 4, 6, 8, 12, 16, 20, 24, 28 weeks post-inoculation using FACs (Bectin Dickinson) analysis. T cell subsets were labeled with OKT4 (CD4; Ortho Diagnostics Systems, Inc.), SP34 (CD3; Pharmigen), or FN18 (CD3; Biosource International) monoclonal antibodies. The number of circulating CD4+ T cells were determined per μl. As a control for FACS analysis, T cell subsets from an uninfected macaque were always performed.

Processing of tissue samples at necropsy

At the time of euthanasia (28 weeks for those macaques inoculated with $SHIV_{VifAAQYLA}$ and 20 weeks for macaque I95), all animals in this study were anesthetized by administration of 10-mg/kg ketamine (IM) followed by intravenous administration of sodium Phenobarbital at 20-30 mg/kg. A laparotomy was performed and the animal exsanguinated by aortic canulation and perfused with one liter of cold Ringer's saline. All aspects of the animal studies were performed according to the institutional guidelines for animal care and use at the University of Kansas Medical Center. Lymphoid and non-lymphoid tissues (brain, heart, lungs, liver, kidney, pancreas, salivary glands, liver, spleen, thymus, small intestine, colon, tonsils, and

mesenteric, inguinal and axillary lymph nodes) were harvested in HBSS (HBSS; 0.137 M NaCl, 5.4 mM KCl, 0.25 mM Na_2HPO_4, 0.44 mM KH_2PO_4, 1.3 mM $CaCl_2$, 1.0 mM $MgSO_4$, 4.2 mM $NaHCO_3$) and aliquots of tissues were either fixed for histological analysis or snap frozen for DNA and RNA assays. Cells were isolated from the thymus, spleen, and mesenteric lymph node and used in an infectious centers assay to determine if infectious virus is present at the time of necropsy.

Histology

Tissues obtained from necropsy listed above were fixed in 10% neutral buffered-formalin, subdivided into smaller blocks, and processed for paraffin embedding. Five μm sections were stained with eosin and hematoxylin. The histological samples were examined for morphological abnormalities and lesions consistent with pathogenic X4 SHIV infection (Stephens et al., 2002).

Plasma viral loads

Plasma viral RNA loads were determined on RNA extracted from 0.5 ml of EDTA-treated plasma. Virus was pelleted using ultracentrifugation (Beckman SW55Ti, 110,000 x g, 2 h) and RNA extracted using the Qiagen viral RNA kit (Qiagen). RNA samples were analyzed by real-time RT-PCR using *gag* primers and a 5'FAM and 3'TAMRA labeled Taqman probe that was homologous to the SIV *gag* gene as previously described (Hofmann-Lehmann et al., 2000). Standard curves were prepared using a series of 12 ten-fold dilutions of viral RNA of known concentration. The sensitivity of the assay was 100 RNA equivalents per ml. Samples were analyzed in

triplicate and the number or RNA equivalents were calculated per ml of plasma. The limit of detection was 100 copies.

Analysis of tissues for viral DNA and RNA

DNA was extracted from the visceral organs listed above as previously described (Hill et al., 2008) and used in nested PCR to amplify SIV *gag* sequence. The 240 base pair amplified product was visualized through a 1.5% agarose gel stained with ethidium bromide. Viral RNA, which is indicative of actively replicating virus, was extracted from approximately 30 mg of each visceral or CNS tissue using the RNAEasy kit (Qiagen) and the manufacturer's instructions. RNA samples were digested with DNase I for 30 minutes and run on agarose formaldehyde gels to check for the presence of contaminating DNA. RT-PCR amplification of the extracted RNA was performed using the Titan One RT-PCR kit (Roche) and the manufacturer's instructions. Each reaction used one microgram of total RNA and was amplified using oligonucleotide primers specific for the $SIV_{mac}239$ *gag* gene. Each RT PCR reaction contained 50 ng of RNA, 0.1 mM dNTP mix, 5 mM DTT solution, 5U RNase inhibitor, 0.4 μM of each primer, 5X RT-PCR buffer, and 1U of Enzyme mix. The oligonucleotides used for the first round of amplification were 5'-CGTCATCTGGTGCATTCACG-3' (sense) and 5'-CTGATTAATGTCATAGGGGGTGC-3' (antisense), which are complementary to bases 1343-1362 and 1636-1658, respectively. The nested primers used were 5'-CACGCAGAAGAGAAAGTGAAACAC-3' (sense) and 5'-GGTGCAACCTTCTGACAGTGC-3' (antisense), which are correspond to bases 1359-1382 and 1620-40, respectively. The reactions were performed with an Applied

Systems 2720 Thermal Cycler using the following thermal profile: 42C for 30 min, 1 cycle; 94C for 2 min, 1 cycle; 94C for 30 s, 55C for 30 s, 68C for 45 s, 10 cycles; 94C for 30 s, 55C for 30 s, and 68C for 2 min; 25 cycles. One microliter of the initial reaction mixture was then added to a nested PCR mixture containing *gag* primers and performed with the following thermal profile: 95C for 10 min, 1 cycle; 30 s, 55C for 30 s, and 68C for 2 min; 35 cycles. The amplified *gag* fragment is 281 base pairs. β-actin was amplified from all of the tissue RNA samples as a control to verify the RNA integrity.

DNA sequence analysis of *vif, vpu, nef,* and *env*

In order to assess the sequence of viral genes, PBMC and tissue DNA was extracted using the QIAamp DNA mini kit (Qiagen) according to the manufacturer's instructions. One μg of isolated genomic DNA was used in a nested DNA polymerase chain reaction using rTaq (Takara) following the manufacturer's instructions and specific nucleotides listed in Table IV. Each PCR reaction contained 1x PCR buffer (Mg^{2+}-free), 4 mM $MgCl_2$, 0.25 mM of each deoxynucleotide triphosphate, 500 nM of each primer, and 1U of rTaq DNA polymerase. The PCR reactions were performed using an Applied Systems 2720 Thermal Cycler with the following thermal profile: 95°C for 2 min; 1 cycle; 95°C for 30 s, 48°C for 30 s, 65°C for 2 min, 35 cycles; 65°C for 7 min. The PCR products were pooled from three separate reactions and separated by electrophoresis on a 1.5% agarose gel, isolated, and directly sequenced. Cycled sequencing reactions were constructed using the BigDye Terminator Cycle Sequencing Ready Reaction kit with AmpliTaq DNA Polymerase, FS (PE Applied Biosystems). Sequence detection

Table IV. Oligonucleotides used in rTaq PCR to amplify SHIV genes.

Gene	Fragment Size (base pairs)	PCR Reaction	Forward (5' to 3')	Reverse (5' to 3')
nef	792	Round 1 Round 2	CCTAGAAGAATAAGACAGGGCTTGG GGAGCTATTTCCATGAGGCGGTCC	GGCTGACAAGAAGGAAACTCGC GGCCTCTTGCGGTTAGCCTTC
vpu	249	Round 1 Round 2	CCTAGACTAGAGCCCTGGAAGCATCC TTAGGCATCTCCTATGGCAGGAAGAAG	GTACCTCTGTATCATATGCTTTAGCAT CACAAAATAGAGTGGTGGTTGCTTCCT
vif	645	Round 1 Round 2	GGCTAAAATTATCAAAGATTATGGAGG GGAGGAGGAAAGAGGTGGATAGCAG	GGTGACATCCCTTGTTCATCATGCC CCAGTATTCCCAAGACCTTTGCC
env	810 765	Round 1 Round 2 Round 1 Round 2	GGTTAATTGATAGACTAATAGAAAGAG GCAGAAGACAGTGGCAATGAGAG GCTGGTTTTGCGATTCTAAAGTG GTAATAATAAGACGTTCAATGG	CCTCCTCTTCTGCTAGACTGCC CAGCAGTTGAGTTGSTACTACTGG GCTTCCTGCTGCTCCCAAGAACCC GGAACAAAGCTCCTATTCCC
gag	240	Round 1 Round 2	CGTGCAACCTTCTGCATTCACG TCATGTTTGAGACCTTCAACACCCCAG	CTGATTAATGTCATAGGGGGTGC CCAAGAAGAAGGCTGGAAGAGTGCC
β-actin	300	Round 1 Round 2	TCATGTTTGAGACCTTCAACACCCCAG CCCCAGCCATGTACGTTGCTATCC	CCAGGAAGGAAGGCTGGAAGAGTGCC GCCTCAGGGCAGCGGAACCGCTCA

was conducted with an Applied Biosystems 377 Prism XL automated DNA sequencer and visualized using the ABI Editview program. A total of 466, 246, 490, and 400 nucleotides from *vif, vpu, env,* and *nef* genes, respectively, were analyzed and compared to the sequence of $SHIV_{KU\text{-}1bMC33}$ using the SE Central Software package.

Immunoprecipitation assays

To determine if macaques developed antibodies to SHIV proteins following inoculation, the plasma obtained at necropsy was used in immunoprecipitation assays. C8166 cells were inoculated with approximately 10^4 $TCID_{50}$ of $SHIV_{KU\text{-}1bMC33}$ for 4 days. The cells were then incubated in methionine/cysteine-free media for 2 h and radiolabeled with 500 μCi of ^{35}S-methionine/cysteine for 15 hours. The cells were lysed in 1 ml of 1x RIPA buffer (50 mM Tris-HCl, pH7.5; 50 mM NaCl, 0.5% deoxycholate; 0.2% SDS; 10 mM EDTA) and nuclei were removed by centrifugation. The cell lysates were incubated overnight at 4°C with 10 μl of plasma from each macaque and protein-A Sepharose beads (Sigma). The immunoprecipitates bound to the beads were washed 3x in 1x RIPA, resuspended in 75 μl of 2x sample reducing buffer (125 mM Tris-HCl pH 6.8; 4% SDS, 10% glycerol. 0.06% bromophenol blue, 1% β-mercaptoethanol), and boiled for 5 min. Proteins were separated on a 10% SDS-PAGE gel and proteins visualized by autoradiography. Controls included pooled prebleed plasma from macaques RAK10, RCS10, and RPL10 (negative control) and plasma from macaques that had been previously inoculated with non-pathogenic SHIV-4 (positive control).

VII. Chapter 3: Replication and persistence of simian-human immunodeficiency viruses in rhesus macaques expressing Vif proteins with mutations in the SLQYLA and HCCH domains

Abstract

The Vif protein of primate lentiviruses interacts with APOBEC3 proteins, which results in shunting of the APOBEC3-Vif complex to the proteosome for degradation. Using the simian-human immunodeficiency virus (SHIV)/macaque model, we compared the replication and pathogenicity of SHIVs that express a Vif protein in which the entire SLQ(Y/F)LA ($SHIV_{Vif5A}$) or HCCH ($SHIV_{VifHCCH(-)}$) domains were substituted with alanine residues. Each virus was inoculated into three macaques and various viral and immunological parameters followed for six months. All macaques maintained stable circulating $CD4^+$ T cells, developed low viral loads, maintained the engineered mutations, yielded no histological lesions, and developed immunoprecipitating antibodies early post-inoculation. Sequence analysis of *nef* and *vpu* from three lymphoid tissues revealed a high percentage of G-to-A-substitutions. Our results show that while the presence of HCCH and SLQ(Y/F)LA domains are critical *in vivo*, there may exist APOBEC3 negative reservoirs that allow for low levels of viral replication and persistence but not disease.

Introduction

Mammals have evolved cellular restriction factors such as apolipoprotein B mRNA editing enzyme catalytic peptide-like 3G (APOBEC3G; hA3G) to inhibit the replication of retroviruses. However, retroviruses, such as human immunodeficiency virus type-1 (HIV-1), have also developed mechanisms to counter defend these restriction factors by subverting the host's proteosomal degradation pathway. For instance, the HIV-1 Vif protein has been shown to interact with A3G promoting its accelerated degradation by the 26S proteosome (Sheehy et al., 2003). APOBEC3G is a cytidine deaminase that, if packaged into HIV-1Δ*vif*/SIV_{mac}239Δ*vif* virions, induces cytidine deamination of newly synthesized minus-strand viral DNA from cytosines to uracils, leading to G to A transitions in plus strand synthesis and inhibition of viral replication (Jarmuz et al., 2002; Harris et al., 2003; Mariani et al., 2003; Mangeat et al., 2003; Sheehy et al., 2003; Virgen et al., 2007; Yu et al., 2004; Zennou et al., 2006).

Previous *in vitro* studies have shown that SIV_{mac}239Δ*vif* has been shown to be restricted by hA3G, hA3F, hA3H and to a lesser extent hA3B, hA3C, hA3D (Dang et al., 2006; Dang et al., 2008; Mariani etal., 2003; Yu et al., 2004b; Zennou et al., 2006). The HIV-1 Vif has limited activity against rhesus and African green monkey A3 proteins while Vif from SIV_{mac}239 and SIV_{agm} have broader specificities. While less is presently known about the rhesus A3 proteins, it is known that HIV-1Δ*vif* can be inhibited by rhA3G, rhA3F, rhA3B, and to a lesser extent rhA3H and rhA3DE (Virgen et al., 2007). SIV_{mac}239Δ*vif* has been shown to be restricted by rhA3G, rhA3F, rhA3C, rhA3B and rhA3DE, and to a lesser extent rhA3H (Virgen et al., 2007; Zennou et al., 2006).

Sequence analysis of Vif proteins from different lentiviruses reveals that there are two highly conserved domains in the carboxyl terminus of Vif required for the assembly of the Vif-CBF-β-Cul5/ElonginB/C/Rbx1 E3 ubiquitin ligase complex, the BC box ^{144}SLQ(Y/F)LAL^{150} and Zn^{++} binding (HCCH; H^{108}-X_5-C^{114}-$X_{17\text{-}18}$-C^{133}-$X_{3\text{-}5}$-H^{139}) motifs (Jäger et al., 2011; Kile et al., 2002; Luo et al., 2005; Mehle et al., 2004; Mehle et al., 2006; Paul et al., 2006; Yu et al., 2003; Yu et al., 2003). As described in the Introduction, the ^{144}SLQ(Y/F)LAL^{150} motif sequence resembles a conserved motif identified in the BC box of the suppressors of cytokine signaling (SOCS) proteins and mediates high affinity binding of Vif to elongin C (Luo et al., 2005; Mehle et al., 2004a; Mehle et al., 2004b; Mehle et al., 2006; Stopak et al., 2003; Yu et al., 2003; Yu et al., 2004c). Located upstream of the BC box is the HCCH motif, which was found to mediate interaction with Cullin-5. Previous studies have shown that substitution of either critical cysteine residue prevents the binding of Zn++ thus affecting the proper folding of the protein (Paul et al., 2006; Xiao et al., 207). Following the binding of N-terminus of Vif to the N-terminus of A3G, both the SLQ(Y/F)LAL and HCCH motifs enable Vif to recruit the Cul5/ElonginB/C/Rbx1 E3 ubiquitin ligase complex to accelerate the polyubiquitination and subsequent 26S proteosomal degradation (Conticello et al., 2003; Marin et al., 2003; Mehle et al., 2004; Stopak et al., 2003; Yu et al., 2003; Yu et al., 2004).

In this study, we constructed simian-human immunodeficiency viruses (SHIVs) in which five amino acids in the SLQYLA motif ($SHIV_{Vif5A}$) and four amino acids of the HCCH ($SHIV_{VifHCCH(-)}$) domain were changed to alanine residues. Our results indicate that rhA3G and rhA3F was efficiently incorporated into both $SHIV_{Vif5A}$ and $SHIV_{VifHCCH(-)}$

virions. However, rhA3F was stable in the presence of wild type and mutant Vif viruses, while only mutant Vif viruses efficiently degraded rhA3G. *In vitro*, rhesus A3G (rhA3G) was more effective at cytidine deamination than rhesus A3F (rhA3F). Macaques inoculated with mutant Vif viruses maintained stable circulating $CD4^+$ T cells, developed low viral loads, and developed immunoprecipitating antibodies. Sequence analysis of both *nef* and *vpu* from the thymus, spleen, and small intestine (ileum) of $SHIV_{VifHCCH(-)}$ inoculated macaques displayed a high percentage of G-to-A substitutions. Our results show that both the HCCH and SLQYLA domains were critical to Vif function *in vivo* but that production of viral RNA only persisted in the macaques inoculated with the $SHIV_{VifHCCH(-)}$.

Results

Replication of $SHIV_{Vif5A}$ and $SHIV_{VifHCCH(-)}$ in A3 positive and negative cell lines

We performed assays to examine the replication of parental $SHIV_{KU-2MC4}$, $SHIV_{Vif5A}$, $SHIV_{VifHCCH(-)}$, $SHIV_{ViAAQYLA}$ and $SHIV_{VifStop}$ in hA3G/F positive (C8166) and negative (SupT1) cell lines as well as rhesus PBMC (rhA3G/F). The sequence of the Vif mutants that were analyzed in this study are shown in Figure 28. We included $SHIV_{VifAAQYLA}$ in these growth curve studies for comparison. The replication of $SHIV_{VifAAQYLA}$ has been previously reported in both tissue culture and rhesus macaques (Schmitt et al., 2009). Cells were inoculated with equivalent amounts (25 ng of p27) of each virus and the levels of p27 (Gag) released into the culture medium were quantified

using a commercial antigen capture assay. All four mutant viruses ($SHIV_{Vif5A}$, $SHIV_{VifHCCH(-)}$, $SHIV_{VifAAQYLA}$ and $SHIV_{VifStop}$) replicated in SupT1 cells to similar levels as parental $SHIV_{KU-2MC4}$ by day 15 post-inoculation, although the kinetics of replication were slower (Figure 29). However, inoculation of $SHIV_{Vif5A}$, $SHIV_{VifHCCH(-)}$, $SHIV_{VifAAQYLA}$ and $SHIV_{VifStop}$ into hA3G/F positive C8166 cell cultures resulted in less than 0.01% of the p27 released compared to parental $SHIV_{KU-2MC4}$ (Figure 29).

Both $SHIV_{Vif5A}$ and $SHIV_{VifHCCH(-)}$ incorporate rhA3G and rhA3F into virus particles

The above results suggested that hA3G and hA3F or rhA3G and rhA3F might be incorporated into maturing virus particles resulting in restriction of replication. As we are most interested in an rhA3G and rhA3F, we transfected 293 cells with plasmids expressing an HA-tagged rhA3G or a V5-tagged rhA3F and the complete genomes of either $SHIV_{Vif5A}$, $SHIV_{VifHCCH(-)}$, $SHIV_{VifSTOP}$, or parental $SHIV_{KU-2MC4}$. At 48 hours post-transfection, the culture medium was collected, clarified, and the virus partially purified and concentrated by ultracentrifugation. The amount of p27 was determined followed by Western blot analysis to detect for the presence or absence of rhA3G or rhA3F. The results shown in Figure 30 indicate that rhA3G was incorporated into $SHIV_{Vif5A}$, $SHIV_{VifHCCH(-)}$, and $SHIV_{VifSTOP}$ virus particles but was excluded from $SHIV_{KU-2MC4}$

Figure 28. The sequence of wild type SIV_{mac}230 Vif and the two mutants assessed in this study.

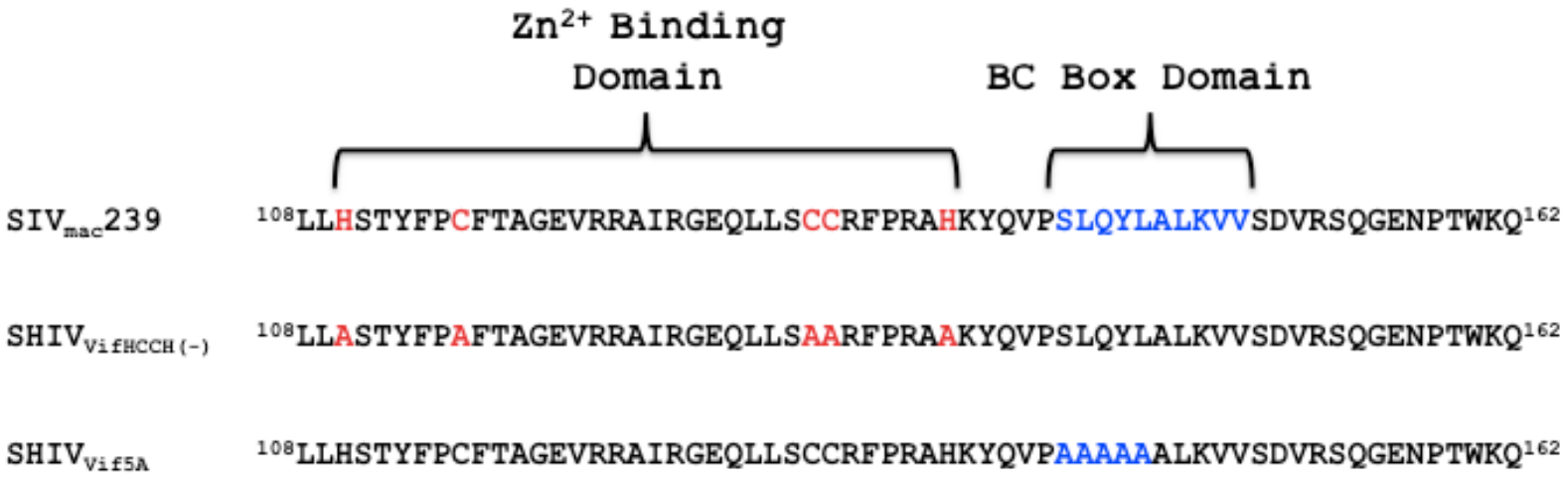
Zn2+ Binding Domain
BC Box Domain
SIVmac239 108LLHSTYFPCFTAGEVRRAIRGEQLLSCCRFPRAHKYQVPSLQYLALKVVSDVRSQGENPTWKQ162
SHIVVifHCCH(-) 108LLASTYFPAFTAGEVRRAIRGEQLLSAARFPRAAKYQVPSLQYLALKVVSDVRSQGENPTWKQ162
SHIVVif5A 108LLHSTYFPCFTAGEVRRAIRGEQLLSCCRFPRAHKYQVPAAAAAALKVVSDVRSQGENPTWKQ162

Figure 29. Replication of $SHIV_{KU-2MC4}$, $SHIV_{VifHCCH(-)}$, $SHIV_{Vif5A}$, and $SHIV_{VifStop}$ in C8166 cells (hA3G/F positive), SupT1 cells (hA3G/F negative) and rhesus macaque PBMC. Cells were inoculated with equal amounts of each virus (25 ng of p27) and the levels of p27 in the culture supernatants was assessed at various time points post-inoculation. Panel A. Replication of viruses in C8166 cells. Panel B. Replication of viruses in C8166 cells. Panel C. Replication of viruses in activated rhesus macaque PBMC. (■) $SHIV_{KU-2MC4}$, (●) $SHIV_{VifHCCH(-)}$, (♦) $SHIV_{Vif5A}$, and (▼) $SHIV_{VifStop}$.

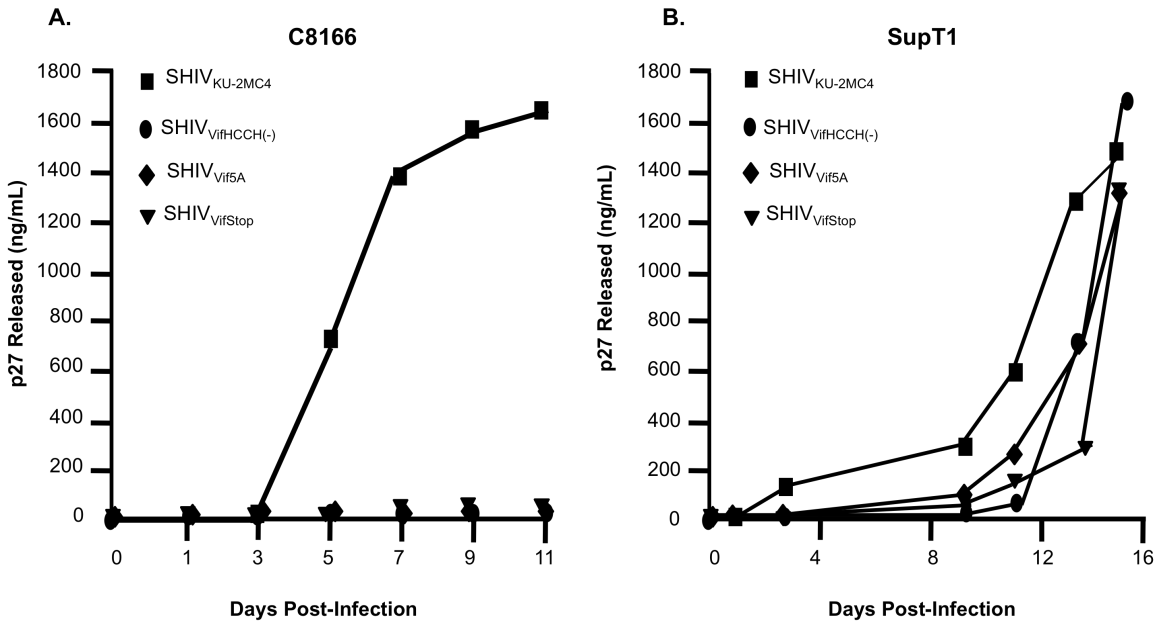
A.
C8166
SHIV KU-2MC4
SHIV VifHCCH(-)
SHIV Vif5A
SHIV VifStop
p27 Released (ng/mL)
1800
1600
1400
1200
1000
800
600
400
200
0
0 1 3 5 7 9 11
Days Post-Infection
B.
SupT1
SHIV KU-2MC4
SHIV VifHCCH(-)
SHIV Vif5A
SHIV VifStop
p27 Released (ng/mL)
1800
1600
1400
1200
1000
800
600
400
200
0
0 4 8 12 16
Days Post-Infection

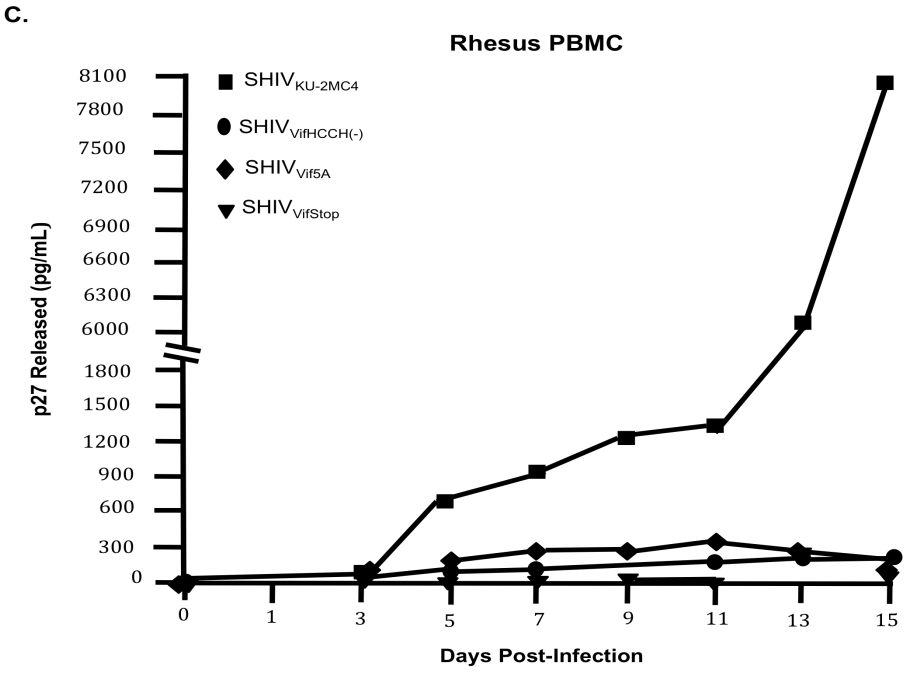
C.
Rhesus PBMC
SHIV KU-2MC4
SHIV VifHCCH(-)
SHIV Vif5A
SHIV VifStop
p27 Released (pg/mL)
8100
7800
7500
7200
6900
6600
6300
6000
1800
1500
1200
900
600
300
0
0 1 3 5 7 9 11 13 15
Days Post-Infection

Figure 30. The incorporation of rhA3G and rhA3F into virus particles. 293 cells were co-transfected with a plasmid that expresses the genome of either $SHIV_{KU-2MC4}$, $SHIV_{Vif5A}$, $SHIV_{VifHCCH(-)}$ or $SHIV_{VifStop}$ and a vector expressing HA-rhA3G or V5-rhA3F. At 48 hours, the culture medium was collected, clarified by low speed centrifugation and concentrated by ultracentrifugation through a 20/60 (w/v) step gradient. Equivalent levels of p27 from each sample were resuspended in sample reducing buffer, boiled and the proteins were separated by 10% SDS-PAGE. The presence of either rhA3G or rhA3F was detected through western blot analysis using an antibody directed by against the HA-tag or V5-tag, respectively. Panel A. Results of the rhA3G incorporation into virus particles. Lane 1. RhA3G proteins detected in lysate from cells transfected with the vector expressing HA-rhA3G alone. Lane 2-5. RhA3G proteins detected in virus from cells transfected with a vector expressing HA-rhA3G and $SHIV_{KU-2MC4}$ (Lane 2), $SHIV_{Vif5A}$ (Lane 3), $SHIV_{VifHCCH(-)}$, (Lane 4) and $SHIV_{VifStop}$ (Lane 5). Lane 6. RhA3G proteins in pelleted supernatant from cells transfected with empty expression vectors. Panel B. The blot in Panel A was stripped and reprobed with an antibody against the p27 protein. Panel C. Results of the rhA3G incorporation of rhA3F into virus particles. Lane 1. RhA3F proteins detected in a lysate from cell transfected with a vector expressing rhA3F alone. Lane 2-5. RhA3F proteins detected in virus from cells transfected with a vector expressing rhA3F and $SHIV_{KU-2MC4}$ (Lane 2), $SHIV_{Vif5A}$ (Lane 3), $SHIV_{VifHCCH(-)}$, (Lane 4) and $SHIV_{VifStop}$ (Lane 5). Lane 6. RhA3F proteins in pelleted supernatant from cells transfected with empty expression

vectors. Panel D. The blot in Panel C was stripped and reprobed with an antibody against the p27 protein.

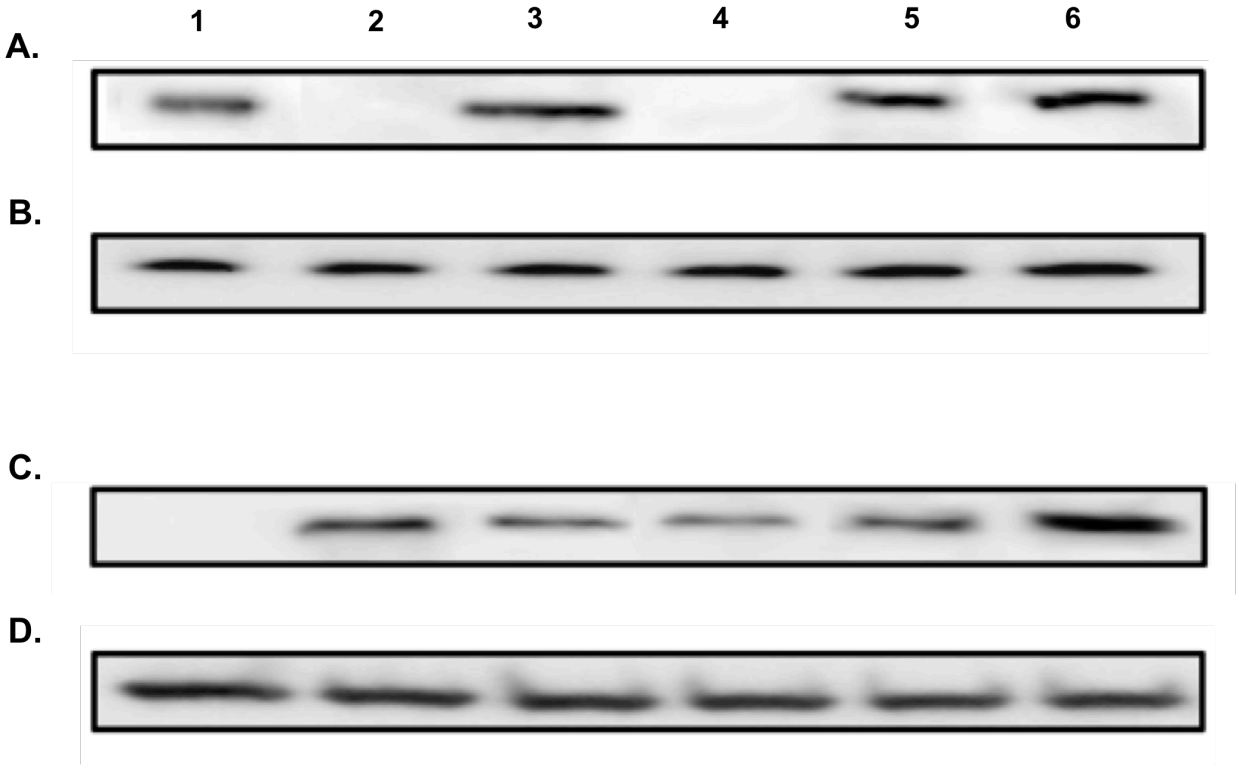

particles. However, we found that the rhA3F protein was incorporated into all four viruses (Figure 30). These results indicate that rhA3G was selectively incorporated only into the Vif mutants while rhA3F was incorporated into all viruses. The inability of $SIV_{mac}239$ Vif to degrade and prevent the incorporation of rhA3F has been previously reported (Virgen et al., 2007).

Rhesus A3F is stable in the presence of SIVmac239 Vif

Since we observed that rhA3F was incorporated into virus particles, we determined the stability of rhA3F and rhA3G in the presence of the viral genome. 293 cells were co-transfected with vectors expressing rhA3G or rhA3F and the genomes of $SHIV_{KU\text{-}2MC4}$, $SHIV_{Vif5A}$, $SHIV_{VifHCCH(-)}$, or $SHIV_{VifSTOP}$. Our results indicate that in the presence of the $SHIV_{KU\text{-}2MC4}$ genome, rhA3G was not stable whereas it was detected in the presence of the $SHIV_{Vif5A}$, $SHIV_{VifHCCH(-)}$ or $SHIV_{VifSTOP}$ (Figure 31). We also found that rhA3F appeared to be stable in the presence of both $SHIV_{KU\text{-}2MC4}$ and also $SHIV_{Vif5A}$, $SHIV_{VifHCCH(-)}$, or $SHIV_{VifSTOP}$ genomes. However, it should be noted that we consistently found higher levels of rhA3F in the presence of the $SHIV_{VifSTOP}$ genome, indicating fundamental differences between the targeting site-directed Vif mutants and the absence of the Vif protein. The results obtained with rhA3F correlate well with the above experiment showing that rhA3F was incorporated into virus particles.

Figure 31. Stability of the rhA3G and rhA3F proteins in the presence of the various *vif* mutant viral genomes. Plasmids expressing the genomes of either $SHIV_{KU\text{-}2MC4}$, $SHIV_{Vif5A}$, $SHIV_{VifHCCH(-)}$ or $SHIV_{VifStop}$ were co-transfected into 293 cells with a vector expressing either HA-rhA3G or V5-rhA3F. At 24 hours post-transfection, cells were lysed and proteins were precipitated using methanol. Proteins were separated on a 10% SDS-PAGE gel and probed using an antibody directed against either the HA or V5-tag. All samples were normalized to the amount of β-actin protein. Panel A. Stability of rhA3G in the presence of $SHIV_{KU\text{-}2MC4}$ (Lane 2), $SHIV_{VifStop}$ (Lane 3), $SHIV_{Vif5A}$ (Lane 4) or $SHIV_{VifHCCH(-)}$ (Lane 5) was assessed. Lanes 1 and 6 were used as positive (HA-rhA3G only, Lane 1) and negative (pcDNA3.1(+) only, Lane 6) controls. Panel B. The stability of rhA3F in the presence of $SHIV_{KU\text{-}2MC4}$ (Lane 2), $SHIV_{VifStop}$ (Lane 3), $SHIV_{Vif5A}$ (Lane 4) or $SHIV_{VifHCCH(-)}$ (Lane 5) was assessed. Lanes 1 and 6 were used as a negative (pcDNA3.1(+) only, Lane 1) or positive (V5-rhA3F only, Lane 6) controls. Similar results were acquired at 48 hours as well (data not shown). Panel B and C. The blot in Panel A and B were stripped and reprobed with an antibody against β-actin protein.

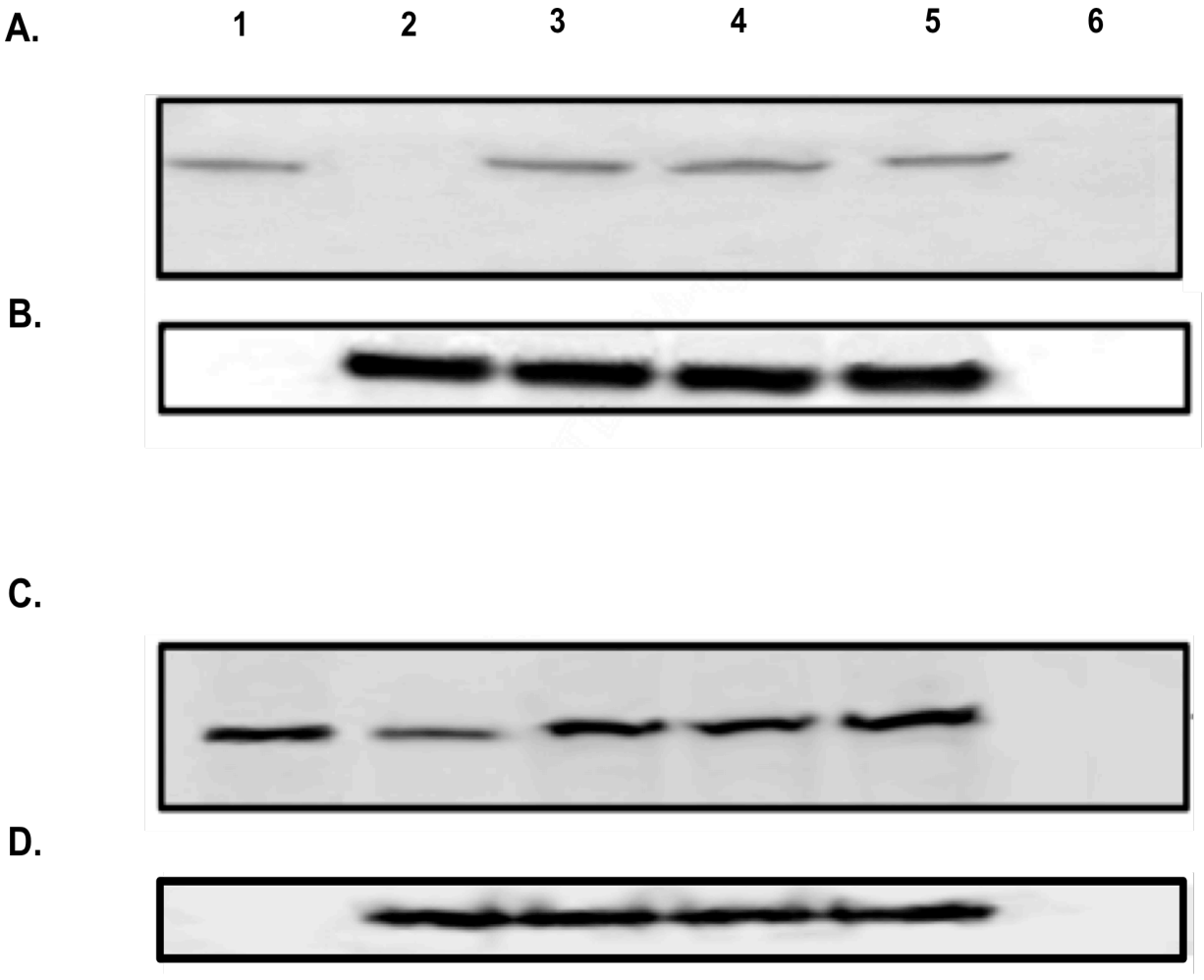
A.
1
2
3
4
5
6
B.
C.
D.

$SHIV_{VifHCCH(-)}$, $SHIV_{VifSTOP}$, or $SHIV_{KU-2MC4}$ and a plasmid expressing either an HA-tagged rhA3G, V5-tagged rhA3F or the empty vector. At 48 hours, the virus containing supernatant was collected, clarified by centrifugation, and the p27 levels quantified. Equivalent levels of p27 from each virus stock were used to titrate infectious virus by a series of 10-fold dilutions onto TZM.bl cells. At 48 hours, the cells were stained for β-galactosidase activity (β-galactosidase is under the control of the LTR and expression of Tat from the incoming virus) and the number of $TCID_{50}$ determined. If rhA3G or rhA3F was packaged into the virions, the virus should be hypermutated resulting in the expression of a non-functional Tat. As shown in Figure 32, $SHIV_{KU-2MC4}$ replicated to approximately the same levels in the presence or absence (empty vector) of rhA3G while the titers of $SHIV_{VifHCCH(-)}$, $SHIV_{Vif5A}$ and $SHIV_{VifSTOP}$ were 100 to 1000 fold less than the unmodified virus ($SHIV_{KU-2MC4}$). With rhA3F, our results indicate that $SHIV_{KU-2MC4}$, $SHIV_{VifHCCH(-)}$ and $SHIV_{Vif5A}$ had an approximate 10-fold decrease in titers and $SHIV_{VifSTOP}$ had greater than a 1000-fold decrease in titer (Figure 32). The results with rhA3F also emphasize the differences in site-directed mutations in $SHIV_{VifHCCH(-)}$, $SHIV_{Vif5A}$ and the severely truncated Vif in $SHIV_{VifSTOP}$.

Rhesus A3G but not rhA3F causes significant G-to-A mutations in the *nef* gene of the SHIV genome

The results above indicated that significant levels of rhA3F were incorporated into virions and rhA3F was stable in cells expressing the wild type genome. We compared the level of G-to-A mutations of the SHIV genome in the presence of either rhA3G or rhA3F. The results are shown in Figure 33 and Table V. Using viral genomes to express the Vif protein, we observed minimal G-to-A changes in $SHIV_{KU-2MC4}$ *nef* in

Figure 32. The incorporation of rhA3G results in less infectious virus. 293 cells were co-transfected with full-length vectors expressing $SHIV_{KU-2MC4}$, $SHIV_{VifHCCH(-)}$, $SHIV_{Vif5A}$ and $SHIV_{VifStop}$ and plasmids expressing either rhA3G of rhA3F. As a control each full-length genome was co-transfected with the empty vector, pcDNA3.1(+), only. At 48 hours, the culture medium was harvested, assessed for p27, and the amount of infectious virus titrated on TZM.bl cells as described in the Material and Methods section. Shown are the infectious titers in the absence or presence of either rhA3G (Panel A) or rhA3F (Panel B).

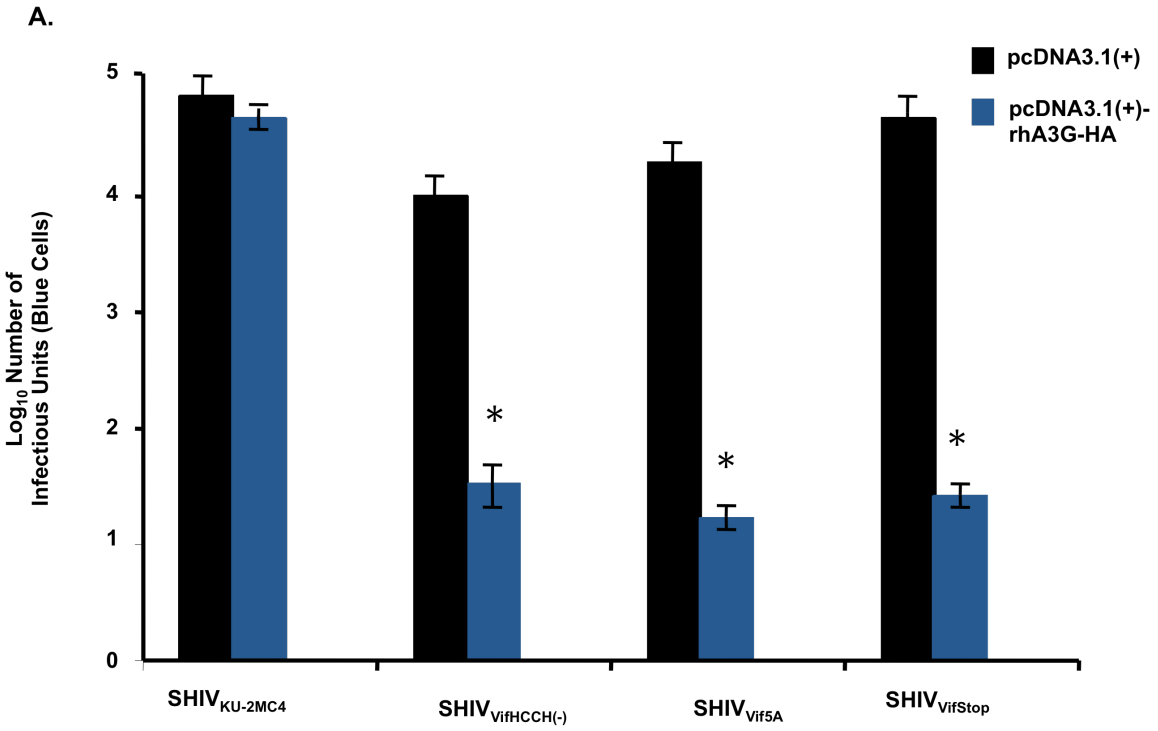
A.
pcDNA3.1(+)
pcDNA3.1(+)-rhA3G-HA
Log10 Number of Infectious Units (Blue Cells)
0
1
2
3
4
5
*
*
*
SHIVKU-2MC4
SHIVVifHCCH(-)
SHIVVif5A
SHIVVifStop

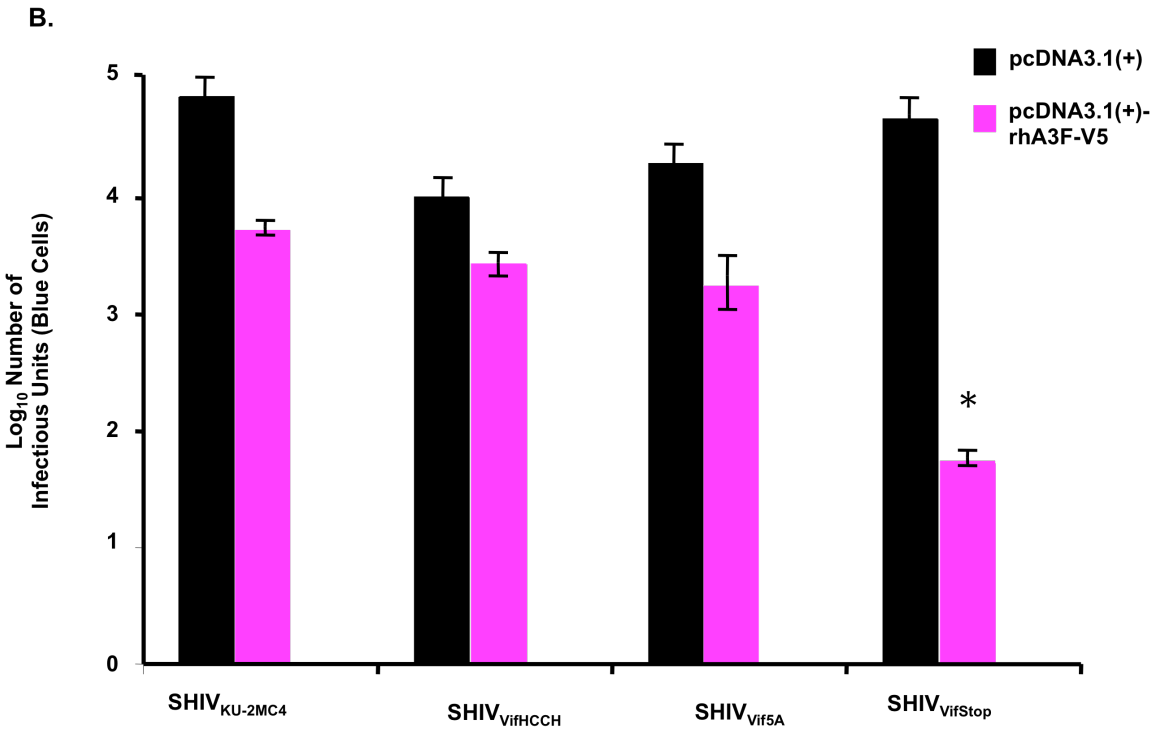
B.
pcDNA3.1(+)
pcDNA3.1(+)-rhA3F-V5
Log10 Number of Infectious Units (Blue Cells)
0
1
2
3
4
5
*
SHIVKU-2MC4
SHIVVifHCCH
SHIVVif5A
SHIVVifStop

Table V. Results of the hypermutation assay of *nef* amplified by rhA3G and rhA3F in the presence of wild type and mutant Vif proteins.

APOBEC3 protein	Virus	[a]Total number of bases sequenced	Total # of G-to-A mutations/percent G-to-A mutations of bases sequenced	Number and context of cytidine deamination		
				5'-GA	5'-GG	5'-GC
rhA3G	$SHIV_{KU-2MC4}$	4875	2 (0.04)	1	1	0
rhA3G	$SHIV_{Vif5A}$	4875	24 (0.49)	23	0	1
rhA3G	$SHIV_{Vif8HCCH(-)}$	4875	26 (0.53)	21	1	4
rhA3G	$SHIV_{Vif5TOP}$	4875	29 (0.59)	27	2	0
rhA3F	$SHIV_{KU-2MC4}$	4875	2 (0.04)	1	1	0
rhA3F	$SHIV_{Vif5A}$	4875	1 (0.02)	1	0	0
rhA3F	$SHIV_{Vif8HCCH(-)}$	4875	2 (0.04)	1	1	0
rhA3F	$SHIV_{Vif5TOP}$	4875	3 (0.06)	2	1	0

[a] A 325 base fragment corresponding to the 5' end of *nef* was amplified, cloned and 15 individual clones were selected for sequence analysis.

Figure 33. RhA3G but not rhA3F induced G-to-A substitutions in single colony sequences obtained from $SIV_{mac}239$ *nef*. Full-length genomes of wild type and *vif* mutant viruses were co-transfected with vectors expressing either rhA3G or rhA3F into 293 cells. At 48 hours post-transfection, the culture medium was collected, clarified by low speed centrifugation, DNase I-treated and used to infect TZM.bl cells. A 325 base pair fragment of $SIV_{mac}239$ *nef* was amplified from DNA at 24 hours post-infection and assessed for G-to-A substitutions. Panel A. A graph depicting the cumulative number of mutations from the 15 independent clones per virus assessed in the presence of rhA3G. Each bar is shaded according to the proportion of G-to-A substitutions that occurred in the context of GA (red), GG (yellow), GT (cyan), GC (gray), or non G-to-A (black). Panel B. A graph depicting the cumulative number of mutations from the 15 independent clones per virus assessed in the presence of rhA3G. Each bar is shaded according to the proportion of G-to-A substitutions that occurred in the context of GA (red), GG (yellow), GT (cyan), GC (gray), or non G-to-A (black). Panel C. A graph depicting the cumulative number of mutations from the 15 independent clones per virus assessed in the presence of rhA3F.

A.

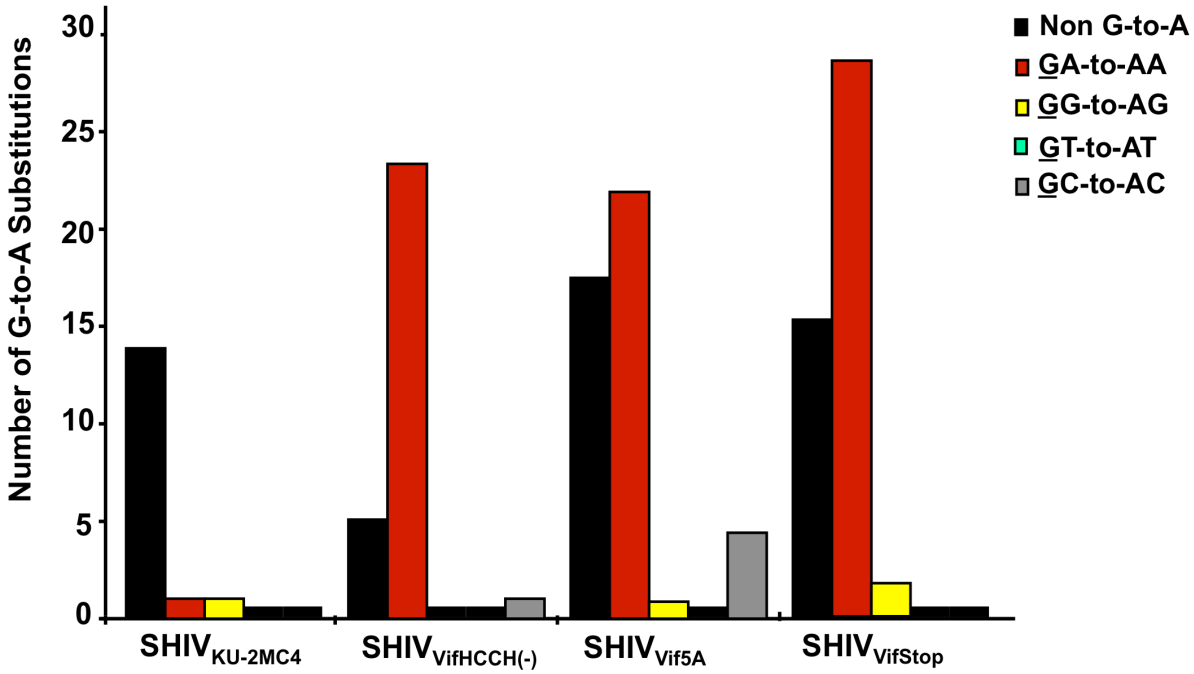
Number of G-to-A Substitutions
30
25
20
15
10
5
0
SHIV KU-2MC4
SHIV VifHCCH(-)
SHIV Vif5A
SHIV VifStop
Non G-to-A
GA-to-AA
GG-to-AG
GT-to-AT
GC-to-AC

B.

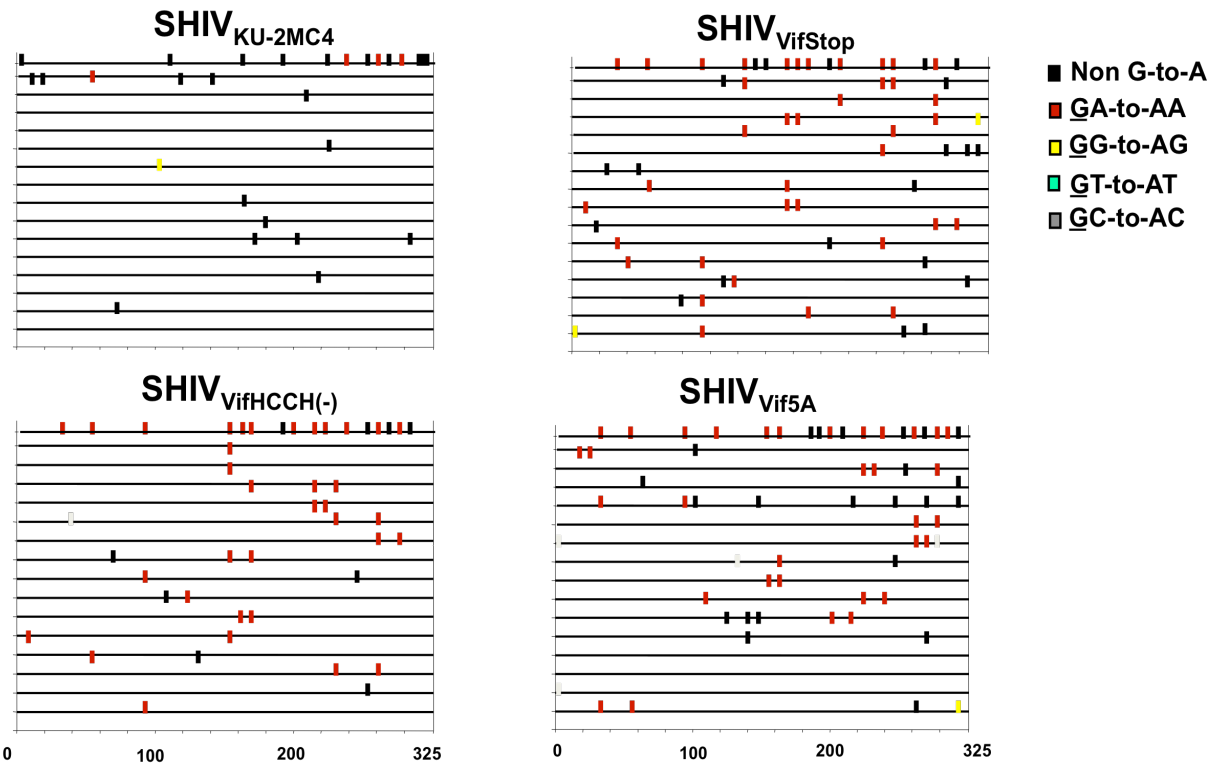
SHIV KU-2MC4
SHIV VifStop
SHIV VifHCCH(-)
SHIV Vif5A
0
100
200
325
0
100
200
325
Non G-to-A
GA-to-AA
GG-to-AG
GT-to-AT
GC-to-AC

C.

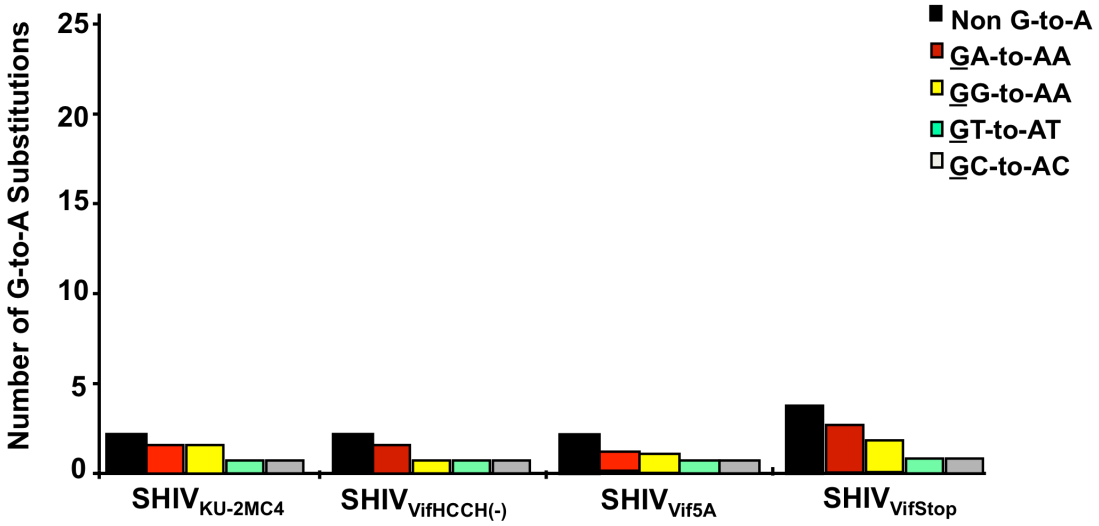
Number of G-to-A Substitutions
25
20
15
10
5
0
Non G-to-A
GA-to-AA
GG-to-AA
GT-to-AT
GC-to-AC
SHIV KU-2MC4
SHIV VifHCCH(-)
SHIV Vif5A
SHIV VifStop

the presence of either rhA3G or rhA3F. In the presence of rhA3G, we found that $SHIV_{Vif5A}$, $SHIV_{VifHCCH(-)}$ or $SHIV_{VifSTOP}$ *nef* had an increase in the number of G-to-A changes (from 2 to 24-29) or approximately 0.5% of the bases sequenced (Table V). However, in the presence of rhA3F, we observed that $SHIV_{Vif5A}$, $SHIV_{VifHCCH(-)}$, and $SHIV_{VifSTOP}$ *nef* had a similar level of G-to-A changes compared to $SHIV_{KU-2MC4}$ (Table V). The results with the rhA3F suggest that incorporation of rhA3F does not result in significant G-to-A substitutions in *nef*.

Assessment of $SHIV_{VifHCCH(-)}$ replication in macaques

We inoculated three macaques with 10^4 $TCID_{50}$ of $SHIV_{VifHCCH(-)}$. Prior to inoculation, macaques AS34, AS51, and AV18 had circulating $CD4^+$ cell levels of 1,509, 1,109, and 400 cells per µl, respectively. These three macaques maintained levels of circulating $CD4^+$ T cells at pre-inoculation levels or higher throughout the course of the six-month infection (Figure 34). All three macaques were euthanized at 26-28 weeks post-inoculation in excellent condition. At necropsy, AS34, AS51, and AV18 had circulating $CD4^+$ T cell levels of 2,124, 1,338, and 1,298 cells/µl, respectively. This contrasts with macaques inoculated with parental $SHIV_{KU-2MC4}$, which developed a severe loss of circulating $CD4^+$ T cells within 3-4 weeks post-inoculation (Figure 34). Analysis of the plasma viral loads revealed a mean viral load of 4.15×10^3 copies per ml at one week post-inoculation (Figure 35), which is approximately 10,000-fold less than the macaques inoculated with parental $SHIV_{KU-2MC4}$ (Figure 35). Following the first week of infection, the plasma viral loads in macaques AS34, AS51, and AV18 were at or just above the limits of detection. At necropsy, viral loads in all three macaques were

Figure 34. Circulating $CD4^+$ T cell levels in macaques inoculated with $SHIV_{VifHCCH(-)}$, $SHIV_{Vif5A}$, and $SHIV_{KU-2MC4}$. Panel A. The levels of circulating $CD4^+$ T cells in three macaques (AS34, ●; AS51, ■; and AV18, ▲) following inoculation with $SHIV_{VifHCCH(-)}$. Panel B. The levels of circulating $CD4^+$ T cells in three macaques (CX54, ●; ER65, ■; and I92, ▲) following inoculation with $SHIV_{Vif5A}$. Panel C. The levels of circulating $CD4^+$ T cells in three macaques (44O, ●; 44N, ■; 35N, ▲) following inoculation with $SHIV_{KU-2MC4}$.

A.

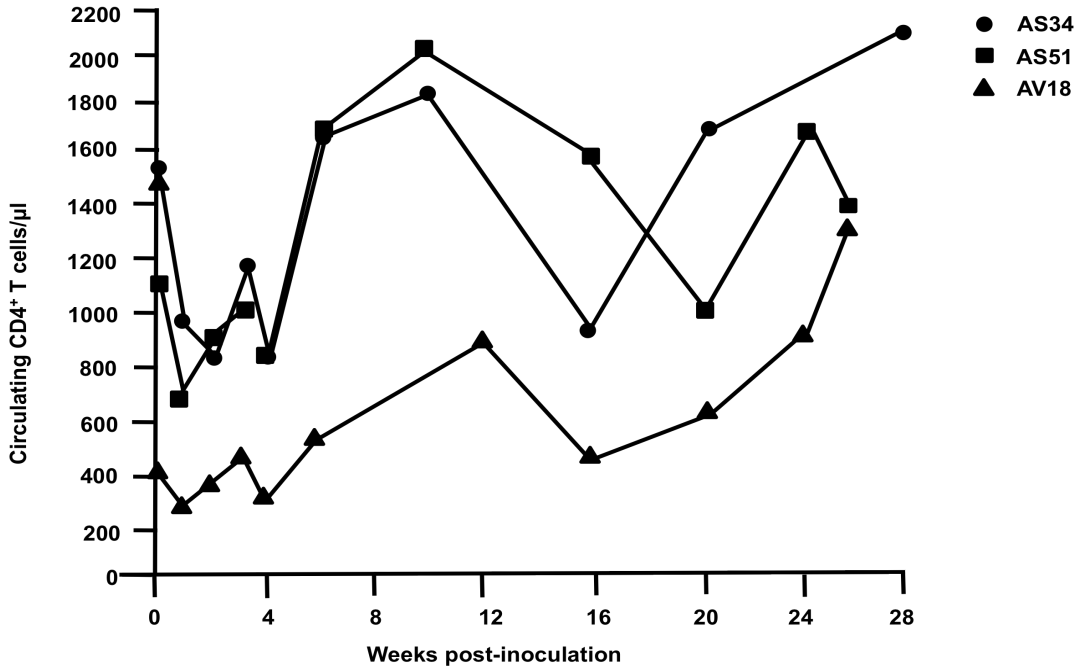
AS34
AS51
AV18
Circulating CD4+ T cells/µl
2200
2000
1800
1600
1400
1200
1000
800
600
400
200
0
0
4
8
12
16
20
24
28
Weeks post-inoculation

B.

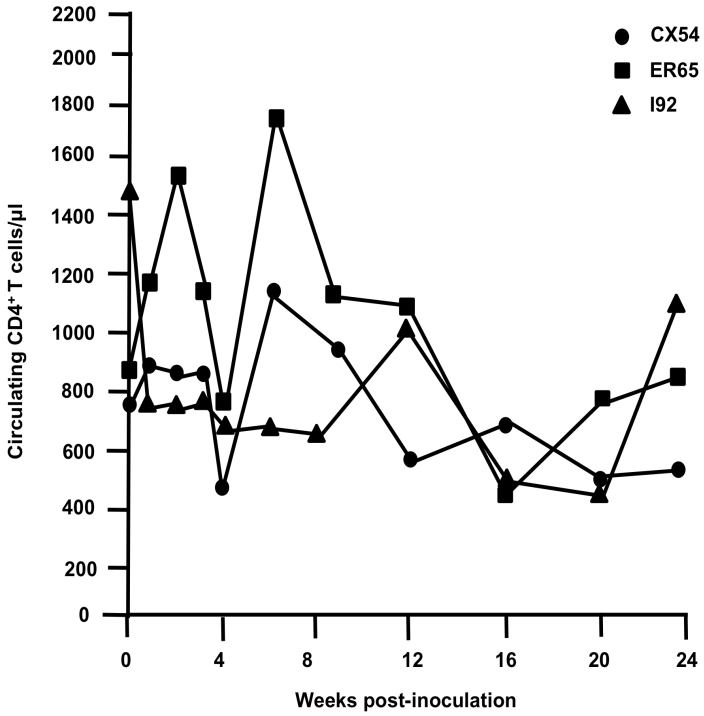
CX54
ER65
I92
Circulating CD4+ T cells/µl
2200
2000
1800
1600
1400
1200
1000
800
600
400
200
0
0
4
8
12
16
20
24
Weeks post-inoculation

C.

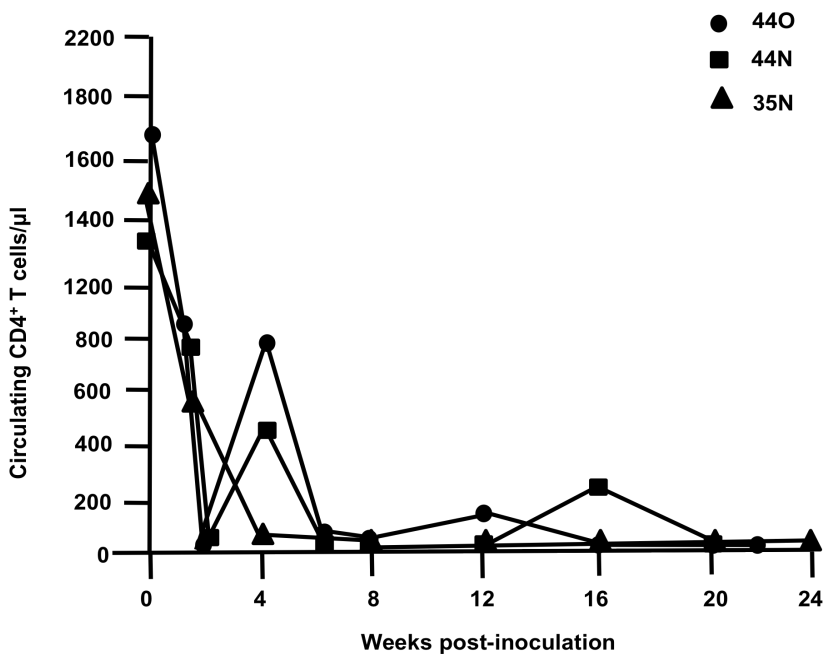
44O
44N
35N
2200
1800
1600
1400
1200
800
600
400
200
0
Circulating CD4+ T cells/µl
0
4
8
12
16
20
24
Weeks post-inoculation

Figure 35. Plasma viral loads in macaques inoculated with $SHIV_{VifHCCH(-)}$, $SHIV_{Vif5A}$, and $SHIV_{KU-2MC4}$ as determined by real-time quantitative PCR. Panel A. Plasma vial loads in three macaques (AS34, ●; AS51, ■; and AV18, ▲) following inoculation with $SHIV_{VifHCCH(-)}$. Panel B. Plasma viral loads in three macaques (CX54, ●; ER65, ■; and I92, ▲) following inoculation with $SHIV_{Vif5A}$. Panel C. Plasma viral loads in three macaques (44O, ●; 44N, ■; 35N, ▲) following inoculation with $SHIV_{KU-2MC4}$.

A.

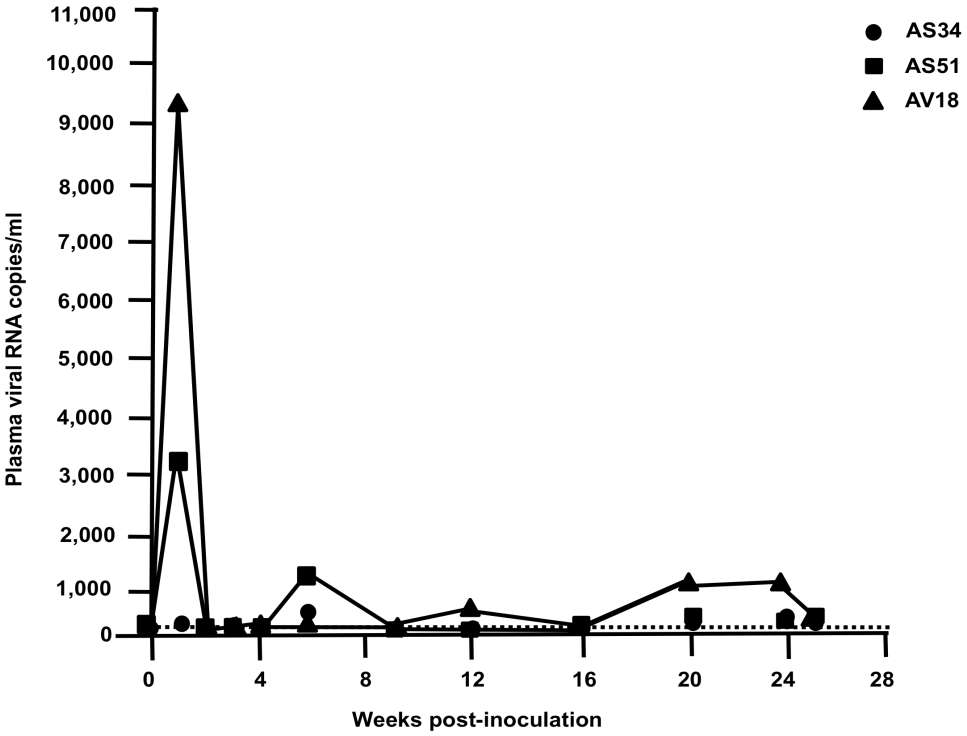
11,000
10,000
9,000
8,000
7,000
6,000
5,000
4,000
3,000
2,000
1,000
0
Plasma viral RNA copies/ml
0
4
8
12
16
20
24
28
Weeks post-inoculation
AS34
AS51
AV18

B.

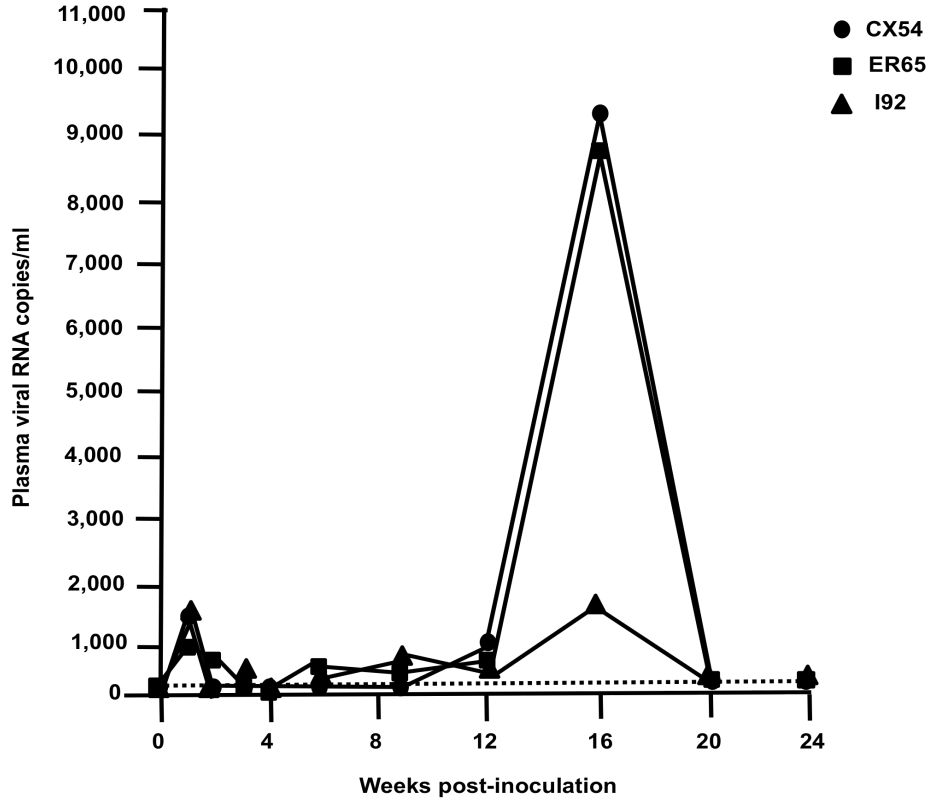
11,000
10,000
9,000
8,000
7,000
6,000
5,000
4,000
3,000
2,000
1,000
0
Plasma viral RNA copies/ml
0
4
8
12
16
20
24
Weeks post-inoculation
CX54
ER65
I92

C.

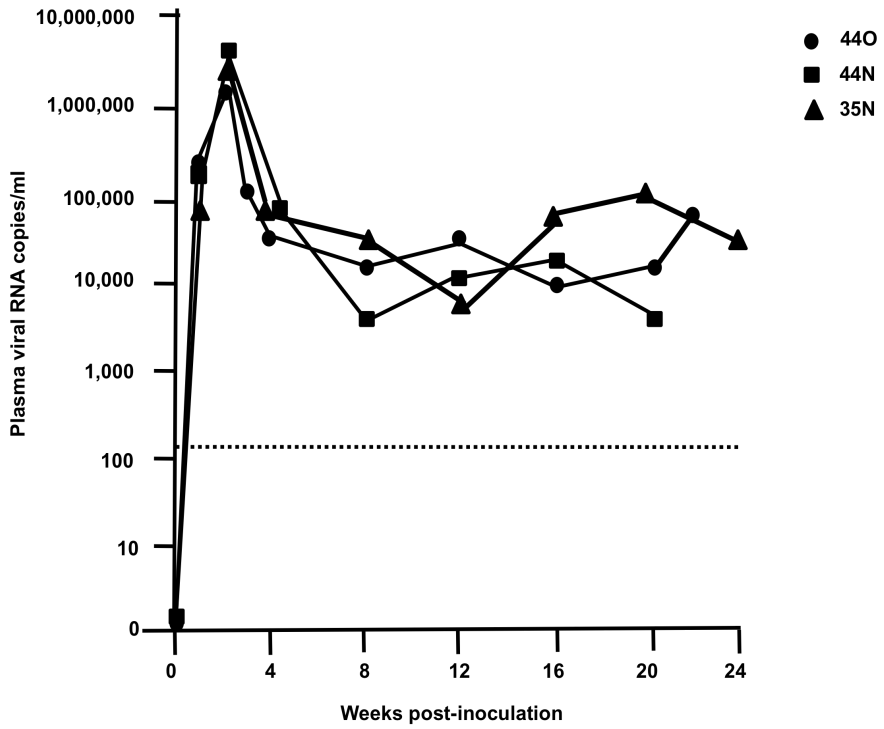
10,000,000
1,000,000
100,000
10,000
1,000
100
10
0
Plasma viral RNA copies/ml
0
4
8
12
16
20
24
Weeks post-inoculation
44O
44N
35N

undetectable. These results indicate that $SHIV_{VifHCCH(-)}$ transiently replicated in these macaques prior to control of the infection.

Assessment of $SHIV_{Vif5A}$ replication in macaques

We also assessed the ability of $SHIV_{Vif5A}$ to replicate in three macaques (CX54, ER65, and I92). Prior to inoculation, macaques CX54, ER65, and I92 had circulating $CD4^+$ T cell levels of 777, 844, and 1,451 cells per µl, respectively (Figure 34). These macaques, similar to those inoculated with $SHIV_{VifHCCH(-)}$, maintained circulating $CD4^+$ T cell levels near the pre-inoculation levels throughout the course of the 6 month infection. All three macaques were euthanized at 26 weeks post-inoculation in excellent condition. At necropsy, CX54, ER65, and I92 had circulating $CD4^+$ T cell levels of 513, 853, and 1192 cells per µl, respectively (Figure 34). This also contrasts with macaques inoculated with parental $SHIV_{KU-2MC4}$ (Figure 34). Analysis of the plasma viral loads of the macaques inoculated with $SHIV_{Vif5A}$ revealed a mean viral load of 1.3 $x10^3$ copies per ml at one week post-inoculation (Figure 35). Following the first week of infection, the plasma viral loads in macaques CX54, ER65, and I92 fell to undetectable levels.

Mutations in vif amplified from isolated DNA of PBMC during the course of infection

We assessed the stability of the engineered mutations in the *vif* gene from DNA isolated PBMC throughout the course of infection. The *vif* sequence was amplified, directly sequenced and compared to the input *vif* sequence of $SHIV_{Vif5A}$ or $SHIV_{VifHCCH(-)}$. We observed that the engineered mutations were stable throughout the course of the six month infection for macaques inoculated with $SHIV_{VifHCCH(-)}$. We performed bulk

Figure 36. Analysis of *vif* sequences amplified from DNA isolated from PBMC at various times post-inoculation. Panel A. Quantitative representation of mutations induced in bulk sequences obtained from a 450 base pair fragment of $SHIV_{VifHCCH(-)}$ Vif. Each vertical bar represents the total number of G-to-A substitutions. Each bar is shaded according to the proportion of G-to-A substitutions that occurred in the context of GA (red), GG (yellow), GT (cyan), or non G-to-A (black). Panel B. A 450 base pair fragment of the SIV Vif was amplified using DNA isolated from macaque PBMC inoculated with $SHIV_{VifHCCH(-)}$. Mutations from bulk sequence analysis from each macaque are shown. Each mutation is denoted by a vertical line that is color coded with respect to the dinucleotide context: GA (red), GG (yellow), GT (cyan), GC (gray) and non-G-to-A substitutions (black).

A.

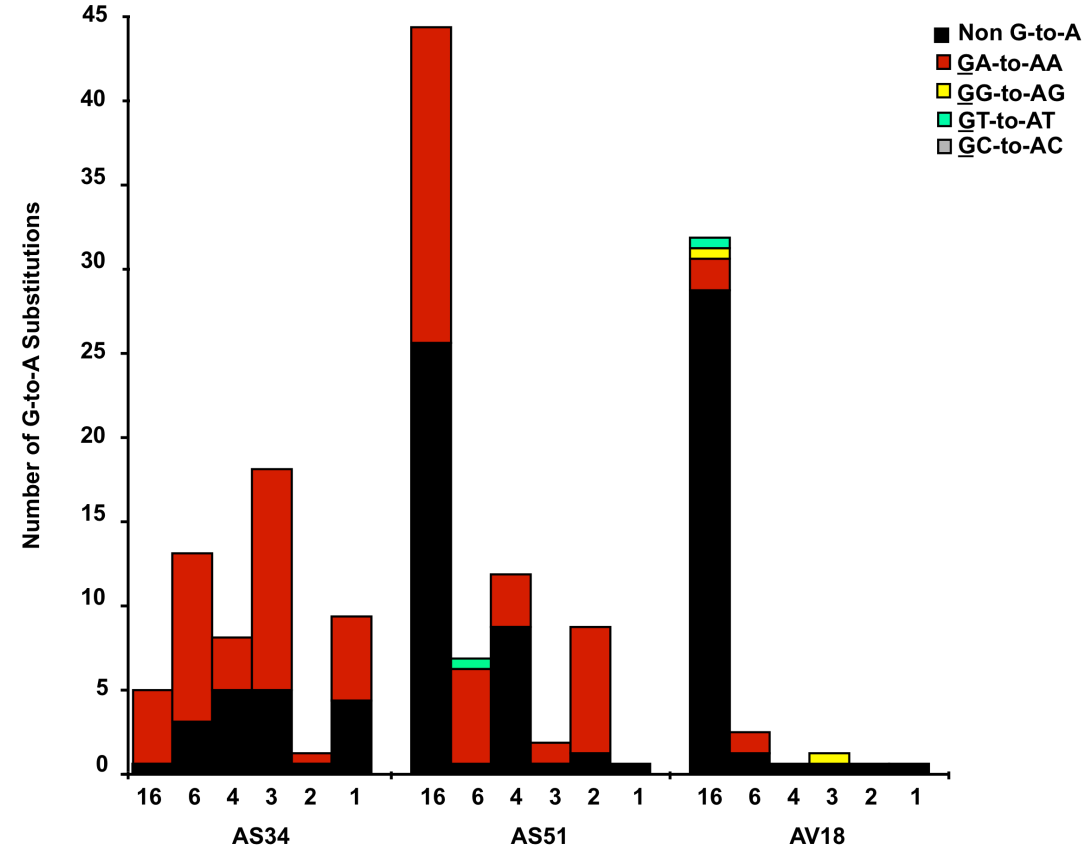
Number of G-to-A Substitutions
45
40
35
30
25
20
15
10
5
0
Non G-to-A
GA-to-AA
GG-to-AG
GT-to-AT
GC-to-AC
16 6 4 3 2 1
AS34
16 6 4 3 2 1
AS51
16 6 4 3 2 1
AV18

B.

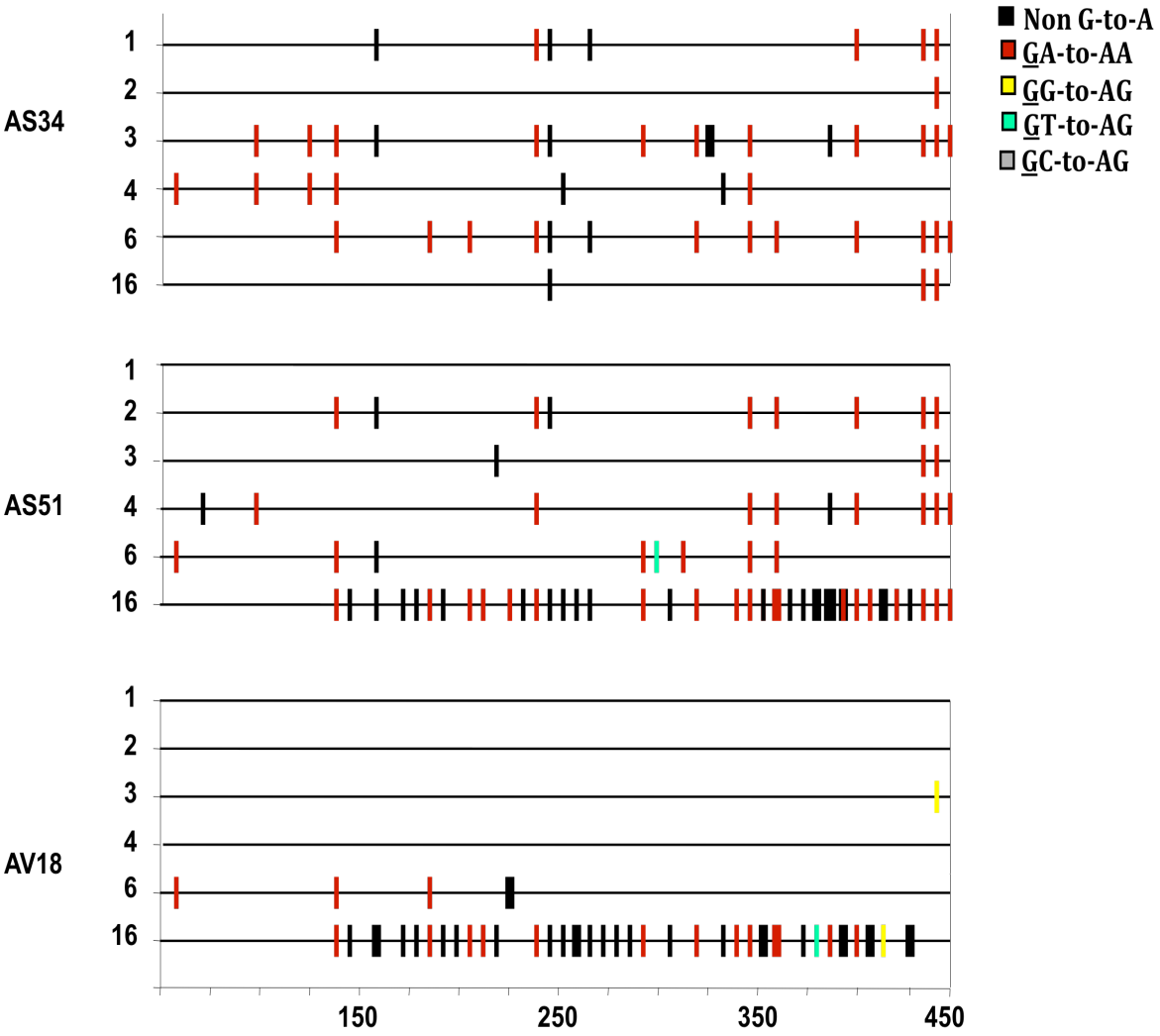
AS34
AS51
AV18
1
2
3
4
6
16
150
250
350
450
Non G-to-A
GA-to-AA
GG-to-AG
GT-to-AG
GC-to-AG

sequencing of the *vif* amplified at 1, 2, 3, 4, 6, and 16 weeks. As shown in Figure 36, the number of G-to-A mutations in the amplified *vif* gene increased with time in two (AS51, AV18) of the three macaques while the third macaque (AS34) appeared to have the largest number of G-to-A mutations at 3 weeks post-inoculation. As we had reported earlier, the majority of the G-to-A mutations were in the context of the 5'-T**C** rather than 5'-C**C** (Schmitt et al., 2009). We were able to amplify part of the *vif* sequence at 1 week from PBMC DNA isolated from macaques inoculated with $SHIV_{Vif5A}$ (CX54, ER65, I92). The sequence analysis also revealed that these *vif* mutations were stable at one week post-inoculation (data not shown). However, from 4 weeks until necropsy, we were unable to amplify the *vif* gene, which correlates with the undetectable plasma viral loads in these macaques after week 1 post-inoculation.

Macaques inoculated with $SHIV_{Vif5A}$ and $SHIV_{VifHCCH(-)}$ developed anti-viral antibody responses early after inoculation

We analyzed the plasma from infected macaques at 12 weeks and at necropsy (26-28 weeks) for the presence of immunoprecipitating antibody responses. At 12 weeks post-inoculation, all three macaques inoculated with $SHIV_{Vif5A}$ had developed antibody responses to p27 but only macaque ER65 developed antibody responses to the Env glycoprotein (Figure 37). For macaques inoculated with $SHIV_{VifHCCH(-)}$, all three macaques developed antibodies to p27 and the Env glycoprotein (Figure 37). At necropsy, we could not detect the presence of immunoprecipitating antibodies from macaques inoculated with either $SHIV_{Vif5A}$ or $SHIV_{VifHCCH(-)}$ (Figure 37). A macaque inoculated with parental $SHIV_{KU-2MC4}$ (44O) did not develop antibodies to the virus at either time point, which is common for macaques that develop severe $CD4^+$ T cell loss

Figure 37. Macaques inoculated with $SHIV_{VifHCCH(-)}$ and $SHIV_{Vif5A}$ developed antibody responses against each virus early after inoculation. C8166 cells were inoculated with $SHIV_{KU-2MC4}$ for 5 days, starved in methionine/cysteine-free DMEM, and then radio labeled overnight with ^{35}S-methionine/cysteine. The culture medium was harvested and used in immunoprecipitation reactions with plasma from AS34, AS51, AV18, CX54, ER65, and I92 as described in the Materials and Methods section. The immunoprecipitates were washed with 1 x RIPA buffer and boiled in 2x sample reducing buffer. The proteins were then separated on a 12%-SDS-PAGE gel and visualized using auto radiographic techniques. Panel A. SHIV proteins immunoprecipitated with plasma obtained at week 12 post-inoculation. Panel B. SHIV proteins immunoprecipitated with plasma obtained at necropsy. (Lanes 1-3) $SHIV_{VifHCCH(-)}$ proteins immunoprecipitated using plasma from either AS34 (Lane 1), AS51 (Lane 2), or AV18 (Lane 3), respectively. (Lanes 4-6) SHIVVif5A proteins immunoprecipitated using plasma from either CX54 (Lane 4), ER65 (Lane 5), or I92 (Lane 6), respectively. (Lane 7) SHIV proteins immunoprecipitated using plasma from an uninfected macaque. (Lane 8) SHIV proteins immunoprecipitated from a positive control plasma sample. The molecular weight standards are shown on the left.

A.

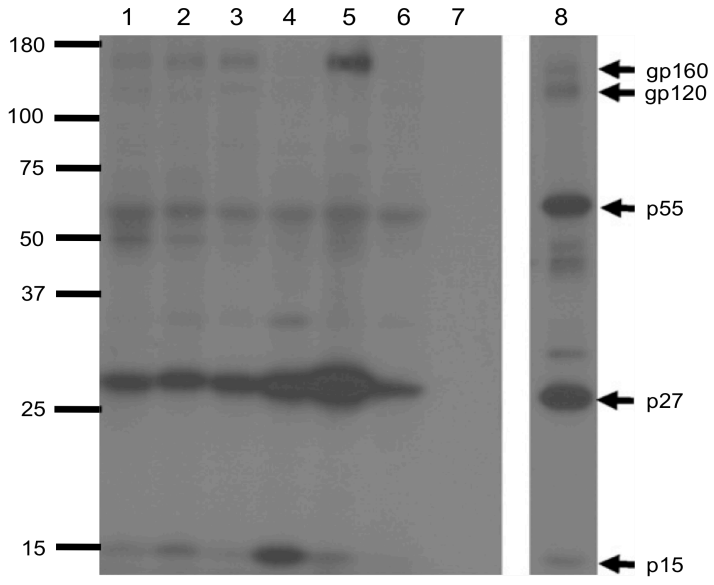
1
2
3
4
5
6
7
8
180
100
75
50
37
25
15
gp160
gp120
p55
p27
p15

B.

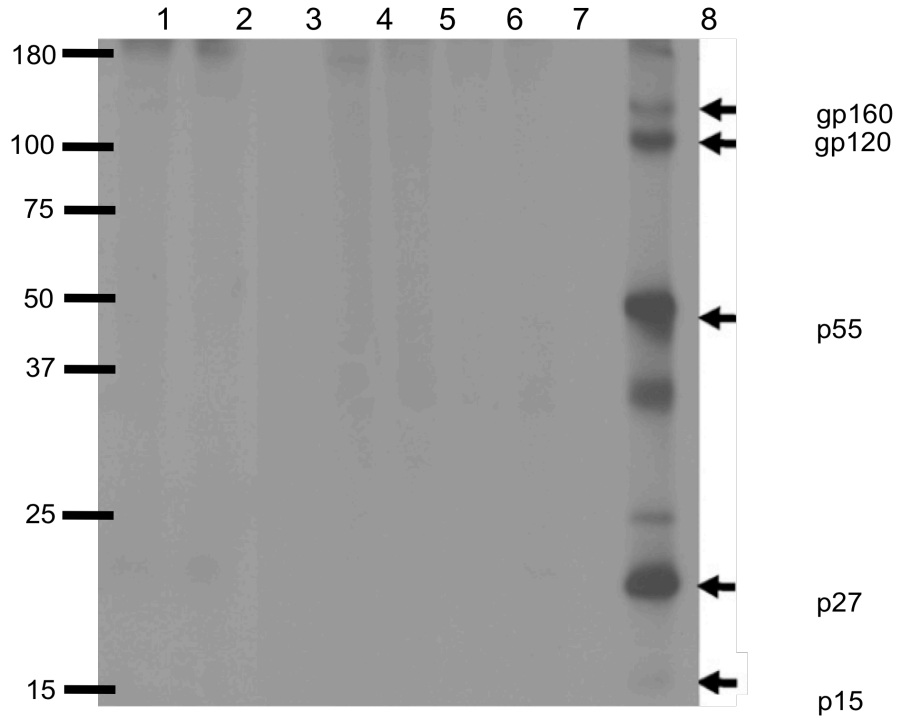
1
2
3
4
5
6
7
8
180
100
75
50
37
25
15
gp160
gp120
p55
p27
p15

during the acute phase (<4 weeks) following inoculation with a pathogenic X4 SHIV (data not shown).

Histological examination of tissues and viral loads in visceral organs of macaques inoculated with $SHIV_{Vif5A}$ and $SHIV_{VifHCCH(-)}$

Tissues from infected macaques were examined for the presence of lesions consistent with this pathogenic X4 SHIV (Joag et al., 1998). Macaques inoculated with either $SHIV_{Vif5A}$ or $SHIV_{VifHCCH(-)}$ did not exhibit histological lesions in any of the 13 visceral organs examined or in the CNS (data not shown). As the plasma viral loads were significantly less than macaques inoculated with $SHIV_{KU-2MC4}$, we assessed the tissue distribution of these two viruses in macaques. RNA was isolated from 13 visceral organs from macaques inoculated with $SHIV_{Vif5A}$ and $SHIV_{VifHCCH(-)}$, DNase I treated, and copy numbers determined by real time quantitative RT-PCR. The number of copies is expressed per 10^6 copies of GADPH. The results obtained from macaques inoculated with $SHIV_{VifHCCH(-)}$ are shown in Figure 38. We found that macaque AS34 had eight tissues (kidney, lung, pancreas, axillary lymph node, inguinal lymph node, spleen, thymus and tonsil) greater than 1,000 copies per 10^6 copies of GAPDH (Figure 38). Macaque AS51 was found to have two tissues (lung and small intestine) with greater than 1,000 copies per 10^6 copies of GAPDH, and macaque AV18 had six tissues (lung, pancreas, axillary lymph node, inguinal lymph node, mesenteric lymph node and spleen) with greater than 1,000 copies per 10^6 copies of GAPDH (Figure 38). Interestingly, the lung had the highest viral copy number in each macaque. In contrast, we were unable to quantify viral RNA from tissues of macaques that were inoculated

Figure 38. Comparison of viral copy numbers in the visceral tissues of macaques inoculated with $SHIV_{KU\text{-}2MC4}$, $SHIV_{VifHCCH(-)}$, and $SHIV_{Vif5A}$. RNA was isolated from different visceral organs of macaques inoculated with either $SHIV_{VifHCCH(-)}$ or $SHIV_{Vif5A}$. The RNA was DNase I treated to remove residual DNA and used in real time quantitative RT-PCR using oligonucleotide primers specific for SIV *gag* as described in the Materials and Methods. The levels of viral RNA are shown per 106 copies of GAPDH RNA. Panel A. The results of the real time quantitative RT-PCR using RNA isolated from tissues of macaque 44O, which was inoculated with $SHIV_{KU\text{-}2MC4}$. Panels B-D. The results of the real time quantitative RT-PCR using RNA isolated from the tissues of macaques AS34 (Panel B), AS51 (Panel C), and AV18 (Panel D), which were inoculated with $SHIV_{VifHCCH(-)}$. Panels E-G. The results of the real time quantitative RT-PCR using RNA isolated from tissues of macaques CX54 (Panel E), ER65 (Panel F), and I92 (Panel G), which were inoculated with $SHIV_{Vif5A}$.

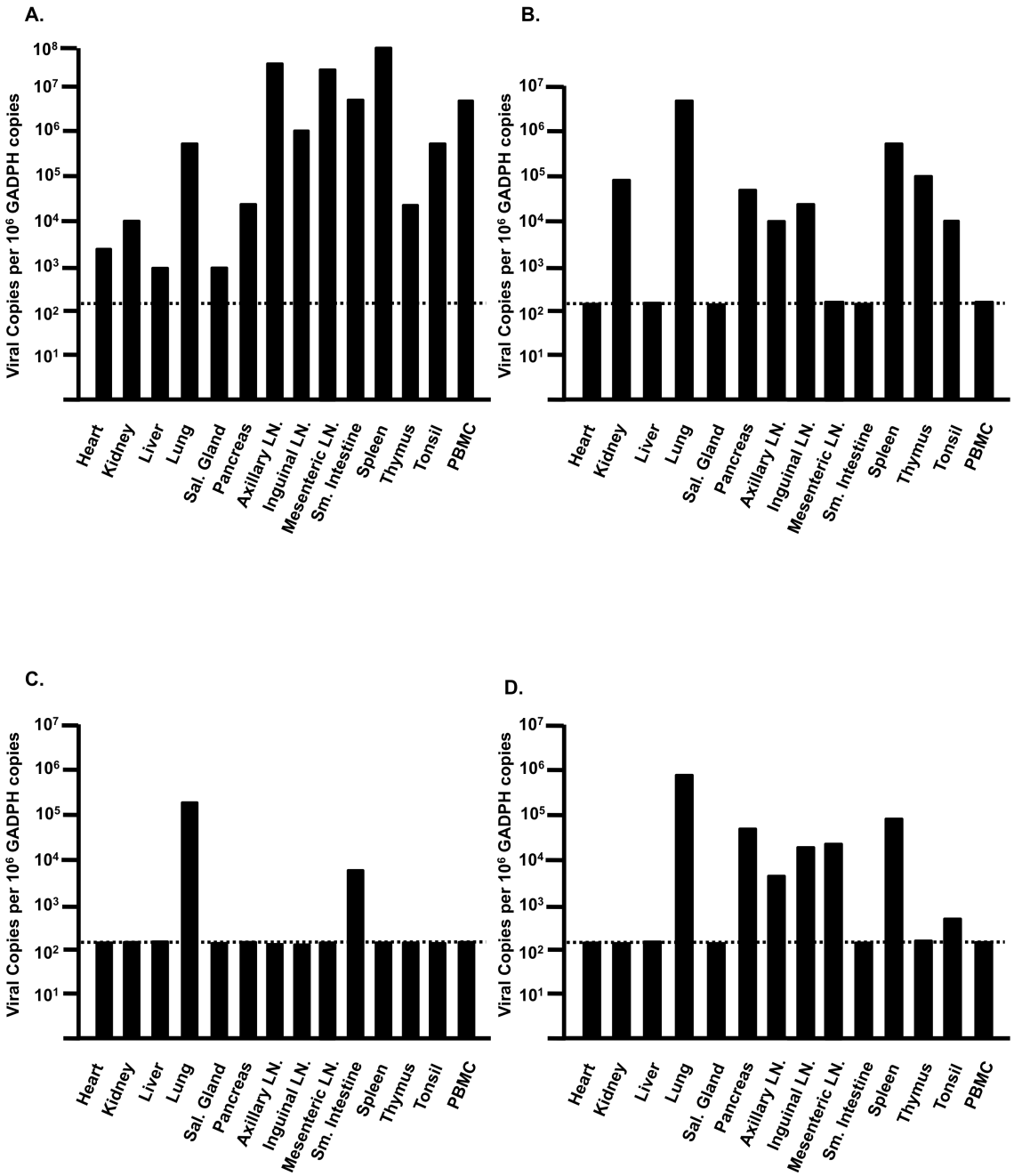
A.
B.
C.
D.
Viral Copies per 10^6 GADPH copies
Heart
Kidney
Liver
Lung
Sal. Gland
Pancreas
Axillary LN.
Inguinal LN.
Mesenteric LN.
Sm. Intestine
Spleen
Thymus
Tonsil
PBMC

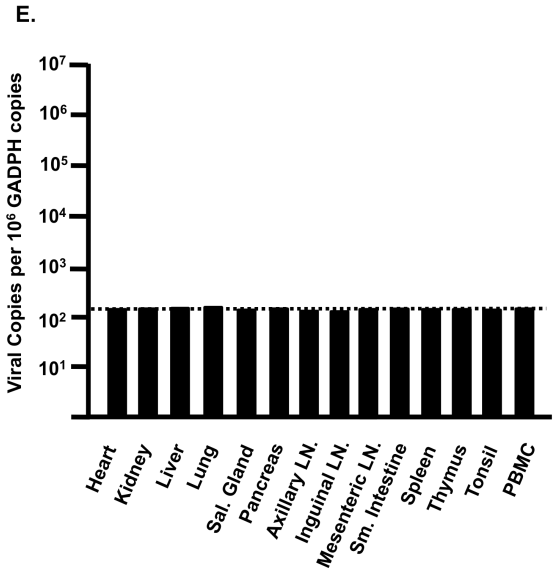
E.
Viral Copies per 10^6 GADPH copies
10^7
10^6
10^5
10^4
10^3
10^2
10^1
Heart
Kidney
Liver
Lung
Sal. Gland
Pancreas
Axillary LN.
Inguinal LN.
Mesenteric LN.
Sm. Intestine
Spleen
Thymus
Tonsil
PBMC

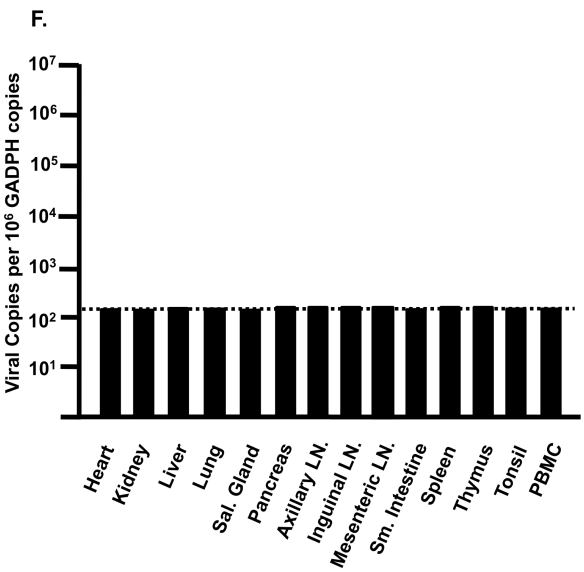
F.
Viral Copies per 10^6 GADPH copies
10^7
10^6
10^5
10^4
10^3
10^2
10^1
Heart
Kidney
Liver
Lung
Sal. Gland
Pancreas
Axillary LN.
Inguinal LN.
Mesenteric LN.
Sm. Intestine
Spleen
Thymus
Tonsil
PBMC

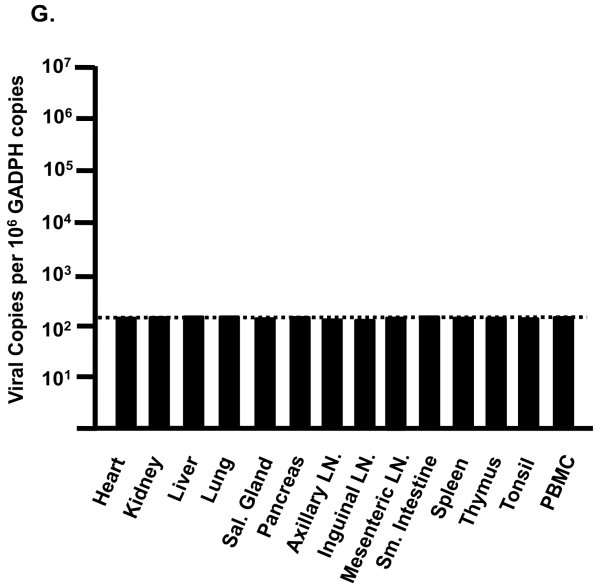
G.
Viral Copies per 10^6 GADPH copies
10^7
10^6
10^5
10^4
10^3
10^2
10^1
Heart
Kidney
Liver
Lung
Sal. Gland
Pancreas
Axillary LN.
Inguinal LN.
Mesenteric LN.
Sm. Intestine
Spleen
Thymus
Tonsil
PBMC

with $SHIV_{Vif5A}$ (data not shown). Macaques inoculated with parental $SHIV_{KU-2MC4}$, 44O and 44N, had high copy numbers of virus in various tissues (Figure 38). Taken together, these results indicate that both $SHIV_{VifHCCH(-)}$ and $SHIV_{Vif5A}$ infections were significantly less widespread compared to macaques inoculated with parental $SHIV_{KU-2MC4}$.

G-to-A mutations in *nef* and *vpu* amplified from DNA of primary and secondary lymph organs

A well documented feature of HIV-1Δ*vif* infection is the incorporation of select APOBEC3 proteins into viral particles leading to cytosine deamination during minus strand DNA synthesis (Yu et al., 2003). This results in hypermutation (guanosine to adenosine transitions) of the viral genome and inhibition of virus replication. We examined the number of G-to-A mutations in the *nef* and *vpu* genes amplified from DNA isolated from one primary lymphoid organ (thymus) and two secondary lymphoid organs (ileum of the small intestine and spleen) from the three macaques inoculated with $SHIV_{VifHCCH(-)}$ and one macaque inoculated with $SHIV_{KU-2MC4}$. We first PCR amplified *nef* and *vpu* sequences from tissue DNA and directly sequenced the amplified products. The results showed that there were multiple G-to-A mutations in the *nef* and *vpu* regions amplified from three tissues. The number of G-to-A mutations ranged from 54 to 88 or 1.2 to 1.9 percent of the total base pairs sequenced (Figure 39; Table VI). While the percentage of mutations observed in the *vpu* was lower (perhaps reflecting the gradient of mutations from *nef* to *vpu*), the overall number of G-to-A mutations in the context of 5'-TC to 5'-CC was approximately 2:1 (75 versus 31 mutations) (Figure 39; Table VI).

Figure 39. Quantitative assessment of mutations in the *nef* gene. Panels A-D. A 300 base pair fragment of *nef* was amplified using DNA isolated from the small intestine (ileum), spleen, and thymus of macaques inoculated with $SHIV_{VifHCCH(-)}$ and one macaque inoculated with $SHIV_{KU-2MC4}$. Mutations obtained using sequence analysis of fifteen independent clones from each macaque is shown. Each vertical bar represents an individual clone, whose height represents the total number of substitutions. Each bar is shaded according to the proportion of G-to-A substitutions that occurred in the dinucleotide context: non-G-to-A (black), GA (red), GG (yellow), GT (cyan), or GC (gray). Panels E-G. A representative hypermutation plot from each macaque illustrating the G-to-A and non-G-to-A substitutions in the clones from the ileum amplified DNA. Mutations obtained from bulk (top line) sequence analysis of fifteen independent clones from each macaque are shown. Each mutation is denoted by a vertical line that is color coded with respect to the the dinucleotide context: non-G-to-A (black), GA (red), GG (yellow), GT (cyan), or GC (gray).

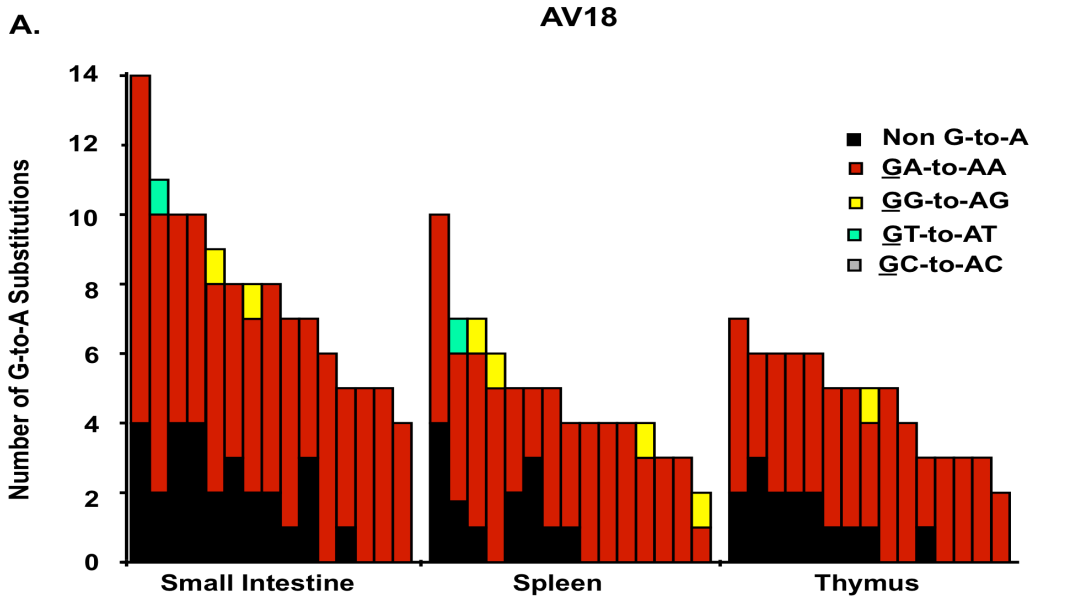
A.
AV18
Number of G-to-A Substitutions
0
2
4
6
8
10
12
14
Small Intestine
Spleen
Thymus
Non G-to-A
GA-to-AA
GG-to-AG
GT-to-AT
GC-to-AC

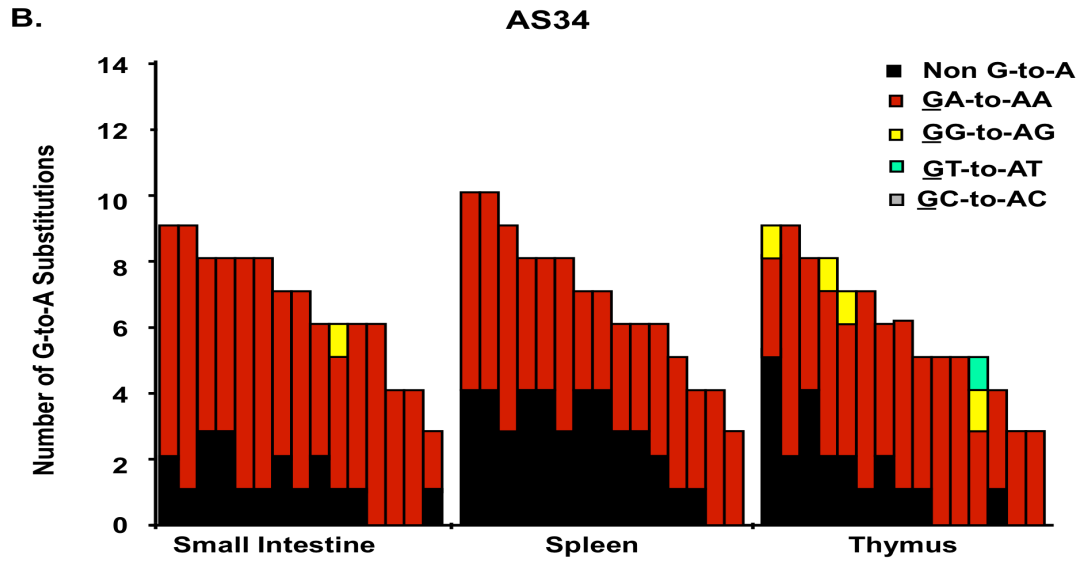
B.
AS34
Number of G-to-A Substitutions
0
2
4
6
8
10
12
14
Small Intestine
Spleen
Thymus
Non G-to-A
GA-to-AA
GG-to-AG
GT-to-AT
GC-to-AC

C.

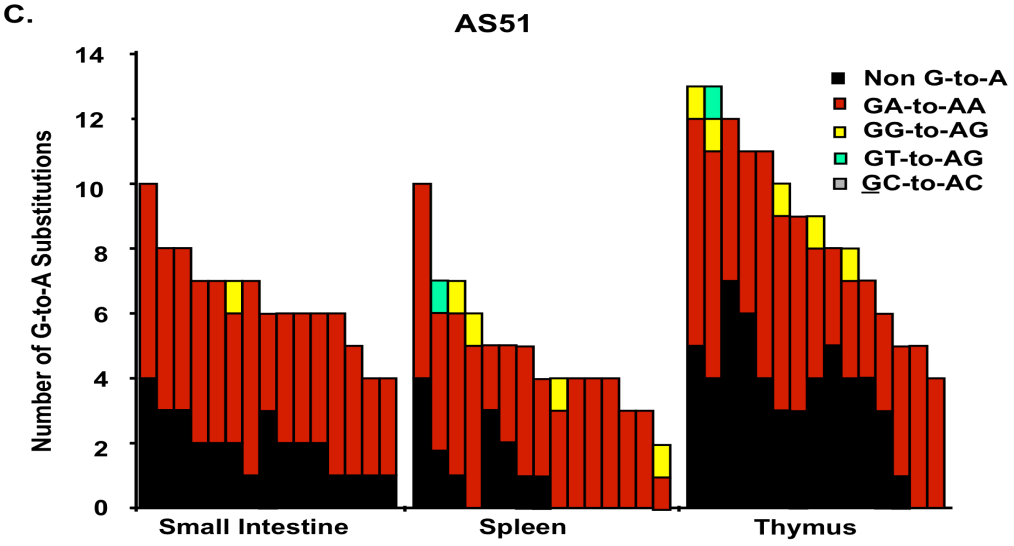
AS51
Number of G-to-A Substitutions
14
12
10
8
6
4
2
0
Non G-to-A
GA-to-AA
GG-to-AG
GT-to-AG
GC-to-AC
Small Intestine
Spleen
Thymus

D.

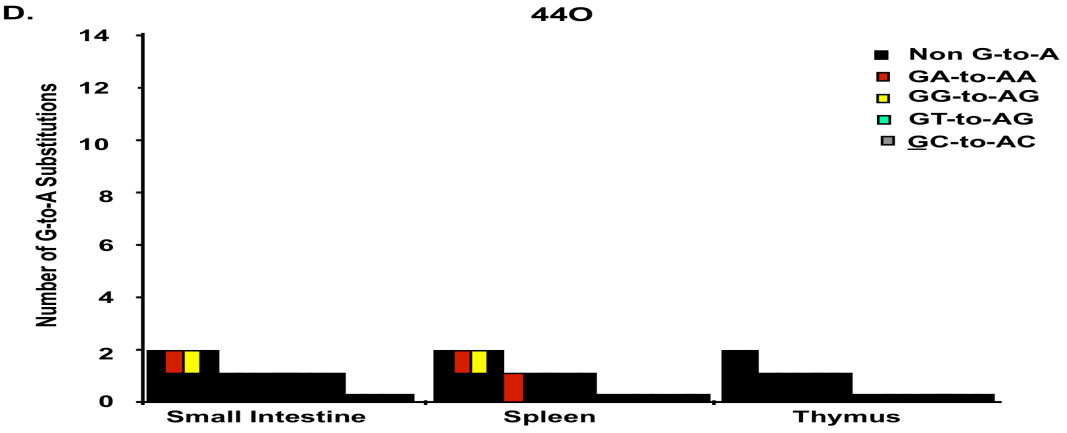
44O
Number of G-to-A Substitutions
14
12
10
8
6
4
2
0
Non G-to-A
GA-to-AA
GG-to-AG
GT-to-AG
GC-to-AC
Small Intestine
Spleen
Thymus

E.

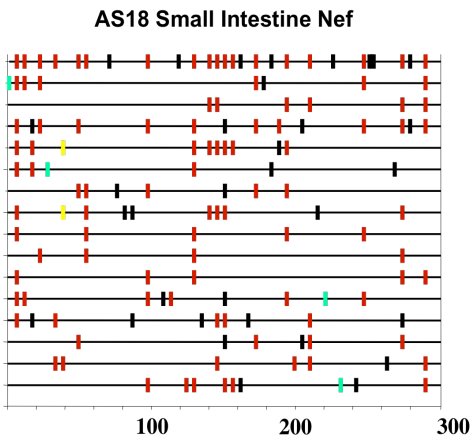
AS18 Small Intestine Nef
100
200
300

F.

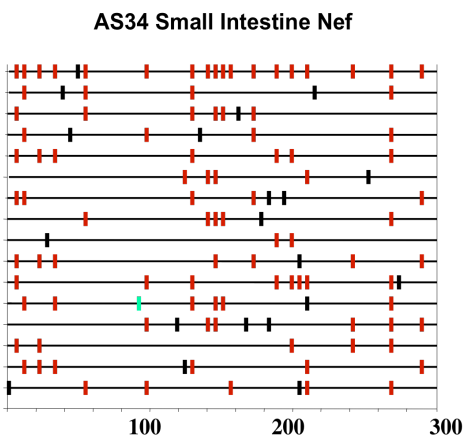
AS34 Small Intestine Nef
100
200
300

G.

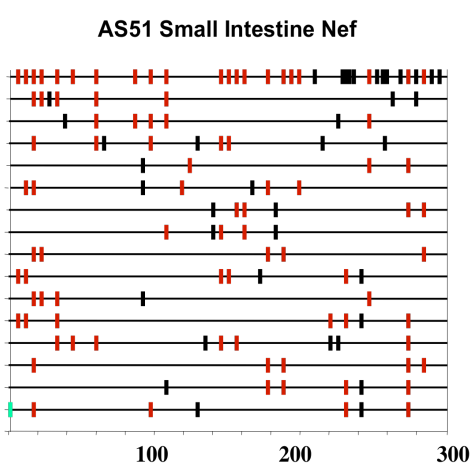
AS51 Small Intestine Nef
100
200
300

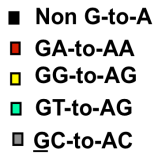
Non G-to-A
GA-to-AA
GG-to-AG
GT-to-AG
GC-to-AC

Table VI. Results of sequence analysis of *nef* amplified from the thymus, ileum, and spleen.

Animal Tissue	[a]Total number of bases sequenced	Total # of G-to-A mutations/percent G-to-A mutations of bases sequenced	Number and context of cytidine deamination		
			5'-GA	5'-GG	% 5'-GA to GG
AS34					
Thymus	4500	71/1.6	67	4	94.3
Spleen	4500	61/1.4	59	2	96.7
Ileum	4500	83/1.8	82	1	98.7
AS51					
Thymus	4500	75/1.7	69	6	92.0
Spleen	4500	62/1.4	62	0	100
Ileum	4500	66/1.5	65	1	98.4
AV18					
Thymus	4500	54/1.2	54	0	100
Spleen	4500	58/1.3	54	4	93.1
Ileum	4500	88/2.0	86	2	97.7

[a] A 300 base fragment corresponding to the 5' end of *nef* was amplified, cloned and 15 separate clones sequenced.

Figure 40. Quantitative assessment of mutations in the *vpu* gene. Panels A-D. A 184 base pair fragment of *vpu* was amplified using DNA isolated from the small intestine (ileum), spleen, and thymus of macaques inoculated with $SHIV_{VifHCCH(-)}$ and one macaque inoculated with $SHIV_{KU-2MC4}$. Substitutions were determined using sequence analysis of fifteen independent clones from each macaque are shown. Each vertical bar represents an individual clone, whose height represents the total number of substitutions. Each bar is shaded according to the proportion of G-to-A substitutions that occurred in the dinucleotide context: non-G-to-A (black), GA (red), GG (yellow), GT (cyan), or GC (gray). Panels E-G. A representative hypermutation plot from each macaque illustrating the G-to-A and non-G-to-A substitutions in the clones from the ileum amplified DNA. Mutations obtained from bulk (top line) sequence analysis of fifteen independent clones from each macaque are shown. Each mutation is denoted by a vertical line that is color coded with respect to the the dinucleotide context: non-G-to-A (black), GA (red), GG (yellow), GT (cyan), or GC (gray).

A.

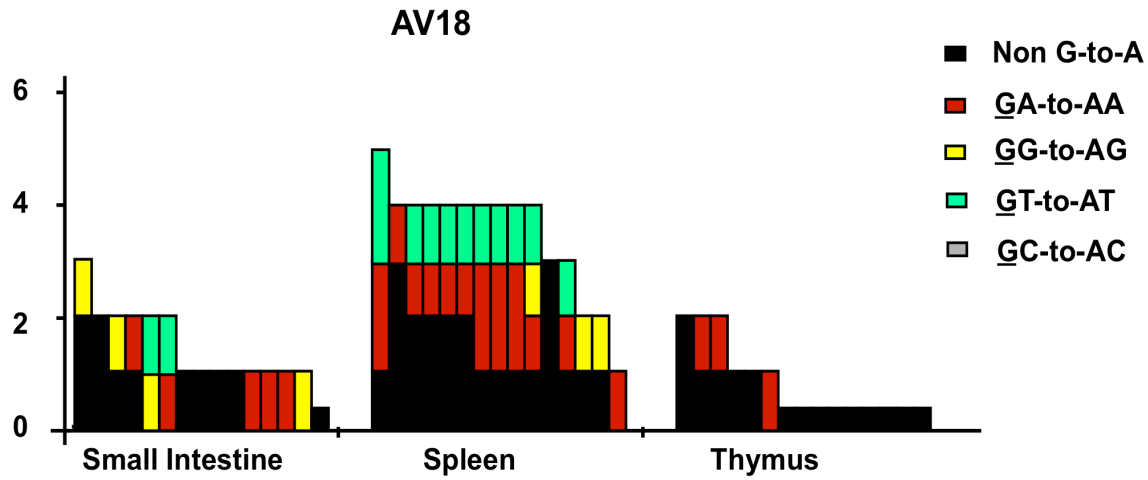
AV18
Non G-to-A
GA-to-AA
GG-to-AG
GT-to-AT
GC-to-AC
6
4
2
0
Small Intestine
Spleen
Thymus

B.

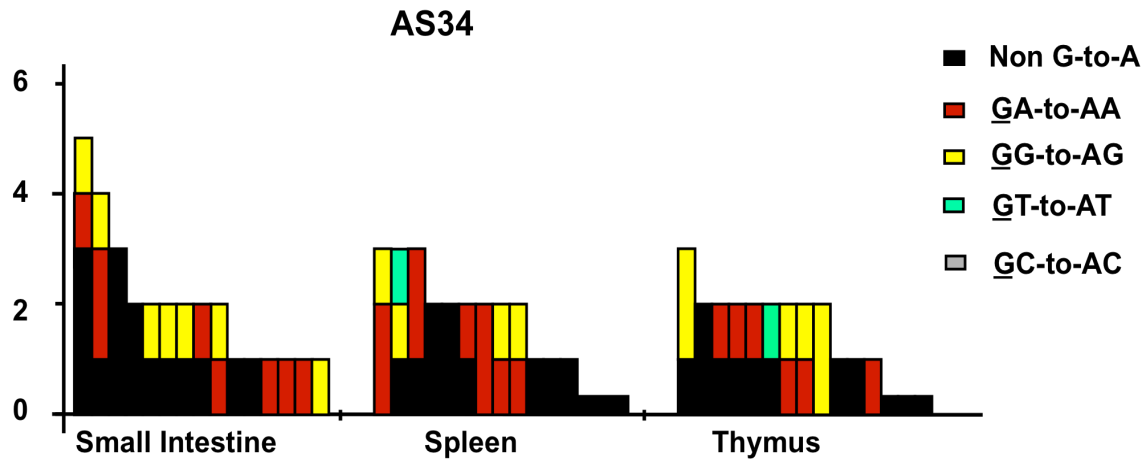
AS34
Non G-to-A
GA-to-AA
GG-to-AG
GT-to-AT
GC-to-AC
6
4
2
0
Small Intestine
Spleen
Thymus

C.

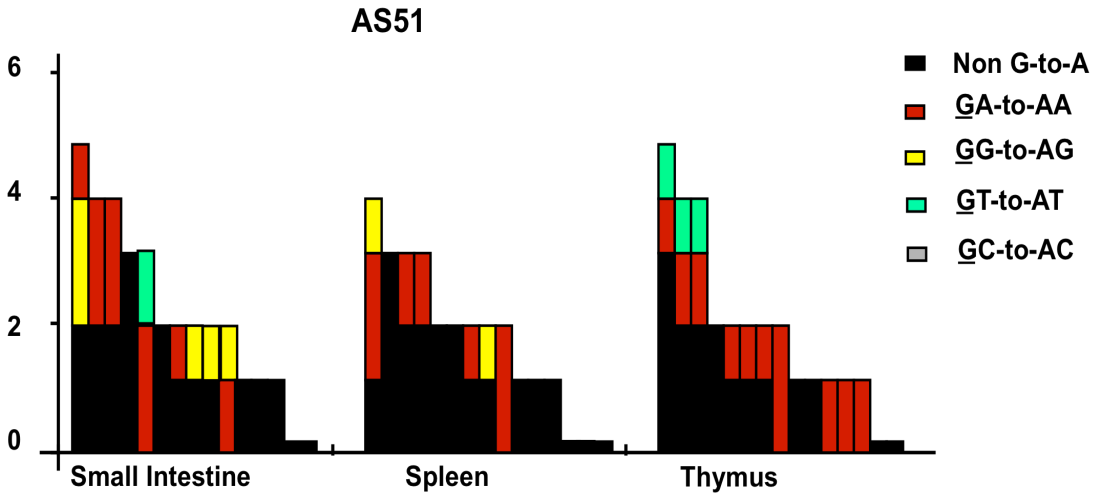
AS51
6
4
2
0
Small Intestine
Spleen
Thymus
Non G-to-A
GA-to-AA
GG-to-AG
GT-to-AT
GC-to-AC

D.

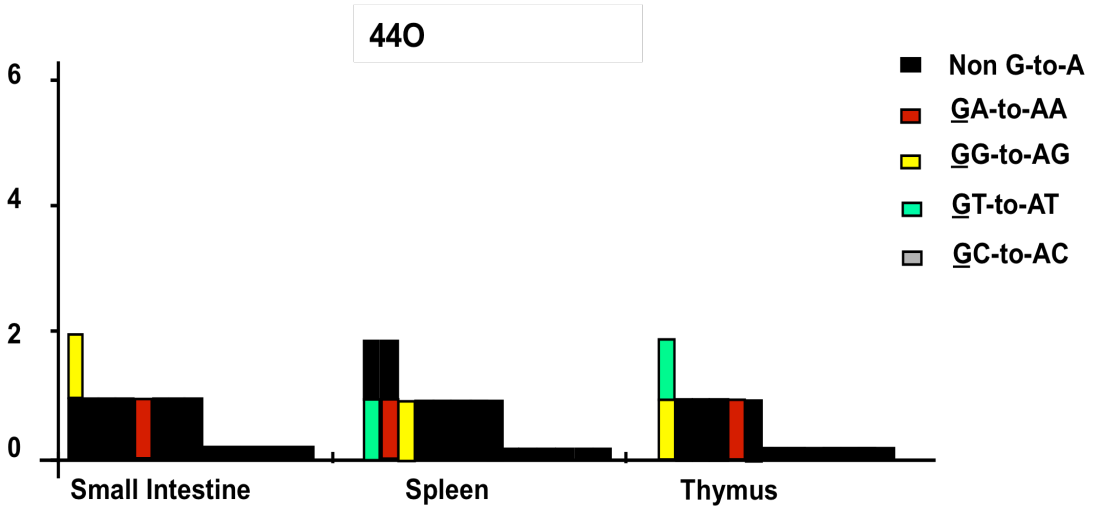
44O
6
4
2
0
Small Intestine
Spleen
Thymus
Non G-to-A
GA-to-AA
GG-to-AG
GT-to-AT
GC-to-AC

E.

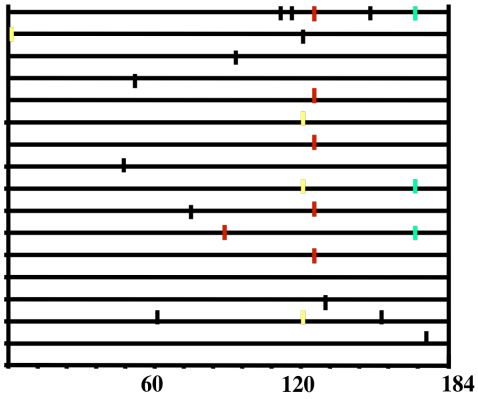
AV18 Small Intestine
60
120
184

F.

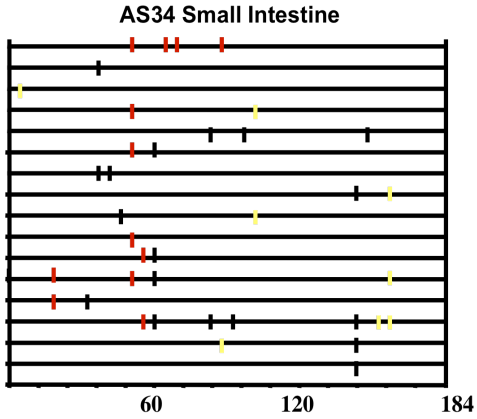
AS34 Small Intestine
60
120
184

G.

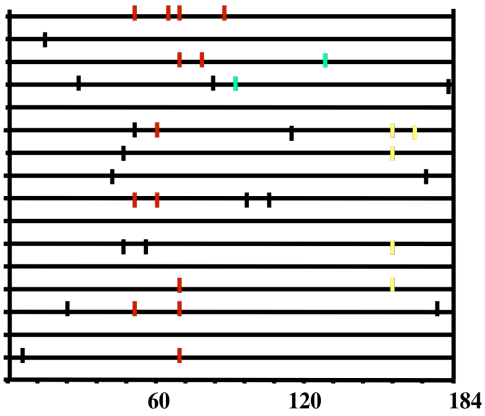
AS51 Small Intestine
60
120
184


Non G-to-A
GA-to-AA
GG-to-AG
GT-to-AT
GC-to-AC

Table VII. Results of sequence analysis of *vpu* amplified from the thymus, ileum, and spleen.

Animal Tissue	[a]Total number of bases sequenced	Total # of G-to-A mutations/percent G-to-A mutations of bases sequenced	Number and context of cytidine deamination		
			5'-GA	5'-GG	% 5'-GA to GG
AS34					
Thymus	2760	13/0.47	6	6	50.0
Spleen	2760	15/0.54	10	4	71.4
Ileum	2760	15/0.54	8	7	53.3
AS51					
Thymus	2760	14/0.51	11	0	100
Spleen	2760	9/0.33	7	2	77.8
Ileum	2760	15/0.54	9	5	64.2
AV18					
Thymus	2760	3/0.12	3	0	100
Spleen	2760	30/1.09	16	3	84.2
Ileum	2760	11/0.40	5	4	55.5

[a] A 184 base fragment corresponding to *vpu* was amplified, sub-cloned and 15 independent clones sequenced.

We confirmed the presence of these G-to-A mutations by sequencing 15 individual clones of the *nef* and *vpu* genes. We plotted the G-to-A mutations obtained from 15 single colony sequences of *nef* and *vpu* amplified from DNA isolated from the ileum of macaques inoculated $SHIV_{VifHCCH(-)}$ (Figures 39 and 40). These results showed that many of the G-to-A mutations found in the direct bulk sequencing products were also found in the individually cloned both genes (Figures 39 and 40). Similar to what we reported previously, the majority of the changes were in the context of 5'-TC (minus strand) (Table VI and VII). Macaque 44O, (inoculated with $SHIV_{KU2\text{-}MC4}$) had very few G-to-A substitutions in *vpu* and *nef* amplified from the same three lymphoid organs, which is similar to other macaques inoculated with this parental virus (unpublished observations). Macaque AV18 yielded the highest number of G-to-A substitutions (88) in the ileum of the small intestine. Taken together these findings suggest that one or more rhA3 proteins that have target sequence preference for 5'-T**C** is the major cytidine deaminase at work *in vivo.*

Discussion

There are only a limited number of studies that have analyzed the role of the Vif protein in the SIV or SHIV/macaque models of HIV-1 disease. In the first study, the role of various accessory proteins expressed from $SIV_{mac}239$ were evaluated in terms of potential to cause disease (Desrosiers et al., 1998). These investigators found that an SIV with deletion of *vif* had only transient viral loads, could only be detected in PBMC for

a short period of time and the macaques did not produce antibodies against SIV proteins. In a second study, investigators showed that a *vif*-deleted virus would generate antibody and cellular immune responses if the virus was administered 2-3 times but was not protective against challenge (Sparger et al., 2008). In both studies, the lymphoid and non-lymphoid tissues were not examined for the presence of viral RNA from these *vif-deleted* viruses. Finally, we previously showed that the introduction of amino acid substitutions into the SLQYLA domain of Vif (to AAQYLA) resulted in a virus ($SHIV_{VifAAQYLA}$) that did not replicate well in hA3G/F positive cells. However, following inoculation into macaques, the plasma viral loads were lowered from approximately 10^7 copies per ml for wild type virus to approximately 10^5 copies per ml for the $SHIV_{VifAAQYLA}$ during the acute phase of infection (Schmitt et al., 2009). In these macaques, the levels of circulating $CD4^+$ T cells were maintained near pre-inoculation levels and they did not develop histological lesions consistent with a pathogenic X4 SHIV. Sequence analysis of the *vif* gene amplified from the PBMC revealed that the engineered AAQYLA motif had mutated to TAQYLA in two of three macaques. Since serine and threonine are hydroxylated amino acids that differ by a methyl group, it was possible that these Vif proteins may have been "partially" functional *in vivo* to permit limited spread within macaques. Examination of the tissues from these macaques revealed that viral RNA was present in select tissues, and the viral sequences contained low levels of G-to-A substitutions. We also showed that the inoculation of plasma from two of these macaques into a naive macaque did not result in detectable viral loads up to five months post-inoculation (Schmitt et al., 2009). Thus, despite the low level of viral replication in

cell culture systems, $SHIV_{VifAAQYLA}$ was still capable of significant *in vivo* replication, thus validating the need to examine targeted Vif mutants in macaques.

In the present study, we have extended our *in vivo* studies using SHIV mutants that express either a Vif protein with the first five amino acids of the SLQYLA domain substituted with alanines ($SHIV_{Vif5A}$) or a Vif with the HCCH domain substituted with alanines ($SHIV_{VifHCCH(-)}$). Interestingly, our restriction assays showed that incorporation of rhA3G but not rhA3F resulted in the greatest reduction of replication, which is somewhat different from the results previously reported (Zennou and Bieniasz, 2006). Our results indicate that unlike the parental virus, both viruses incorporated rhA3G while both the parental and mutant viruses incorporated rhA3F into virions. Our analysis of rhA3F and rhA3G stability in the presence of viral genome indicated that rhA3F is stable while rhA3G is degraded. The incorporation of rhA3F into wild type virions is in agreement with a previous study (Zennou and Bieniasz, 2006; Virgen and Hatzioannou, 2007). These paradoxical findings suggest that rhA3F can be incorporated in the presence of SIV_{mac} Vif and that the virus can seemly replicate without the accumulation of lethal mutations. In the former study, these investigators found that rhA3F was resistant to the SIV_{mac} Vif protein. They suggested that rhA3F may not exert a strong negative presence on SIV_{mac} *in vivo* and that the SIV_{mac} Vif may actually permit some degree of mutagenesis by rhA3F. This was supported by analysis of HIV-1 *gag*, *pol*, and *env* for potential editing sites (GG or GA) that would yield a termination codon if mutated. Their analysis revealed that the percentage of GA editing sites leading to termination codons was lower than GG sites in the *gag*, *pol*, and *env.* Analysis of the SIV *gag*, *pol*, *vif*, *vpr*, *vpx*, and *nef* (the SIV genes of our SHIV) also revealed this trend

(unpublished observations) yet the mutations observed in the SIV_{mac} *nef* were predominantly in the context of GA and not GG. Whether this was due to lethal GG-to-AG mutations that were subsequently cleared (or not detectable) or whether this was due to rhA3F or another rhA3 protein is unknown at this time. However, it should be noted that there were differences in our study and the previous study. First, in the previous study the investigators used a HIV-1Δ*vif* genome and we used an SIV-based viral genome with targeted mutations in the *vif*. We showed that replication of $SHIV_{VifSTOP}$ was much lower compared to $SHIV_{Vif5A}$ and $SHIV_{VifHCCH(-)}$ in the presence of rhA3F. Thus, the results of $SHIV_{VifSTOP}$ in our study and HIV-1Δ*vif* in their study is comparable. Our study also shows that our viruses with targeted mutations ($SHIV_{Vif5A}$ and $SHIV_{VifHCCH(-)}$) were restricted less efficiently in the presence of rhA3F compared to $SHIV_{VifSTOP}$, suggesting that the presence of an intact, "crippled" Vif protein can impose some restriction compared to having a ΔVif virus. This may relate to the ability of the $Vif_{HCCH(-)}$ and the Vif_{5A} proteins to still bind to rhA3F. Previous studies have defined regions of the HIV-1 Vif that are required for binding various hA3 proteins. Many of these regions are in the amino terminal region of the protein. Previous studies demonstrated that HIV-1 Vif residues ^{40}YRHHY^{44} and ^{12}QVDRMR^{17} are important for the interaction with hA3G and hA3F/C, respectively (Russell and Pathak, 2007; Mehle et al., 2007). In a more recent study, a conserved YXXL domain at residues 69-72 of the HIV-1 Vif was found to be important for the interaction of Vif with hA3G, hA3F and hA3C (Pery et al., 2009). While the ^{12}QVDRMR^{17} and ^{40}YRHHY^{44} are not conserved in the SIV_{mac}239 Vif, there is a lysine at position 27 of the SIV_{mac} Vif that is required for interaction with rhA3G (Chen et al., 2009; Dang et al., 2009). The YWGL domain of the

HIV-1 Vif is also conserved in the SIV Vif (as YWHL). Thus, it is possible that the Vif proteins with targeted amino acid substitutions may still bind and incorporate rhA3Finto virus particles but may be inefficient in deamination because of its association with Vif. A second difference in the two studies is the hypermutation assay used to analyze the percentage of G-to-A changes in the genome. While the previous study showed that rhA3F caused G-to-A hypermutation at levels higher than rhA3G, we found that rhA3F produced little hypermutation in the viral genome. In the previous study, these investigators used a VSV pseudotyped HIV-1 vector with the *vif* deleted as well as other genes and analyzed hrGFP sequences. In our system, we used complete SIV viral genomes expressing the Vif mutant.

One goal of these studies was to determine if $SHIV_{Vif5A}$ was effectively controlled by macaques during the primary phase of infection or if viral variants would emerge that would permit limited replication in macaque tissues. Our results indicate that following inoculation of $SHIV_{Vif5A}$ into macaques, there was a further reduction of plasma viral loads compared to $SHIV_{VifAAQYLA}$ (Schmitt et al., 2009). The mean peak plasma virus load (week 1) was 1.3×10^3 viral copies per ml or approximately 4,000-fold lower than parental $SHIV_{KU\text{-}2MC4}$. However, following this initial burst of replication, viral RNA from macaques inoculated with $SHIV_{Vif5A}$ was near or below the limits in this assay (~180 copies). It should be noted that the virus was not completely eliminated because viral RNA was occasionally detected in the plasma throughout the 6-month infection using nested RT-PCR (data not shown). At necropsy, the number of copies of viral RNA could not be quantified from various organs of these macaques (detection limit 180 copies) but could be detected by nested RT-PCR. We were unable to detect the virus in PBMC by 3

weeks post-inoculation and were unable to amplify the *nef* gene at necropsy for sequence analysis. While the results presented here may be predicted based on studies in cell culture systems, these results demonstrate for the first time that a primate lentivirus expressing a Vif protein with only targeted mutations in a critical domain can be completely controlled by the host. Taken together, these results indicate that the $SHIV_{Vif5A}$ replicated similarly to a virus that does not express a functional Vif protein (Desrosiers et al., 1998).

No studies have analyzed the role of the Zn^{++} binding domain of Vif *in vivo*. Previous studies have shown that this domain is critical to Vif function, interacting with Cul 5 of the Cul 5/ ElonginB/C/ Rbx E3 ligase (Luo et al., 2005; Xiao et al., 2007). Our results showed that these macaques had slightly higher initial viral loads at one week post-inoculation than macaques inoculated with $SHIV_{Vif5A}$, however the virus was effectively controlled by the macaques by 3 weeks post-inoculation. Similar to our previous study, the majority of the G-to-A mutations were in the context of 5'-T**C** (minus strand) and not 5'-C**C**. In addition, we observed that the majority of the G-to-A changes found in the *vif* gene amplified from PBMC DNA occurred during the first weeks of infection. This correlated well with the plasma viral loads, which indicated the viral replication primarily occurred during this time period.

Taken together, our results show that abolishing the SLQYLA domain of Vif may be more detrimental to the virus *in vivo* than the HCCH domain. These data bring up the question, "Why were we able to quantify viral RNA from tissues of macaques inoculated with $SHIV_{VifHCCH(-)}$ but not $SHIV_{Vif5A}$?" While the answer is unknown, several possibilities exist. First, the virus may have initially replicated in cells expressing active rhA3

proteins and incorporated one or more rhA3 proteins into the viral progeny. In the next round of replication the genome was mutated but not to the extent that RNA polymerase II could not transcribe viral RNA. Second, there may be a tissue/cellular reservoir for virus replication that do not express the rhA3 proteins that would restrict the crippled SIV_{mac}239 Vif protein. We previously showed using immunohistochemistry that rhA3G was not expressed in all cell types in the brain and kidneys (Hill et al., 2006; 2007). Finally, during the initial rounds of replication and potential deamination, G-to-A mutations may have led to compensating mutations that made the viral Vif partially functional. The later scenario is not likely as our sequence analysis did not identify consensus mutations in either the $SHIV_{Vif5A}$ or $SHIV_{VifHCCH(-)}$-inoculated macaques.

As previous studies showed that antibody responses were not generated with a single inoculation of *vif-deleted* viruses (Desrosiers et al., 1998; Sparger et al., 2008), we determined if a single inoculation of either virus would result in an antibody response against viral proteins. Comparison of the antibody responses from macaques inoculated with either $SHIV_{VifHCCH(-)}$ or $SHIV_{Vif5A}$ shows that at 12 weeks post-inoculation macaques had developed antibody responses against the virus but these were undetectable at necropsy. This would argue that the viral RNA detected in tissues at necropsy may not have been translated into viral proteins. This would also suggest that infectious virus was cleared by the macaque and that antigenic stimulation through viral proteins did not occur. However, this study provides evidence that such viruses containing site-directed mutations in *vif* could be used to “prime” the immune system and suggests that such a virus could be useful in a prime-boost strategy. It will be of interest to determine if multiple inoculations will result in stronger immune responses (both humoral and cellular)

and a further reduction of viral loads with increasing inoculations. If successful, it will be of interest to determine if the immune responses are protective against challenge. While the use of live attenuated lentiviruses has led to useful information concerning the role of accessory genes in replication of the virus *in vivo*, the use of such vaccines has several underlying risks (Koff et al., 2006). First, these vaccines have relied on the deletion/disruption of accessory genes (*nef, vpu, vpx/vpr*) that enhance replication but are not absolutely required for replication *in vivo*. For this reason these viruses can select for compensating mutations that ultimately result in the virus becoming pathogenic (Baba et al., 1995; 1999). The second problem is the risk of recombination of the viral genome to yield a pathogenic virus (Kim et al., 2005). A vaccine based on a "crippled Vif" that allows for limited replication resulting in G-to-A substitutions and inactivation of the virus should prevent the scenarios discussed above. It would be of interest to determine if inoculation of macaques with two viruses, one harboring a mutation in *vif* and another having a mutation in another accessory gene such as *nef* can recombine *in vivo* to generate a wild type virus causing $CD4^+$ T cell loss and disease prior to the virus accumulating G-to-A mutations.

Experimental Methods

Cells, plasmids, and viruses

The C8166 and SupT1 lymphocyte cell lines were used for transfections of full-length SHIVs and as indicator cells to measure infectivity and cytopathicity of the viruses

used in this study. Both cell lines were maintained in RPMI-1640, supplemented with 10 mM Hepes buffer pH 7.3, 2 mM glutamine, 5 µg per ml gentamicin, 100 units/µg penicillin-streptomycin and 10% fetal bovine serum (R10FBS). Rhesus macaque PBMCs were obtained from uninfected animals and isolated on Ficoll/Hypaque gradients for p27 growth curves. The 293 cell line was maintained in Dulbecco's minimal essential medium (DMEM) with 10% fetal bovine serum and the antibiotics described above. The derivation of $SHIV_{KU-2MC4}$ has been previously described (Joag et al., 1998). The pcDNA3.1(+)-HA-rhesus APOBEC3G and pcDNA3.1(+)-rhesus APOBEC3F-V5 were kindly provided by Nathaniel Landau (New York University School of Medicine, New York, New York).

Construction of $SHIV_{Vif5A}$, $SHIV_{VifHCCH(-)}$ and $SHIV_{VifSTOP}$

For the construction of $SHIV_{VifHCCH(-)}$, the PacI/SphI fragment (nucleotides 5132 to 6452) from the p5'-SHIV4 was subcloned into the pGEM3Zf (+) vector. The histidine to alanine substitution at position 110 of Vif was introduced using oligonucleotides (only sense strand shown) 5'-GCAGACATTTTACTGGCTAGCACTTATTTCC- 3'. The cytidine to alanine substitution at position 116 of Vif was introduced using oligonucleotides (only sense strand shown) 5'- GCACTTATTTCCCTGCCTTTACAGCGGGAG- 3'. The cysteines at positions 134 and 135 of Vif were substituted for alanines using the oligonucleotides (only sense strand shown) 5'-CAACTGCTGTCTGCCGCCAGGTTCCCG-3'. The histidine to alanine substitution at position 144 of Vif was introduced using oligonucleotides (only sense strand shown) 5'-GGTTCCCGAGAGCTGCTAAGTACCAGGTACC –3'. All substitutions were made using

the Quick-Change Mutagenesis Kit (Stratagene) following the manufacturer's instructions. The resulting PacI/SphI fragment was digested, isolated, and subcloned into full length $SHIV_{KU-2MC4}$. The resulting plasmid was sequenced to ensure that the desired mutations were introduced as expected.

For the construction of $SHIV_{Vif5A}$, the PacI/SphI fragment (nucleotides 5132 to 6452) from full-length $SHIV_{KU-2MC4}$ was subcloned into the pGEM3zf (+) vector. The serine and leucine at positions 147 and 148 were substituted for alanines using the oligonucleotides (sense strand shown) 5'-CCAGGTACCAGCCGCACAGTACTTAGCAC-3'. The glutamine and tyrosine at positions 149 and 150 were substituted for alanines using the oligonucleotides (sense strand shown) 5'-CCAGGTACCAGCCGCAGCGGCCTTAGCACTGAAAGTAGTAAGC-3'. The leucine at position 151 was substituted for an alanine using the oligonucleotide (sense strand shown) 5'-GGTACCAGCCGCAGCGGCCGCAGCACTGAAGTAGTAAGCG-3'. All substitutions were made using the Quick-Change Mutagenesis Kit (Stratagene) following the manufacturer's instructions and virus constructed and prepared as described above.

For the construction of $SHIV_{VifSTOP}$, the tyrosine and leucine at amino acid positions 28 and 29 were engineered to have stop codons using site-directed mutagenesis in order to produce a full-length SHIV that does not express a functional Vif protein. The oligonucleotide used to introduce these mutations was 5'-GCCTCATTAAAATAGTAGAAATATAAAACTAAAG-3' (only sense strand shown). The substitutions were made using the Quick-Change Mutagenesis Kit (Stratagene) following the manufacturer's instructions. The resulting PacI/SphI fragment was digested,

isolated, and subcloned into full length $SHIV_{KU-2MC4}$. The resulting plasmid was sequenced to ensure that the desired mutations were introduced as expected. For all three viruses, the plasmids containing the full-length genomes were transfected into SupT1 cells as previously described (Stephens et al., 2002; Hout et al., 2005). Stocks of $SHIV_{VifHCCH(-)}$, $SHIV_{Vif5A}$, and $SHIV_{VifSTOP}$ were prepared, tittered on SupT1 cells, and stored at -86°C.

Analysis of the replication of $SHIV_{Vif5A}$ and $SHIV_{VifHCCH(-)}$ in APOBEC3G/F positive and negative cells

C8166 (A3G/F positive) and SupT1 (A3G/F negative) cells were inoculated with equivalent levels (25 ng) of parental $SHIV_{KU-2MC4}$, $SHIV_{Vif5A}$, $SHIV_{VifHCCH(-)}$, $SHIV_{VifAAQYLA}$, or $SHIV_{VifSTOP}$ for 4 hours at 37C. For rhesus PBMC, cells were isolated on Ficoll-Hypaque gradients, stimulated for 48 hours in R10FBS supplemented with concanvalin A (10 µg/ml) and interleukin-2 (IL-2; 50 ng/ml). The cells were washed, and inoculated with virus (25 ng) incubated in R10FBS containing interleukin-2 (50 ng/ml) for 4 hours. At 4 hours, cells were centrifuged, washed 3 times to remove the inoculum and incubated in fresh medium (medium for the rhesus PBMC also contained 50 ng/ml IL-2) at 37C for up to 15 days. Aliquots of culture supernatants were obtained at 0, 1, 3, 5, 7, 9, 11, 13, and 15 days post-inoculation and the levels of p27 assessed using commercial p27 antigen capture kits (Zeptometrix).

APOBEC3G/F incorporation assays

Plasmids containing the genomes viruses (derived from $SHIV_{KU-2MC4}$) expressing each of the mutant Vif proteins described above were co-transfected into 293 cells using

PEI Transfection reagent (Ex-Gen 500) along with plasmids expressing either HA-rhA3G or V5-rhA3F. At 48 hours, the virus containing supernatants were harvested and clarified by low speed centrifugation. The clarified supernatant was then subjected to ultracentrifugation to pellet the virus (SW41 rotor, 247,000xg, 1 hour). The pellet was resuspended in PBS (pH 7.4) and layered on a 20/60% sucrose step gradient and again subject to ultracentrifugation (SW55Ti, 247,000xg, 1 hour). The virus (at the interface) was harvested, pelleted again by ultracentrifugation described above, and resuspended in 200µl of 1x PBS (pH 7.4). An aliquot was saved to determine the p27 content by antigen capture assay (Zeptometrix). The remaining sample was boiled in sample reducing buffer. Equivalent amounts of p27 were loaded on a 12% SDS-PAGE gel and transferred to PVDF membranes. APOBEC3 proteins were detected by Western blotting using an antibody directed against either the HA tag (HA-probe; Santa Cruz) or V5 tag (Clone V5-10; Sigma). Blots were stripped in 1X stripping buffer (62.5 mM Tris-HCl, pH 6.8 and 2% SDS) and reprobed using a rabbit polyclonal antibody specific for p27. As a control, plasmids expressing either rhA3G or rhA3F were transfected into 293 cells using PEI transfection reagent (ExGen500, Fermentas). At 48 hours post-transfection, cells were lysed in 1x RIPA and the nuclei were removed. Whole protein was precipitated with methanol and resuspended in 2x sample buffer. Normalized to β-actin, the samples were run on a 12%-SDS-PAGE gel, and probed with the antibodies stated above.

Stability of rhA3G and rhA3F in the presence of SHIV genomes

We determined if rhA3G or rhA3F were stable in the presence of $SHIV_{KU-2MC4}$, $SHIV_{VifHCCH(-)}$, $SHIV_{Vif5A}$, or $SHIV_{VifSTOP}$. Full-length mutated SHIVs were co-transfected in a 2:1 ratio with either APOBEC3G-HA or APOBEC3F-V5 using polyethylenimine transfection reagent (PEI, Fermentas). Twenty-four hours post-transfection, the supernatant was removed and the cells were harvested and lysed using 1 x RIPA (50 mM Tris-HCl, pH 7.5; 50 mM NaCl; 0.5% deoxycholate; 0.2% SDS; 10 mM EDTA). Following lysis, the nuclei were removed by microcentrifugation at 1400 rpm for 15 minutes. The protein was prepared using methanol, resuspended in 2X sample reducing buffer, and boiled for 5 minutes. Proteins were separated on a 10% SDS-PAGE gel and probed using commercially available rabbit polyclonal HA antibody (HA-probe, Santa Cruz) for rhA3G-HA or mouse monoclonal V5 antibody (Clone V5-10, Sigma) for rhA3F. All samples were normalized to the amount of β-actin protein using a mouse monoclonal antibody (Novous Biologicals) specific for β-actin.

Hypermutation assays in the presence of rhA3G or rhA3F

Hypermutation of various SHIVs in the presence of rhesus APOBEC3G/F 293 cells were transfected with $SHIV_{KU-2MC4}$, $SHIV_{VifHCCH(-)}$, $SHIV_{Vif5A}$, or $SHIV_{VifSTOP}$ in the presence of either rhA3G or rhA3F using polyethylenimine transfected reagent (PEI, Fermentas). Twenty-four hours post-transfection, cells were washed and fresh DMEM was added. After forty-eight hours, the supernatant containing virus was subjected to low speed centrifugation. The resulting supernatant was DNase-I—treated (Fermentas) at 37°C for 30 minutes to eliminate any trace of plasmid carry-over from the initial

transfection. The DNase-I-treated supernatant was titrated on TZM-bl cells to both assess infectivity and hypermutation. Twenty-four hours post-infection, total DNA cellular DNA was harvested and extracted using the DNeasy kit and the manufacturer's instructions (Qiagen). The DNA was used in a nested DNA polymerase chain reaction to amplify a 300 base pair fragment of *nef*. The PCR reaction was carried out using rTaq, the manufacturer's instructions (Takara), and the oligonucleotides listed below. 1 µl of the first PCR product was added to a nested reaction. The PCR reactions were perfomed using an Applied Systems 2720 Thermal Cycler with the following thermal profile: 95°C for 2 minutes, 1 cycle; 95°C for 30 seconds, 48°C for 30 seconds, 65°C for 2 minutes, 35 cycles; 65°C for 7 minutes. The PCR products were separated by electrophoresis, isolated, purified, sequenced and sub-cloned into pGEM-TEasy (Promega) as described below. Fifteen independent clones were sequenced and assessed for each mutant SHIV as described above.

Restriction of Vif Mutants on rhA3G or rhA3F

We determined the effect of the Vif mutants on the suppression of rhA3G and rhA3F. Full-length mutated SHIVs were co-transfected with either rhA3G or rhA3F using PEI transfection reagent (ExGen500, Fermentas). Forty-eight hours post-transfection, the supernatant was harvested and purified by low speed centrifugation. Equivalent amounts of p27 were serially diluted using 10-fold dilutions from 10^1 to 10^6 and used to inoculate TZM-bl cells. Forty-eight hours later, the media was removed, cells washed with 1X PBS and the monolayer fixed using 1% formaldehyde-0.2% glutaraldehyde in

phosphate-buffered saline (1 x PBS). The cells were washed and incubated in a solution for 2 hours at 37C in 4 mM potassium ferrocyanide, 4 mM potassium ferricyanide, 4 mM magnesium chloride, and 0.4 mg X-gal per ml. The reaction was stopped and the number of $TCID_{50}$ were calculated (Derdeyn et al., 2000; Wei et al., 2002).

Macaques analyzed in this study

Three rhesus macaques (*Macaca mulatta*: CX54, ER65, and I92) were intravenously inoculated with 1 ml of undiluted culture supernatant from SupT1 grown virus stocks (containing 10^4 $TCID_{50}$ per ml). Three additional rhesus macaques (AS34, AS51, and AV18) were inoculated with 10^4 $TCID_{50}$ $SHIV_{VifHCCH(-)}$ (titered in SupT1 cells). The animals were housed in the AAALAC-approved animal facility at the University of Kansas Medical Center. All aspects of the animal studies were performed according to the institutional guidelines for animal care and use at the University of Kansas Medical Center. Heparinized blood was collected weekly for the first 4 weeks, then at 2-week intervals for the next month and at monthly intervals thereafter.

Assays for circulating $CD4^+$ T cells

Changes in the levels of $CD4^+$ T cells after viral inoculations were monitoredsequentially by flow cytometric analysis (BD Biosciences). T cell subsets were labeled with a commercially available anti-CD3/CD4/CD8 mixture. T cell subsets from a normal uninfected macaque were always performed at the same time to serve as a control for the flow cytometry analysis.

Processing of tissue samples at necropsy

At the time of euthanasia (26 or 28 weeks), all macaques in this study were anesthetized by administration of 10 mg/kg ketamine (IM) followed by intravenous administration of sodium phenobarbital at 20-30 mg/kg. At the time of necropsy, all macaques were in a healthy condition. A laparotomy was performed. The animal was exsanguinated by aortic canulation and perfused with one liter of cold Ringer's saline. Lymphoid and non-lymphoid tissues (heart, kidneys, liver, lungs, mesenteric, inguinal and axillary lymph nodes, pancreas, salivary gland, small intestine, spleen, thymus, and tonsils) were obtained and aliquots of tissue snap frozen for DNA and RNA assays. Aliquots of lymphoid tissues were immersed in HBSS to quantify levels of infectious virus in tissues using infectious centers assays with SupT1 cells.

Sequence analysis of the vif, nef, and vpu genes

To determine the stability of the mutations that were introduced into *vif* and assess whether these macaques acquired G-to-A mutations*,* the *vif, nef,* and *vpu* genes were amplified from either PBMCs at different time points during infection (*vif*) or from several tissue DNA samples taken at necropsy (*nef* and *vpu*) that were positive for viral RNA. One hundred nanograms of extracted genomic DNA was used in a nested DNA polymerase chain reaction (Takara, Madison, WI) following the manufacturer's instructions. The oligonucleotides employed during the first round to amplify *vif* were 5'-GGCTAAAATTATCAAAGATTATGGAGG-3' (sense) and 5'-

GGTGACATCCCTTGTTCATCATGCC-3' (antisense), which corresponds to bases 5326-5352 and 5984-6008, respectively. The nested oligonucleotides were 5'-GGAGGAGGAAAAGAGGTGGATAGCAGTTCCC-3' (sense) and 5'-CCAGTATTCCCAAGACCTTTGCC-3' (antisense), which corresponds to bases 5348-5378 and 5963-5985, respectively. The oligonucleotides used during the first round to amplify the *nef* gene were 5'-GGTGGAGCTATTTCCATGAGG-3' (sense) and 5'-GTCTTCTTGGACTGTAATAAATCCC-3' (antisense), which corresponds to bases 9445-9465 and 9832-9856, respectively. The nested oligonucleotides were 5'-CCATGAGGCGGTCCAGGCAGTCTAGAG-3' (sense) and 5'-CCTCCCAGTCCCCCCTTTTC-3' (antisense), which corresponds to bases 9458-9484 and 9814-9833, respectively. The oligonucleotides used during the first round to amplify the *vpu* gene were 5'-CCTAGACTAGAGCCCTGGAAGCATCC-3' (sense) and 5'-GTACCTCTGTATCATATGCTTTAGCAT-3' (antisense), which corresponds to bases 6486-6511 and 7034-7061, respectively. The nested oligonucleotides used were 5'-TTAGGCATCTCCTATGGCAGGAAGAAG-3' (sense) and 5'-CACAAAATAGAGTCCTGGTTGCTTCCT-3' (antisense), which corresponds to bases 6597-6623 and 7001-7027, respectively.

For sequence analysis, the PCR products from three separate PCR reactions were pooled and separated by electrophoresis in a 1.5% agarose gel, isolated, and each PCR reaction directly sequenced. Cycle sequencing reactions using the BigDye Terminator Cycle Sequencing Ready Reaction Kit with AmpliTaq DNA polymerase, FS (PE Applied Biosystems, Foster City, CA) sequence detection was conducted with an

Applied Biosystems 377 Prism XL automated DNA sequencer and visualized using the ABI Editview program. Sequences were compared to the sequence of $SHIV_{KU-2MC4}$. A total of 615 nucleotides were analyzed from *vif*, 300 nucleotides analyzed from *nef*, and 184 nucleotides from *vpu* using the SE Central Software package. In order to isolate and analyze single sequences, bulk PCR reactions were subcloned into the pGEM-TEasy (Promega) cloning vector. Fifteen clones were selected, sequenced as described above, and analyzed to assess the number of G-to-A substitutions that occurred.

Plasma virus loads

Plasma viral RNA loads were determined on RNA extracted from 1 ml of EDTA-treated plasma. Virus was pelleted using ultracentrifugcation (Beckman SW55Ti, 250,000xg, 2 hours) and RNA extracted using the Qiagen viral RNA kit (Qiagen). RNA samples were analyzed by real-time RT-PCR using *gag* primers and a 5'FAM and 3'TAMRA labeled Taqman probe that is homologous to the SIV *gag* gene as previously described (Hofmann-Lehmann *et al.*, 2000). Standard curves were prepared using a series of six ten-fold dilutions of viral SIV *gag* RNA of known concentration. The sensitivity of the assay was 100 RNA equivalents per ml. Samples were analyzed in triplicate and the number of RNA equivalents per ml of plasma were calculated. Viral RNA was also quantified from in visceral tissues using this primer/probe reaction. In order to quantify the amount of viral RNA, GAPDH was used as a control and data is presented as copies per 10^6 GAPDH molecules (Marcario et al., 2008).

Immunoprecipitation assays

To determine if the macaques developed antibodies to SHIV proteins following inoculation, the plasma at 12 weeks and at necropsy was used in immunoprecipitation assays. C8166 cells were inoculated with approximately 10^4 $TCID_{50}$ of $SHIV_{KU-2MC4}$ for 5 days. The cells were then incubated in methionine/cysteine-free media for 2 hours and radiolabeled labeled with 500 µCi of ^{35}Smethionine/cysteine for 15 hours. The cells were lysed in 1ml of 1X RIPA buffer and nuclei were removed by centrifugation. The cell lysates were incubated overnight at 4^{o}C with 10 µl of plasma from each macaque and protein A Sepharose beads. The immunoprecipitates bound to the beads were washed three times in 1X RIPA, resuspended in 75 µl of 2X sample reducing buffer, and boiled for 5 minutes. Proteins were separated on a 10% SDS-PAGE gel and visualized by autoradiography. Controls included pooled prebleed plasma from macaques (negative control) and plasma from macaques that had been previously inoculated with a non-pathogenic SHIV ($SHIV_{TM,}$ positive control).

VIII. Chapter 4: Differential virus restriction patterns of rhesus macaque and human APOBEC3A: Implications for lentivirus evolution

Abstract

The human apolipoprotein B mRNA editing enzyme catalytic peptide-like 3 (APOBEC3; A3) family of proteins (A3A-H) are known to restrict various retroviruses and retroelements, but the full complement of rhesus macaque A3 proteins remains unclear. We report the isolation and characterization of the hA3A homologue from rhesus macaques (rhA3A) and show that the rhesus macaque and human *A3* genes are orthologous. RhA3A is expressed at high levels in activated $CD4^+$ T cells, is widely expressed in macaque tissues, and is degraded in the presence of the human immunodeficiency virus (HIV-1) and simian-human immunodeficiency virus (SHIV) genomes. Our results indicate that rhA3A is a potent inhibitor of SHIVΔ*vif* and to a lesser extent HIV-1Δ*vif*. Unlike hA3A, rhA3A did not inhibit adeno-associated virus 2 (AAV-2) replication and L1 retrotransposition. These data suggest an evolutionary switch in primate A3A virus specificity and provide the first evidence that a primate A3A virus specificity and provide the first evidence that a primate A3A can inhibit lentivirus replication.

Introduction

In the last decade several host restriction factors have been discovered that can restrict the replication of HIV-1. One of these restriction factors, Apolipoprotein B

mRNA-editing catalytic polypeptide-like 3 (APOBEC3; A3), has been shown to inhibit a wide range of retroviruses and other viruses such as the parvoviruses, papillomaviruses, and hepadnaviruses (Abe et al., 2009; Baumert et al., 2007; Bonvin et al., 2006, 2007; Chen et al., 2006; Henry et al., 2009; Jarmuz et al., 2002; Köck et al., 2008; Mahieux et al., 2005; Narvaiza et al., 2009; Noguchi et al., 2007; Paprotka et al., 2010; Sheehy et al., 2002; Strebel et al., 2005; Turelli et al., 2004; Vartanian et al., 2008; Zhang et al., 2008). A3 proteins comprise a family of seven cytidine deaminases (A3A, A3B, A3C, A3D, A3F, A3G, and A3H) that catalyze the deamination of cytidine to uracil on single-stranded DNA or RNA through a highly conserved Zn^{+2}-binding motif (C/H-X-E-X_{23-28}-P-C-X_{2-4}-C) (Chiu et al., 2009; Goila-Gaur and Strebel., 2008; Huthoff et al., 2005; Yu et al., 2004). These proteins also contain a key glutamate required for proton shuttling during catalysis and two aromatic amino acids residues required for RNA substrate binding (Jarmuz et al., 2002).

The A3 proteins can be divided into those with a single (A3A, A3C, A3H) or double (A3B, A3D, A3F, and A3G) cytidine deaminase domains (CDA). The double CDA proteins A3D, A3F, and A3G have been shown to restrict the replication of HIV-1 isolates that do not express a functional Vif protein while A3B could inhibit HIV-1 independent of Vif (Dang et al., 2006; Doehle et al., 2005; Kao et al., 2003; Liddament et al., 2004; Sheehy et al., 2002; Smith et al., 2010; Wiegand et al., 2004; Yu et al., 2004; Zheng et al., 2004). The Vif protein is known to bind to select A3 proteins and shunt the A3 proteins to the proteasome for degradation (Liu et al., 2004; Marin et al., 2003; Mehle et al., 2004; Sheehy et al., 2003; Yu et al., 2003). Mutagenesis studies have shown that the N-terminal CDA lacks catalytic activity and is responsible for

binding the RNA while the C-terminal CDA mediates sequence-specific deamination of single-stranded DNA (Yu et al., 2004). In addition to deaminase dependent functions, hA3G and hA3F inhibit virus replication by deaminase-independent mechanisms (Holmes et al., 2007a,b). Human A3G (hA3G) and hA3F can also inhibit DNA synthesis, which may involve interference of t-RNA Lys3 primer annealing, initiation and elongation of DNA synthesis and minus or plus strand DNA transfers (Bishop et al., 2008; Guo et al., 2006, 2007; Holmes et al., 2007a; Iwatani et al., 2007; Li et al., 2007; Luo et al., 2007; Newman et al., 2005; Ooms et al., 2010). Of the single CDA A3 proteins, hA3A has no activity against HIV-1 while hA3C can be incorporated into virions but only has weak activity against HIV-1 and foamy virus (Langlois et al., 2005; Perkovic et al., 2009). Human A3H is now known to have seven haplotypes, several of which can be stably expressed (Harai et al., 2009; Ooms et al., 2010; Wang et al., 2011). However, attempts to detect hA3H in isolated peripheral blood mononuclear cells (PBMC) has been unsuccessful (Li et al., 2010).

Human A3A is a nucleocytoplasmic protein that is expressed mainly in primary monocytes and keratinocytes (Koning et al., 2009; Madsen et al., 1999; Peng et al., 2007). Sequences consistent with hA3A-mediated editing have been observed in the genome of papilloma virus, which is known to infect both cutaneous and mucosal keratinocytes (Vartanian et al., 2008). Previous studies shown that hA3A lacks antiviral activity against HIV-1, but inhibits the replication of adeno-associated virus 2 (AAV-2), intracisternal A particles (IAP), and long interspersed nuclear element 1 (L1) (Bogerd et al., 2006a,b; Chen et al., 2006; Muckenfuss et al., 2006). The expression of HA3A is

induced by foreign DNA detection and interferon (IFN) in phagocytes, which leads to the degradation and clearance of foreign DNA (Stenglein et al., 2010).

Although hA3A contains one CDA, the deaminase activity of hA3A is not required for its inhibitory role against AAV or retrotransposons, suggesting that a deaminase-independent mechanism of inhibition is occurring (Narvaiza et al., 2009). Human A3A also contains significant homology to the N-terminal half of hA3G, does not associate with the viral nucleocapsid complex (NPC) of HIV-1 but is readily incorporated into virions (Goila-Gaur et al., 2007).

Simian immunodeficiency (SIV) and simian-human immunodeficiency (SHIV) viruses have been invaluable models for studying various aspects of HIV-1 pathogenesis. Sequencing of the rhesus macaque genome has led to the identification of rhesus homologues of A3B, A3C, A3D, A3F, A3G and A3H. Here we describe the identification of an A3A homologue in rhesus macaques (rhA3A) and present evidence that the human and macaque *Apobec3* genes are orthologous. We show that the rhA3A protein is expressed well in activated macaque $CD4^+$ T cells and other rhesus macaque tissues, is incorporated into virions, is degraded by both HIV-1 and SHIV in a Vif dependent manner, and restricts the replication of SHIV (expressing the SIV_{mac}239 Vif) and HIV-1.

Results

Molecular cloning of rhesus macaque A3A

Humans encode seven *APOBEC3 (hA3)* genes that are tandemly arrayed on chromosome 22, but there is uncertainty on whether a similar array of *rhA3* genes is expressed in the syntenic region on rhesus macaque chromosome 10. In particular, no *rhA3A* gene has been cloned from rhesus macaques suggesting that this gene may have been deleted in the genome of this primate species (OhAinle et al., 2008; Virgen et al., 2007). However, a recent study showed that *A3A* is encoded in the genome of several monkey species, including African green and owl monkeys (Bulliard et al., 2011). The evolutionary conservation of *A3A* therefore suggested that the *rhA3A* gene was missed in previous cloning attempts. To determine whether *rhA3A* is expressed, we took advantage of the sequencing of the rhesus macaque genome (Rhesus Macaque Genome Sequencing and Analysis Consortium, 2007). BLAST analysis of the *hA3A* sequence revealed that the first exon has a counterpart on the rhesus macaque chromosome 10, thus providing a potential forward primer for PCR amplification. However, counterparts of other *hA3A* exons were not detected in the rhesus macaque genome immediately downstream of this putative exon 1 sequence. Thus, the last exon of *hA3A* was used as a reverse primer.

Human A3A is not expressed in resting peripheral blood mononuclear cells (PBMC), but is substantially induced by cellular activation and cytokines (Koning et al., 2009; Refsland et al., 2010). We therefore utilized cDNA from Concanavilin A-activated rhesus macaque PBMCs in an attempt to detect *rhA3A*. A dominant band of the correct size was amplified in the first attempt by PCR. BLAST analysis of the cloned amplicon revealed 89% nucleotide identity with *hA3A*. Alignment of the amino acid sequence with recently identified A3A sequences showed the highest identity (90%) with A3A from

Figure 41. Sequence analysis of the rhA3A proteins. Panel A. Protein sequence alignment of primate A3A proteins. Dashes correspond to indels, while residues highlighted in pink or orange are conserved or mathed the consensus, respectively. Some indels were associated with specific primate taxons. This includes homiind-specific deletion at amino acid positions 27 to 29, and a deletion in residues 108-109 in New World monkeys. Panel B. A3A phylogeny. The amino acid sequence alignment was subjected to phylogenic analysis using the neighbor joining method, excluding sequence gaps, and rooted using the C-terminal half of rhesus macaque A3G as an outgroup. Numbers correspond to the percentage of clustering following 1000 subreplicates. RhA3A clustered most significantly with A3A from another Old World monkey species, African Green monkey (AGM).

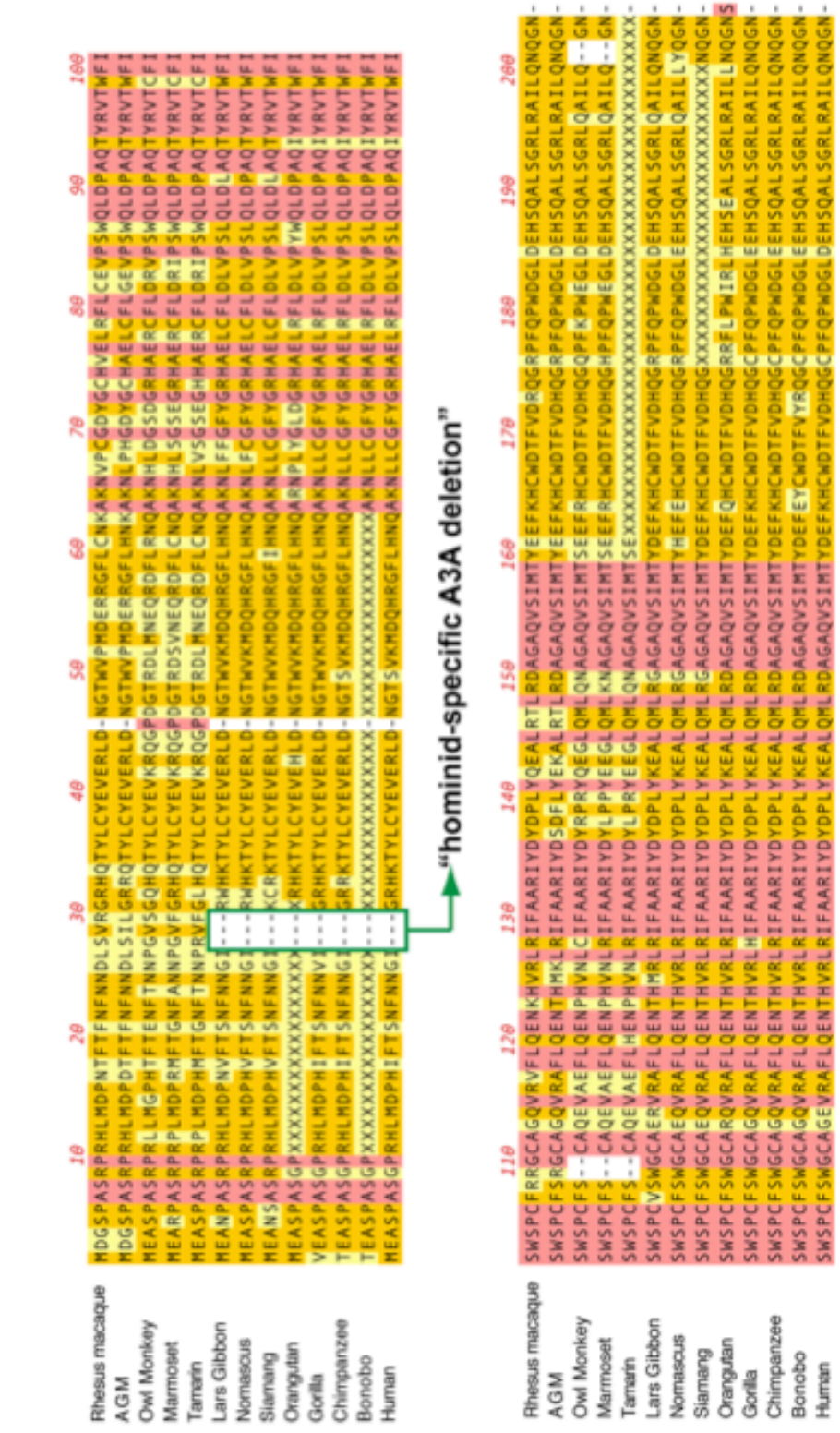
A.
"hominid-specific A3A deletion"
Rhesus macaque
AGM
Owl Monkey
Marmoset
Tamarin
Lars Gibbon
Nomascus
Siamang
Orangutan
Gorilla
Chimpanzee
Bonobo
Human

B.

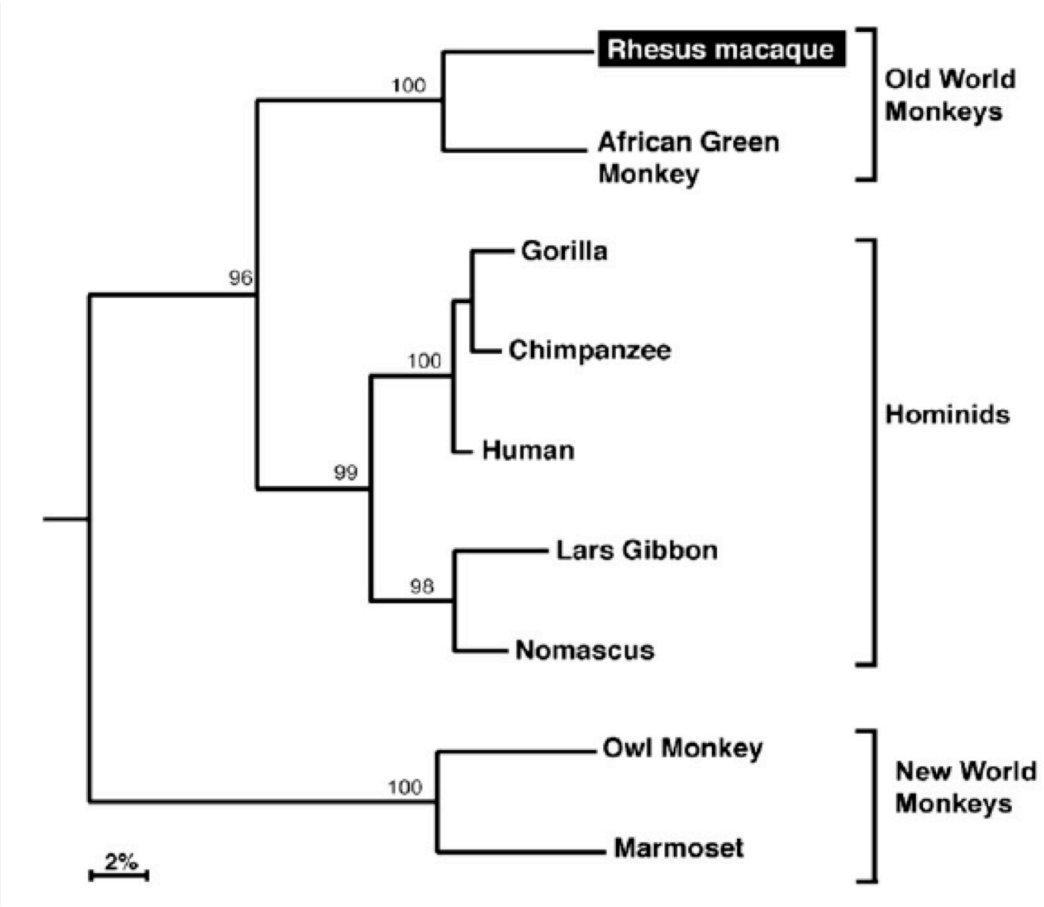
Rhesus macaque
African Green Monkey
Old World Monkeys
Gorilla
Chimpanzee
Human
Lars Gibbon
Nomascus
Hominids
Owl Monkey
Marmoset
New World Monkeys
100
96
100
99
98
100
2%

African green monkeys, which, together with Asian macaques, are considered as “Old World” monkeys (Figure 41). This alignment also revealed primate lineage-specific insertions/deletions (indels). In particular, we observed deletions at positions 27 to 29 in the hominid A3A genes. To further explore the clustering of A3A sequences with specific primate lineages, we constructed a phylogenetic tree that excluded the contribution of indels. As shown in Figure 41, A3A sequences clustered accordingly with their corresponding primate taxons. These analyses demonstrate that the cloned *rhA3A* gene is a *bona fide* member of the *A3A* gene family.

Evidence that seven A3 genes are tandemly arrayed on chromosome 10 of rhesus macaques

While the sequence of the rhesus macaque genome has been “completed,” it still remains unclear why this did not reveal the *rhA3A* gene. We attempted to determine the position of the cloned *rhA3A* sequence in relation with other *rhA3* genes. At the time that the analyses were performed, only the nucleotide sequences for rhesus macaque *rhA3C*, *rhA3F*, *rhA3G* and *rhA3H* had been deposited into GenBank. BLAST analysis of these cDNA sequences against the rhesus macaque genome revealed their distinct positions as shown in Figure 42. The position of rhesus macaque *rhA3B* and *rhA3DE* remains unknown, although their amino acid sequences were published (Virgen et al., 2007). We first attempted to determine the relative positions of *rhA3B* and *rhA3D* in chromosome 10 based solely on the genome sequence. Using the geneid program (http://genome.crg.es/geneid.html), genome sequences between *rhA3C* and *rhA3F*

predicted *rhA3D* (Figure 43), while genomic and previously unlocalized sequences upstream of *rhA3C* predicted *rhA3B* (Figure 44).

The relative placement of *rhA3B* and *rhA3D* in the rhesus macaque genome suggested a similar *A3* gene organization as found in humans, with the notable uncertainty of *rhA3A*. We therefore focused on genomic sequences immediately upstream of *rhA3B*. BLAST analysis of the cloned *rhA3A* sequence revealed an identical sequence corresponding to *rhA3A* exon 1 in the genome. This putative *rhA3A* exon 1 was immediately followed by 560 bp of CT-rich repeat sequences and 16.8 kb of unresolved sequence. It is possible that these repeat sequences interfered with accurate sequencing of this region. On the other hand, exons 2 to 4 of *rhA3A* mapped to an unlocalized chromosome 10 genomic scaffold sequence with GenBank Accession NW_001096321.1. The 3,764 bp NW_001096321.1 sequence could easily be accommodated in the 16.8 kb genomic gap. Notably, the NW_001096321.1 sequence contained 838 bp of intron sequence upstream of exon 2. We therefore investigated whether the NW_001096321.1 links directly with the genome by amplifying rhesus macaque genomic DNA with primers designed in exon 1 and 2 of *rhA3A* (Figure 42). Direct sequencing of the 1.8-kb amplicon revealed identity with the flanking sequences following the putative exon 1 in the genome and prior to exon 2 in NW_001096321.1 (Figure 42**).** These results provide strong evidence that *rhA3A* is likely encoded in the rhesus macaque genome immediately upstream of *rhA3B*. Overall, these analyses suggest that the seven *rhA3* members are tandemly arrayed in the rhesus macaque genome, similar to humans.

Figure 42. Sequence characterization of the rhesus macaque *A3* locus. Panel A. Genome organization of rhesus macaque *A3* genes. (*Top*) Published cDNA sequences for *rhA3C, rhA3F, rhA3G,* and *rhA3H* were subjected to BLAST analysis against the rhesus macaque genome. Matching exons were plotted against assigned genome coordinates, shown here in 20 kb intervals. **RhA3B* and *rhA3D* were predicted by subjecting the genome sequences upstream from *rhA3C* or flanked by *rhA3C* and *rhA3F* to the geneid prediction program (http://genome.crg.es/geneid.html), respectively. *RhA3A* amplified from activated PBMC was subjected to BLAST analysis. *RhA3A* exon 1 mapped in the genome directly upstream of *A3B*, but this was followed by a 16.8 kb of unresolved sequence (dotted lines). (*Bottom) A3A* exons 2 to 4 matched sequences from an unlocalized chromosome 10 genomic scaffold sequence. Primers based on *A3A* exons 1 and 2 amplified a 1.8 kb product that matched flanking sequences after exon 1 in the genome and before exon 2 in the unlocalized genomic scaffold (gray lines). This provides strong evidence for the current placement of *rhA3A* in the rhesus macaque genome. Panel B. Phylogeny of rhesus macaque and human A3 proteins. Amino acid sequences from rhesus macaque and human A3 genes were aligned, with the double-CDA members split into an N- and C-terminal half. For example, A3B-C corresponds to the C-terminal half of A3B. RhA3A clustered with the C-terminal half of A3B and A3G, forming the *Z1* clade. Each rhesus macaque *A3* gene clustered significantly with the corresponding human *A3* gene, suggesting that rhesus macaque and human A3 proteins are orthologous.

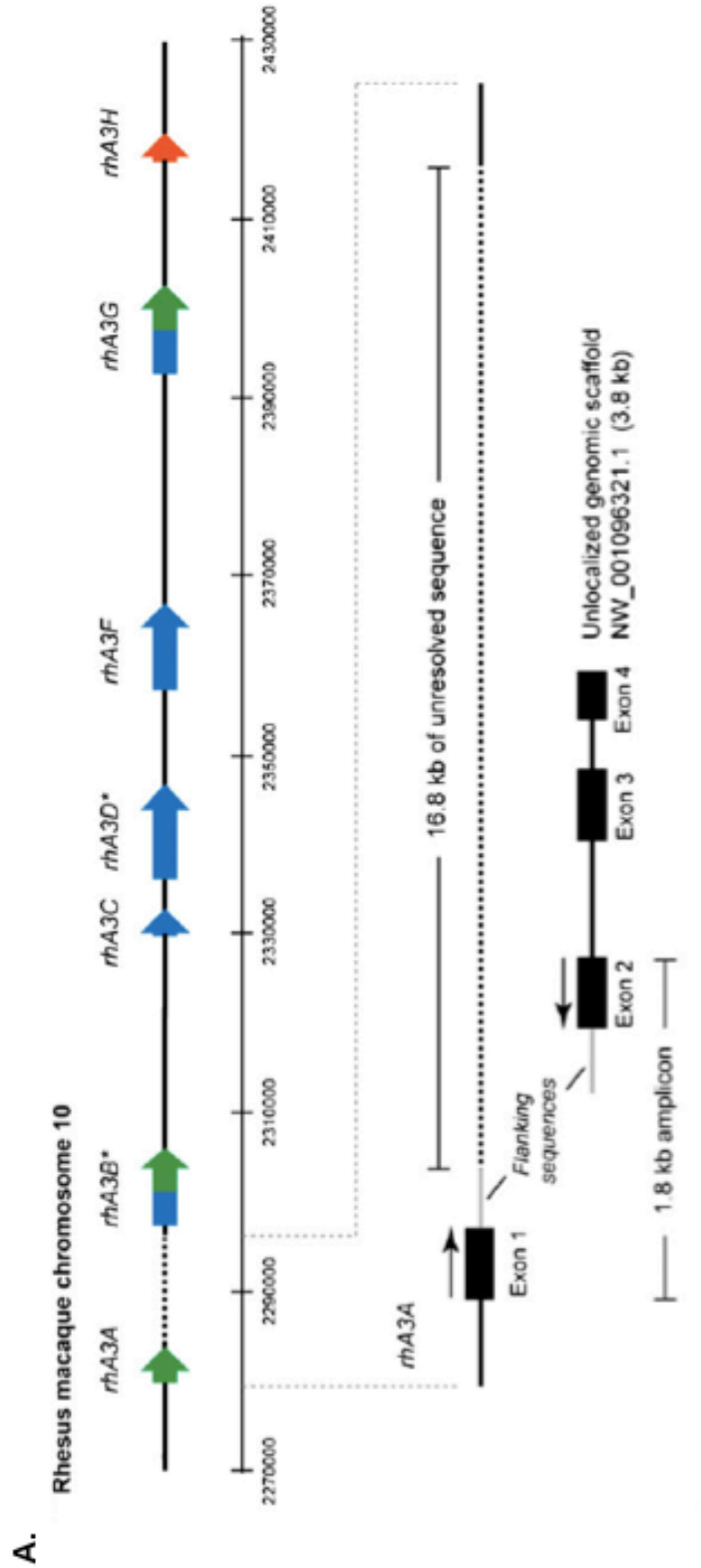
A.
Rhesus macaque chromosome 10
rhA3A
rhA3B*
rhA3C
rhA3D*
rhA3F
rhA3G
rhA3H
2270000
2290000
2310000
2330000
2350000
2370000
2390000
2410000
2430000
rhA3A
16.8 kb of unresolved sequence
Exon 1
Flanking sequences
Exon 2
Exon 3
Exon 4
Unlocalized genomic scaffold
NW_001096321.1 (3.8 kb)
1.8 kb amplicon

B.

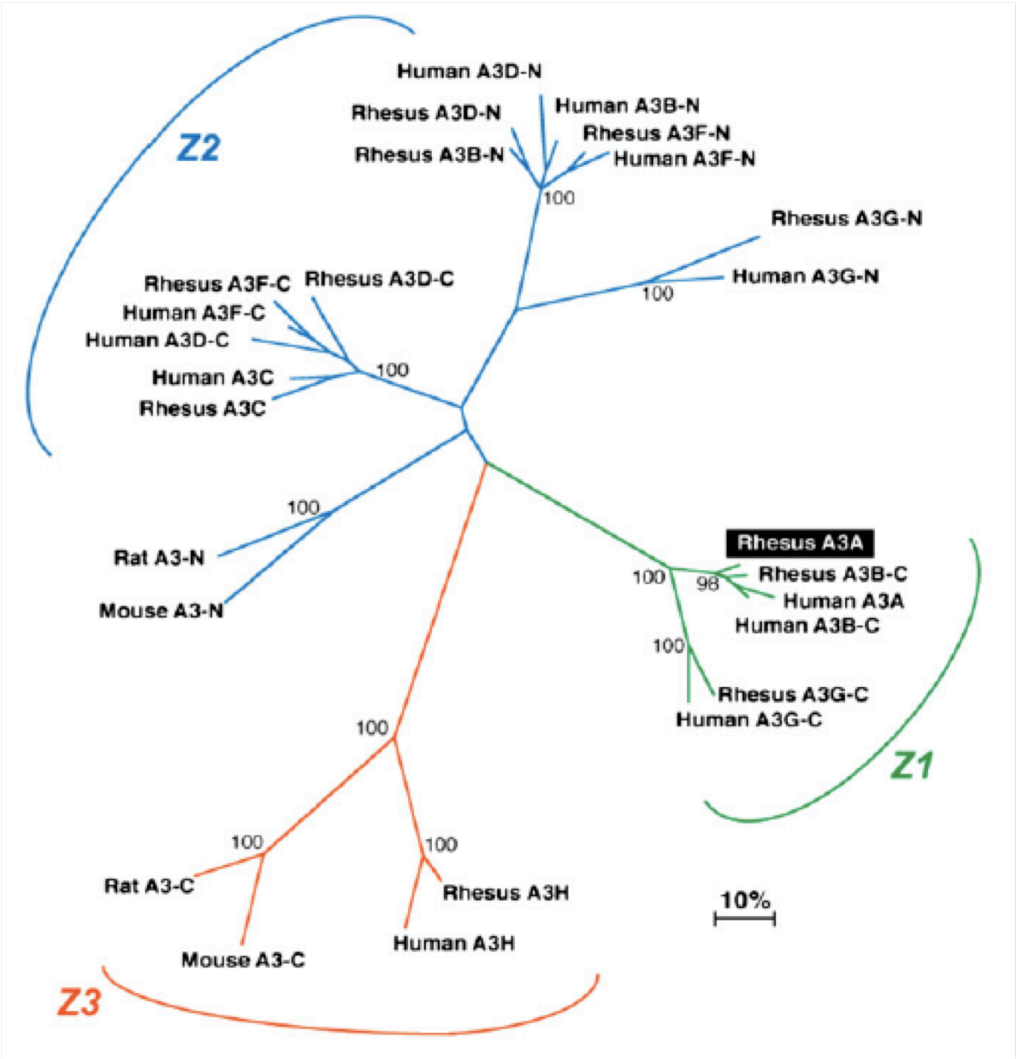
Human A3D-N
Rhesus A3D-N
Human A3B-N
Rhesus A3F-N
Rhesus A3B-N
Human A3F-N
Z2
100
Rhesus A3G-N
Human A3G-N
100
Rhesus A3F-C
Rhesus A3D-C
Human A3F-C
Human A3D-C
Human A3C
Rhesus A3C
100
100
Rat A3-N
Mouse A3-N
Rhesus A3A
100
98
Rhesus A3B-C
Human A3A
Human A3B-C
100
Rhesus A3G-C
Human A3G-C
Z1
100
100
100
Rat A3-C
Rhesus A3H
Human A3H
Mouse A3-C
10%
Z3

Figure 43. Nucleotide sequence alignment of *huA3D* and genome-predicted *rhA3D.* The rhesus macaque genome sequence flanking *rhA3C* and *rhA3F* could potentially encode *rhA3D.* To investigate this possibility, we subjected this genomic sequence to a gene prediction program, (http://genome.crg.es/geneid.html). This analysis revealed a putative *rhA3D* gene that exhibited 86% nucleotide identity with *hA3D*. However, multiple attempts to clone the full-length gene in activated rhesus macaque PBMCs failed, likely due to the fact that the reverse primer cross-reacted significantly with the more highly expressed *rhA3C* gene and that *rhA3D* is very poorly expressed in these cells. In contrast, the 5' half of this gene was cloned (unpublished data).

```
huA3DE              1 ATGAATCCACAGATCAGAAATCCGATGGAGCGGATGTATCGAGACACATTCTACGACAAC   60
rhA3DE*             1 -------------------------ATGGAGCGGATGTATCGACGCACATTCAACTACAAC   36
                                              .................  ....... .. .....

huA3DE             61 TTTGAAAACGAACCCATCCTCTATGGTCGGAGCTACACTTGGCTGTGCTATGAAGTGAAA  120
rhA3DE*            37 TTTGAAAATGAACCCATCCTCTATGGTCGGAGCTACACCTGGCTGTGCTACGAAGTGAAA   96
                      ........ ............................. ........... .........

huA3DE            121 ATAAAGAGGGGCCGCTCAAATCTCCTTTGGGACACAGGGGTCTTTCGAGGCCCGGTACTA  180
rhA3DE*            97 ATAAGGAAGGACCCCTCAAAGCTCCCTTGGGACACAGGGGTCTTTCGAGGCCAGGTACGA  156
                      .... .. .. .. ...... .... ........................... ..... .

huA3DE            181 CCCAAACGTCAGTCGAATCACAGGCAGGAG----------------------------GTG  213
rhA3DE*           157 CCCAAACTTCAGTCGAATCGTAGGTACGAACTAAGCAACTGGGAATGCAGAAAACACGTG  216
                      ....... ...........  ... . ..                             ...

huA3DE            214 TATTTCCGGTTTGAGAACCACGCAGAAATGTGCTTCTTATCTTGGTTCTGTGGCAACCGA  273
rhA3DE*           217 TATTTCCAGCCTCAGTACCACGCAGAAATGTGCTTCCTCTCTTGGTTCTGTGGCAACCAG  276
                      ....... .   . .. ..................... . ..................

huA3DE            274 CTGCCTGCTAACAGGCGCTTCCAGATCACCTGGTTTGTATCATGGAACCCCTGCCTGCCC  333
rhA3DE*           277 CTGCCTGCTTACAAGCGCTTCCAGATCACCTGGTTTGTATCCTGGAACCCCTGCCCGGAC  336
                      ......... ... ............................. ............ .  .

huA3DE            334 TGTGTGGTGAAGGTGACCAAATTCTTGGCTGAGCACCCCAATGTCACCCTGACCATCTCT  393
rhA3DE*           337 TGTGTGGCAAAGGTGACCGAATTCCTGGCTGAGCACCCTAATGTCACCCTGACCATCTCC  396
                      .......  ......... ..... ............ ..................

huA3DE            394 GCCGCCCGCCTCTACTACTACCGGGATAGAGATTGGCGGTGGGTGCTCCTCAGGCTGCAT  453
rhA3DE*           397 GCCGCCCGCCTCTACTACTATTGGGGTAAAGATTGGCGGAGGGCGCTCCGCAGGCTGCAT  456
                      ..................  ... .. .......... ... ..... ..........

huA3DE            454 AAGGCAGGGGCCCGTGTGAAGATCATGGACTATGAAGACTTTGCATACTGCTGGGAAAAC  513
rhA3DE*           457 CAGGCAGGGGCTCTCGTGAAGATCATGGACTATGAAGAATTTGCATACTGCTGGGAAAAC  516
                       .......... .  ....................... ..................

huA3DE            514 TTTGTGTGCAATGAAGGTCAGCCATTCATGCCTTGGTACAAATTCGATGACAATTATGCA  573
rhA3DE*           517 TTTGTGTACAATGAAGGTCAGTCATTCATGCCTTGGGACAAATTCGATGACAATTATGCA  576
                      ....... ............. ............. ......................

huA3DE            574 TCCCTGCACCGCACGCTAAAGGAGATTCTCAGAAACCCGATGGAGGCAATGTACCCACAC  633
rhA3DE*           577 TCCCTGCACTGCAAGCTAAAGGAGATTCTCAGAAACCCGATGAAGGCAATGTATCCACAC  636
                      ......... ... ............................. .......... ......

huA3DE            634 ATATTCTACTTCCACTTTAAAAACCTACTGAAAGCCTGTGGTCGGAACGAAAGCTGGCTG  693
rhA3DE*           637 ACATTCTACTTCCACTTTGAAAACCTACAGAAAGCCTATGGTCGGAATGAAACCTGGCTG  696
                      . ............... ......... ........ ......... .... .......

huA3DE            694 TGCTTCACCATGGAAGTTACAAAGCACCACTCAGCTGTCTTCCGGAAGAGGGGCGTCTTC  753
rhA3DE*           697 TGCTTCGCCGTGGAAATTATAAAGCAGCACTCAACTGTCTCCTGGAAGACGGGCGTCTTC  756
                      ...... .. ..... ... ...... ...... ...... . ...... ..........

huA3DE            754 CGAAACCAGGTGGATCCTGAGACCCATTGTCATGCAGAAAGGTGCTTCCTCTCTTGGTTC  813
rhA3DE*           757 CGAAACCAGGTTGATCCTGAGACCCATTGTCATGCAGAAAGGTGCTTCCTCTCTTGGTTC  816
                      ........... ..................................................

huA3DE            814 TGTGACGACATACTGTCTCCTAACACAAACTACGAGGTCACCTGGTACACATCTTGGAGC  873
rhA3DE*           817 TGCGACAACACACTGTCTCCTAAGAAAAACTACCAGGTCACCTGGTACATATCTTGGAGC  876
                      .. ... ... ............ . ....... .............. ..........

huA3DE            874 CCTTGCCCAGAGTGTGCAGGGGAGGTGGCCGAGTTCCTGGCCAGGCACAGCAACGTGAAT  933
rhA3DE*           877 CCTTGTCCAGAGTGTGCAGGGGAGGTGGCCGAGTTCCTGGCCACGCACAGCAACGTGAAG  936
                      ..... ..................................... ..............

huA3DE            934 CTCACCATCTTCACCGCCCGCCTCTGCTACTTCTGGGATACAGATTACCAGGAGGGGCTC  993
rhA3DE*           937 CTCACCATCTATACCGCCCGCCTCTACTACTTCTGGGATACAGATTACCAGGAGGGGCTC  996
                      ..........  ............ ..................................

huA3DE            994 TGCAGCCTGAGTCAGGAAGGGGCCTCCGTGAAGATCATGGGCTACAAAGATTTTGTATCT 1053
rhA3DE*           997 CGCAGCCTGAGTGAGGAAGGGGCCTCCATGGAGATCATGGGCTACGAAGATTTTAAATAT 1056
                       .......... ............ .. ............ ........  .. .
```

Figure 44. Nucleotide sequence alignment of *hA3B* and genome-predicted *rhA3B.* Upstream of *rhA3C* are genome sequences that matched some exons of *hA3B*. Closer inspection revealed unresolved sequences in regions that could putatively encode exons 2, 7, and 8. A substantial portion of these gaps was resolved with the inclusion of "unlocalized genomic scaffold sequences" from chromosome 10. In particular, chromosome 10 sequences designated with GenBank Accession numbers AANU01162607.1 and AANU01065938.1 encoded putative exons 2 and 7 of *A3B* and formed contiguous bases to bridge a portion of the unresolved regions. A 2.7-kb gap that likely encodes the last 4 amino acids of *A3B* still remains unresolved in the macaque genome. Using the geneid program, the *rhA3B* nucleotide sequence was predicted, and this sequence exhibited 85% identity with *hA3B*. These analyses provided strong evidence for the current position of *rhA3B* upstream of *rhA3C*. However, our multiple attempts to clone *rhA3B* from activated rhesus macaque PBMC mRNA were unsuccessful.

The rhesus macaque and human A3 genes are orthologous

```
huA3B          1 ATGAATCCACAGATCAGAAATCCGATGGAGCGGATGTATCGAGACACATTCTACGACAAC   60
rhA3B*         1 ATGAATCCACAGATCAGAAATCCGATGGAGCGGATGTATCAACGCACATTCTACTACCAC   60
                 ........................................ .  .......... .. ..

huA3B         61 TTTGAAAACGAACCCATCCTCTATGGTCGGAGCTACACTTGGCTGTGCTATGAAGTGAAA  120
rhA3B*        61 TTTGAAAATAAACCCATCCTCTATGGTCGGAGCTACACCTGGCTGTGCTACGAAGTGAAA  120
                 ........  ........................... ..........  .........

huA3B        121 ATAAAGAGGGGCCGCTCAAATCTCCTTTGGGACACAGGGGTCTTTCGAGGCCAGGTGTAT  180
rhA3B*       121 ATAAGGAAGGACCCCTCAAAGCTCCCTTGGGACACAGGGGTCTTTCGAGGCCAGGTGTAT  180
                 .... .. .. .. ...... .... ..................................

huA3B        181 TTCAAGCCTCAGTACCACGCAGAAATGTGCTTCCTCTCTTGGTTCTGTGGCAACCAGCTG  240
rhA3B*       181 TCCAAGCCTGAGCACCACGCAGAAATGTGCTTCCTCTCTCGGTTCTGTGGCAACCAGCTG  240
                 . ....... .. ........................... ..................

huA3B        241 CCTGCTTACAAGTGTTTCCAGATCACCTGGTTTGTATCCTGGACCCCCTGCCCGGACTGT  300
rhA3B*       241 CCTGCTTACAAGCGCTTCCAGATCACCTGGTTTGTATCCTGGAACCCCTGCCCGGACTGT  300
                 ............ . ............................. ..............

huA3B        301 GTGGCGAAGCTGGCCGAATTCCTGTCTGAGCACCCCAATGTCACCCTGACCATCTCTGCC  360
rhA3B*       301 GTGGCGAAGGTGATTGAATTCCTGGCTGAGCACCCTAATGTCACCCTGACCATCTCTACC  360
                 ......... ..   ......... .......... ..................... ..

huA3B        361 GCCCGCCTCTACTACTACTGGGAAAGAGATTACCGAAGGGCGCTCTGCAGGCTGAGTCAG  420
rhA3B*       361 GCCCGCCTCTACTACTACTGGGGTAGAGATTGGCAGAGGGCGCTCTGCAGGCTGCGTCAG  420
                 ......................  .......  .  ................... .....

huA3B        421 GCAGGAGCCCGCGTGACGATCATGGACTATGAAGAATTTGCATACTGCTGGGAAAACTTT  480
rhA3B*       421 GCAGGGGCCCGAGTGAAGATCATGGACTATGAAGAATTTGCATACTGCTGGGAAAACTTT  480
                 ..... ..... .... ..........................................

huA3B        481 GTGTACAATGAAGGTCAGCAATTCATGCCTTGGTACAAATTCGATGAAAATTATGCATTC  540
rhA3B*       481 GTGTACAATGAAGATCAGTCATTCATGCCTTGGTACAAATTCAATGACAATTATGCATTC  540
                 ............. ....  ....................... .... ............

huA3B        541 CTGCACCGCACGCTAAAGGAGATTCTCAGATACCTGATGGATCCAGACACATTCACTTTC  600
rhA3B*       541 CTGCACCGCATGCTAAAGGAGATTCTCAGACACCTGATGGATCCAGACACGTTCACTTCC  600
                 .......... ................... ..................... ....... .

huA3B        601 AACTTTAATAATGACCCTTTGGTCCTTCGACGGCGCCAGACCTACTTGTGCTATGAGGTG  660
rhA3B*       601 AACTTTAACAATGACGTTTCGGTCCGTGGACGGCACCAGACCTACTTGTGCTACGAGGTG  660
                 ........ ......  .. ..... . ...... ................... ......

huA3B        661 GAGCGCCTGGACAATGGCACCTGGGTCCTGATGGACCAGCACATGGGCTTTCTATGCAAC  720
rhA3B*       661 GAGCGCCTGGACAATGGCACCTGGGTCCCGATGGACCAGCACTGGGGATTTCTATGCAAC  720
                 ............................. ............  ... ............

huA3B        721 GAGGCTAAGAATCTTCTCTGTGGCTTTTACGGCCGCCATGCGGAGCTGCGCTTCTTGGAC  780
rhA3B*       721 CAGGCTAAGAATGTTCTCCGTGGTGATTATGGCTGCCACGCGGAGCTGTGCTTCCTGGGC  780
                 ........... ..... ....   ... ... .... ......... ..... ... .

huA3B        781 CTGGTTCCTTCTTTGCAGTTGGACCCGGCCCAGATCTACAGGGTCACTTGGTTCATCTCC  840
rhA3B*       781 TGGGTTCCTTCCTGGCAGTTGGACCCGGCCCAGACGTACAGGGTCACTTGGTTCATCTCC  840
                 ......... . ..................  ......................

huA3B        841 TGGAGCCCCTGCTTCTCCTGGGGCTGTGCCGGGGAAGTGCGTGCGTTCCTTCAGGAGAAC  900
rhA3B*       841 TGGAGCCCCTGCTTCAGCTGGGGCTGTGCCGAGCAAGTGCGTGCGTTCCTTCAGGAGAAC  900
                 .............  ............. . ....................

huA3B        901 ACACACGTGAGACTGCGCATCTTCGCTGCCCGCATCTATGATTACGACCCCCTATATAAG  960
rhA3B*       901 ACACACGTGAGACTGCACATCTTTGCTGCCCGCATCTATGATTACGACCCCCTGTATCAG  960
                 ................ ...... ............................. ... ..

huA3B        961 GAGGCGCTGCAAATGCTGCGGGATGCTGGGGCCCAAGTCTCCATCATGACCTACGATGAG 1020
rhA3B*       961 GAGGCACTGCGAACGCTGCGGGATGCTGGGGCCCAAGTCTCCATCATGACCTATGATGAA 1020
                 ..... .... .. ......................................... .....

huA3B       1021 TTTGAGTACTGCTGGGACACCTTTGTGTACCGCCAGGGATGTCCCTTCCAGCCCTGGGAT 1080
rhA3B*      1021 TTTGAGTACTGCTGGGACACCTTTGTGGACCGCCAGGGACGTCCCTTCCAGCCCTGGGAT 1080
                 ............................ ............ ....................
```

Rodents encode a single *A3* gene, while humans encode seven. Other mammals, such as dogs, pigs, horses and sheep encode a variety of *A3* genes that reveal substantial duplication, unequal cross-over and divergent evolution of individual members and are therefore considered paralogues (Conticello et al., 2005; LaRue et al., 2006). This pattern of "evolutionary shuffling" could be roughly inferred in phylogenetic trees, where *A3* segments containing the canonical deoxycytidine deaminase motif can be classified into *Z1, Z2* and *Z3* clades (LaRue et al., 2006). To extend this classification to *rhA3* genes, a phylogenetic tree comparing the human, rodent and rhesus macaque A3 amino acid sequences was constructed (Figure 42B). The *rhA3* genes consistently clustered with the *hA3* counterparts (Figure 42B). Thus, each of the seven rhesus macaque and human *A3* genes appear to originate from a common ancestor, indicating that the genes are orthologous. In other words, we found no evidence for significant "shuffling events" in the *A3* locus after the evolutionary split between monkeys and humans.

Expression of rhA3 genes in rhesus macaque tissues and activated $CD4^+$ T cells

We next determined *rhA3A* mRNA expression in various perfused rhesus macaque organs and tissues. Specific *rhA3A* primers were used to determine expression in 14 visceral organs and 12 regions of the central nervous system (CNS) by RT-PCR. GAPDH was used to assess the integrity of RNA in the samples (data not shown). Our results indicate that *rhA3A* was not only widely expressed in the visceral organs but also in different regions of the CNS (Figure 45A). We verified the specificity

of the *rhA3A* amplification by directly sequencing the PCR amplicons (data not shown). Extensive detection of *rhA3A* in various lymphoid organs raised the possibility that *rhA3A* may also be expressed in $CD4^+$ T cells, a primary cellular target of SHIV and SIV infection *in vivo*.

To determine the relative expression of *rhA3A* against other *rhA3* members, we developed Taqman-based real-time PCR assays to specifically quantify each of the seven *rhA3* genes (Table VIII). To evaluate specificity, we first performed an end-point PCR and determined by agarose gel electrophoresis whether the primers could amplify other *rhA3* cDNAs. If some cross-reactivity with the primers was observed, we subjected 10^8 *rhA3* cDNA copies in a real-time PCR reaction that also includes the probe. The results of these analyses are presented in Table VIIII. Most of the assays developed did not cross-react with other *A3* family members. In those instances where some cross-reactivity was observed, detection of similar *A3* members were least 10^4

Figure 45. Expression of *rhA3A* in rhesus macaque tissues and $CD4^+$ T cells. Panel A. *RhA3A* expression profile in visceral organs and the CNS. Multiple tissues were obtained from an SIV negative rhesus macaque. RNA from these tissues was analyzed for the presence of *rhA3A* mRNA by RT-PCR. Amplicons were run on 1.5% agarose gels and visualized by staining with ethidium bromide. Amplicons were directly sequenced and found to correspond to *rhA3A*. All samples were positive for GAPDH RNA to control for integrity of RNA in the samples (data not shown). *Upper gel, rhA3A* mRNA from 14 visceral organs. *Lower gel, rhA3A* mRNA from 12 regions of the central nervous system (CNS). The size markers (in base pairs) are shown to the left. Panel B. Expression of *A3* genes in rhesus macaque $CD4^+$ T cells. *Upper,* Activation of rhesus $CD4^+$ T cells. Rhesus macaque PBMCs were activated with 2.5 µg/ml SEB overnight, and subjected to FACS analysis. FACS histograms of CD25 expression in $CD3^+CD4^+$ cells before (resting, blue) and after SEB activation (activated; red) are shown. $CD4^+$ T cells were magnetically purified by negative selection, and RNA was extracted for quantitative RT-PCR analyses. *Lower, rhA3* mRNA levels in activate rhesus macaque $CD4^+$ T cells, *A3* cDNA was subjected to real-time quantitative RT-PCR using primers specific for individual *rhA3* genes (Table VIIII) Dashed lines correspond to the assay limit of detection (5 input copies/reaction), while error bars correspond to standard deviation from triplicate determinations.

A.

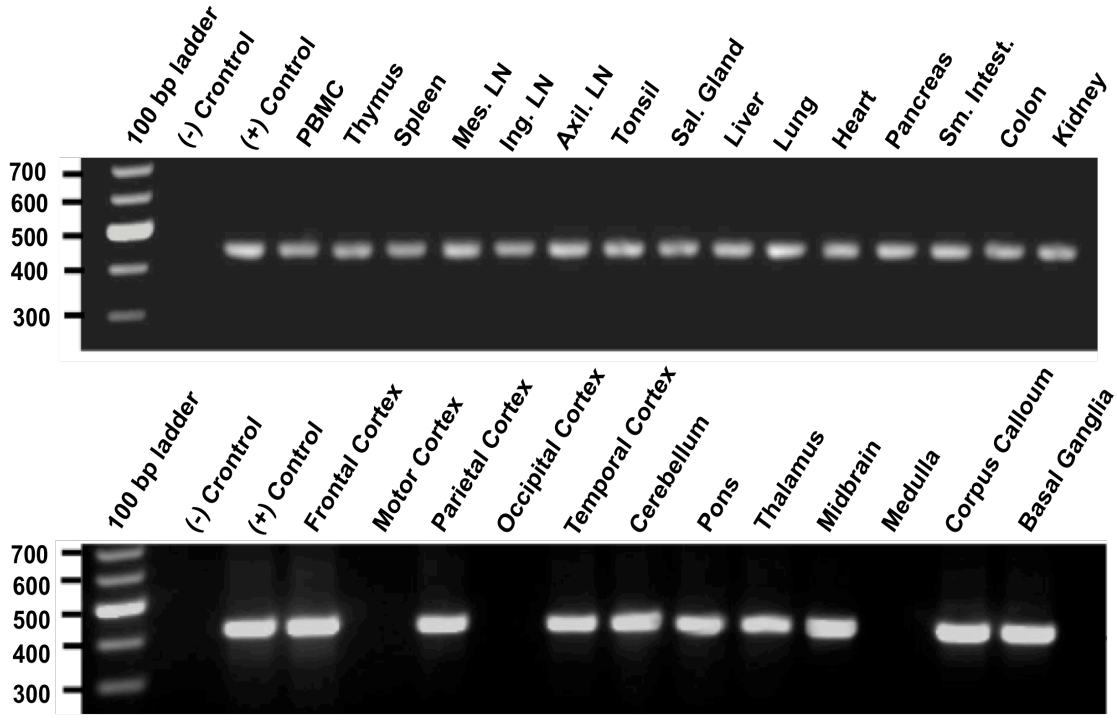
100 bp ladder
(-) Crontrol
(+) Control
PBMC
Thymus
Spleen
Mes. LN
Ing. LN
Axil. LN
Tonsil
Sal. Gland
Liver
Lung
Heart
Pancreas
Sm. Intest.
Colon
Kidney
700
600
500
400
300
100 bp ladder
(-) Crontrol
(+) Control
Frontal Cortex
Motor Cortex
Parietal Cortex
Occipital Cortex
Temporal Cortex
Cerebellum
Pons
Thalamus
Midbrain
Medulla
Corpus Calloum
Basal Ganglia
700
600
500
400
300

B.

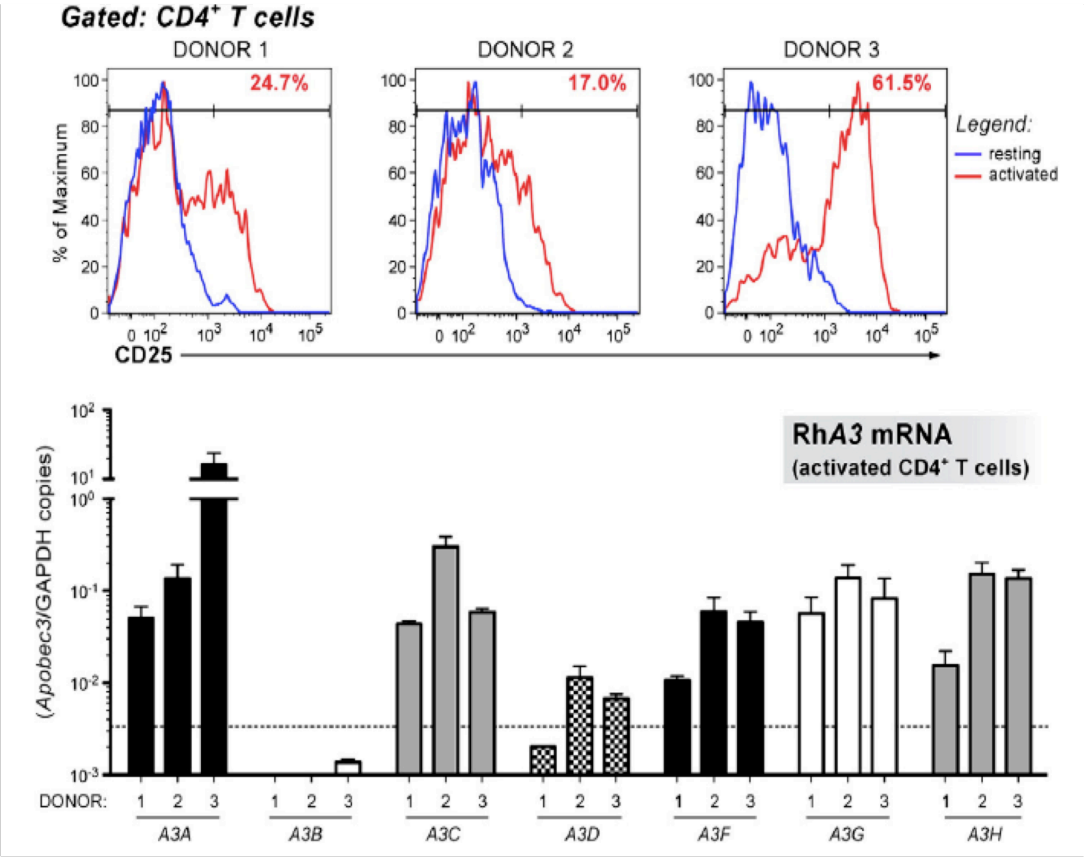
Gated: CD4+ T cells
DONOR 1
DONOR 2
DONOR 3
24.7%
17.0%
61.5%
% of Maximum
CD25
Legend:
resting
activated
RhA3 mRNA
(activated CD4+ T cells)
(Apobec3/GAPDH copies)
DONOR:
A3A
A3B
A3C
A3D
A3F
A3G
A3H

Table VIII. Rhesus macaque *A3* real-time PCR primers and probes.

Apobec3	Primers[a]	Primer size (nt)	PCR product (nt)	T_a (°C)
RhA3A	Forward: CAAGGCTAAGAATGTTCCCT	20	201	59
	Reverse: ATGCGCAGTCTCACGTGTTT	20		
	Probe: [6-FAM]TGAGGTTCCTTCTTGGCAGT[TAMRA-6-FAM]	20		
RhA3B	Forward: TGGGGTAGAGATTGGCAGAG	20	224	59
	Reverse: TTGGAAGTGAACGTGTCTGG	20		
	Probe: [6-FAM]CCGCATGCTAAAGGAGATTC[TAMRA-6-FAM]	20		
RhA3C	Forward: AGGTGCTTCCTCTCCTGGTT	20	197	59
	Reverse: CCCTGCTGGTAATTCGGATA	20		
	Probe: [6-FAM]GGCACAACAATGTGATGCTC[TAMRA-6-FAM]	20		
RhA3D	Forward: GTCTTCCGAAACCAGGTTGA	20	245	59
	Reverse: AGCCCCTCCTGGTAATCTGT	20		
	Probe: [6-FAM]CTCTTGGTTCTGCGACAACA[TAMRA-6-FAM]	20		
RhA3F	Forward: GAAGGTGGCCGAATTCCTA	19	264	60
	Reverse: TTTCTGAGAATCTCCTTTAGCTTGT	25		
	Probe:[6-FAM]ACTGGGAAACAGATTATCGCA[TAMRA-6-FAM]	21		
RhA3G	Forward: GCCATTTAAGCCTTGGAACA	20	230	60.5
	Reverse: GAGCCTGGTTGCGTAGAAAG	20		
	Probe: [6-FAM]AACCTTGGGTCAGTGGACAG[TAMRA-6-FAM]	20		
RhA3H	Forward: AAGGACCATGCAGAAATTCG	20	239	59
	Reverse: ACCTGGGATCCACACAGAAG	20		
	Probe: [6-FAM]AACTATCAGGAGGGGCTGCT[TAMRA-6-FAM]	20		

[a] PCR conditions were as follows: 95 °C for 10 min followed by 40 cycles of 95 °C for 15 s and the corresponding annealing temperature (T_a) for 45 s.

Table VIIII. Specificity evaluation of *rhA3* primers and probes

Primer-probe set	Template cross-reactivity (input: 5×10^8 copies)						
	RhA3A	*RhA3B*[a]	*RhA3C*	*RhA3D*[a]	*RhA3F*	*RhA3G*	*RhA3H*
RhA3A		NT	–	NT	9.9×10^1	2.7×10^3	–
RhA3B	–		–	2.0×10^3	–	–	–
RhA3C	–	NT		NT	–	–	1.5×10^4
RhA3D	–	1.5×10^2	–		–	–	–
RhA3F	6.5×10^3	NT	–	NT		3.4×10^1	–
RhA3G	–	NT	–	NT	5.1×10^4		–
RhA3H	–	NT	1.7×10^3	NT	–	–	

[a] *RhA3B* (340nt) and *rhA3D* (370nt) templates were synthetic oligos based on predicted sequences. –, no cross-reactivity observed based on endpoint-PCR and gel electrophoresis; NT: not tested.

fold lower in magnitude than what would be expected for the gene of interest. Thus, the real-time PCR methods could be used to distinguish the relative levels of the individual *A3* members.

Rhesus macaque PBMCs from three uninfected donors were stimulated with Staphylococcal Enterotoxin B (SEB), previously determined to be a potent activator of rhesus macaque T cells (Kakimoto et al., 1999). However, SEB-stimulation still did not result in consistent activation, since the levels of CD25 expression in $CD4^+$ T cells varied between the 3 donors (Figure 45B). Total RNA was extracted from magnetically purified $CD4^+$ T cells from these activated PBMCs, and subjected to real-time RT-PCR. Consistent with our failure to clone *rhA3B* from activated PBMCs, *rhA3B* mRNA was not detected in any donor (Figure 45A). With one exception (*rhA3A* donor 3), the expression of individual *rhA3* genes between the donors did not vary more than 10-fold, and did not appear to correlate with $CD25^+$ expression levels. Since *rhA3G* is well accepted as a biologically relevant restriction factor against SIV (Schmitt et al., 2009; 2010; Schrofelbauer 2006; Sui et al., 2010), we compared the expression of other *rhA3* genes relative to *rhA3G*. Setting the average *rhA3G* level from the 3 donors as 1, only *rhA3A* (excluding donor 3), *rhA3C* and *rhA3H* exhibited mRNA expression levels that are similar in magnitude (1.0-1.5 fold) to that of *rhA3G*. In contrast, *rhA3F* and *rhA3D* were on average expressed at 2.4- and 13.6-fold lower than *rhA3G,* respectively. Thus, *rhA3A, rhA3C* and *rhA3H* mRNAs are expressed to similar levels as *rhA3G* in SEB-activated rhesus macaque $CD4^+$ T cells.

Nucleocytoplasmic localization of HA-tagged rhA3A

Previous studies have shown that the cytoplasmic localization of hA3G and the nucelocytoplasmic localization of hA3A could partially explain the differences in the range of retroviruses or retrotransposons that were inhibited by these proteins (Bogerd et al., 2006a,b; Chen et al., 2006; Giola-Gaur et al., 2007; Muckenfuss et al., 2006). To determine whether rhA3A exhibited a similar subcellular localization, we generated a molecular clone of rhA3A with an HA-tag at the amino terminal end for detection purposes. A plasmid expressing either rhA3G or rhA3A (Figure 46A) was transfected into 293 cells and the expression examined by Western blot analysis using an antibody directed against the HA tag. As shown in Figure 46A, 293 cells transfected with the vector expressing rhA3G expressed a protein with an M_r of 45kD while cells transfected with the vector expressing rhA3A expressed a protein with an M_r of 24kD, which reflects the size of the two different proteins (363 amino acids for rhA3G versus 202 amino acids for rhA3A). Using confocal microscopy, we found that rhA3G was observed exclusively in the cytoplasm (Figures 46B, C, D) and that rhA3A was detected in both the cytoplasm and nucleus as it co-localized with a nuclear marker (Figures 46B, E, F, G). Similar to other studies, hA3A was observed rhA3A in both the nucleus and cytoplasm (Figures 46G, H, I). Thus any differences in the retroviral restriction properties of hA3A and rhA3A could not be explained by the subcellular localization.

Figure 46. Expression of an HA-tagged rhA3A. Panel A. 293 cells were transfected with 1.5 µg of HA-tagged rhA3A, rhA3G, or the empty expression vectors. At 48 h, cells were lysed and proteins separated by SDS-PAGE and analyzed by Western blot using an antibody directed against the HA-tag. Sizes of the molecular standards are to the right. RhA3A migrates at about half the molecular weight than rhA3G, consistent with their amino acid sequences. Panel B-J. Subcellular localization of rhA3G, rhA3A, and hA3A. 293 cells were transfected with HA-tagged vectors expressing rhA3A, rhA3G, or hA3A and a vector expressing an eGFP tagged nuclear marker (Clontech). At 48 h, cells were fixed and stained with anti-HA for 1 h, washed, and detected using a horse anti-rabbit-Ig Cy5 antibody. Cells were examined under a Nikon A1 fluorescent microscope and micrographs taken using a 100x objective with a 2x digital zoom using the E2-C1 software package as described in the Materials and Methods.

Minimal inhibition of foreign DNA reporter gene expression by rhA3A and hA3A

A.

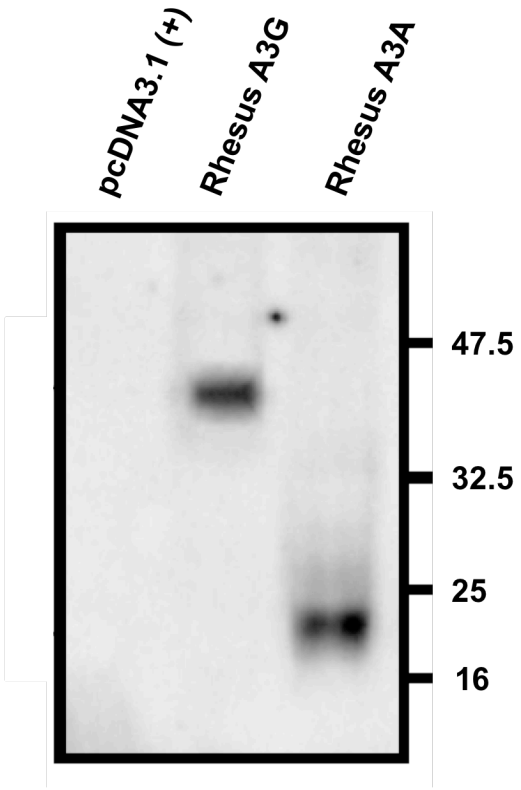

B.

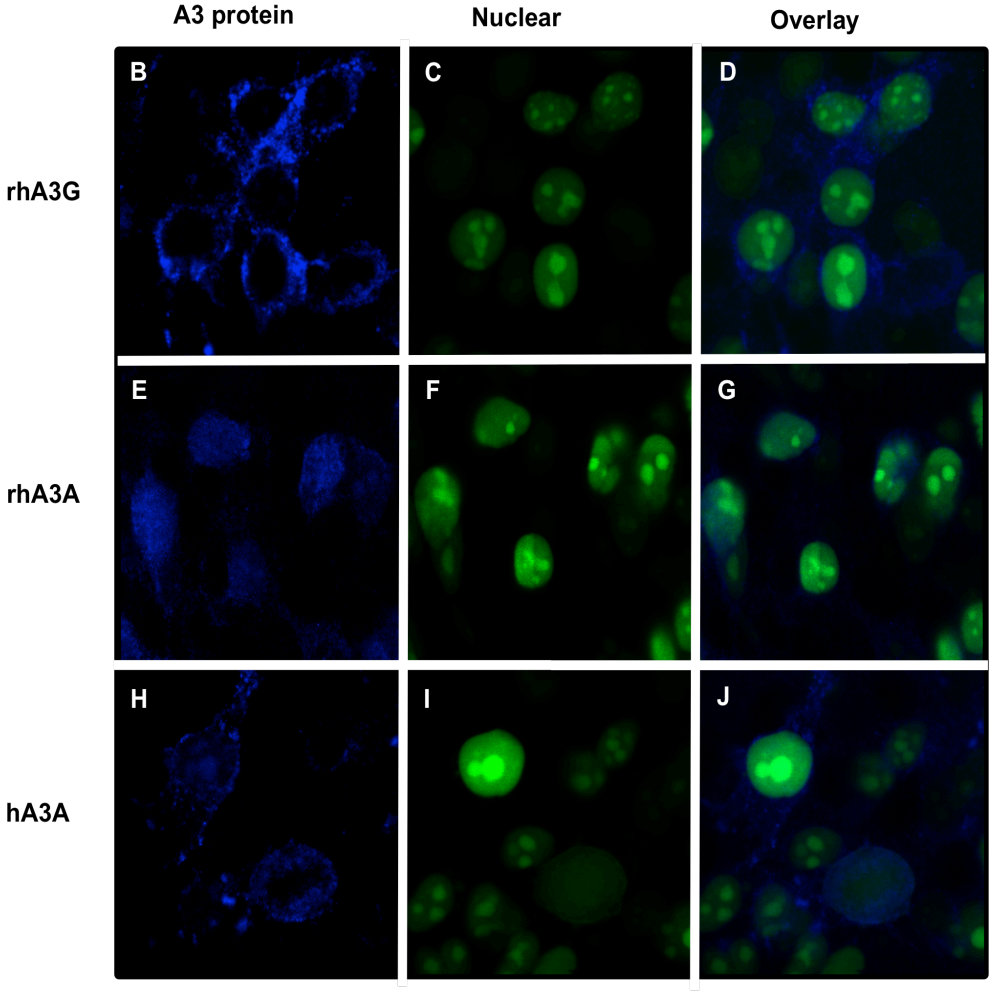

In a recent study, hA3A was shown to inhibit the expression of transfected plasmid DNA by deamination of the incoming plasmid DNA (Stenglein et al., 2010). Co-transfection of an eGFP reporter plasmid with hA3A in 293 cells resulted in approximately 20% reduction in the number of cells expressing eGFP signal 2 days. In these investigators' model, the incoming DNA induces an interferon-induced up-regulation of hA3A expression, the cytidine residues are deaminated resulting in uracils, which are excised by UNG2. This will eventually result in cleavage and degradation of the DNA backbone (Stenglein et al., 2010). This phenomenon could significantly confound experiments that involve co-transfection of A3A with viral plasmid constructs.

Since our virus experiments involving rhA3A or hA3A lasted no longer than 48 h, we determined whether rhA3A, hA3A or rhA3G interfered with the expression of enhanced green fluorescent protein (eGFP) from a foreign plasmid. Plasmids expressing either rhA3A, hA3A or rhA3G were co-transfected into 293 cells 24 h prior to transfection with the plasmid expressing eGFP under the control of the CMV promoter. At 2 days post-transfection of eGFP, the cells were analyzed for fluorescence by flow cytometry. We detected 14.1, 14.5, 11.2, and 14.6% eGFP positive cells in the presence of empty vector, rhA3A, hA3A, or rhA3G, respectively (Figure 47A). These results indicate that hA3A had minimal impact (<20%) while rhA3A had no impact on reporter gene expression from foreign plasmids at 48 h.

Human and rhesus macaque A3A does not inhibit SHIV or HIV-1 production in 293 cells

Figure 47. Minimal restriction of foreign DNA by rhA3A and hA3A. Panel A. Expression constructs (3 μg) of HA-tagged rhA3A, hA3A, and rhA3G were first transfected into 293 cells for 24 h. At 24 h post-transfection, the 293 cells were re-transfected with a plasmid encoding a CMV-driven eGFP reporter and assayed for reporter expression. The cells were removed from the plate and fixed. All samples were analyzed by a flow cytometer and the mean fluorescence intensity (MFI) for eGFP positive cells was calculated. The MFI ratio and percentage of eGFP cells were calculated for each sample and the experiment was run in triplicate. All groups were compared to the pcDNA3.1(+) plus EGFP control using a Student's *t*-test with $p<0.05$ considered significant. Panel B. SHIVΔVif production in the presence of rhA3A, hA3A and rhA3G. Cells were first transfected with 0.5 μg of plasmids expressing HA-tagged rhA3A, hA3A, rhA3G or empty vector. At 24 h post-transfection, the 293 cells were re-transfected with a plasmid containing the SHIVΔ*vif*. Virus supernatants were harvested at 2 days post-transfection with the viral genome. Mean Gag p27 levels as measured using a commercially available ELISA kit (Zeptometrix) are shown. In all panels, error bars correspond to standard deviations from triplicate determinations. Panel C. HIV-1Δ*vif* production in the presence of hA3A and rhA3A. Cells were first transfected with 0.5 μg of plasmids expressing HA-tagged rhA3A, hA3A, rhA3G, or empty vector. At 24 h post-transfection, the 293 cells were re-transfected with a 1 μg plasmid containing the HIV-1Δ*vif*. Virus supernatants were harvested at 2 days post-transfection with the viral genome. Mean Gag p24 levels as measured

using a commercially available ELISA kit (Zeptometrix) are shown. In all panels, error bars correspond to standard deviations from triplicate determinations.

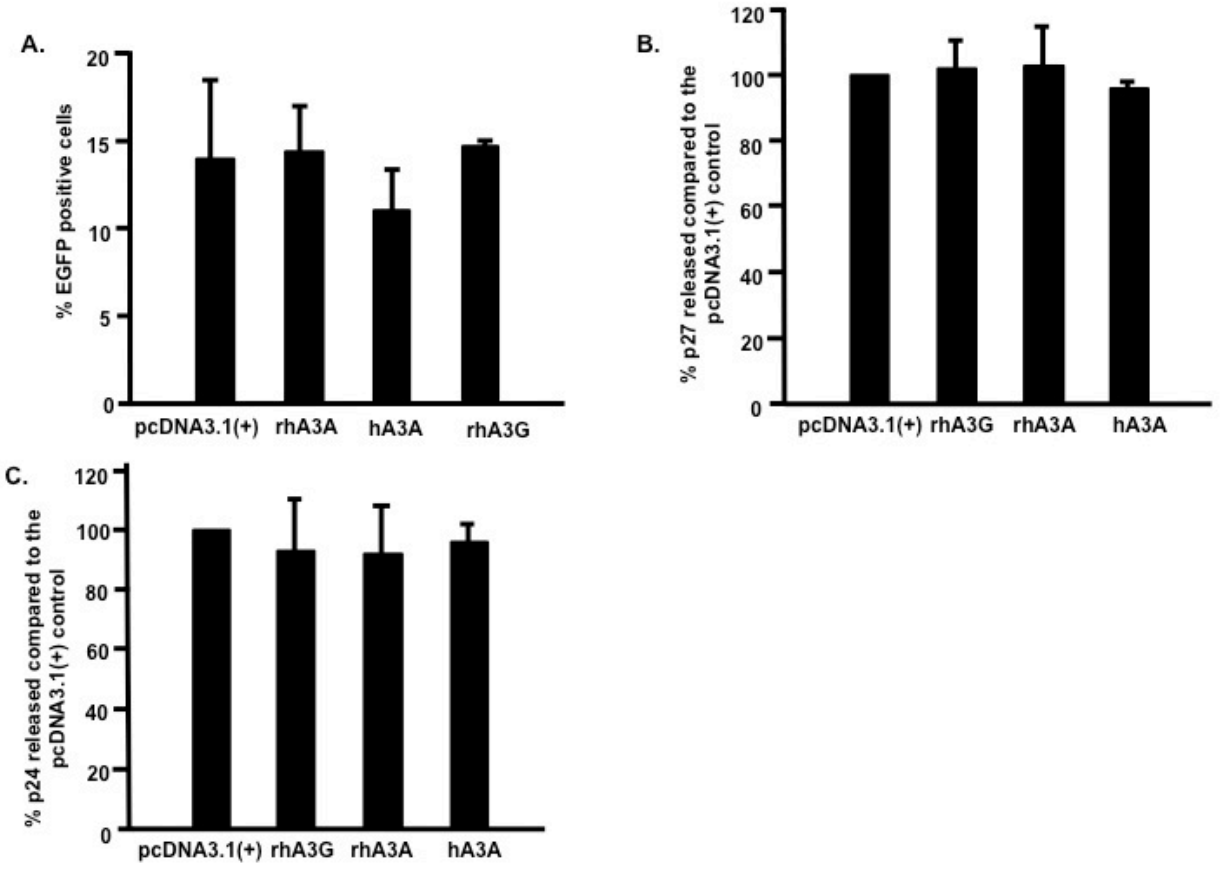

It can be argued that the slight inhibition of plasmid reporter gene expression by hA3A may be amplified with typically longer plasmids containing a full-length viral genome. Similarly, the absence of an effect by rhA3A in plasmid reporter expression may be enhanced in the context of a full-length viral molecular clone. We conjectured that if A3A can degrade viral infectious molecular clones, then virus production would be significantly inhibited. We therefore investigated whether virus production was inhibited in cells transfected with rhA3A or hA3A. 293 cells were transfected with the plasmids expressing hA3A, rhA3A, rhA3G or the empty plasmid 24 hours prior to transfection with plasmids with the SHIVΔ*vif* or HIV-1Δ*vif* constructs. At 2 days post-transfection with the viral genomes, the culture medium was assayed for either p27 (SHIV) or p24 (HIV-1). We did not observe a significant decrease in the level of SHIVΔ*vif* p27 released into the culture medium in cells co-transfected with empty vector, rhA3A, hA3A, or rhA3G at 5 days post-transfection (Figure 47B). Similar findings were observed for *HIV*-1Δvif (Figure 47C). These data suggests that rhA3A and hA3A likely have no post-entry restriction activity against SHIV or HIV-1 and reinforce the conclusion that rhA3A and hA3A have minimal impact on plasmid DNA stability at 2 days post-transfection. Thus, our subsequent experiments, which involve analyzing cells within 48 h, should not be influenced by potential plasmid-specific restriction.

Rhesus macaque A3A inhibits the infectivity of SHIVΔvif and HIV-1Δvif

We next determined if rhA3A could inhibit the infectivity of SHIV and SHIVΔ*vif*. For comparison, we also co-transfected these viral constructs with plasmids expressing

rhA3G, rhA3C, or hA3A. Virion infectivity was measured by taking the ratio of infectious titer in TZM-bl cells and comparing to the wild-type SHIV construct co-transfected with empty vector control. Our results indicate that rhA3A and rhA3G reduced the level of infectious SHIVΔ*vif* nearly 20-fold compared to the parental SHIV, while hA3A reduced the infectivity of SHIVΔ*vif* approximately 10-fold (Figure 48A). In contrast, rhA3C did not inhibit the level of infectious virus released from cells. SHIV virions produced in the presence of rhA3A, hA3A or rhA3G were purified and concentrated by ultracentrifugation and analyzed by Western blot. Consistent with the virion infectivity data, rhA3A was incorporated into SHIVΔ*vif* and to a lesser extent in SHIV (Figure 48B). However, we were unable to detect hA3A in either SHIV or SHIVΔ*vif* virions.

We also tested whether rhA3A had activity against HIV-1. HIV-1(NL4-3) and HIV-1Δ*vif* constructs were co-transfected with plasmids expressing rhA3A, hA3A, or hA3G. Consistent with previous reports, hA3A did not inhibit infectivity of HIV-1Δ*vif* virions, while hA3G reduced HIV-1Δ*vif* virion infectivity by 10-fold. Surprisingly, rhA3A reduced HIV-1Δ*vif* virion infectivity approximately 3-fold (Figure 48C). HIV-1 virions released from 293 cells expressing either hA3G, hA3A or rhA3A were partially purified by ultracentrifugation. The resulting virions were analyzed by Western blot using an anti-HA antibody. Consistent with previously published data, hA3A was detected in both HIV-1 and HIVΔ*vif* virions. However, rhA3A was not detected in HIV-1 and HIVΔ*vif* virions (Figure 48D). Together, these findings indicate that unlike hA3A, rhA3A reduces the infectivity of both SHIVΔ*vif* and HIV-1Δ*vif*.

Figure 48. Inhibition of SHIVΔVif and HIV-1ΔVif virion infectivity by rhA3A. Panel A. RhA3A restricts SHIVΔ*vif*. 293 cells were co-transfected with 1 μg wild-type SHIV or SHIVΔ*vif* molecular clones and 0.5 μg plasmids expressing either empty vector (pcDNA3.1), rhA3A, hA3A, or rhA3G. At 48 h, the culture medium was harvested and virion infectivity measured by taking the ratio of infectious viral titers on TZM-bl cells. Shown is the percentage virion infectivity with the empty plasmid control normalized to 100%. Panel B. 293 cells were transfected with wild-type SHIV or SHIVΔ*vif* molecular clones and HA-tagged rhA3A, hA3A, or rhA3G. At 48 h, the culture medium was collected, clarified by low speed centrifugation, and concentrated by ultracentrifugation through a 20%/60% (w/v) step-gradient. Each sample was resuspended in 2x sample reducing buffer, boiled, and the proteins were separated by SDS-PAGE. The presence of rhA3G, hA3A, or rhA3A was detected by Western blot using an antibody directed against the HA-tag (Upper panel) and the presence of p27 using an antibody directed against p27 (Middle panel*).* The lower panel are 293 cells transfected with vectors expressing rhA3G, hA3A, rhA3A, or pcDNA3.1(+) vector in the absence of the viral genome. Panel C. RhA3A restricts HIV-1Δ*vif* genomes were co-transfected with HA-tagged hA3A, hA3G, or rhA3A as described for the SHIV experiments in Panel A. Shown is the percentage virion infectivity with the empty plasmid control normalized to 100%. Panel D. Undetectable rhA3A in HIV-1Δ*vif* virions. Virions were purified as described for the SHIV experiments in Panel B, and hA3G, hA3A, and rhA3A incorporation were detected by Western blot using an anti-HA

antibody, normalizing for Gag p24 levels. The lower panel are 293 cells transfected with vectors expressing rhA3G, hA3A, rhA3A, or pcDNA3.1(+) vector in the absence of the viral genome. Mean values in triplicate experiments are shown, and the statistical differences with the wild-type control were evaluated using a two-tailed Student's *t*-test, with $p<0.05$, (▲) considered significant.

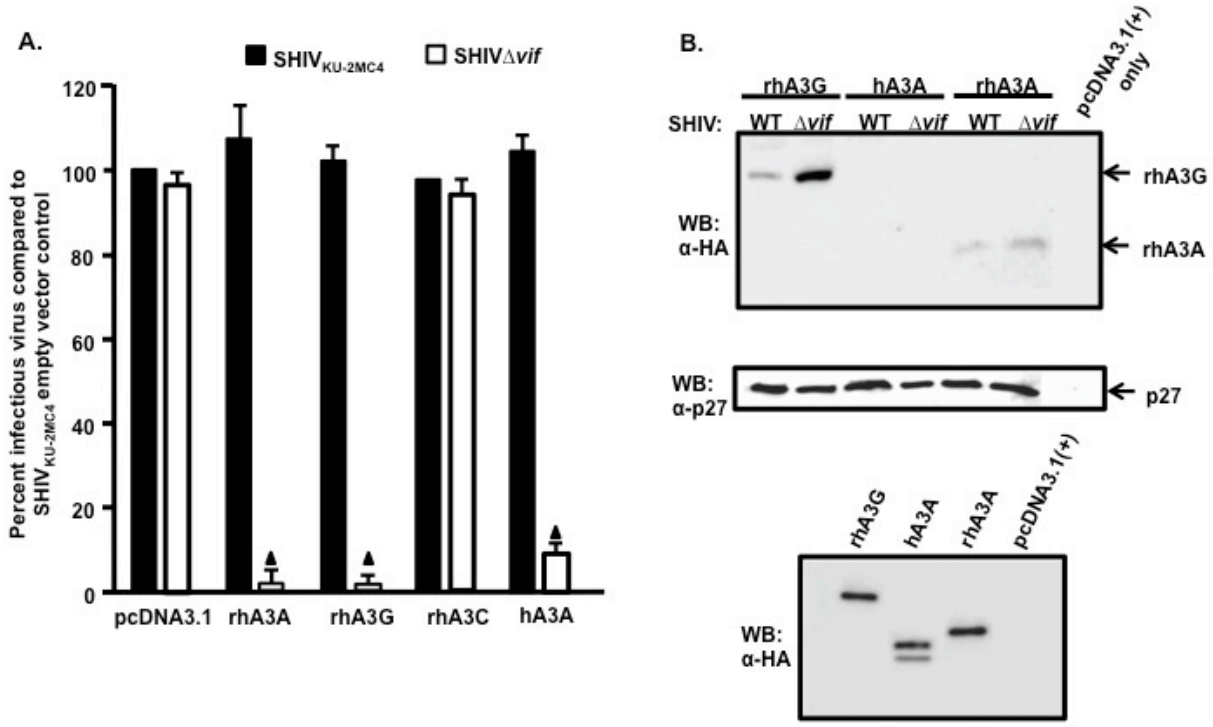
A.
SHIV$_{KU-2MC4}$
SHIVΔ*vif*
Percent infectious virus compared to SHIV$_{KU-2MC4}$ empty vector control
120
100
80
60
40
20
0
pcDNA3.1
rhA3A
rhA3G
rhA3C
hA3A
B.
rhA3G
hA3A
rhA3A
pcDNA3.1(+) only
SHIV:
WT
Δ*vif*
WT
Δ*vif*
WT
Δ*vif*
WB: α-HA
rhA3G
rhA3A
WB: α-p27
p27
rhA3G
hA3A
rhA3A
pcDNA3.1(+)
WB: α-HA

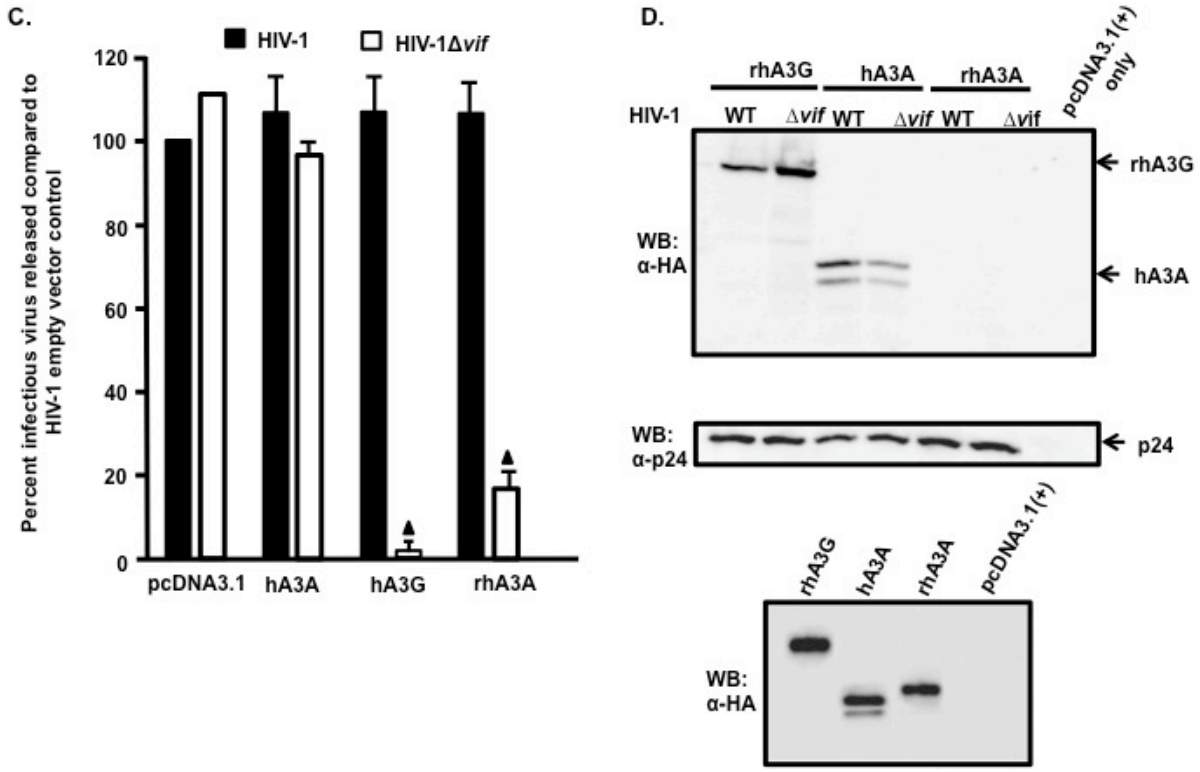
C.
HIV-1
HIV-1Δvif
Percent infectious virus released compared to HIV-1 empty vector control
120
100
80
60
40
20
0
pcDNA3.1
hA3A
hA3G
rhA3A
D.
rhA3G
hA3A
rhA3A
pcDNA3.1(+) only
HIV-1
WT
Δvif
WT
Δvif
WT
Δvif
WB: α-HA
rhA3G
hA3A
WB: α-p24
p24
rhA3G
hA3A
rhA3A
pcDNA3.1(+)
WB: α-HA

Deletion of amino acids 27-29 of rhA3A abolishes its anti-viral activity

Hominid and monkey A3As can be distinguished by a 3 amino-acid indel between residues 27 to 29. We hypothesize that this region may contribute to the differential activity of rhA3A and hA3A against SHIVΔvif and HIV-1Δvif. To test this hypothesis, we constructed a rhA3A mutant in which amino acids 27-29 (SVR) were deleted. The resulting mutant, rhA3AΔSVR, was found to be stable in cells (data not shown). Interestingly, rhA3AΔSVR was inactive against SHIVΔvif (Figure 49A) and HIV-1Δvif (Figure 49B). However, when the amino acids 27-29 (SVR) were introduced into hA3A, we restored the ability of hA3A to partially inhibit HIV-1Δvif (Figure 49B). These findings suggested that these monkey-specific A3A residues were critical for lentivirus inhibition, but was functionally lost in the hominid lineage.

RhA3A, but not hA3A, is sensitive to SIV and HIV-1 Vif-mediated degradation

We next determined the stability of rhA3A and hA3A in the presence of the SHIV, SHIVΔ*vif*, HIV-1, or HIVΔ*vif* genomes. Each full-length molecular clone was co-transfected into 293 cells along with plasmids expressing HA-tagged rhA3A, rhA3G, hA3A, or rhA3AΔSVR. At 24 h, the cells were lysed, proteins precipitated, and analyzed by Western blot using an antibody specific to the HA-tag. Our results show that rhA3G was degraded in the presence of the parental SHIV but not in cells co-transfected with the SHIVΔ*vif* genome. In contrast, hA3A was stable in the presence of parental SHIV or SHIVΔ*vif* (the apparent difference of the hA3A in lanes 4 and 5 is due to less protein

Figure 49. Deletion of three amino acids from the N-terminus region of rhA3A abolishes restriction. Panel A. RhA3AΔSVR is inactive against SHIVΔ*vif*. 293 cells were co-transfected with (1.0 μg) SHIV and SHIVΔ*vif* molecular clones with vectors expressing (0.5 μg) rhA3A, rhA3AΔSVR, rhA3G, or empty vector (pcDNA3.1) in a 12-well plate. At 48 h, the culture medium was harvested, assessed for p27 and the amount of infectious virus titrated onto TZM-bl cells. Panel B. RhA3AΔSVR is inactive against HIV-1Δ*vif*. 293 cells were co-transfected with (1.0 μg) HIV-1 and HIV-1Δ*vif* molecular clones with vectors expressing (0.5 μg) rhA3A, rhA3AΔSVR, hA3AΔSVR, hA3A, or empty vector (pcDNA3.1) in a 12-well plate. Virion infectivity was calculated normalizing to the wild-type HIV-1 empty vector control. In both panels, A and B, the assays were run at least in triplicate. Significance in the restriction was determined with respect to the wild-type empty vector control using a two-tailed Student's *t*-test ($p<0.05$; ▲)

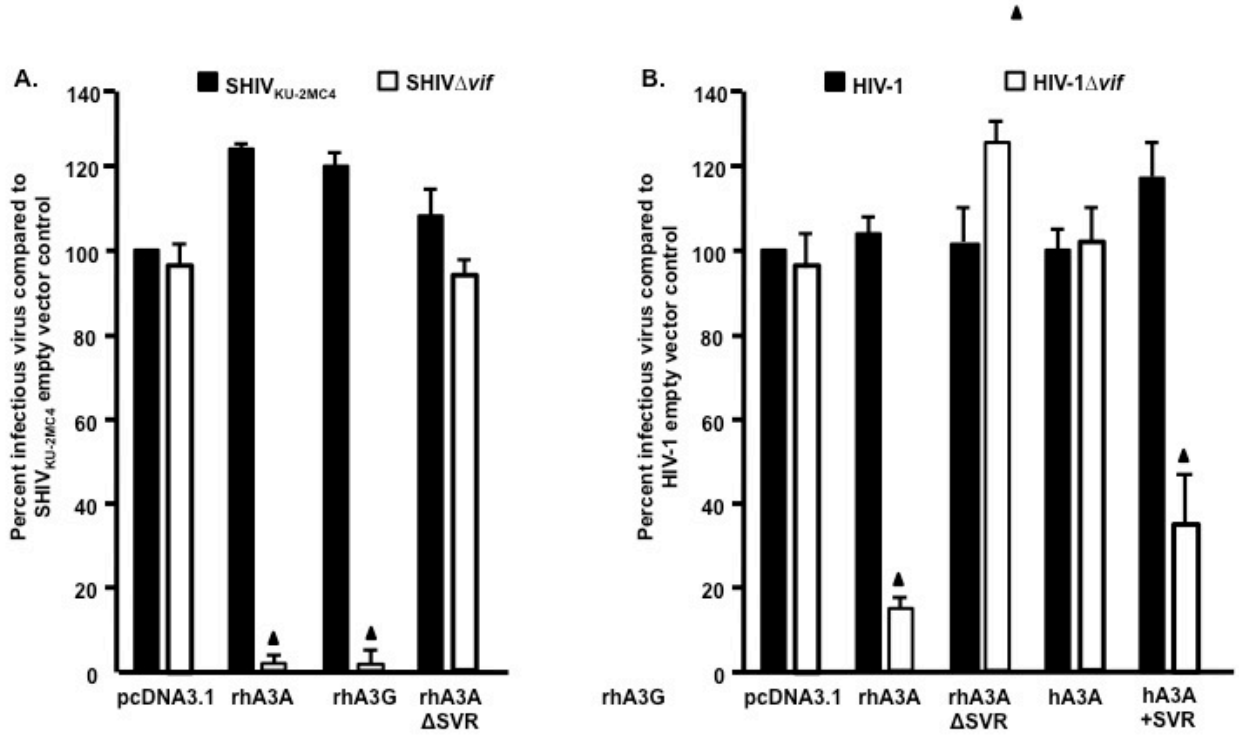
A.
SHIV$_{KU-2MC4}$
SHIVΔ*vif*
Percent infectious virus compared to SHIV$_{KU-2MC4}$ empty vector control
140
120
100
80
60
40
20
0
pcDNA3.1
rhA3A
rhA3G
rhA3A ΔSVR
B.
HIV-1
HIV-1Δ*vif*
Percent infectious virus compared to HIV-1 empty vector control
140
120
100
80
60
40
20
0
rhA3G
pcDNA3.1
rhA3A
rhA3A ΔSVR
hA3A
hA3A +SVR

Figure 50. Sensitivity of rhA3A to lentivirus Vif-mediated degradation. Panel A. SHIV Vif mediates rhA3A degradation. SHIV and SHIVΔ*vif* molecular clones were co-transfected with rhA3G, hA3A, rhA3A, or rhA3AΔSVR. At 24 h post-transfection, cells were lysed and proteins were precipitated using methanol. Proteins were separated on a 12% SDS-PAGE gel and probed using an antibody directed against the HA-tag. All samples were normalized to the amount of β-actin. Panel B. HIV-1 Vif mediates rhA3A degradation. HIV-1 and HIV-1Δ*vif* molecular clones were co-transfected with rhA3G, hA3A, rhA3A, and rhA3AΔSVR. In both panels, blots were stripped and re-probed with an antibody against β-actin. All assays were performed twice.

A.

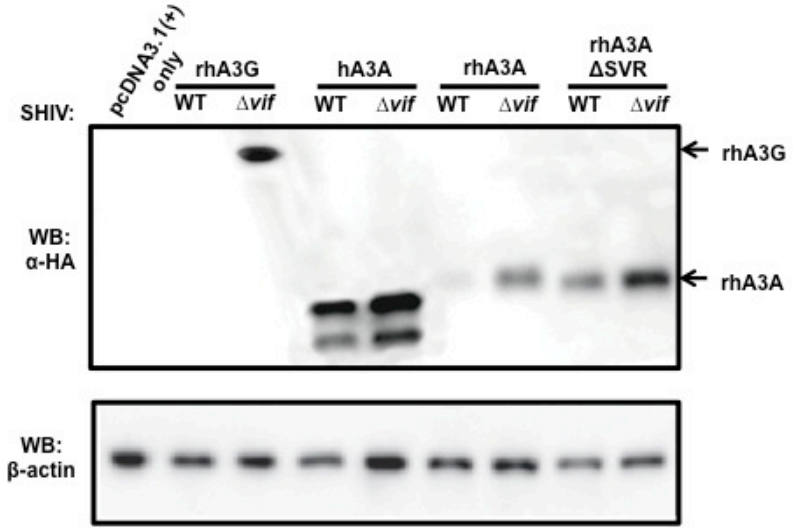
pcDNA3.1(+) only
rhA3G
hA3A
rhA3A
rhA3A ΔSVR
SHIV:
WT
Δvif
WT
Δvif
WT
Δvif
WT
Δvif
WB: α-HA
rhA3G
rhA3A
WB: β-actin

B.

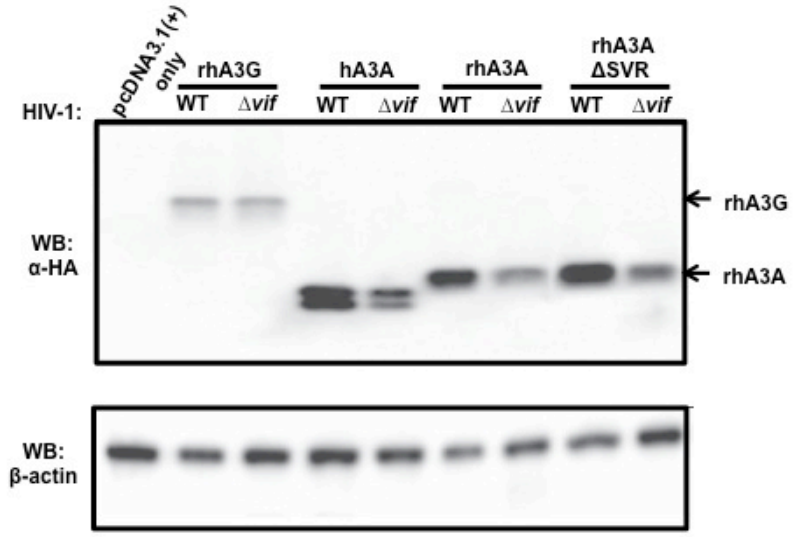
pcDNA3.1(+) only
rhA3G
hA3A
rhA3A
rhA3A ΔSVR
HIV-1:
WT
Δvif
WT
Δvif
WT
Δvif
WT
Δvif
WB: α-HA
rhA3G
rhA3A
WB: β-actin

loaded in lane 4). Unlike hA3A, rhA3A was degraded in the presence of the SHIV genome but stable in the presence of the SHIVΔ*vif* genome (Figure 50A). From these results we conclude that rhA3A interacts with the SIV Vif protein. Finally, rhA3A appeared to be less stable in the presence of the HIV-1 genome and more stable in the presence of NL4-3Δvif (Figure 50B). Similar results were observed at 48 h post-transfection (data not shown). From these results we conclude that the SIV and HIV-1 Vif proteins may interact with rhA3A promote its rapid turnover.

RhA3A causes low levels of G-to-A mutations in nascent SHIVΔVif reverse transcripts

RhA3A incorporation into SHIVΔ*vif* virions led to a significant decrease in infectivity (Figures 48B). Our previous study revealed that rhA3G inhibition of SHIVΔ*vif* virions in target cells was accompanied by substantial G-to-A mutations (Schmitt et al., 2010). To determine whether rhA3A has a similar effect, we amplified a 300 bp region in *nef* from target TZM-bl cells and sequenced 15 independent clones.

The results indicate that while rhA3G caused 33 G-to-A mutations in 15 clones (300 bases sequenced in each clone or total of 4,500 bp) in the *nef* gene of SHIVΔ*vif*, most of which (29) were in the context of 5'-TCT-3' (Schmitt et al., 2010), while only 7 such mutations were detected with rhA3A (Figures 51B). As expected, the corresponding wild-type SHIV had significantly lower G-to-A mutation frequencies

Figure 51. RhA3A induces low frequencies of G-to-A mutations in SHIVΔ*vif* nascent reverse transcripts. TZM-bl cells were infected with DNase-I treated SHIV or SHIVΔ*vif* virions and DNA was extracted after 24 h. A 300-bp segment of *nef* was amplified, cloned, and 15 independent clones were sequenced. Panel A. Moderate G-to-A mutations induced by rhA3A on SHIVΔ*vif*. Panel B. Graph depicting the cumulative number of mutations from the 15 clones. RhA3A induced 5-fold lower G-to-A mutations than rhA3G against SHIVΔVif. Panel C. Lack of G-to-A mutations in wild-type SHIV in the presence of either rhA3A or rhA3G. Panel D. Graph of cumulative substitutions in wild type SHIV. In panels A and C, each mutation is denoted by a vertical line that is color coded with respect to the dinucleotide context: GA (red), GG (yellow), or non-G-to-A (black). In panels B and D, each bar is shaded according to the proportion of G-to-A substitutions that occurred in the context of GA (red), GG (yellow), or non-G-to-A (black).

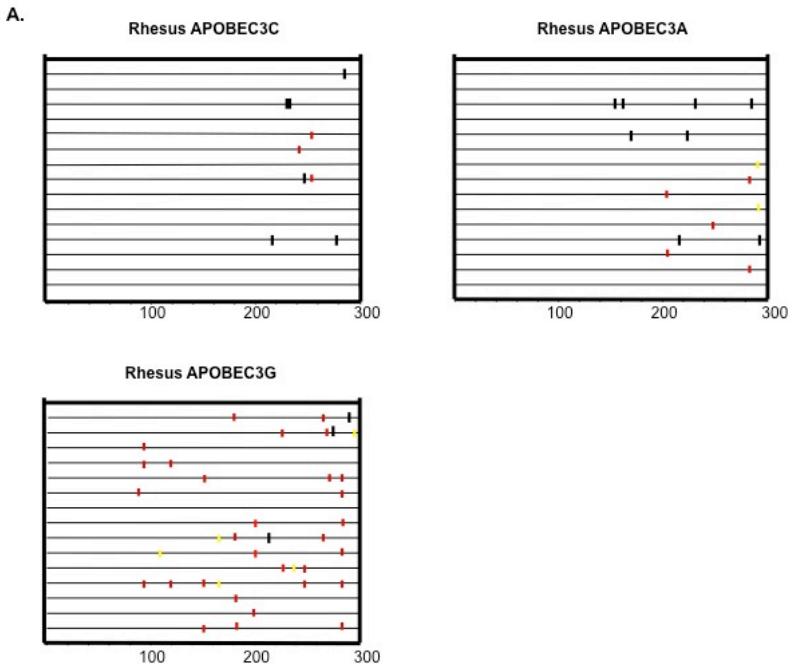
A.
Rhesus APOBEC3C
Rhesus APOBEC3A
Rhesus APOBEC3G
100
200
300

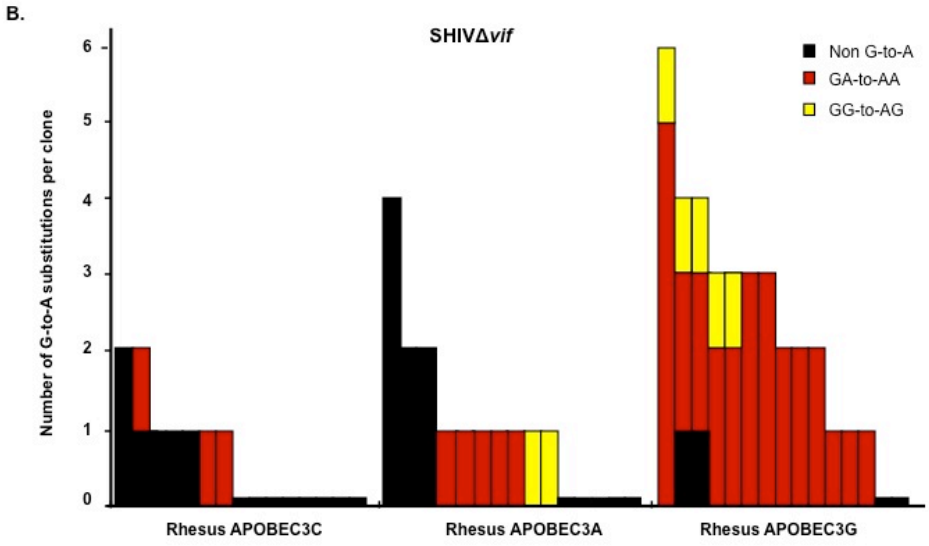
B.
SHIVΔvif
Non G-to-A
GA-to-AA
GG-to-AG
Number of G-to-A substitutions per clone
0
1
2
3
4
5
6
Rhesus APOBEC3C
Rhesus APOBEC3A
Rhesus APOBEC3G

C.

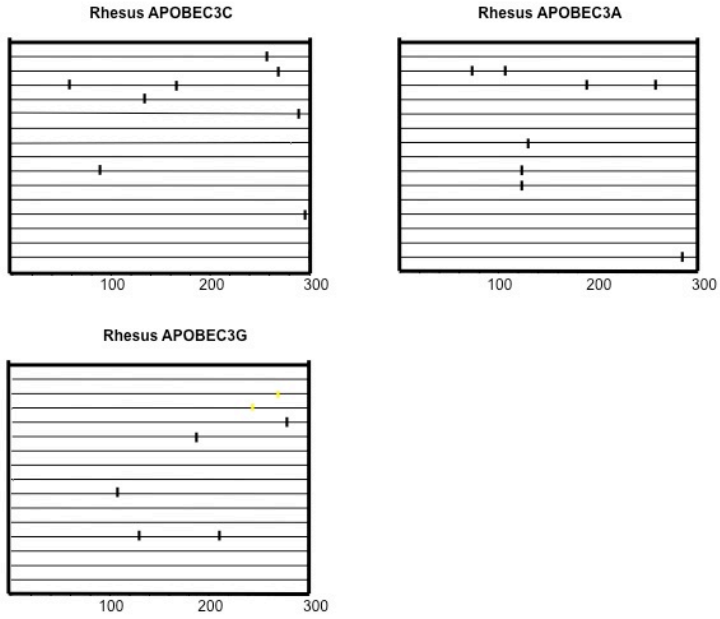
Rhesus APOBEC3C
Rhesus APOBEC3A
Rhesus APOBEC3G
100
200
300

D.

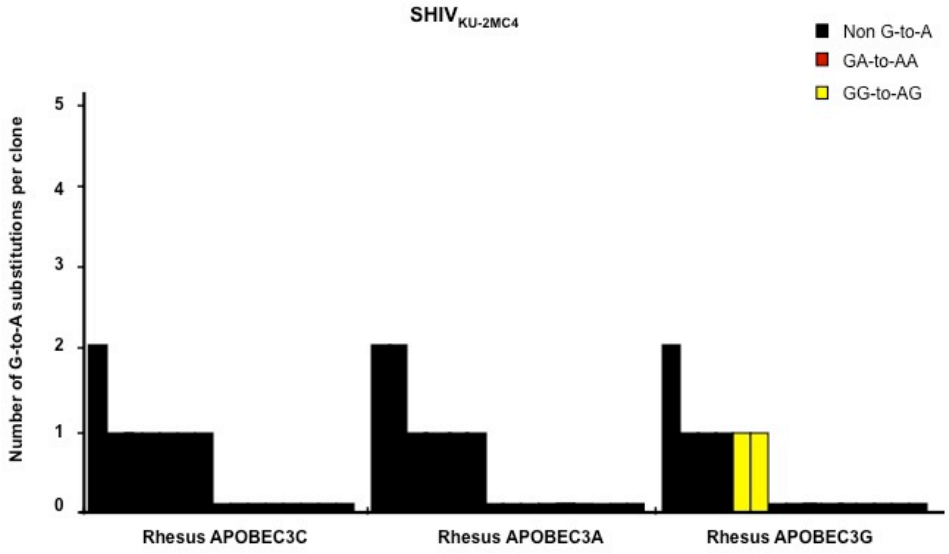
SHIV KU-2MC4
Non G-to-A
GA-to-AA
GG-to-AG
Number of G-to-A substitutions per clone
0
1
2
3
4
5
Rhesus APOBEC3C
Rhesus APOBEC3A
Rhesus APOBEC3G

Figure 52. RhA3A does not inhibit AAV-2 replication. Panel A. Low molecular weight DNA extracted from 293 cells transfected with recombinant AAV-2 plasmids and either empty vector (pcDNA3.1), hA3A, rhA3A, or rhA3G. A 1% Southern blot was run and hybridized with a ^{32}P-labeled probe from SSV9 as previously described (Qiu and Pintel, 2002). The following AAV replication products are shown as RF (double recombinant form), RF (recombinant form), and ssDNA. These experiments were performed two times with identical results. Panel B. A Western blot was performed on an aliquot of the lysate to show that each A3 protein was expressed.

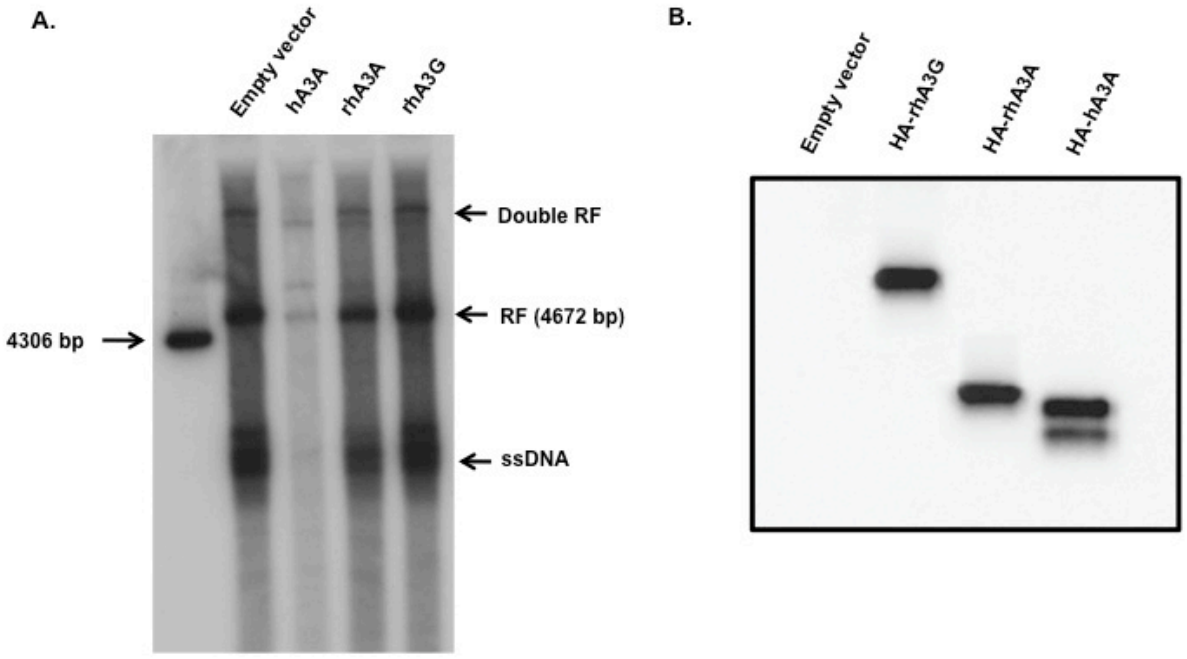
A.
Empty vector
hA3A
rhA3A
rhA3G
Double RF
RF (4672 bp)
4306 bp
ssDNA
B.
Empty vector
HA-rhA3G
HA-rhA3A
HA-hA3A

(**Figures 53D**). These results suggest that while rhA3A and rhA3G appear to have similar antiviral potency against SHIVΔ*vif* (Figure 51D), rhA3A produced an approximately 5-fold decrease in the number of G-to-A mutations in SHIVΔ*vif* compared to rhA3G.

Rhesus A3A does not inhibit adeno-associated virus 2 (AAV-2)

Previous studies have shown that hA3A can inhibit the replication of AAV-2 and autonomously replicating parvoviruses (Chen et al., 2006). We determined if rhA3A could inhibit the replication of AAV-2. 293 cells were transfected with vectors expressing hA3A, rhA3G, rhA3A or the empty vector and plasmids expressing AAV-2 and a helper plasmid. At 48 h, the cells were harvested, the extrachromosomal DNA isolated by Hirt extraction and analyzed using Southern blots for the presence of replicating AAV-2 DNA. The results, shown in Figure 52A, indicate that hA3A, but not rhA3G, inhibited AAV-2 replication, as previously reported (Narvaiza et al., 2009; Chen et al., 2006). In contrast, rhA3A did not significantly inhibit AAV-2 replication. A Western blot from an aliquot of the 293 lysates showed that the A3 proteins were similarly expressed (Figure 52B).

RhA3A does not inhibit LINE-1 retrotransposition

L1 elements are autonomous non-LTR retrotransposons that constitute about 17% of the human genome (Babushok and Kazazian, 2007). L1 elements, through the ORF2 gene product, also facilitate the retrotransposition of *Alu* elements, which are present in an additional 11% of the genome. These *in vitro* retrotransposition assays require the co-transfection of hA3A with L1 plasmids (Rangwala and Kazazian, 2009) and assaying after 3-4 days, a timepoint where significant hA3A inhibition of plasmid DNA may be observed (Stenglein et al., 2010).

To determine whether rhA3A could inhibit L1 retrotransposition, we used an L1-eGFP plasmid construct that contains a self-splicing intron in the opposite orientation within eGFP (pLRE3-EF1-mEGFPI) (Wissing et al., 2007). As a positive control, an intronless isogenic construct that encoded an intact eGFP (pLRE3-EF1-mEGFP) was used. L1 (1 µg) and A3A (200 ng) plasmids were co-transfected into 293T cells and the cells were harvested at 2 and 4 days. Similar to our earlier results (Figure 53B), at 2 days post-transfection, we observed minimal (22%) inhibition of the eGFP control plasmid, while rhA3A had no effect (data not shown). However, the L1 signals we obtained at 2 days were still very low, which is line with previous reported data (Kroutter et al., 2009). By 4 days post-transfection, we observed detectable L1 retrotransposition (Figure 53A). As expected, hA3A potently inhibited L1 retrotransposition. In contrast, rhA3A, as well as the rhA3A_SVR mutant, had no effect (Figure 53A). The effect of hA3A on L1 retrotransposition could be partially attributed to foreign DNA restriction, since at 4 days post-transfection, we observed a 2-fold reduction in eGFP signal from

the control plasmid (Figure 53A). However, it should be noted that substantial eGFP signals were still detected, in contrast to near-complete inhibition of L1 by hA3A (Figure 53A). Importantly, under conditions where we detected significant foreign DNA restriction by hA3A, no such activity was observed for rhA3A and rhA3A_SVR. Thus, we conclude that unlike hA3A, rhA3A does not restrict L1 retrotransposons and/or foreign DNA.

Discussion

SIV and SHIV infections of rhesus macaques have been used extensively as models for studying HIV pathogenesis and in vaccine development. The fact that the dose, timing and route of infection can be controlled also makes it ideal for investigating the earliest events following pathogenic lentivirus infection, including innate immune responses. Recent discoveries have shown that specific lentivirus genes could antagonize the effects of host innate restriction factors. Thus, the macaque/SIV or SHIV models provides a compelling system to explore how these restriction factors are regulated *in vivo* following lentivirus infection.

Figure 53. RhA3A does not inihibit retrotransposition. One microgram of L1 constructs containing eGFP with or without the γ-globin intron in the opposite orientation and 200 ng of empty vector, hA3A, rhA3A, or rhA3AΔSVR plasmid were co-transfected into 293 T cells using Fugene 6 (Roche). At 4 days post-transfection, cells were harvested and analyzed for eGFP expression using a FACSCalibur machine (BD Biosciences) with 150,000 events. Panel A. Results of co-transfection of LINE 1 plasmid (with intron) with either the empty vector, hA3A, or rhA3A plasmids. To minimize autofluorescence background, the percentage of eGFP+ cells from the untransfected control was gated against an empty fluorescence channel (FL3). Panel B. Results of co-transfection of eGFP control plasmid (no introns) with either the empty vector, hA3A, or rhA3A plasmids.

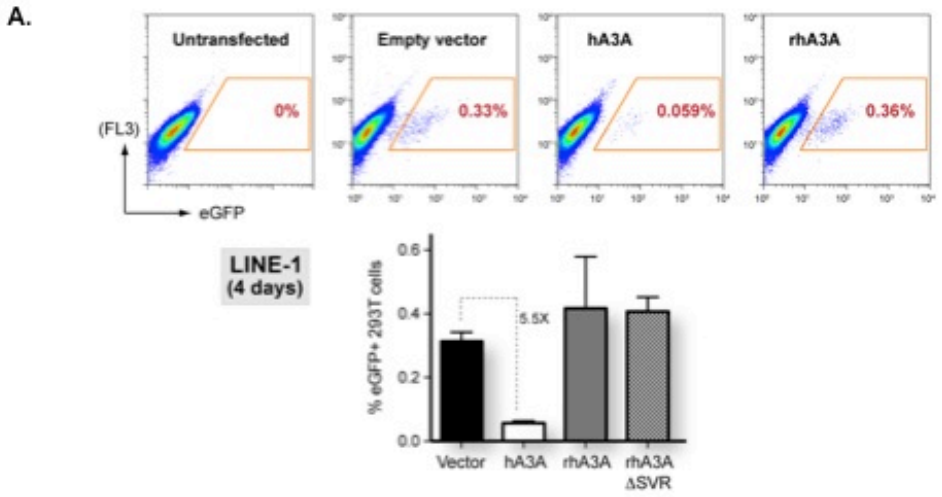
A.
Untransfected
Empty vector
hA3A
rhA3A
0%
0.33%
0.059%
0.36%
(FL3)
eGFP
LINE-1
(4 days)
% eGFP+ 293T cells
5.5X
Vector
hA3A
rhA3A
rhA3A
ΔSVR
B.
Untransfected
Empty vector
hA3A
rhA3A
0.047%
27.8%
15.6%
30.4%
SSC
eGFP
eGFP control
(4 days)
% eGFP+ 293T cells
2.0X
Vector
hA3A
rhA3A
rhA3A
ΔSVR

Identification of rhA3A as a novel lentivral restriction factor

The APOBEC3 family of deoxycytidine deaminases function as potent antiretroviral factors. Incorporation of select A3 proteins can inhibit reverse transcription and/or induce G-to-A hypermutation in nascent reverse transcripts in the next target cell (Bishop et al., 2004; Celico et al., 2006; Russell et al, 2009; Sova et al., 1993; von Schwedler et al., 1993; Zheng et al., 2005). Seven *A3* genes are encoded in the human genome, but only a subset, *hA3G*, and to a lesser extent, *hA3F* and *hA3C*, are expressed in CD4+ T cells, inhibit HIV-1 and are counteracted by the HIV-1 encoded Vif protein (Koning et al., 2009; Refsland et al., 2010). There is uncertainty whether a similar complement of *A3* genes are present in rhesus macaques, particularly since no *rhA3A* gene has yet to be identified. In this study, we cloned the *rhA3A* gene. This result is consistent with a recent study that revealed evolutionary conservation of *A3A* among hominids, Old World and New World monkeys (Bulliard et al., 2011). In addition, analysis of the rhesus macaque genome provided evidence of seven encoded *A3* members that based on phylogenetic analyses are orthologous to the corresponding *hA3* genes. These findings suggest that the seven rhA3 genes have been maintained after the evolutionary split between monkeys and humans. Thus, the *vif* genes of various SIV strains naturally infecting Old World monkey species have likely been co-evolving with the same set of *A3* genes for millions of years.

Rhesus macaque A3G is a potent A3 deaminase against SIV, SHIV and HIV-1 (Schmitt et al., 2010; Virgen et al., 2007; Zennou et al., 2006). We therefore determined

the expression of the other rhesus macaque *A3* genes in primary, activated $CD4^+$ T cells, the main cellular targets of SIV and SHIV *in vivo*, in relation to rhA3G. Our results indicate that *rhA3B* mRNA is not expressed and that *rhA3D* mRNA is expressed at levels that are likely not biologically relevant *in vivo*. *RhA3F* is expressed at 2-fold lower levels than *rhA3G*, but rhA3F appears to be incorporated promiscuously into virions and is not as functional as rhA3G in side-by-side co-transfection studies (Schmitt et al., 2010). Only *rhA3A*, *rhA3C* and *rhA3H* are expressed at similar or higher levels than *rhA3G*. RhA3H has been previously shown to have potent antiretroviral activity against HIV-1 (OhAinle et al., 2008) and we found significant activity against SHIV (unpublished data). We also found no significant antiviral activity of rhA3C against SHIV. Surprisingly, rhA3A exhibited potent antiretroviral activity. Based on this data, we conclude that rhA3A, rhA3G, and rhA3H most likely are the dominant rhesus macaque APOBEC3 deaminases that could restrict SHIV or SIV *in vivo*.

Insights on rhA3A restriction of lentiviruses

Rhesus macaque A3G inhibits SHIVΔ*vif* and HIV-1Δ*vif* virion infectivity through a mechanism that involves virion incorporation. Virion incorporated rhA3G blocks reverse transcription and/or induces G-to-A hypermutation in the next target cell. Consistent with this mechanism, we readily detected rhA3G in SHIVΔ*vif* and HIV-1Δ*vif* virions, and observed substantial G-to-A mutations in reverse transcripts newly formed in target cells. Given these consistent phenotypes, we used rhA3G as a positive control for evaluating the antiretroviral activity of rhA3A. In this study, we found that rhA3A is as

potent as rhA3G in restricting virus infectivity. Both proteins inhibited SHIVΔ*vif* infectivity by approximately 20-fold. In addition, rhA3A modestly inhibited HIVΔ*vif* infectivity by about 3-fold. We found that in contrast to rhA3G, rhA3A was incorporated at low levels into SHIVΔ*vif* virions and was undetectable in HIVΔ*vif* virions (Figure 48). The results may be due to the sensitivity of the Western blots and that rhA3A is incorporated into virions at very low levels compared to rhA3G. This would also suggest that rhA3A enzymatic activity may be higher than rhA3G on a per-molar basis.

As a first step in gaining mechanistic insights on *rhA3A*-mediated restriction of SHIV and HIV-1, we evaluated whether two rhA3A domains are critical for restriction. Comparison of the amino acid sequences of human and rhesus macaque A3A reveals a monkey-specific insertion at position 27-29 (SVR) that is critical for SHIVΔ*vif* and HIV-1ΔVif inhibition by rhA3A that was lost in the hominid lineage (Figure 41). In a recent modeling study of hA3A, it was shown that amino acids 29 and 30 likely form part of a polynucleotide accommodating groove near the active-site pocket (Bulliard et al., 2011). We observed that the rhA3A ΔSVR mutant is totally inactive, while remaining sensitive to SHIV and HIV-1 Vif-dependent degradation. In addition, we made just the opposite mutation, the addition of the SVR motif to hA3A. We found that this mutant gained partial activity against HIV-1Δ*vif* but was not as active as rhA3A, suggesting that other amino acid substitutions are likely involved in this function. We also determined if the canonical cytidine deaminase Zn^{+2} binding domain (C/H-X-E-X_{23-28}-P-C-X_{2-4}-C) was critical for rhA3A anti-lentiviral activity. Mutation of the histidine at position 70 to glutamic acid resulted in no restriction of SHIVΔ*vif* (unpublished data). Thus, the

monkey-specific residues SVR (27-29) and the canonical Zn^{+2} binding domain are critical for rhA3A-mediated Δ*vif* lentivirus restriction.

Human A3A is largely inactive against HIV-1ΔVif, but when targeted to the viral nucleocapsid, it has potent activity against HIV-1ΔVif (Goila-Gaur et al., 2007). Since hA3A and the C-terminal region of hA3G are derived from a common ancestor, the N-terminal domain of hA3G was fused to hA3A (hA3G-A3A). This hA3G-A3A fusion protein localized to the cytoplasm, incorporated into the viral nucleoprotein complexes, and inhibited HIV-1 replication (Goila-Gaur et al., 2007). Similarly, fusion of hA3A to the Vpr protein resulted in its incorporation into viral nucleoprotein complexes and inhibition of HIV-1 and SIV replication (Aguiar et al., 2008). These results suggested that the reason that hA3A could not restrict lentiviruses is that it could not be targeted to the virion core. While hA3A had no substantial activity against HIV-1ΔVif, hA3A surprisingly decreased SHIVΔVif virion infectivity by approximately 10-fold. Although we did not detect hA3A in virions; it is possible that like rhA3A, very little is incorporated into nascent virions and is below the limits of detection by Western blot analysis.

Evidence for recent evolutionary gain of function of DNA restriction in hominids

Previous studies have shown that while hA3A is inactive against HIV-1, it can block endogenous retroviral elements such as LTR-retrotransposons or *Alu* elements (Chen et al., 2006; Bogerd et al., 2006b). Human A3A has antiviral activity against autonomous (minute virus of mice; MVM) and non-autonomous (AAV-2) replicating

parvoviruses and has editing activity against the human papillomavirus genome (Chen et al., 2006; Narvaiza et al., 2009; Vartanian et al., 2008). Finally, hA3A has been shown to counteract foreign DNA (Stenglein et al., 2010) and promote DNA damage (Landry et al., 2011). These studies suggest that hA3A biology is intimately linked to the restriction of double-stranded DNA elements. Surprisingly, we found no evidence for rhA3A restricting AAV-2, L1 elements and foreign DNA. While it can be argued that rhA3A may have activity against rhesus macaque AAV, no infectious macaque AAVs have been isolated to date. Thus, the DNA restriction properties of A3A may have been a recent evolutionary development in the hominid lineage.

The mammalian *A3* locus encodes genes that have among the highest detectable evolutionary pressures known (Sawyer et al., 2004). This is thought to reflect a long-standing host-pathogen genetic conflict that eventually helps dictate current trends in cross-species transmission and viral host range. Our findings now enter A3A into this select group of genes, given the divergent virus specificities of the human and monkey homologues. RhA3A inhibits the SHIVΔ*vif* and HIV-1ΔVif, but not the DNA virus AAV-2 and L1 retroelements, while hA3A inhibits SHIVΔ*vif*, AAV-2 and L1 elements but not HIV-1Δ*vif*. Thus, it would appear that rhA3A could inhibit a broader range of lentiviruses at the cost of having no activity against DNA viruses. On the other hand, hA3A appears to have acquired activity against DNA viruses, at the expense of losing broad potency against lentiviruses. The rhA3A mutant with amino acids 27-29 deleted (rhA3AΔSVR) was incapable of restricting SHIVΔ*vif* and HIV-1Δ*vif*. Thus, the divergent

viral specificities of hA3A and rhA3A may be dictated, at least in part, by an evolutionary switch that involved alterations in the polynucleotide-binding groove of A3A. The 81% identity between hA3A and rhA3A at the amino acid level should enable structure-based domain-swap experiments to determine which residues account for differential virus restriction. These types of studies should provide a biologically relevant system to interrogate which changes in the molecular determinants of nucleic acid specificity of the A3A proteins dictates the antiviral activity of A3A against lentiviruses, parvoviruses and L1 retroelements.

Experimental Methods

Cells, viruses, and plasmids

HeLa and 293 cells were used for transfections of vectors expressing various APOBEC3 proteins, full-length SHIV or HIV-1 (NL4-3). The TZM-bl cell line was used as an indicator cell line to measure the infectivity of viruses (Derdeyn et al., 2000; Platt et al., 2009; Takeuchi et al., 2008; Wei et al., 2002). Both cell lines was maintained in Dulbecco's minimal essential medium (DMEM) with 10% fetal bovine serum (R10FBS), 10 mM Hepes buffer, pH 7.3, and 100 U/μg penicillin-streptomycin and 5 μg gentamicin. Rhesus macaque PBMCs were obtained from uninfected animals and isolated on Ficoll/Hypaque gradients. The derivation of $SHIV_{KU\text{-}2MC4}$ (a pathogenic molecular clone; referred to in the text as SHIV) and $SHIV_{VifSTOP}$ (referred to in the text as SHIVΔ*vif*) *has*

been previously described (Liu et al., 1999; Schmitt et al., 2010). A plasmid with the genome of HIV-1 strain NL4-3 (referred to in the text as HIV-1) was used to construct a *Δvif* version (referred to in text as HIV-1Δ*vif*) (pNL4-3; NIH AIDS Research and Reference Reagent Program). This plasmid was digested with PflM1, phenol: chloroform extracted, and ethanol precipitated. The 5'-protruding ends were filled using DNA Polymerase I Large Fragment (Klenow; Promega). The resulting Klenow fragment reaction produced blunt ended fragments that were purified and re-ligated. The resulting plasmid was sequenced and found to contain a deletion in pNL4-3 *vif* between base pairs 5301 to 5308. Therefore, only the first 79 amino acids of pNL4-3 Vif could be expressed. The plasmids pcDNA3.1(+)-HA-rhA3G and pcDNA3.1(+)-HA-hA3A were kindly provided by Nathaniel Landau (New York University School of Medicine). A plasmid expressing HA-rhA3C was constructed in this laboratory and cloned into the pCruz-HA vector (Santa Cruz Biotechnology) using restriction sites *Sca* I and *Kpn* I. A plasmid expressing pcDNA3.1(+)-HA-hA3G used in these studies was provided by the NIH AIDS Reference and Reagent Program.

Molecular cloning of rhA3A

Total RNA from mitogen-activated rhesus macaque PBMCs was isolated using the RNAEasy Kit (QIAGEN; Valencia, CA). Three hundred ng of sample was subjected to random hexamer priming using the RT^2 EZ first strand kit (SA Biosciences), and 4 µl of this cDNA was subjected to a 40 µl PCR reaction consisting of 1x Sweet PCR Mix (SA Biosciences), 12.5 pmol of rhA3A.F (5'-GACAAGCACATGGACGGCAG) and rhA3A.R

(5'-CATCCTTCAGTTTCCCTGAT) primers, designed based on the first and last exons of human *A3A* (*hA3A*). Amplification conditions included 95^{o}C for 15 min hot-start, followed by 40 cycles at 94^{o}C 30 s, 50^{o}C 30 s and 72^{o}C 3 min in a PE 9700 machine (Perkin Elmer). A dominant PCR amplicon of 600 bp was subcloned into the TOPO-TA vector (Invitrogen) and sequenced. The sequence for rhesus macaque *A3A* (*rhA3A*) was submitted to GenBank with Accession number JF831054. An expression construct containing rhA3A linked to an N-terminal HA-tag was synthesized (GenScript). The HA-rhA3A gene was subcloned into pcDNA3.1(+) using restriction sites *Kpn* I and *Eco* RV sites of pcDNA3.1(+) and sequence-confirmed.

Positioning of rhA3 genes in the rhesus macaque genome

Analysis of the *Apobec3* loci was performed using NCBI Build 1.2 version of the macaque chromosome 10 sequence. *RhA3C* (Accession # EU381233), *rhA3G* (XM_001094452), *rhA3F* (DQ514917) and *rhA3H* (DQ507277) cDNA sequences were subjected to BLAST analysis against the macaque genome, and the corresponding coordinates were obtained. To characterize the intronic sequence flanked by exons 1 and 2 of *rhA3A*, exon 1 (5'-AGAAGAGACAAGCACATGGAC) and exon 2 (5'-GCTCCACCTCGTAGCACAA) specific primers were used to directly amplify rhesus macaque genomic DNA. The resulting PCR amplicon was directly sequenced (**Figure 42**; see text for details). *RhA3B* and *rhA3DE* sequences were predicted based on the genome sequences upstream of *rhA3C* and between *rhA3C and rhA3F*, respectively, using the geneid program (http://genome.crg.es/geneid.html) (**Figures 43 and 44**).

Phylogenetic analysis of rhApobec3A

The *A3A* amino acid sequences from various primate species were obtained from (Bulliard et al. 2011). Sequences were aligned using ClustalX using the Gonnet series, and neighbor-joining trees were constructed with 1000 subreplicates, correcting for multiple substitutions and excluding gaps. The C-terminal half of rhA3G was used as outgroup. A3 amino acid sequences from human, mouse, rat and rhesus macaque were likewise aligned using Clustal X, after splitting the sequences of rodent A3 and primate A3B, A3DE, A3F and A3G into N-terminal and C-terminal halves. Neighbor-joining trees were performed unrooted, with 1000 subreplicates and excluding gaps.

Expression of rhA3A in rhesus macaque tissues

A rhesus macaque that euthanized and perfused with 2 liters of Ringer's saline to remove contaminating blood was used to examine the expression of *rhA3A* mRNA in different tissues (visceral organs and brain). *RhA3A* was amplified from 30 µg of each visceral and CNS tissue using the RNAEasy kit (Qiagen; Valencia, CA). RNA was digested with 1 U/µl DNase-I (Fermentas) for 30 min. RT-PCR was performed using the Titan One RT-PCR kit (Roche). Each reaction used 100 ng of total RNA and was amplified using oligonucleotide primers specific for *rhA3A*. The oligonucleotides used for the reverse transcriptase reaction and first round PCR were 5'-GGACGGCAGCCCAGCATCCAGGCCCAG-3' (sense) and 5'-CGTAGGTCATGATGGAGACTTGGGC -'3 (antisense), which are complementary to

bases 3-29 and 451-475, respectively. The nested oligonucleotides used were 5'-CCAGGCCCAGACACTTGATGGATCC-3' (sense) and 5'-CCGCAGCGTTCGCAGTGCCTCCTGATACAGG-3' (antisense), which are complementary to bases 20-44 and 411-441, respectively. As a control, GAPDH was amplified to verify the integrity the RNA using oligonucleotides 5'-GCCATCACTGCCACCCAG-3' (sense) and 5'-GCCACATACCAGGAAATGAGC-3' (antisense). The nested oligonucleotides used were 5'-CCTCCGGGAAACTGTGGC-3' (sense) and 5'-CGTTGAGGGCAATGCCAG-3' (antisense). The reactions were performed in an ABI 2720 Thermal Cycler using the following thermal profile: 42°C 30 min for 1 cycle; 94°C 2 min for 1 cycle, 94°C 30 s, 55°C 30 s, and 68°C 45s for 10 cycles; 94°C for 30 s, 55°C 30 s, and 68°C 2 min for 25 cycles. One µl of the initial reaction mixture used for nested PCR using r*Taq* (Takara) and performed with the following thermal cycle profile: 95°C for 1 min, 48°C 2 min, and 72°C 3 min for 35 cycles. The 450 bp amplicon was visualized in a 1.5% agarose gel, excised and gel purified (Qiagen; Valencia, CA) and directly sequenced.

Expression of rhA3 genes in activated $CD4^+$ T cells

Rhesus PBMCs were obtained from three donors by Ficoll separation. 5×10^6 cells were seeded into each well of a 6-well plate containing 3 ml RPMI medium (Mediatech) with 10% Fetal Bovine Serum (Gemini Biosciences). Half of the cultured PBMCs were activated with 2.5 µg/ml Staphylococcal Enterotoxin B (SEB; Toxin Technology) overnight. The following day, the PBMCs were stained with CD3-V450

(clone SP34-2), CD4-APC-H7 (L200) and CD25-PerCP-Cy5.5 (M-A251) (BD Biosciences) and analyzed in an LSR-II flow cytometer (BD Biosciences). Histogram plots to highlight CD25 expression in $CD4^+$ T cells were constructed using the FlowJo software (Treestar). $CD4^+$ T cells were purified from activated PBMCs by negative selection with magnetic beads (Miltenyi Biotec). Total RNA was extracted from $CD4^+$ T cells using the RNAEasy kit, and cDNA was synthesized by random hexamer priming using the RT^2 EZ first strand kit (SA Biosciences). The cDNA was used for triplicate real-time PCR evaluations (25 µl) with optimized *A3*-specific primers and a housekeeping gene, GAPDH, in a BioRad real-time PCR machine. Briefly, 5 µl of cDNA was mixed with 12.5 µl of 1´ Universal Master Mix (Applied Biosystems), 10 pmol of primers and 5 pmol of probe and subjected to 40 cycles of denaturation and annealing/elongation. The *A3*-specific primers, probes and cycling conditions are listed in **Table VIII**. Cloned cDNA sequences were used as standards and for evaluating cross-reactivity (**Table VIIII**). The *A3*-specific assays had a limit of detection of 5 copies per reaction, and standard curves had r^2 values >98%.

Subcellular localization of rhA3A

For intracellular localization of rhA3A, 293 cells were plated onto 13 mm cover slips in a 6 well plate and transiently co-transfected with vectors expressing HA-tagged hA3A, rhA3G or rhA3A and one expressing a eGFP tagged nuclear marker using a polyethylenimine (PEI) transfection reagent (ExGen^{TM} 500, MBI Fermentas) according to the manufacturer's instructions. Cultures were maintained for 36-48 h before being

were fixed in 2% paraformaldehyde (4°C) for 10 min and washed twice for 5 min in 1x PBS (pH7.4). Cover slips were incubated with a rabbit polyclonal anti-HA antibody (HA-probe, Santa Cruz) for 1 h at ambient temperature in 1x PBS plus 1% BSA. Cover slips were washed twice for 5 min in PBS and reacted with a Cy-5 conjugated secondary antibody (Abcam) 1x PBS plus 1% BSA for 30 min. The cover slips were washed twice for 5 min in 1x PBS and mounted in glycerol containing mounting media (Slowfade antifade solution A, Invitrogen). A Nikon A1 confocal microscope was used to collect 100x images with a 2x digital zoom, using EZ-C1 software. The pinhole was set to large for all wavelengths used with Cy5 and eGFP excited using a 638 nm and 488 nm diode lasers, respectively. Images were collected using a 670 nm filter for Cy5 and 525/25 nm fiter for eGFP.

Foreign DNA restriction by rhA3A

293 cells were seeded into 6-well tissue culture plates 24 h prior to transfection. Cells were first transfected with 3 mg of either HA-rhA3A, HA-hA3A, HA-rhA3G HA-rhA3ADSVR or pcDNA3.1(+) vector using a polyethylenimine transfection reagent (ExGen^{TM} 500, MBI Fermentas) according to the manufacturer's instructions. After 24 h, the cells were re-transfected with 3 mg of a vector expressing eGFP. Cells were incubated at 37^{o}C in 5% CO_2 atmosphere for either 2 or 5 days. The cells were removed from the plate using $Ca^{2+/}Mg^{2+-}$free PBS containing 10 mM EDTA. Cells were then fixed in 2% paraformaldehyde, for 5 min. The cells were washed twice in 1x PBS plus and analyzed using an LSRII flow cytometer. The mean fluorescence intensity

(MFI) for eGFP positive cells was calculated. The MFI ratio and percentage of eGFP positive cells was calculated for each sample. Normalized ratios from three separate experiments were averaged and the standard error calculated. All groups were compared to pcDNA3.1(+) plus eGFP control using a Student's *t*-test with $p<0.05$ considered significant.

Production of HIV-1ΔVif and SHIVΔVif virions in the presence of A3A

293 cells were seeded into a 12-well tissue culture plate 24 h prior to transfection. Cells were first transfected with 1 mg of HA-tagged rhA3A, hA3A, rhA3G or pcDNA3.1(+) vector using PEI (Fermentas). After 24 h, cells were transfected with 1 mg of SHIVΔ*vif* or HIV-1Δ*vif* plasmid. Cells were incubated at 37°C in 5% CO_2 atmosphere for 48 h. Supernatants were collected and cellular debris removed by low speed centrifugation. The cells were lysed in 500 ml of RIPA (50 mM Tris-HCl, pH 7.5, 50 mM NaCl, 0.5% deoxycholate, 0.2% SDS, 10 mM EDTA) and the nuclei were removed through high-speed centrifugation. The amount of Gag p27 or p24 present in the viral supernatants was measured using a commercially available p27 and p24 ELISA kits (Zeptometrix). The experiment was run at least three separate times, normalized to the empty vector control samples. Differences between mean percentages were calculated using a two-tailed Student's *t*-test with $p<0.05$ considered significant.

Inhibition of SHIV and HIV-1 virion infectivity by A3A

SHIV, SHIVΔVif, HIV-1 or HIVΔVif infectious molecular clones (3 μg) were co-transfected (1.5 μg) with plasmids expressing rhA3A, rhA3AΔSVR, rhA3G, rhA3C, hA3A, hA3A+SVR, or hA3G using PEI (Fermentas) in a 6-well plate. At 48 h post-transfection, the culture medium was harvested and clarified by low speed centrifugation. Equivalent amounts of p27 were serially diluted using 10-fold dilutions from 10^1 to 10^6 and used to inoculate TZM-bl cells. At 48 h post-inoculation, the media was removed, cells washed with PBS and the monolayer fixed using 1% formaldehyde-0.2% glutaraldehyde in PBS. The cells were washed and incubated in a solution for 2 h at 37°C containing 4 mM potassium ferrocyanide, 4 mM potassium ferricyanide, 4 mM magnesium chloride, and 0.4 mg X-gal per ml. The reaction was stopped and the infectious units (IU) per ml were calculated (Derdeyn et al., 2000; Wei et al., 2002).

Site-directed mutagenesis

Mutations introduced into all plasmids were accomplished using a QuikChange site-directed mutagenesis kit (Stratagene) according to the manufacturer's protocol. All plasmid inserts were sequenced to ensure the validity of the mutations and that no other mutations were introduced during the cloning process.

Virion incorporation assays

SHIV, SHIVΔVif, HIV-1 or HIVΔVif infectious molecular clones (3 μg) were co-transfected with 1.5 μg of plasmids expressing either rhA3A, rhA3G, hA3G or hA3A proteins into 293 cells using PEI reagent (Ex-Gen™ 500, Fermentas) in each well of a

6-well plate. At 48 h, virus supernatants were harvested and clarified by low speed centrifugation. The clarified supernatant was ultracentrifuged to pellet virions (SW41 rotor, 247,000x*g*, 1 h, 4°C). The pellet was resuspended in PBS and layered on a 20%/60% sucrose step gradient and again subjected to ultracentrifugation (SW55Ti, 247,000´*g*, 1 h) at 4^{O}C. The interface (containing virions) was harvested, pelleted again by ultracentrifugation as described above, and resuspended in 150 µl of PBS. An aliquot was saved to determine the p27 or p24 content by antigen capture assay (Zeptometrix). The remaining sample was boiled in 2´ sample reducing buffer. Equivalent amounts of p27 or p24 were loaded on a 12% SDS-PAGE gel. A3 proteins were detected by Western blotting using an anti-HA antibody (HA-probe; Santa Cruz). Blots were placed in stripping buffer (25 mM glycine, pH 2.0 and 1% SDS) and reprobed using either rabbit polyclonal antibody specific for p27 or a mouse monoclonal antibody to p24 (NIH AIDS Research and Reference Reagent Program).

Stability of rhA3A in the presence of SHIV and HIV-1 genomes

Infectious molecular clones of HIV-1, HIV-1Δvif or SHIV and SHIVΔvif were co-transfected in a 2:1 ratio with rhA3A, rhA3AΔSVR, rhA3G, hA3G, or hA3A using PEI transfection reagent (Ex-Gen500; Fermentas) into a 12-well plate. At 24 h post-transfection, the supernatant was removed, the cells were harvested and lysed using RIPA buffer. Following lysis, the nuclei were removed by centrifugation at 14,000 rpm for 15 min in a microfuge at 4°C. The protein was precipitated using methanol, resuspended in 2x sample reducing buffer, and boiled for 5 min. Proteins were

separated on a 12% SDS-PAGE gel and probed using commercially available rabbit polyclonal HA antibody (HA-probe, Santa Cruz). All samples were normalized to the same amount of b-actin protein using a mouse monoclonal antibody specific for b-actin (AC15; Novous Biologicals).

Hypermutation assays in the presence of rhA3A

To determine whether virion-incorporated rhA3A can induce G-to-A mutations in nascent reverse transcripts, 293 cells were co-transfected with vectors containing the genomes SHIV or SHIVΔVif and vectors expressing rhA3G (positive control), rhA3C (negative control) or rhA3A using PEI (Fermentas). At 24 h post-transfection, cells were washed and fresh DMEM was added. At 48 h, the supernatant containing virus was subjected to ultracentrifugation through a 20% sucrose cushion. The resulting supernatant was DNase-I-treated (Fermentas) at 37°C for 30 min to minimize plasmid carry-over. Infectious titers in the supernatants were measured on TZM-bl cells. In addition, at 24 h post-infection of TZM-bl cells, total cellular DNA was harvested and extracted using the DNeasy kit (Qiagen). The DNA was used in a nested DNA PCR to amplify a 300 base pair fragment of *nef*. The PCR reaction was carried out using rTaq and the manufacturer's instructions (Takara). The oligonucleotides employed during in the first round PCR to amplify SIV *nef* were 5'-GGTGGAGCTATTTCCATGAGG-3' (sense) and 5'-GTCTTCTTGGACTGTAAT AAATCCC-3' (anti-sense). One µl of the first PCR product was added to a nested reaction. The oligonucleotides used during the nested PCR reaction were 5'-CCATGAGGCGGTCCAGGCAGTCTAGAG-3' (sense)

and 5'-CCTCCCAGTCCCCCCT TTTC-3' (anti-sense). The PCR reactions were performed using an ABI 2720 Thermal Cycler with the following thermal profile: 95°C for 2 min, 1 cycle; 95°C for 30 s, 55° for 30 s, 65°C for 2 min, for 35 cycles; 65°C for 7 min. The PCR products were separated by electrophoresis, isolated, purified, sequenced and sub-cloned into pGEM-TEasy (Promega). Fifteen independent clones were sequenced and assessed for each mutant SHIV as described above for each condition.

Adeno-associated virus-2 (AAV-2) replication assay

The ability of rhA3A to inhibit the replication of AAV2 was assessed. 293 cells were transfected using LipoD 293 transfection reagent (SignaGen Labs;, Rockville, MD) into 60 mm dishes in duplicate with 1 mg SSV9 (an AAV2 infectious clone, psub201) (Qiu et al., 2002), 2mg pHelper (Stratagene, La Jolla, CA) (Xiao et al., 1998), and 1 mg of an A3 expression vector, rhA3G, hA3A, rhA3A, or as a negative control pBluescript SK (+) (Stratagene, La Jolla, CA). Forty-eight h post-transfection, the cells were harvested and resuspended in PBS. The supernatant was discarded and Hirt DNA was extracted using Hirt solution (10 mM Tris, 10 mM EDTA, pH 7.5, 0.6% SDS) at room temperature for 10 min followed by 5 M NaCl at 4°C overnight. The mixture was centrifuged at 14,000 rpm at 4^{o}C for 20 min. Following centrifugation, the pellet was discarded and the supernatant was treated with Proteinase K (50 mg/ml) at 37°C for 1 h. The low molecular weight (LMW) DNA was extracted twice with saturated phenol and once with chloroform/isoamyl alcohol. The resulting DNA was ethanol precipitated and column purified using the Qiagen gel extraction kit (Qiagen). The LMW DNA was run on

a 1% agarose gel, transferred to nitrocellulose and analyzed by Southern hybridization using a ^{32}P-labeled probe consisting of a fragment representing nucleotides 184-4490 (*Xba* I digestion) from SSV9 as previously described (Qiu et al., 2002). To ensure that all samples were expressing the desired A3 proteins, aliquots of harvested cells utilized in the Southern blot were lysed in RIPA buffer. The nuclei were removed and the protein was precipitated using methanol, resuspended in 2X sample reducing buffer, and boiled for 5 min. Proteins were separated on a 12% SDS-PAGE gel and probed using a rabbit polyclonal anti-HA antibody (HA-probe, Santa Cruz).

L1 retrotransposition assay

The engineered L1 enhanced green fluorescent protein (EGFP) reporter (Ostertag et al., 2000) was cloned into the *pLRE3-EF1-mEGFPI,* which contains a retrotransposition competent L1 element (LRE3) (Brouha et al., 2003) under the control of an EF-1α promoter in addition to the internal 5' UTR promoter. The enhanced GFP (eGFP) retrotransposition indicator cassette is under the control of an ubiquitin promoter (UBC), and the SV40 late polyadenylation signal. The construct was cloned into *pBSKS-II+* (Stratagene). The positive control *pLRE3-EF1-mEGFP(Δintron)* is similar to the *pLRE3-EF1-mEGFPI* but lacks the intron in the *mEGFPI* indicator cassette and therefore serves as a positive control for transfection efficiency. One μg of L1 construct and 200 ng of empty vector, hA3A, rhA3A or rhA3AΔSVR plasmid was co-transfected into 293T cells using Fugene 6 (Roche). All transfections were performed in triplicate.

Cells were harvested at 2 and 4 days and analyzed for eGFP expression using a FACSCalibur machine (BD Biosciences), collecting 150,000 events.

Previous research has shown that human APOBEC3A (hA3A) lacks antiviral activity against HIV-1, but inhibits the replication of adeno-associated virus 2 (AAV-2), intracisternal A particles (IAP), and long interspersed nuclear element 1 (L1) (Bogerd et al., 2006a,b; Chen et al., 2006; Muckenfuss et al., 2006). Although hA3A contains one CDA, the deaminase activity of hA3A is not required for its inhibitory role against AAV or retrotransposons, suggesting that a deaminase-independent mechanism of inhibition is occurring (Narvaiza et al., 2009). Human A3A also contains significant homology to the N-terminal half of hA3G, does not associate with the viral nucleocapsid complex (NPC) of HIV-1 but is readily incorporated into virions (Goila-Gaur et al., 2007).

SIV and SHIV have been invaluable models for studying various aspects of HIV-1 pathogenesis. Sequencing of the rhesus macaque genome has led to the identification of rhesus homologues of A3B, A3C, A3D, A3F, A3G and A3H. Here we describe the identification of an A3A homologue in rhesus macaques (rhA3A) and present evidence that the human and macaque *Apobec3* genes are orthologous. We show that the rhA3A protein is expressed well in activated macaque $CD4^+$ T cells and other rhesus macaque tissues, is incorporated into virions, is degraded by both HIV-1 and SHIV in a Vif dependent manner, and restricts the replication of SHIV (expressing the SIV_{mac}239 Vif) and HIV-1.

IX. Conclusion

In the last thirty years, HIV-1 has become one of the most devastating infectious diseases in humans. Developing countries display the greatest HIV-1-related morbidity and mortality, which is primarily due to the fact that only 10% of infected patients receive HAART therapy. HAART therapy prolongs the lifespan of HIV-1 infected patients by decreasing $CD4^+$ T cell loss and progression to AIDS. Presently, HAART therapy does not cure the patient, and there is an increased frequency of multidrug resistant HIV-1 strains. Therefore, new small molecule inhibitors or a vaccine to prevent infection or reduce transmission of HIV-1 is necessary to minimize the expansion of this epidemic.

In addition to humans, HIV-1 only infects chimpanzees and a practical alternative to studying the role of HIV-1 accessory genes in viral pathogenesis is to use macaques infected with non-human primate lentiviruses (Heeney et al., 2006). Amino acid substitutions in these proteins can be studied using Asian (rhesus or pig-tailed) macaques infected with either SIV or SHIV to study disease progression, test anti-retroviral therapy, and possible vaccine strategies (Ambrose et al., 2007). While these models have provided us with insight into the role of these genes in pathogenesis, they also have short comings such as: 1) the diversity of viral protein sequences between different primate lentiviral lineages; 2) the evaluation of viral proteins in replication or as antiviral targets *in vivo*; 3) the testing of vaccine epitopes only identified in HIV-1; and 4) anti-retroviral drug efficacy and efficiency (Thippeshappa et al., 2011). Our laboratory has studied the role of HIV-1 Vpu and its various domains in $CD4^+$ T cell loss, virus release, and pathogenesis in macaques using the chimeric SHIVs: $SHIV_{KU\text{-}1bMC33}$ and

$SHIV_{KU-2MC4}$ (Stephens et al., 2002; Singh et al., 2003; Hout et al., 2005; 2006; Hill et al., 2008).

Highly Conserved Domains in the C-Terminus of Primate Lentivirus Vif Proteins

Cellular proteins termed restriction factors have been identified and found to function in preventing the spread of retroviruses and endogenous mobile genetic elements (Goff et al., 2004; Malim et al., 2008; Albin et al., 2010). As a consequence, many retroviruses have evolved mechanisms to counter this restriction. The HIV-1 accessory protein Vif is required for lentivirus infectivity of specific cell types (except EIAV); therefore, HIV-1 virions deficient in the Vif protein cannot sustain a productive infection in either primary $CD4^+$ T cells, macrophages, and many established $CD4^+$ T cell lines (H9, C8166, CEMx174) (Gabuzda et al., 1992; Madani et al., 1998; Simon et al., 1998; Sova et al., 1993). These nonpermissive cells express an antiviral restriction factor known as APOBEC3G (A3G) (Sheehy et al., 2002). Vif binds APOBEC3 through non-linear binding sites in the N-terminus. Following the Vif-APOBEC3G interaction, Vif recruits the E3 ubiquitin ligase complex, which consists of elongin B (EloB), elongin C (EloC), Cullin-5 (Cul5), and Rbx-1 (Kao et al., 2003; Mehle et al., 2004a; 2006; Yu et al., 2003). This complex induces polyubiquitination of APOBEC3G and subsequent degradation by the 26S proteosome (Conticello et al., 2009; Marin et al., 2003; Mehle et al., 2004; Sheehy et al., 2003; Stopak et al., 2003; Yu et al., 2004). There are two highly conserved domains near the carboxy-terminus of Vif that have been implicated in the recruitment of the Cul5-E3 ubiquitin ligase machinery. One of the domains identified is

the SLQ(Y/F)LA motif, which was shown to mediate the binding of Vif to EloC (Mehle et al., 2004b; Yu et al., 2003; Yu et al., 2004). Therefore, one of the goals of this dissertation was to study highly conserved domains of primate lentivirus Vif *in vivo,* and determine their roles in pathogenicity.

Previous *in vitro* research has shown that mutation of the serine, leucine, and glutamine prevent the association of Elongin BC complex subsequently disruption of the proteasomal targeting and degradation of the A3 proteins resulting in a non-productive infection (Fang et al., 2007; Mehle et al., 2004; Yu et al., 2003; Yu et al., 2004). Mutations in this motif have also been shown to increase A3 incorporation into virions resulting G-to-A hypermutation (Kobayashi et al., 2005). The importance of the SLQ(Y/F)LA domain of Vif in its interaction with the Elongin BC complex in viral pathogenesis is essential to understanding the specific motifs required for the degradation of A3 proteins. This data can potentially assist in the development of small molecule inhibitors or attenuated *vif* vaccines targeting both conserved and functional domains of Vif that limit viral replication and increase the host immune response. Therefore, the first study focused on determining if specific mutations in the SLQYLA motif of $SIV_{mac}239$ Vif were critical for viral pathogenesis in rhesus macaques.

We mutated two residues of the highly conserved SLQYLA motif in SHIV, which expresses a $SIV_{mac}239$ Vif. The serine at amino acid position 147 and the leucine at amino acid position 148 were mutated to alanine residues resulting in a virus called $SHIV_{VifAAQYLA,}$ which was used to inoculate three rhesus macaques. These macaques developed no significant loss in circulating CD4+ T cells, displayed 100-fold lower viral

loads, no histological lesions, and fewer visceral tissues positive for viral *gag* DNA or RNA in two of the three macaques, when compared to macaques inoculated with $SHIV_{KU\text{-}1bMC33}$. In two of the three macaques (RAK10 and RCS10), specific tissues such as the mesenteric, axillary, and inguinal lymph nodes, tonsil, and thymus, were positive for both viral RNA and DNA. The presence of viral RNA suggests that these macaques have active viral replication in the primary and secondary lymphoid organs and that the virus may have persisted in these tissue populations. Recently, Refsland and colleagues published studies regarding the profiling of the *A3* mRNA repertoire in human lymphocytes and tissues using quantitative PCR methods (Refsland et al., 2010). From their studies they profiled the expression of *A3* mRNA in twenty tissues such as adipose, bladder, brain, cervix, colon, esophagus, heart, kidney, liver, lung, ovary, placenta, prostate, skeletal muscle, small intestine, spleen, testes, thymus, thyroid, and the trachea. Interestingly, the lung, adipose, spleen, bladder, thymus, heart, and cervix were among the tissues that showed a broad expression of *A3* mRNA (Refsland et al., 2010). Previously, our laboratory used immunohistochemical analysis to determined whether A3G was expressed in the brain and kidney. It was found that A3G expression in brain was limited to the pyramidal neurons in the gray matter of the cerebral and cerebellar cortices and restricted to the proximal convoluted tubules of kidney in the pig-tailed macaque (Hill et al., 2006; 2007). However, since we are using the rhesus macaque as a model of SHIV infection, both the visceral tissues and specific regions of the brain need to be identified for the expression of rhesus *A3A/B/C/D/F/G/H* mRNA. No studies to date have examined this, and experimentally it would allow laboratories using

the rhesus macaque as a nonhuman primate to study the restricted replication patterns or identify reservoirs of *vif* attenuated SHIV replication. The replication of virus in specific tissues may be explained by the expression patterns of *A3* mRNA in those tissues.

In HIV-1 Vif deficient viruses, A3 proteins are incorporated into the virion, which are effectively introduced into the target cell upon the next round of infection (Soros et al., 2007). The A3 proteins can then mediate extensive dC to dU mutations of the minus-strand of viral DNA during reverse transcription (Suspene et al., 2004; Yu et al., 2004). These mutated reverse transcripts can then be destroyed either by the DNA base repair enzymes such as uracil DNA glycosylase or apurinic-apyrimidinic endonuclease or survive to serve as a template for plus-strand synthesis resulting in the accumulation of G-to-A substitutions (Harris et al., 2003; Mangeat et al., 2003). If these G-to-A substitutions (plus strand) exceed 10% of all of the viral dG residues, this is referred to a "hypermutation" of the viral genome (Harris et al., 2003; Lecossier et al., 2003; Mangeat et al., 2003; Zhang et al., 2003). These mutations can result in alteration of viral open reading frames, decreased tRNALys3 primer annealing to the primer binding site on the genomic RNA, and mutation of essential viral genes required for a productive HIV-1 infection (Harris et al., 2003; Lecossier et al., 2003; Mangeat et al., 2003; Suspene et al., 2004; Yu et al., 2004; Zhang et al., 2003). Often the G-to-A mutations (plus strand) occur within highly polarized mutational gradients in the viral genome from 5' to 3' due to the time that these regions of the minus-strand of DNA remain single-stranded (Suspene et al., 2006; Yu et al., 2004). Our sequencing results of the thymus, mesenteric, axilary,

and inguinal lymph nodes of macaques inoculated with $SHIV_{VifAAQYLA}$ indicated that a definite 5' to 3' (minus strand) gradient of G-to-A substitutions occurred in the viral genome. The *vif, vpu, nef,* and *env* genes were sequenced and assessed in these tissues resulting in an overall gradient in two of the three macaques analyzed, *nef>env>vpu>vif*. The exception to this gradient was macaque RPL10 who displayed an overall high number of G-to-A (plus strand) transitions in all four genes. Over 85% of these mutations were in the dinucleotide sequence context of 5'-TC, we concluded that an A3 protein besides A3G was involved in the cytidine deamination mutational patterns observed. It is important to note that not all lymphoid tissues showed G-to-A substitutions above background levels. Since A3F, A3D, A3B, A3C, and A3H can display this mutational pattern, it is hard to decipher if one or many of these A3 proteins were involved in the cytidine deamination. Therefore, tissue specific expression patterns of various *A3* mRNA would help us further determine which of those four tissues we analyzed expressed higher levels of one A3 protein over another. Recently, we discovered the A3A protein in the rhesus macaque and looked at an expression panel of *rhA3* mRNA in Staphylococcal Enterotoxin B (SEB) activated $CD4^+$ T cells. Using quantitative real-time RT-PCR, the expression level of *A3A, A3C,* and *A3H* relative to *A3G* were 1.0-1.5-fold similar in magnitude, while *A3F* and *A3D* were expressed on average 2.4- and 13.6-fold lower in magnitude than *A3G*, respectively. Therefore, one of these three A3 proteins (A3A, A3C, A3G, or A3H) is most likely causing cytidine deamination in the viral DNA with a dinucleotide context of 5'-TC (minus strand).

Interestingly, when assessing sequences from $SHIV_{VifAAQYLA}$-inoculated macaque PBMC DNA at weeks 1, 3, 4, 8, 12, and 28 weeks post-inoculation, two of the three macaques (RPL10 and RAK10) displayed a G-to-A mutation at four weeks. This mutation resulted in the mutation of the site-directed alanine at amino acid position 147 to a threonine in the ^{147}AAQYLA^{152} (to ^{147}TAQYLA^{152}) motif of Vif. The mutation of amino acid residue 147 demonstrates that not all G-to-A substitutions are detrimental to the viral genome. While we do not know why RAK10 and RPL10 selected for this mutation or how pathogenicity of the virus is affected, we do know that it did not alter viral burdens or levels of circulating CD4+ T cells in these macaques beyond four weeks post-inoculation. One possible theory could be that the A147T mutation could have permitted a more productive SHIV infection in these macaques resulting in a better antigenic stimulus. Macaques RAK10 and RPL10 both had higher viral burders and developed immunoprecipitating antibodies similar to the positive control; whereas, macaque RCS10 retained the A147A mutation, had lower viral burdens, and significantly less immunoprecipitating antibodies. More research is needed to assess the replication fitness, pathogenicity, and structural/mechanistic implications of the A147T mutation selected from these rhesus macaques.

To extend our *in vivo* studies and further cripple the $SHIV_{VifAAQYLA}$ mutant, we constructed a SHIV mutant that expresses a Vif protein with the first five amino acids of the SLQYLA substituted for alanine residues ($SHIV_{Vif5A}$). *In vitro* $SHIV_{Vif5A}$ in the presence of rhesus A3G was readily incorporated into virions, displayed a 1,000-fold decrease in viral infectivity, revealed a high frequency of G-to-A substitutions in the

dinucleotide context of 5'-TC (minus strand) in the *nef* gene. Macaque inoculated with $SHIV_{Vif5A}$ displayed a further reduction in plasma viral loads compared to the $SHIV_{VifAAQYLA}$ inoculated macaques. The initial burst of replication occurred at one-week post-inoculation and occasionally detected in the plasma thoughtout the duration of infection, but maintained levels of circulating $CD4^+$ T cells at pre-inoculation levels. However, sequences were obtained from PBMC only during the first three weeks of infection. At necropsy, the viral RNA copy number in the visceral and central nervous system tissues could not be quantified due to the limit of detection for this assay being ~100 copies. Since we were unable to sequence the *nef* gene in the PBMC through out the course of infection or at necropsy, we were unable to assess the number of G-to-A substitutions in the viral genome. Also, these macaques produced immunoprecipitating antibodies by 12 weeks post-inoculation that waned by necropsy. Since viral RNA was not detected in the visceral tissues of macaques inoculated with $SHIV_{Vif5A}$ at necropsy, the infectious virus could have been readily cleared by the macaque, and viral proteins may not have been produced to provide an antigenic stimulus for an increased immune response against the infection. We were unable to detect any viral loads in the visceral organs or the CNS tissue in macaques inoculated with $SHIV_{Vif5A}$. These results could be due to $SHIV_{Vif5A}$ replicating initially in cell types that express a wide range of APOBEC3 proteins that were incorporated into the virion and exerted an antiviral affect on the next target cell. During the next round of replication, the viral genome could have been highly mutated with G-to-A substitutions, and the RNA polyermase II could not transcribe the viral RNA efficiently. Also, there may have been tissue or cellular reservoirs where

APOBEC3 proteins are not expressed and there is no restriction on the replication of $SHIV_{Vif5A}$. As described above, further studies will be needed to determine if cell populations exist that do or do not express APOBEC3 proteins. These results show that primate lentiviruses expressing a Vif protein with targeted mutations in a highly conserved domain (SLQ(Y/F)LA) can be controlled by the host, are more detrimental to the virus *in vivo*, and that this domain is critical to Vif function *in vivo*.

In addition, another highly conserved motif is the zinc-binding motif H-X_5-C-X_{17-18}C-X_{3-5}-H (HCCH) motif, which has been shown to interact with Cul5 (Luo et al., 2005; Mehle et al., 2004; Yu et al., 2004). Previous tissue culture studies showed that mutation of the two cysteine residues or chelation of zinc inhibited proper folding of HIV-1 Vif and prevented the recruitment of Cul5 resulting in the inability of Vif to recruit the E3 ubiquitin ligase complex (Mehle et al., 2006; Paul et al., 2006; Xiao et al, 2006; 2007a; 2007b). For this study, we constructed a SHIV where four amino acids in the HCCH motif of the Vif protein were mutated to alanine residues, resulting in the virus $SHIV_{VifHCCH(-)}$. *In vitro* $SHIV_{VifHCCH(-)}$ in the presence of rhesus A3G, readily incorporated rhA3G, showed a 100-fold decrease in viral titer, and displayed an increase in the number of G-to-A substitutions in the *nef* gene in the context of 5'-TC and not 5'-CC (minus strand). Macaques inoculated with $SHIV_{VifHCCH(-)}$ showed slightly higher viral loads than $SHIV_{Vif5A}$ at one week post-inoculation. However, by three weeks post-inoculation, the virus was effectively controlled by the macaque with bursts of replication at weeks 6, 20 and 24. These bursts of replication correlated with G-to-A substitutions in the dinucleotide context of 5'TC (minus strand) that we observed in the *vif* gene amplified

from PBMC DNA. Immunoprecipitating antibodies were detected at 12 weeks post-inoculation, and were non-existent by necropsy. We also assessed the distribution of viral loads in the visceral tissues of macaques inoculated with $SHIV_{VifHCCH(-)}$ relative to $SHIV_{KU-2MC4}$. We found that there was a significant decrease in viral loads of macaques infected with $SHIV_{VifHCCH(-)}$, when compared to macaques inoculated with $SHIV_{KU-2MC4}$, suggesting that $SHIV_{VifHCCH(-)}$ infection is significantly less widespread. As described above, these results suggest that $SHIV_{VifHCCH(-)}$ may replicate in the macaque in a cell type-specific manner depending on APOBEC3 expression. Also, the viral RNA detected in visceral tissues of macaques inoculated with $SHIV_{VifHCCH(-)}$ at necropsy may not have been translated into viral proteins due to excessive G-to-A mutation; therefore, the infection may have been cleared by the macaque because no antigenic stimulation through viral proteins could occur. Also, due to hypermutation viral quasipecies may exist allowing for the co-existence of functional, deleted, or truncated *vif* genes which can determine the degree of viral attenuation depending on the site and extension of the deletion (Rangel et al., 2009).

Using lentiviruses as a live attenuated vaccine candidate has been involved in the removal of “non-essential” viral genes such as *vpr, vpx, nef,* or *vpu*, which results in low levels of viral replication, the accumulation of compensatory mutations in other genes, and/or recombination or reversion to a more pathogenic phenotype. These live attenuated virus vaccines are usually based on non-virulent cloned viral variants or clones engineered with deletions in accessory genes (Abel et al., 2003; Almond and Scott, 1999; Daniel et al., 1992; Lohman et al., 1994). Following vaccination, challenge

with pathogenic SIV or SHIV should protect the host by suppressing the challenge viral loads, increasing the survival of the host, and preservation of the CD4+ T cell population. The live attenuated vaccine approach is not always successful in protecting against SIV and the length of time between vaccination and challenge seems to be a variable that influences efficacy; however, many of the factors required to determine the protective efficacy have not yet been identified (Clements et al., 1995; Marthas et al., 1990; Wyand et al., 1996). While the immune correlates for HIV-1 infection are still unknown, a vaccine needs to ensure relative safety and induce a potent protective immune response in the host (Wyand et al., 1996). Vaccines consisting of the deletion or inactivation of one or more viral genes on HIV-1 or SIV seem to be the most effective (Koff et al., 2006).

Macaque studies examining *vif*-deleted lentiviruses are limited, but all of the studies thus far have shown that Vif is required for viral replication *in vivo* (Desrosiers et al., 1998; Gabuzda et al., 1994; Harmache et al., 1996; Inoshima et al., 1996; Kristbjornsdottir et al., 2004; Lockridege et al., 1999; Sparger et al., 2008). In a previous study the roles of various accessory proteins of $SIV_{mac}239$, including the *vif* gene, were assessed. Rhesus macaques inoculated with $SIV_{mac}239\Delta$*vif* maintained low viral loads, did not show any viral DNA in PBMC at weeks 2 or 16, and did not produce antibodies to SIV viral proteins such as *vpx* or *vpr* (Desrosiers et al., 1998). In a second study, investigators showed that a *vif*-deleted proviral DNA vaccine inoculated into rhesus macaques was immunogenic displaying a virus-specific T cell proliferative response even though the virus was severely attenuated. Even though the virus was administered as a booster at 6 and 22 weeks post-inoculation, the vaccine was not protective against

challenge with $SIV_{mac}251$ (Sparger et al., 2008). Our studies showed that both $SHIV_{VifHCCH(-)}$ and $SHIV_{Vif5A}$ were effectively controlled by rhesus macaques during the primary phase of infection. This suggests that viruses containing mutations in the conserved domains of *vif* may be useful to create a vaccine candidate for HIV-1. Since these macaques were singly inoculated with each virus and developed an immunoprecipitating antibody response at 12 weeks post-inoculation, it would be of interest to determine if multiple inoculations would result in a stronger immune response that could protect against challenge with a pathogenic SHIV. Since the Vif protein is required for replication of HIV-1 (SHIV/SIV) in CD4+ T cells and macrophages, mutations targeted in conserved motifs of Vif could permit limited replication and effective immune responses (both humoral and cell mediated) thus representing a novel means of producing a live attenuated lentivirus vaccine candidate. Furthermore, more research is required to determine if mutations in other conserved motifs in Vif my permit more replication to improve immune responses prior to being controlled by the host, and whether they would protect against challenge with pathogenic virus. For instance, while the C-terminal region of Vif has been studied in this dissertation, the N-terminal region of Vif has not been assessed *in vivo* (Figure 13). The N-terminal region of HIV-1 consists of various non-linear binding sites for A3 proteins. Since there is only 50% amino acid homology between HIV-1 SIVmac239, it would be of interest to determine the amino acids in $SIV_{mac}239$ that are responsible for binding A3 proteins. It is important to functionally understand and identify these domains to determine if they are highly conserved, like “SLIK” or “YxxL.” This would provide more conserved binding sites in Vif

that could be used as attenuated viruses to boost the host immune response and protect against challenge.

Identification of Rhesus APOBEC3A

Human APOBEC3 (hA3) genes are a large family of tissue specific cytidine deaminases that are tandemly arrayed on chromosome 22 (Jarmuz et al., 2002). Human A3B, A3C, A3D, A3G, and A3F have been shown to inhibit the replication of HIV-1Δ*vif* and SIV_{mac}239Δ*vif* to various extents (Dang et al., 2006; 2008; Doehle et al., 2005; Mariani et al., 2003; Wiegand et al., 2004; Yang et al., 2007; Yu et al., 2004b; Zennou and Bieniasz, 2006; Zheng et al., 2004). While hA3A lacks antiviral activity against HIV-1 and HIV-1Δ*vif*, it inhibits the replication of adeno-associated virus 2 (AAV2), intracisternal A particles (IAP), long interspersed nuclear element 1 (LINE-1, L1), and *Alu*, through deaminase-independent mechanisms (Bogerd et al., 2006a; 2006b; Chen et al., 2006; Goila-Gaur et al., 2007; Muckenfuss et al., 2006). Even though hA3A lacks antiviral activity, it is still readily incorporated into the virions in the absence of the viral nucleoprotein complex (NPC) in the presence of a functional Vif. Human A3A contains significant homology to the C-terminal region of hA3G. Therefore, when the N-terminal half of hA3G was fused to hA3A, the A3G-A3A chimera was effectively packaged into only HIV-1Δ*vif* virions by associating with the NPC, showed cytoplasmic localization similar to hA3G, and exhibited a strong antiviral activity against HIV-1Δ*vif* (Goila-Gaur et al., 2007).

While hA3A has been extensively studied, no rhesus A3A (rhA3A) counterpart had been cloned from the rhesus macaque, suggesting that rhA3A may have been deleted in the rhesus macaque genome (OhAinle et al., 2008; Virgen and Hatziioannou, 2007). However, a recent publication showed that human *A3A* contains orthologs in eleven different non-human primate species such as owl and African green monkeys (Bulliard et al., 2011). Therefore, we were interested in the isolating and characterizing the antiviral activities of rhesus A3A against HIV-1 and $SIV_{mac}239$ Vif. Based on the rhesus macaque genome sequence, we were able to clone rhesus A3A and determine that this gene is tandemly arrayed with the other six rhesus A3 genes on chromosome 10 in the rhesus macaque. We determined that the *rhA3A* cloned amplicon revealed 82% nucleotide sequence identity with *hA3A*, and that the rhesus sequence together with Asian macaques ("Old World" monkeys) contained a primate lineage-specific insertion at amino acid positions 27 to 30 in *A3A* genes. We further classified the *rhA3A* gene in a phylogenetic analysis determining that the rhesus macaque and human *A3A* genes are orthologous.

We found that rhesus A3A is widely expressed in both the visceral and central nervous system tissues of the rhesus macaque, is expressed at high levels in Staphylococcal Enterotoxin B (SEB) activated $CD4^+$ T cells from three donor macaques, and degraded in the presence of both HIV-1 and $SIV_{mac}239$ genomes. While it is thought that localization can partially explain the differences in antiviral activity against retroviruses and retrotransposons, this was not the case (Bogerd et al., 2006a; 2006b; Chen et al., 2006; Goila-Gaur et al., 2007; Muckenfuss et al., 2006). In our study, rhA3A

displayed nucleocytoplasmic localization similar to hA3A. However, previous reports suggest that hA3A can inhibit AAV-2, IAP, L1, and *Alu*. In our studies rhA3A did not restrict the replication of AAV-2 or L1 retrotransposition (Bogerd et al., 2006a; 2006b; Chen et al., 2006; Goila-Gaur et al., 2007; Muckenfuss et al., 2006).

Recent research by Stenglein and colleagues suggests that hA3A *in vitro* can inhibit the expression of transfected plasmid DNA through deaminase-dependent mechanisms, while genomic DNA is not affected. These authors suggest that foreign DNA restriction is a conserved innate immune defense mechanism predominantly in monocytes, macrophages, and neutrophils (Stenglein et al., 2010; 25, 29). Therefore, genetic engineering, gene therapy, and DNA vaccines may be influenced by this foreign DNA defense mechanism effecting the efficiency and fidelity of these treatments (Stenglein et al., 2010). However, our studies using an eGFP expression plasmid or full-length viral molecular clones co-transfected with either hA3A or rhA3A did not show significant differences at 48 hours (the length of most of our tissue culture experiments). Human A3A had minimal impact (<20%), while rhA3A did not have an impact on either reporter gene expression or full-length viral DNA molecular clone. Also, when we examined the release of virus from these cells, rhA3A and hA3A had no post-entry restriction activity against SHIV or HIV-1. Therefore, our studies should have minimal impact on plasmid DNA stability throughout the duration of our experiments. Also, the DNA restriction properties of hA3A may be a recent evolutionary development in the hominid lineage.

Similar to rhA3G, rhA3A was a potent inhibitor of SHIVΔ*vif* by reducing the levels of infectious virus by 20-fold. Interestingly, we also found that hA3A effectively inhibited SHIVΔ*vif* to a lesser extent by reducing the levels of infectious virus by 10-fold. Unlike SHIVΔ*vif*, rhA3A only reduced the infectivity of HIV-1Δ*vif* by 3-fold. Therefore, for the first time we were able to show an evolutionary switch in the antiviral activities of primate A3A by showing that rhA3A can inhibit lentiviral replication. Previous research suggests that virion incorporation of A3 proteins is necessary for A3 to exhibit its antiviral deamination-dependent effects on HIV-1 in the next target cell (Gladdis et al., 2003; Sheehy et al., 2002; Suspene et al., 2004). However, we were only able to detect small amounts of rhA3A incorporation into SHIV virions and unable to detect its incorporation into HIV-1 virions. Also, even though hA3A inhibited SHIVΔ*vif*, hA3A was not detected in SHIV virions. This may be due to the sensitivity our virion incorporation technique suggesting that small amounts of rhA3A or hA3A are incorporated into SHIV virions. Using *in vitro* hypermutation assays, we were able to observe G-to-A (plus strand) substitutions in *nef* of SHIVΔ*vif* in the presence of rhA3A. However, the frequency of G-to-A substitutions observed with rhA3A was significantly less (a 5-fold decrease) than the G-to-A substitutions observed with rhA3G. Therefore, rhA3A may be potently restricting SHIVΔ*vif* through both deaminase-dependent and deaminase-independent mechanisms.

Since the hominid and monkey A3A's are distinguished by a three amino acid indel (insertion and/or deletion) between residues 27 to 29 (SVR), we sought to determine if this region is necessary for the differential antiviral activity of hA3A and

rhA3A. When the “SVR” amino acids were removed from rhA3A, SHIVΔ*vif* and HIV-1Δ*vif* were no longer restricted by rhA3AΔSVR but still remained sensitive to SHIV and HIV-1 Vif-mediated degradation. However, when the “SVR” amino acids were inserted into hA3A, hA3A+SVR gained partial activity against HIV-1Δ*vif*. This demonstrates that these amino acid residues are critical for rhA3A lentiviral inhibition, but they may have been functionally lost during the evolutionary split between humans and monkeys. A recent publication by Bulliard and colleagues modeled the structure of hA3A based upon the known crystal structure of the hA3G C-terminus (Holden et al., 2008; Shandilya et al., 2010). This analysis found that the hA3A structure tightly correlates with loop 1 of the predicted DNA docking/editing groove (polynucleotide-accommodating groove) in the C-terminus of hA3G. Based upon their work, the “SVR” amino acids point towards the protein core providing stabilization to rhA3A and form a groove that accommodate a single-stranded DNA molecule for cytidine deamination (Bulliard et al., 2010).

Previous research has determined that hA3A inhibits the replication of AAV-2, autonomously replicating parvoviruses, intracisternal A particles (IAP), long interspersed nuclear element 1 (LINE-1, L1), and *Alu*, through deaminase-independent mechanisms (Bogerd et al., 2006a; 2006b; Chen et al., 2006; Goila-Gaur et al., 2007; Muckenfuss et al., 2006). As previously reported, we found that hA3A can inhibit AAV-2, while rhA3G cannot (Chen et al., 2006; Narvaiza et al., 2009). However, we showed that rhA3A was unable to restrict the replication of AAV-2 and LINE-1 elements. This necessity may not be required as no infectious AAVs have been isolated from rhesus macaques.

Based on of these results, further studies are needed to examine the restriction patterns of primate A3A genes from both a structural and evolutionary perspective. Therefore, experiments designed to determine why hA3A does not restrict HIV-1Δ*vif* and why rhA3A potently restricts of SHIVΔ*vif* and to a lesser extent HIV-1Δ*vif* are necessary. Using the C-terminal crystal structure of hA3G and determining a molecular model obtained using the interactive SWISS-MODEL program of both hA3A and rhA3A, we will be able to identify residues near the polynucleotide binding groove or residues that are solvent exposed, suggesting that they may have the ability to interact with single-stranded DNA (Figure 53) (Bulliard et al., 2010; Holden et al., 2008; Shandilya et al., 2010). In order to study this we would need to construct chimeric domain swapping protein mutants, this will allow us to examine which changes in molecular determinants of nucleic acid specificity of A3A proteins dictates the antiviral activity of A3A against lentiviruses or the restriction of AAV-2 replication and LINE-1 retrotransposition. These domain-swapping proteins would be constructed as follows: AC-Loop1 (accommodating loop 1; D35G, L26I, S27, V28, R29, Q33K), AC-Loop 2, AC-Loop 3 (C59H, K61Q, V64L, P66I, D69F, C72R, V74A), AC-Loop 5 (R106S, R107W), and α-helix 4 (Q140K, R144Q, T145M) (Bulliard et al., 2010; Holden et al., 2008; Shandilya et al., 2010). The AC-Loop 1 is thought to have proximity to the active center and bind the target DNA for deamination, while α-helix 4 may be important for A3A specificity and polynucleotide binding. These studies will allow us to understand the structural basis involved in restriction of lentivirus and parvovirus replication as well as the inhibition of LINE-1 retrotransposition. Also, determining if the biological properties of the restriction by A3A

proteins from Old World and New World monkeys would be interesting. This is because New World macaques have not been evolutionarily driven by SIV like Old World macaques. Looking at these A3A proteins would help us deterimine the potential driving forces for A3A evolution. For example, sequence analysis shows that A3A proteins from various Old World monkeys contain variable amino acids in the "SVR" motif. Therefore, it would be interesting to see if other mutations from various Old World monkeys would still inhibit lentiviral replication.

Viral protein X (Vpx) is uniquely encoded by HIV-2 and SIV (SIV_{mac}/SIV_{sm}) and has been found to bind hA3A to counteract its antiviral effects (Berger et al., 2010; Horton et al., 1994; Wolfrun et al., 2007). Vpx is required for the infection of human monocytes and monocyte-derived cells such as macrophages and dendritic cells *in vitro* but dispensable for the infection of primary lymphocytes and cell lines (Berger et al., 2010; Cheng et al., 2008; Fletcher et al., 1996; Sharova et al., 2008; Wolfrum et al., 2007). SIV_{mac} Vpx partially binds hA3A and decreases its steady-state levels within the cell through degradation during the early phase of myeloid cell infection allowing for the replication of SIV_{mac}. A single-point mutation in SIV_{mac} Vpx, H82A, prevents binding hA3A allowing hA3A to abrogate the infection of monocytes (Berger et al., 2010; Berger et al., 2011). Therefore, it would be interesting to design experiments to determine if SIV_{mac} Vpx binds rhesus A3A allowing rhA3A to abrogate the infection of monocytes. With the domain swap mutant proteins described above, we could determine which domains of human and rhesus A3A are required for this interaction. This could reveal

another novel role for rhA3A by inhibiting lentiviral replication and shed light on the importance of myeloid cells during primate lentiviral pathogenesis.

Figure 53: Structural differences between human and rhesus A3A. Panel A. The predicted human A3A structure based off of the x-ray crystal structure of the C-terminal half of human A3G (Bulliard et al., 2010; Holden et al., 2008). Panel B. The predicted structure of rhesus A3A based on the SWISS-MODEL program and the x-ray crystal structure of the C-terminal half of human A3G (Dr. Xiaojiang Chen, University of Southern California).

A.

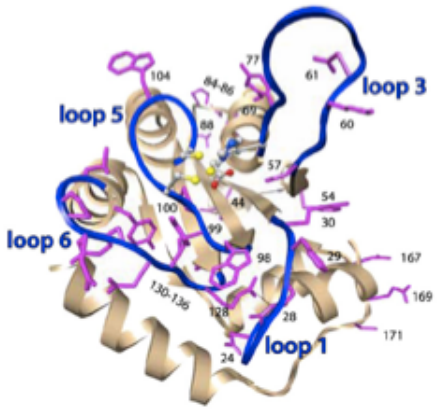
loop 5
loop 3
loop 6
loop 1
104
84-86
77
61
88
60
57
54
100
44
30
99
98
29
167
169
130-136
128
28
171
24

B.

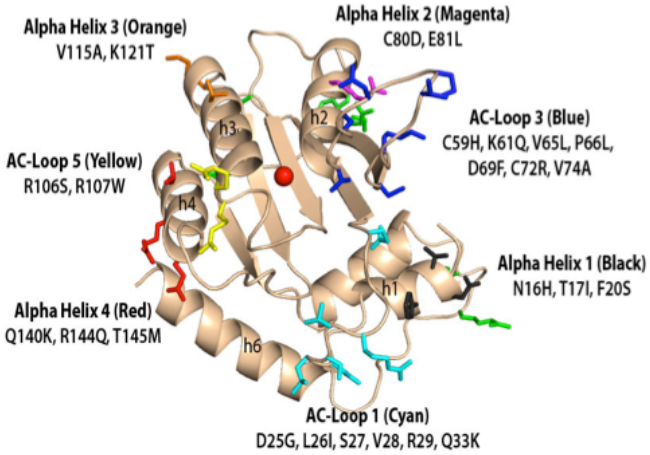
Alpha Helix 3 (Orange)
V115A, K121T
Alpha Helix 2 (Magenta)
C80D, E81L
AC-Loop 3 (Blue)
C59H, K61Q, V65L, P66L,
D69F, C72R, V74A
AC-Loop 5 (Yellow)
R106S, R107W
Alpha Helix 1 (Black)
N16H, T17I, F20S
Alpha Helix 4 (Red)
Q140K, R144Q, T145M
AC-Loop 1 (Cyan)
D25G, L26I, S27, V28, R29, Q33K
h1
h2
h3
h4
h6

X. References

1 Abe, H. *et al.* Effects of structural variations of APOBEC3A and APOBEC3B genes in chronic hepatitis B virus infection. *Hepatology research : the official journal of the Japan Society of Hepatology* **39**, 1159-1168, doi:10.1111/j.1872-034X.2009.00566.x (2009).

2 Abel, K. *et al.* Simian-human immunodeficiency virus SHIV89.6-induced protection against intravaginal challenge with pathogenic SIVmac239 is independent of the route of immunization and is associated with a combination of cytotoxic T-lymphocyte and alpha interferon responses. *Journal of virology* **77**, 3099-3118 (2003).

3 Accola, M. A., Bukovsky, A. A., Jones, M. S. & Gottlinger, H. G. A conserved dileucine-containing motif in p6(gag) governs the particle association of Vpx and Vpr of simian immunodeficiency viruses SIV(mac) and SIV(agm). *Journal of virology* **73**, 9992-9999 (1999).

4 Adessi, C. & Soto, C. Converting a peptide into a drug: strategies to improve stability and bioavailability. *Current medicinal chemistry* **9**, 963-978 (2002).

5 Advani, A. *et al.* Role of VEGF in maintaining renal structure and function under normotensive and hypertensive conditions. *Proceedings of the National Academy of Sciences of the United States of America* **104**, 14448-14453, doi:10.1073/pnas.0703577104 (2007).

6 Agopian, K., Wei, B. L., Garcia, J. V. & Gabuzda, D. A hydrophobic binding surface on the human immunodeficiency virus type 1 Nef core is critical for association with p21-activated kinase 2. *Journal of virology* **80**, 3050-3061, doi:10.1128/JVI.80.6.3050-3061.2006 (2006).

7 Aguiar, R. S., Lovsin, N., Tanuri, A. & Peterlin, B. M. Vpr.A3A chimera inhibits HIV replication. *The Journal of biological chemistry* **283**, 2518-2525, doi:10.1074/jbc.M706436200 (2008).

8 Aiken, C. Pseudotyping human immunodeficiency virus type 1 (HIV-1) by the glycoprotein of vesicular stomatitis virus targets HIV-1 entry to an endocytic pathway and suppresses both the requirement for Nef and the sensitivity to cyclosporin A. *Journal of virology* **71**, 5871-5877 (1997).

9 Aiken, C., Krause, L., Chen, Y. L. & Trono, D. Mutational analysis of HIV-1 Nef: identification of two mutants that are temperature-sensitive for CD4 downregulation. *Virology* **217**, 293-300, doi:10.1006/viro.1996.0116 (1996).

10 Albin, J. S. & Harris, R. S. Interactions of host APOBEC3 restriction factors with HIV-1 in vivo: implications for therapeutics. *Expert reviews in molecular medicine* **12**, e4, doi:10.1017/S1462399409001343 (2010).

11 Almond, N. & Stott, J. Live attenuated SIV--a model of a vaccine for AIDS. *Immunology letters* **66**, 167-170 (1999).

12 Ambrose, Z., KewalRamani, V. N., Bieniasz, P. D. & Hatziioannou, T. HIV/AIDS: in search of an animal model. *Trends in biotechnology* **25**, 333-337, doi:10.1016/j.tibtech.2007.05.004 (2007).

13 Ammosova, T. *et al.* Phosphorylation of HIV-1 Tat by CDK2 in HIV-1 transcription. *Retrovirology* **3**, 78, doi:10.1186/1742-4690-3-78 (2006).

14 Anderson, J. L. *et al.* Proteasome inhibition reveals that a functional preintegration complex intermediate can be generated during restriction by diverse TRIM5 proteins.

Journal of virology **80**, 9754-9760, doi:10.1128/JVI.01052-06 (2006).

15 Anderson, S. J., Lenburg, M., Landau, N. R. & Garcia, J. V. The cytoplasmic domain of CD4 is sufficient for its down-regulation from the cell surface by human immunodeficiency virus type 1 Nef. *Journal of virology* **68**, 3092-3101 (1994).

16 Andersson, S. *et al.* Plasma viral load in HIV-1 and HIV-2 singly and dually infected individuals in Guinea-Bissau, West Africa: significantly lower plasma virus set point in HIV-2 infection than in HIV-1 infection. *Archives of internal medicine* **160**, 3286-3293 (2000).

17 Andersson, S., Norrgren, H., Dias, F., Biberfeld, G. & Albert, J. Molecular characterization of human immunodeficiency virus (HIV)-1 and -2 in individuals from guinea-bissau with single or dual infections: predominance of a distinct HIV-1 subtype A/G recombinant in West Africa. *Virology* **262**, 312-320, doi:10.1006/viro.1999.9867 (1999).

18 Andrew, A. J., Miyagi, E., Kao, S. & Strebel, K. The formation of cysteine-linked dimers of BST-2/tetherin is important for inhibition of HIV-1 virus release but not for sensitivity to Vpu. *Retrovirology* **6**, 80, doi:10.1186/1742-4690-6-80 (2009).

19 Angers, S. *et al.* Molecular architecture and assembly of the DDB1-CUL4A ubiquitin ligase machinery. *Nature* **443**, 590-593, doi:10.1038/nature05175 (2006).

20 Antinori, A. *et al.* Updated research nosology for HIV-associated neurocognitive disorders. *Neurology* **69**, 1789-1799, doi:10.1212/01.WNL.0000287431.88658.8b (2007).

21 Arens, M. *et al.* Alterations in spliced and unspliced HIV-1-specific RNA detection in

peripheral blood mononuclear cells of individuals with varying CD4-positive lymphocyte counts. *AIDS research and human retroviruses* **9**, 1257-1263 (1993).

22 Arold, S. T. & Baur, A. S. Dynamic Nef and Nef dynamics: how structure could explain the complex activities of this small HIV protein. *Trends in biochemical sciences* **26**, 356-363 (2001).

23 Arora, V. K. *et al.* Lentivirus Nef specifically activates Pak2. *Journal of virology* **74**, 11081-11087 (2000).

24 Atkins, K. M. *et al.* HIV-1 Nef binds PACS-2 to assemble a multikinase cascade that triggers major histocompatibility complex class I (MHC-I) down-regulation: analysis using short interfering RNA and knock-out mice. *The Journal of biological chemistry* **283**, 11772-11784, doi:10.1074/jbc.M707572200 (2008).

25 Ayouba, A. *et al.* HIV-1 group O infection in Cameroon, 1986 to 1998. *Emerging infectious diseases* **7**, 466-467 (2001).

26 Ayouba, A. *et al.* HIV-1 group N among HIV-1-seropositive individuals in Cameroon. *AIDS* **14**, 2623-2625 (2000).

27 Ayyavoo, V. *et al.* HIV-1 viral protein R (Vpr) regulates viral replication and cellular proliferation in T cells and monocytoid cells in vitro. *Journal of leukocyte biology* **62**, 93-99 (1997).

28 Baba, T. W. *et al.* Pathogenicity of live, attenuated SIV after mucosal infection of neonatal macaques. *Science* **267**, 1820-1825 (1995).

29 Babushok, D. V. & Kazazian, H. H., Jr. Progress in understanding the biology of the human mutagen LINE-1. *Human mutation* **28**, 527-539, doi:10.1002/humu.20486

(2007).

30 Bachand, F., Yao, X. J., Hrimech, M., Rougeau, N. & Cohen, E. A. Incorporation of Vpr into human immunodeficiency virus type 1 requires a direct interaction with the p6 domain of the p55 gag precursor. *The Journal of biological chemistry* **274**, 9083-9091 (1999).

31 Bai, C. *et al.* SKP1 connects cell cycle regulators to the ubiquitin proteolysis machinery through a novel motif, the F-box. *Cell* **86**, 263-274 (1996).

32 Balliet, J. W. *et al.* Distinct effects in primary macrophages and lymphocytes of the human immunodeficiency virus type 1 accessory genes vpr, vpu, and nef: mutational analysis of a primary HIV-1 isolate. *Virology* **200**, 623-631, doi:10.1006/viro.1994.1225 (1994).

33 Barlow, K. L., Ajao, A. O. & Clewley, J. P. Characterization of a novel simian immunodeficiency virus (SIVmonNG1) genome sequence from a mona monkey (Cercopithecus mona). *Journal of virology* **77**, 6879-6888 (2003).

34 Barouch, D. H. Challenges in the development of an HIV-1 vaccine. *Nature* **455**, 613-619, doi:10.1038/nature07352 (2008).

35 Batzer, M. A. & Deininger, P. L. Alu repeats and human genomic diversity. *Nature reviews. Genetics* **3**, 370-379, doi:10.1038/nrg798 (2002).

36 Baumert, T. F., Rosler, C., Malim, M. H. & von Weizsacker, F. Hepatitis B virus DNA is subject to extensive editing by the human deaminase APOBEC3C. *Hepatology* **46**, 682-689, doi:10.1002/hep.21733 (2007).

37 Beale, R. C. *et al.* Comparison of the differential context-dependence of DNA

deamination by APOBEC enzymes: correlation with mutation spectra in vivo. *Journal of molecular biology* **337**, 585-596, doi:10.1016/j.jmb.2004.01.046 (2004).

38 Beauregard, A., Curcio, M. J. & Belfort, M. The take and give between retrotransposable elements and their hosts. *Annual review of genetics* **42**, 587-617, doi:10.1146/annurev.genet.42.110807.091549 (2008).

39 Beer, B. E. *et al.* Simian immunodeficiency virus (SIV) from sun-tailed monkeys (Cercopithecus solatus): evidence for host-dependent evolution of SIV within the C. lhoesti superspecies. *Journal of virology* **73**, 7734-7744 (1999).

40 Beer, B. E. *et al.* Characterization of novel simian immunodeficiency viruses from red-capped mangabeys from Nigeria (SIVrcmNG409 and -NG411). *Journal of virology* **75**, 12014-12027, doi:10.1128/JVI.75.24.12014-12027.2001 (2001).

41 Bejerano, G. *et al.* A distal enhancer and an ultraconserved exon are derived from a novel retroposon. *Nature* **441**, 87-90, doi:10.1038/nature04696 (2006).

42 Belancio, V. P., Deininger, P. L. & Roy-Engel, A. M. LINE dancing in the human genome: transposable elements and disease. *Genome medicine* **1**, 97, doi:10.1186/gm97 (2009).

43 Belancio, V. P., Hedges, D. J. & Deininger, P. Mammalian non-LTR retrotransposons: for better or worse, in sickness and in health. *Genome research* **18**, 343-358, doi:10.1101/gr.5558208 (2008).

44 Belancio, V. P., Roy-Engel, A. M. & Deininger, P. The impact of multiple splice sites in human L1 elements. *Gene* **411**, 38-45, doi:10.1016/j.gene.2007.12.022 (2008).

45 Bennasser, Y. & Bahraoui, E. HIV-1 Tat protein induces interleukin-10 in human

peripheral blood monocytes: involvement of protein kinase C-betaII and -delta. *The FASEB journal : official publication of the Federation of American Societies for Experimental Biology* **16**, 546-554 (2002).

46 Bennett, E. A. *et al.* Active Alu retrotransposons in the human genome. *Genome research* **18**, 1875-1883, doi:10.1101/gr.081737.108 (2008).

47 Bennett, R. P. *et al.* APOBEC-1 and AID are nucleo-cytoplasmic trafficking proteins but APOBEC3G cannot traffic. *Biochemical and biophysical research communications* **350**, 214-219, doi:10.1016/j.bbrc.2006.09.032 (2006).

48 Bennett, R. P., Presnyak, V., Wedekind, J. E. & Smith, H. C. Nuclear Exclusion of the HIV-1 host defense factor APOBEC3G requires a novel cytoplasmic retention signal and is not dependent on RNA binding. *The Journal of biological chemistry* **283**, 7320-7327, doi:10.1074/jbc.M708567200 (2008).

49 Bennett, R. P., Salter, J. D., Liu, X., Wedekind, J. E. & Smith, H. C. APOBEC3G subunits self-associate via the C-terminal deaminase domain. *The Journal of biological chemistry* **283**, 33329-33336, doi:10.1074/jbc.M803726200 (2008).

50 Bergamaschi, A. *et al.* The human immunodeficiency virus type 2 Vpx protein usurps the CUL4A-DDB1 DCAF1 ubiquitin ligase to overcome a postentry block in macrophage infection. *Journal of virology* **83**, 4854-4860, doi:10.1128/JVI.00187-09 (2009).

51 Berger, A. *et al.* Interaction of Vpx and apolipoprotein B mRNA-editing catalytic polypeptide 3 family member A (APOBEC3A) correlates with efficient lentivirus infection of monocytes. *The Journal of biological chemistry* **285**, 12248-12254, doi:10.1074/jbc.M109.090977 (2010).

52 Berger, G. *et al.* APOBEC3A is a specific inhibitor of the early phases of HIV-1 infection in myeloid cells. *PLoS pathogens* **7**, e1002221, doi:10.1371/journal.ppat.1002221 (2011).

53 Berkhout, B. & de Ronde, A. APOBEC3G versus reverse transcriptase in the generation of HIV-1 drug-resistance mutations. *AIDS* **18**, 1861-1863 (2004).

54 Betts, L., Xiang, S., Short, S. A., Wolfenden, R. & Carter, C. W., Jr. Cytidine deaminase. The 2.3 A crystal structure of an enzyme: transition-state analog complex. *Journal of molecular biology* **235**, 635-656, doi:10.1006/jmbi.1994.1018 (1994).

55 Bhaskaran, K. *et al.* Changes in the incidence and predictors of human immunodeficiency virus-associated dementia in the era of highly active antiretroviral therapy. *Annals of neurology* **63**, 213-221, doi:10.1002/ana.21225 (2008).

56 Bieniasz, P. D. Intrinsic immunity: a front-line defense against viral attack. *Nature immunology* **5**, 1109-1115, doi:10.1038/ni1125 (2004).

57 Bishop, K. N., Holmes, R. K. & Malim, M. H. Antiviral potency of APOBEC proteins does not correlate with cytidine deamination. *Journal of virology* **80**, 8450-8458, doi:10.1128/JVI.00839-06 (2006).

58 Bishop, K. N. *et al.* Cytidine deamination of retroviral DNA by diverse APOBEC proteins. *Current biology : CB* **14**, 1392-1396, doi:10.1016/j.cub.2004.06.057 (2004).

59 Bishop, K. N., Verma, M., Kim, E. Y., Wolinsky, S. M. & Malim, M. H. APOBEC3G inhibits elongation of HIV-1 reverse transcripts. *PLoS pathogens* **4**, e1000231, doi:10.1371/journal.ppat.1000231 (2008).

60 Blanc, D., Patience, C., Schulz, T. F., Weiss, R. & Spire, B. Transcomplementation of

VIF- HIV-1 mutants in CEM cells suggests that VIF affects late steps of the viral life cycle. *Virology* **193**, 186-192 (1993).

61 Bogerd, H. P., Doehle, B. P., Wiegand, H. L. & Cullen, B. R. A single amino acid difference in the host APOBEC3G protein controls the primate species specificity of HIV type 1 virion infectivity factor. *Proceedings of the National Academy of Sciences of the United States of America* **101**, 3770-3774, doi:10.1073/pnas.0307713101 (2004).

62 Bogerd, H. P., Wiegand, H. L., Doehle, B. P. & Cullen, B. R. The intrinsic antiretroviral factor APOBEC3B contains two enzymatically active cytidine deaminase domains. *Virology* **364**, 486-493, doi:10.1016/j.virol.2007.03.019 (2007).

63 Bogerd, H. P., Wiegand, H. L., Doehle, B. P., Lueders, K. K. & Cullen, B. R. APOBEC3A and APOBEC3B are potent inhibitors of LTR-retrotransposon function in human cells. *Nucleic acids research* **34**, 89-95, doi:10.1093/nar/gkj416 (2006).

64 Bogerd, H. P. *et al.* Cellular inhibitors of long interspersed element 1 and Alu retrotransposition. *Proceedings of the National Academy of Sciences of the United States of America* **103**, 8780-8785, doi:10.1073/pnas.0603313103 (2006).

65 Bohnlein, E., Berger, J. & Hauber, J. Functional mapping of the human immunodeficiency virus type 1 Rev RNA binding domain: new insights into the domain structure of Rev and Rex. *Journal of virology* **65**, 7051-7055 (1991).

66 Bollinger, R. C., Egan, M. A., Chun, T. W., Mathieson, B. & Siliciano, R. F. Cellular immune responses to HIV-1 in progressive and non-progressive infections. *AIDS* **10 Suppl A**, S85-96 (1996).

67 Bonvin, M. *et al.* Interferon-inducible expression of APOBEC3 editing enzymes in

human hepatocytes and inhibition of hepatitis B virus replication. *Hepatology* **43**, 1364-1374, doi:10.1002/hep.21187 (2006).

68 Bonvin, M. & Greeve, J. Effects of point mutations in the cytidine deaminase domains of APOBEC3B on replication and hypermutation of hepatitis B virus in vitro. *The Journal of general virology* **88**, 3270-3274, doi:10.1099/vir.0.83149-0 (2007).

69 Borjabad, A., Brooks, A. I. & Volsky, D. J. Gene expression profiles of HIV-1-infected glia and brain: toward better understanding of the role of astrocytes in HIV-1-associated neurocognitive disorders. *Journal of neuroimmune pharmacology : the official journal of the Society on NeuroImmune Pharmacology* **5**, 44-62, doi:10.1007/s11481-009-9167-1 (2010).

70 Borman, A. M., Quillent, C., Charneau, P., Dauguet, C. & Clavel, F. Human immunodeficiency virus type 1 Vif- mutant particles from restrictive cells: role of Vif in correct particle assembly and infectivity. *Journal of virology* **69**, 2058-2067 (1995).

71 Bour, S., Boulerice, F. & Wainberg, M. A. Inhibition of gp160 and CD4 maturation in U937 cells after both defective and productive infections by human immunodeficiency virus type 1. *Journal of virology* **65**, 6387-6396 (1991).

72 Bour, S., Schubert, U. & Strebel, K. The human immunodeficiency virus type 1 Vpu protein specifically binds to the cytoplasmic domain of CD4: implications for the mechanism of degradation. *Journal of virology* **69**, 1510-1520 (1995).

73 Bouyac-Bertoia, M. *et al.* HIV-1 infection requires a functional integrase NLS. *Molecular cell* **7**, 1025-1035 (2001).

74 Breuer, S. *et al.* Biochemical indication for myristoylation-dependent conformational

changes in HIV-1 Nef. *Biochemistry* **45**, 2339-2349, doi:10.1021/bi052052c (2006).

75 Briggs, J. A., Wilk, T., Welker, R., Krausslich, H. G. & Fuller, S. D. Structural organization of authentic, mature HIV-1 virions and cores. *The EMBO journal* **22**, 1707-1715, doi:10.1093/emboj/cdg143 (2003).

76 Briggs, S. D., Lerner, E. C. & Smithgall, T. E. Affinity of Src family kinase SH3 domains for HIV Nef in vitro does not predict kinase activation by Nef in vivo. *Biochemistry* **39**, 489-495 (2000).

77 Brouha, B. *et al.* Hot L1s account for the bulk of retrotransposition in the human population. *Proceedings of the National Academy of Sciences of the United States of America* **100**, 5280-5285, doi:10.1073/pnas.0831042100 (2003).

78 Brown, G. V. *et al.* Energy-dependent excitation cross section measurements of the diagnostic lines of Fe XVII. *Physical review letters* **96**, 253201 (2006).

79 Bulliard, Y. *et al.* Structure-function analyses point to a polynucleotide-accommodating groove essential for APOBEC3A restriction activities. *Journal of virology* **85**, 1765-1776, doi:10.1128/JVI.01651-10 (2011).

80 Buonaguro, L., Tornesello, M. L. & Buonaguro, F. M. Human immunodeficiency virus type 1 subtype distribution in the worldwide epidemic: pathogenetic and therapeutic implications. *Journal of virology* **81**, 10209-10219, doi:10.1128/JVI.00872-07 (2007).

81 Burnett, A. & Spearman, P. APOBEC3G multimers are recruited to the plasma membrane for packaging into human immunodeficiency virus type 1 virus-like particles in an RNA-dependent process requiring the NC basic linker. *Journal of virology* **81**, 5000-5013, doi:10.1128/JVI.02237-06 (2007).

82 Callinan, P. A. & Batzer, M. A. Retrotransposable elements and human disease. *Genome dynamics* **1**, 104-115, doi:10.1159/000092503 (2006).

83 Camaur, D. & Trono, D. Characterization of human immunodeficiency virus type 1 Vif particle incorporation. *Journal of virology* **70**, 6106-6111 (1996).

84 Campbell, B. J. & Hirsch, V. M. Vpr of simian immunodeficiency virus of African green monkeys is required for replication in macaque macrophages and lymphocytes. *Journal of virology* **71**, 5593-5602 (1997).

85 Campbell, E. M., Nunez, R. & Hope, T. J. Disruption of the actin cytoskeleton can complement the ability of Nef to enhance human immunodeficiency virus type 1 infectivity. *Journal of virology* **78**, 5745-5755, doi:10.1128/JVI.78.11.5745-5755.2004 (2004).

86 Campbell, E. M., Perez, O., Anderson, J. L. & Hope, T. J. Visualization of a proteasome-independent intermediate during restriction of HIV-1 by rhesus TRIM5alpha. *The Journal of cell biology* **180**, 549-561, doi:10.1083/jcb.200706154 (2008).

87 Cao, J., Isaacson, J., Patick, A. K. & Blair, W. S. High-throughput human immunodeficiency virus type 1 (HIV-1) full replication assay that includes HIV-1 Vif as an antiviral target. *Antimicrobial agents and chemotherapy* **49**, 3833-3841, doi:10.1128/AAC.49.9.3833-3841.2005 (2005).

88 Carr, D. B. *et al.* Gestational diabetes mellitus increases the risk of cardiovascular disease in women with a family history of type 2 diabetes. *Diabetes Care* **29**, 2078-2083, doi:10.2337/dc05-2482 (2006).

89 Chang, H. C., Samaniego, F., Nair, B. C., Buonaguro, L. & Ensoli, B. HIV-1 Tat protein

exits from cells via a leaderless secretory pathway and binds to extracellular matrix-associated heparan sulfate proteoglycans through its basic region. *AIDS* **11**, 1421-1431 (1997).

90 Chelico, L., Pham, P., Calabrese, P. & Goodman, M. F. APOBEC3G DNA deaminase acts processively 3' --> 5' on single-stranded DNA. *Nature structural & molecular biology* **13**, 392-399, doi:10.1038/nsmb1086 (2006).

91 Chen, G., He, Z., Wang, T., Xu, R. & Yu, X. F. A patch of positively charged amino acids surrounding the human immunodeficiency virus type 1 Vif SLVx4Yx9Y motif influences its interaction with APOBEC3G. *Journal of virology* **83**, 8674-8682, doi:10.1128/JVI.00653-09 (2009).

92 Chen, H. *et al.* APOBEC3A is a potent inhibitor of adeno-associated virus and retrotransposons. *Current biology : CB* **16**, 480-485, doi:10.1016/j.cub.2006.01.031 (2006).

93 Chen, J. M., Ferec, C. & Cooper, D. N. LINE-1 endonuclease-dependent retrotranspositional events causing human genetic disease: mutation detection bias and multiple mechanisms of target gene disruption. *Journal of biomedicine & biotechnology* **2006**, 56182, doi:10.1155/JBB/2006/56182 (2006).

94 Chen, J. M., Stenson, P. D., Cooper, D. N. & Ferec, C. A systematic analysis of LINE-1 endonuclease-dependent retrotranspositional events causing human genetic disease. *Human genetics* **117**, 411-427, doi:10.1007/s00439-005-1321-0 (2005).

95 Chen, K. M. *et al.* Structure of the DNA deaminase domain of the HIV-1 restriction factor APOBEC3G. *Nature* **452**, 116-119, doi:10.1038/nature06638 (2008).

96 Chen, L. L. & Carmichael, G. G. Gene regulation by SINES and inosines: biological consequences of A-to-I editing of Alu element inverted repeats. *Cell Cycle* **7**, 3294-3301 (2008).

97 Chen, P., Mayne, M., Power, C. & Nath, A. The Tat protein of HIV-1 induces tumor necrosis factor-alpha production. Implications for HIV-1-associated neurological diseases. *The Journal of biological chemistry* **272**, 22385-22388 (1997).

98 Chen, R., Le Rouzic, E., Kearney, J. A., Mansky, L. M. & Benichou, S. Vpr-mediated incorporation of UNG2 into HIV-1 particles is required to modulate the virus mutation rate and for replication in macrophages. *The Journal of biological chemistry* **279**, 28419-28425, doi:10.1074/jbc.M403875200 (2004).

99 Chen, R., Yang, Z. & Zhou, Q. Phosphorylated positive transcription elongation factor b (P-TEFb) is tagged for inhibition through association with 7SK snRNA. *The Journal of biological chemistry* **279**, 4153-4160, doi:10.1074/jbc.M310044200 (2004).

100 Chen, Z. *et al.* Human immunodeficiency virus type 2 (HIV-2) seroprevalence and characterization of a distinct HIV-2 genetic subtype from the natural range of simian immunodeficiency virus-infected sooty mangabeys. *Journal of virology* **71**, 3953-3960 (1997).

101 Cheng, J. *et al.* Neuronal excitatory properties of human immunodeficiency virus type 1 Tat protein. *Neuroscience* **82**, 97-106 (1998).

102 Cheng, X., Belshan, M. & Ratner, L. Hsp40 facilitates nuclear import of the human immunodeficiency virus type 2 Vpx-mediated preintegration complex. *Journal of virology* **82**, 1229-1237, doi:10.1128/JVI.00540-07 (2008).

103 Chesebro, B., Wehrly, K., Nishio, J. & Perryman, S. Macrophage-tropic human immunodeficiency virus isolates from different patients exhibit unusual V3 envelope sequence homogeneity in comparison with T-cell-tropic isolates: definition of critical amino acids involved in cell tropism. *Journal of virology* **66**, 6547-6554 (1992).

104 Chiu, Y. L. & Greene, W. C. The APOBEC3 cytidine deaminases: an innate defensive network opposing exogenous retroviruses and endogenous retroelements. *Annual review of immunology* **26**, 317-353, doi:10.1146/annurev.immunol.26.021607.090350 (2008).

105 Chiu, Y. L. & Greene, W. C. APOBEC3G: an intracellular centurion. *Philosophical transactions of the Royal Society of London. Series B, Biological sciences* **364**, 689-703, doi:10.1098/rstb.2008.0193 (2009).

106 Chiu, Y. L. *et al.* Cellular APOBEC3G restricts HIV-1 infection in resting CD4+ T cells. *Nature* **435**, 108-114, doi:10.1038/nature03493 (2005).

107 Chiu, Y. L. *et al.* High-molecular-mass APOBEC3G complexes restrict Alu retrotransposition. *Proceedings of the National Academy of Sciences of the United States of America* **103**, 15588-15593, doi:10.1073/pnas.0604524103 (2006).

108 Chowers, M. Y. *et al.* Optimal infectivity in vitro of human immunodeficiency virus type 1 requires an intact nef gene. *Journal of virology* **68**, 2906-2914 (1994).

109 Christenson, R. H. *et al.* Toward standardization of cardiac troponin I measurements part II: assessing commutability of candidate reference materials and harmonization of cardiac troponin I assays. *Clin Chem* **52**, 1685-1692, doi:10.1373/clinchem.2006.068437 (2006).

110 Clements, J. E., Gdovin, S. L., Montelaro, R. C. & Narayan, O. Antigenic variation in lentiviral diseases. *Annual review of immunology* **6**, 139-159, doi:10.1146/annurev.iy.06.040188.001035 (1988).

111 Clements, J. E. *et al.* Cross-protective immune responses induced in rhesus macaques by immunization with attenuated macrophage-tropic simian immunodeficiency virus. *Journal of virology* **69**, 2737-2744 (1995).

112 Coetzer, M. *et al.* Evolution of CCR5 use before and during coreceptor switching. *Journal of virology* **82**, 11758-11766, doi:10.1128/JVI.01141-08 (2008).

113 Coffin, J. M. HIV population dynamics in vivo: implications for genetic variation, pathogenesis, and therapy. *Science* **267**, 483-489 (1995).

114 Coleman, S. H., Day, J. R. & Guatelli, J. C. The HIV-1 Nef protein as a target for antiretroviral therapy. *Expert opinion on therapeutic targets* **5**, 1-22, doi:10.1517/14728222.5.1.1 (2001).

115 Comeaux, M. S., Roy-Engel, A. M., Hedges, D. J. & Deininger, P. L. Diverse cis factors controlling Alu retrotransposition: what causes Alu elements to die? *Genome research* **19**, 545-555, doi:10.1101/gr.089789.108 (2009).

116 Connor, R. I., Chen, B. K., Choe, S. & Landau, N. R. Vpr is required for efficient replication of human immunodeficiency virus type-1 in mononuclear phagocytes. *Virology* **206**, 935-944, doi:10.1006/viro.1995.1016 (1995).

117 Conticello, S. G., Harris, R. S. & Neuberger, M. S. The Vif protein of HIV triggers degradation of the human antiretroviral DNA deaminase APOBEC3G. *Current biology : CB* **13**, 2009-2013 (2003).

118 Conticello, S. G., Thomas, C. J., Petersen-Mahrt, S. K. & Neuberger, M. S. Evolution of the AID/APOBEC family of polynucleotide (deoxy)cytidine deaminases. *Molecular biology and evolution* **22**, 367-377, doi:10.1093/molbev/msi026 (2005).

119 Cordaux, R. & Batzer, M. A. The impact of retrotransposons on human genome evolution. *Nature reviews. Genetics* **10**, 691-703, doi:10.1038/nrg2640 (2009).

120 Cormier, E. G. & Dragic, T. The crown and stem of the V3 loop play distinct roles in human immunodeficiency virus type 1 envelope glycoprotein interactions with the CCR5 coreceptor. *Journal of virology* **76**, 8953-8957 (2002).

121 Cost, G. J., Feng, Q., Jacquier, A. & Boeke, J. D. Human L1 element target-primed reverse transcription in vitro. *The EMBO journal* **21**, 5899-5910 (2002).

122 Costa, L. J. *et al.* Nef binds p6* in GagPol during replication of human immunodeficiency virus type 1. *Journal of virology* **78**, 5311-5323 (2004).

123 Crise, B., Buonocore, L. & Rose, J. K. CD4 is retained in the endoplasmic reticulum by the human immunodeficiency virus type 1 glycoprotein precursor. *Journal of virology* **64**, 5585-5593 (1990).

124 Cullen, B. R. Retroviruses as model systems for the study of nuclear RNA export pathways. *Virology* **249**, 203-210, doi:10.1006/viro.1998.9331 (1998).

125 Cullen, B. R. Role and mechanism of action of the APOBEC3 family of antiretroviral resistance factors. *Journal of virology* **80**, 1067-1076, doi:10.1128/JVI.80.3.1067-1076.2006 (2006).

126 Curran, J. W. *et al.* Epidemiology of HIV infection and AIDS in the United States. *Science* **239**, 610-616 (1988).

127 Daly, T. J., Cook, K. S., Gray, G. S., Maione, T. E. & Rusche, J. R. Specific binding of HIV-1 recombinant Rev protein to the Rev-responsive element in vitro. *Nature* **342**, 816-819, doi:10.1038/342816a0 (1989).

128 Dang, Y., Davis, R. W., York, I. A. & Zheng, Y. H. Identification of 81LGxGxxIxW89 and 171EDRW174 domains from human immunodeficiency virus type 1 Vif that regulate APOBEC3G and APOBEC3F neutralizing activity. *Journal of virology* **84**, 5741-5750, doi:10.1128/JVI.00079-10 (2010).

129 Dang, Y. *et al.* Human cytidine deaminase APOBEC3H restricts HIV-1 replication. *The Journal of biological chemistry* **283**, 11606-11614, doi:10.1074/jbc.M707586200 (2008).

130 Dang, Y., Wang, X., Esselman, W. J. & Zheng, Y. H. Identification of APOBEC3DE as another antiretroviral factor from the human APOBEC family. *Journal of virology* **80**, 10522-10533, doi:10.1128/JVI.01123-06 (2006).

131 Dang, Y., Wang, X., York, I. A. & Zheng, Y. H. Identification of a critical T(Q/D/E)x5ADx2(I/L) motif from primate lentivirus Vif proteins that regulate APOBEC3G and APOBEC3F neutralizing activity. *Journal of virology* **84**, 8561-8570, doi:10.1128/JVI.00960-10 (2010).

132 Dang, Y., Wang, X., Zhou, T., York, I. A. & Zheng, Y. H. Identification of a novel WxSLVK motif in the N terminus of human immunodeficiency virus and simian immunodeficiency virus Vif that is critical for APOBEC3G and APOBEC3F neutralization. *Journal of virology* **83**, 8544-8552, doi:10.1128/JVI.00651-09 (2009).

133 Daniel, M. D., Kirchhoff, F., Czajak, S. C., Sehgal, P. K. & Desrosiers, R. C. Protective effects of a live attenuated SIV vaccine with a deletion in the nef gene. *Science* **258**,

1938-1941 (1992).

134 Daniel, M. D., Kirchhoff, F., Czajak, S. C., Sehgal, P. K. & Desrosiers, R. C. Protective effects of a live attenuated SIV vaccine with a deletion in the nef gene. *Science* **258**, 1938-1941 (1992).

135 De Clercq, E. Anti-HIV drugs: 25 compounds approved within 25 years after the discovery of HIV. *International journal of antimicrobial agents* **33**, 307-320, doi:10.1016/j.ijantimicag.2008.10.010 (2009).

136 de Mareuil, J. *et al.* HIV-1 Tat protein enhances microtubule polymerization. *Retrovirology* **2**, 5, doi:10.1186/1742-4690-2-5 (2005).

137 Deacon, N. J. *et al.* Genomic structure of an attenuated quasi species of HIV-1 from a blood transfusion donor and recipients. *Science* **270**, 988-991 (1995).

138 Dehart, J. L. & Planelles, V. Human immunodeficiency virus type 1 Vpr links proteasomal degradation and checkpoint activation. *Journal of virology* **82**, 1066-1072, doi:10.1128/JVI.01628-07 (2008).

139 Deininger, P. L. & Batzer, M. A. Alu repeats and human disease. *Molecular genetics and metabolism* **67**, 183-193, doi:10.1006/mgme.1999.2864 (1999).

140 Delebecque, F. *et al.* Restriction of foamy viruses by APOBEC cytidine deaminases. *Journal of virology* **80**, 605-614, doi:10.1128/JVI.80.2.605-614.2006 (2006).

141 Demarchi, F., Gutierrez, M. I. & Giacca, M. Human immunodeficiency virus type 1 tat protein activates transcription factor NF-kappaB through the cellular interferon-inducible, double-stranded RNA-dependent protein kinase, PKR. *Journal of virology* **73**, 7080-7086 (1999).

142 Demarest, J. F. *et al.* Immunologic and virologic analyses of an acutely HIV type 1-infected patient with extremely rapid disease progression. *AIDS research and human retroviruses* **17**, 1333-1344, doi:10.1089/08892220152596597 (2001).

143 Deng, L. *et al.* Acetylation of HIV-1 Tat by CBP/P300 increases transcription of integrated HIV-1 genome and enhances binding to core histones. *Virology* **277**, 278-295, doi:10.1006/viro.2000.0593 (2000).

144 Deng, L. *et al.* Enhancement of the p300 HAT activity by HIV-1 Tat on chromatin DNA. *Virology* **289**, 312-326, doi:10.1006/viro.2001.1129 (2001).

145 Derdeyn, C. A. *et al.* Sensitivity of human immunodeficiency virus type 1 to the fusion inhibitor T-20 is modulated by coreceptor specificity defined by the V3 loop of gp120. *Journal of virology* **74**, 8358-8367 (2000).

146 Derdowski, A., Ding, L. & Spearman, P. A novel fluorescence resonance energy transfer assay demonstrates that the human immunodeficiency virus type 1 Pr55Gag I domain mediates Gag-Gag interactions. *Journal of virology* **78**, 1230-1242 (2004).

147 Desrosiers, R. C. HIV with multiple gene deletions as a live attenuated vaccine for AIDS. *AIDS research and human retroviruses* **8**, 1457 (1992).

148 Desrosiers, R. C. *et al.* Identification of highly attenuated mutants of simian immunodeficiency virus. *Journal of virology* **72**, 1431-1437 (1998).

149 Dewannieux, M., Esnault, C. & Heidmann, T. LINE-mediated retrotransposition of marked Alu sequences. *Nature genetics* **35**, 41-48, doi:10.1038/ng1223 (2003).

150 Doehle, B. P., Schafer, A. & Cullen, B. R. Human APOBEC3B is a potent inhibitor of HIV-1 infectivity and is resistant to HIV-1 Vif. *Virology* **339**, 281-288,

doi:10.1016/j.virol.2005.06.005 (2005).

151 Donahue, J. P., Vetter, M. L., Mukhtar, N. A. & D'Aquila, R. T. The HIV-1 Vif PPLP motif is necessary for human APOBEC3G binding and degradation. *Virology* **377**, 49-53, doi:10.1016/j.virol.2008.04.017 (2008).

152 Douglas, J. L. *et al.* Vpu directs the degradation of the human immunodeficiency virus restriction factor BST-2/Tetherin via a {beta}TrCP-dependent mechanism. *Journal of virology* **83**, 7931-7947, doi:10.1128/JVI.00242-09 (2009).

153 Drewes, G., Ebneth, A. & Mandelkow, E. M. MAPs, MARKs and microtubule dynamics. *Trends in biochemical sciences* **23**, 307-311 (1998).

154 Dube, M. *et al.* Suppression of Tetherin-restricting activity upon human immunodeficiency virus type 1 particle release correlates with localization of Vpu in the trans-Golgi network. *Journal of virology* **83**, 4574-4590, doi:10.1128/JVI.01800-08 (2009).

155 Dussart, S. *et al.* The Vif protein of human immunodeficiency virus type 1 is posttranslationally modified by ubiquitin. *Biochemical and biophysical research communications* **315**, 66-72, doi:10.1016/j.bbrc.2004.01.023 (2004).

156 Duthie, M. S. & Kahn, S. J. During acute Trypanosoma cruzi infection highly susceptible mice deficient in natural killer cells are protected by a single alpha-galactosylceramide treatment. *Immunology* **119**, 355-361, doi:10.1111/j.1365-2567.2006.02439.x (2006).

157 Dutko, J. A., Schafer, A., Kenny, A. E., Cullen, B. R. & Curcio, M. J. Inhibition of a yeast LTR retrotransposon by human APOBEC3 cytidine deaminases. *Current biology : CB* **15**, 661-666, doi:10.1016/j.cub.2005.02.051 (2005).

158 Eckstein, D. A. *et al.* HIV-1 actively replicates in naive CD4(+) T cells residing within human lymphoid tissues. *Immunity* **15**, 671-682 (2001).

159 Embretson, J. *et al.* Massive covert infection of helper T lymphocytes and macrophages by HIV during the incubation period of AIDS. *Nature* **362**, 359-362, doi:10.1038/362359a0 (1993).

160 Esnault, C. *et al.* APOBEC3G cytidine deaminase inhibits retrotransposition of endogenous retroviruses. *Nature* **433**, 430-433, doi:10.1038/nature03238 (2005).

161 Esnault, C., Millet, J., Schwartz, O. & Heidmann, T. Dual inhibitory effects of APOBEC family proteins on retrotransposition of mammalian endogenous retroviruses. *Nucleic acids research* **34**, 1522-1531, doi:10.1093/nar/gkl054 (2006).

162 Espeland, M. A. *et al.* Consent for genetics studies among clinical trial participants: findings from Action for Health in Diabetes (Look AHEAD). *Clin Trials* **3**, 443-456, doi:10.1177/1740774506070727 (2006).

163 Ewart, G. D., Sutherland, T., Gage, P. W. & Cox, G. B. The Vpu protein of human immunodeficiency virus type 1 forms cation-selective ion channels. *Journal of virology* **70**, 7108-7115 (1996).

164 Fackler, O. T., Luo, W., Geyer, M., Alberts, A. S. & Peterlin, B. M. Activation of Vav by Nef induces cytoskeletal rearrangements and downstream effector functions. *Molecular cell* **3**, 729-739 (1999).

165 Fan, L. & Peden, K. Cell-free transmission of Vif mutants of HIV-1. *Virology* **190**, 19-29 (1992).

166 Fang, Q. *et al.* [The apoptosis-inducing activity of human selenoprotein P shorter

isoform]. *Zhonghua zhong liu za zhi [Chinese journal of oncology]* **26**, 652-656 (2004).

167 Federau, T. *et al.* Solution structure of the cytoplasmic domain of the human immunodeficiency virus type 1 encoded virus protein U (Vpu). *International journal of peptide and protein research* **47**, 297-310 (1996).

168 Feng, Q., Moran, J. V., Kazazian, H. H., Jr. & Boeke, J. D. Human L1 retrotransposon encodes a conserved endonuclease required for retrotransposition. *Cell* **87**, 905-916 (1996).

169 Ferrari, A. *et al.* Caveolae-mediated internalization of extracellular HIV-1 tat fusion proteins visualized in real time. *Molecular therapy : the journal of the American Society of Gene Therapy* **8**, 284-294 (2003).

170 Fischer, U., Huber, J., Boelens, W. C., Mattaj, I. W. & Luhrmann, R. The HIV-1 Rev activation domain is a nuclear export signal that accesses an export pathway used by specific cellular RNAs. *Cell* **82**, 475-483 (1995).

171 Fisher, A. G. *et al.* The sor gene of HIV-1 is required for efficient virus transmission in vitro. *Science* **237**, 888-893 (1987).

172 Flach, E. J., Stevenson, M. F. & Henderson, G. M. Aspergillosis in gentoo penguins (Pygoscelis papua) at Edinburgh Zoo, 1964 to 1988. *The Veterinary record* **126**, 81-85 (1990).

173 Fletcher, T. M., 3rd *et al.* Nuclear import and cell cycle arrest functions of the HIV-1 Vpr protein are encoded by two separate genes in HIV-2/SIV(SM). *The EMBO journal* **15**, 6155-6165 (1996).

174 Fonseca, V. A. & Kahn, S. E. Commentary: Of HOPEs and DREAMs: the quest to

prevent type 2 diabetes. *The Journal of clinical endocrinology and metabolism* **91**, 4762-4763, doi:10.1210/jc.2006-2164 (2006).

175 Fornerod, M., Ohno, M., Yoshida, M. & Mattaj, I. W. CRM1 is an export receptor for leucine-rich nuclear export signals. *Cell* **90**, 1051-1060 (1997).

176 Forshey, B. M., Shi, J. & Aiken, C. Structural requirements for recognition of the human immunodeficiency virus type 1 core during host restriction in owl monkey cells. *Journal of virology* **79**, 869-875, doi:10.1128/JVI.79.2.869-875.2005 (2005).

177 Foti, M. *et al.* Nef-mediated clathrin-coated pit formation. *The Journal of cell biology* **139**, 37-47 (1997).

178 Frankel, A. D. & Young, J. A. HIV-1: fifteen proteins and an RNA. *Annual review of biochemistry* **67**, 1-25, doi:10.1146/annurev.biochem.67.1.1 (1998).

179 Freed, E. O. HIV-1 replication. *Somatic cell and molecular genetics* **26**, 13-33 (2001).

180 Friew, Y. N., Boyko, V., Hu, W. S. & Pathak, V. K. Intracellular interactions between APOBEC3G, RNA, and HIV-1 Gag: APOBEC3G multimerization is dependent on its association with RNA. *Retrovirology* **6**, 56, doi:10.1186/1742-4690-6-56 (2009).

181 Fujita, M. *et al.* Expression of HIV-1 accessory protein Vif is controlled uniquely to be low and optimal by proteasome degradation. *Microbes and infection / Institut Pasteur* **6**, 791-798, doi:10.1016/j.micinf.2004.04.011 (2004).

182 Fujita, M. *et al.* Vpx is critical for reverse transcription of the human immunodeficiency virus type 2 genome in macrophages. *Journal of virology* **82**, 7752-7756, doi:10.1128/JVI.01003-07 (2008).

183 Fujita, M. *et al.* Amino acid residues 88 and 89 in the central hydrophilic region of

human immunodeficiency virus type 1 Vif are critical for viral infectivity by enhancing the steady-state expression of Vif. *Journal of virology* **77**, 1626-1632 (2003).

184 Furukawa, A. *et al.* Structure and real-time monitoring of the enzymatic reaction of APOBEC3G which is involved in anti-HIV activity. *Nucleic Acids Symp Ser (Oxf)*, 87-88, doi:10.1093/nass/nrp044 (2009).

185 Gabuzda, D. H. *et al.* Role of vif in replication of human immunodeficiency virus type 1 in CD4+ T lymphocytes. *Journal of virology* **66**, 6489-6495 (1992).

186 Gabuzda, D. H. *et al.* Essential role of vif in establishing productive HIV-1 infection in peripheral blood T lymphocytes and monocyte/macrophages. *J Acquir Immune Defic Syndr* **7**, 908-915 (1994).

187 Gallois-Montbrun, S. *et al.* Comparison of cellular ribonucleoprotein complexes associated with the APOBEC3F and APOBEC3G antiviral proteins. *Journal of virology* **82**, 5636-5642, doi:10.1128/JVI.00287-08 (2008).

188 Gallois-Montbrun, S. *et al.* Antiviral protein APOBEC3G localizes to ribonucleoprotein complexes found in P bodies and stress granules. *Journal of virology* **81**, 2165-2178, doi:10.1128/JVI.02287-06 (2007).

189 Gandhi, S. K., Siliciano, J. D., Bailey, J. R., Siliciano, R. F. & Blankson, J. N. Role of APOBEC3G/F-mediated hypermutation in the control of human immunodeficiency virus type 1 in elite suppressors. *Journal of virology* **82**, 3125-3130, doi:10.1128/JVI.01533-07 (2008).

190 Gao, F. *et al.* Origin of HIV-1 in the chimpanzee Pan troglodytes troglodytes. *Nature* **397**, 436-441, doi:10.1038/17130 (1999).

191 Gao, F. *et al.* Evidence of two distinct subsubtypes within the HIV-1 subtype A radiation. *AIDS research and human retroviruses* **17**, 675-688, doi:10.1089/088922201750236951 (2001).

192 Gao, F. *et al.* Genetic diversity of human immunodeficiency virus type 2: evidence for distinct sequence subtypes with differences in virus biology. *Journal of virology* **68**, 7433-7447 (1994).

193 Garcia, J. V. & Miller, A. D. Serine phosphorylation-independent downregulation of cell-surface CD4 by nef. *Nature* **350**, 508-511, doi:10.1038/350508a0 (1991).

194 Gasior, S. L., Wakeman, T. P., Xu, B. & Deininger, P. L. The human LINE-1 retrotransposon creates DNA double-strand breaks. *Journal of molecular biology* **357**, 1383-1393, doi:10.1016/j.jmb.2006.01.089 (2006).

195 Gattone, V. H., 2nd *et al.* SIV-associated nephropathy in rhesus macaques infected with lymphocyte-tropic SIVmac239. *AIDS research and human retroviruses* **14**, 1163-1180 (1998).

196 Gerchman, F. *et al.* Superiority of the Modification of Diet in Renal Disease equation over the Cockcroft-Gault equation in screening for impaired kidney function in Japanese Americans. *Diabetes research and clinical practice* **77**, 320-326, doi:10.1016/j.diabres.2006.11.001 (2007).

197 Geyer, M., Fackler, O. T. & Peterlin, B. M. Structure--function relationships in HIV-1 Nef. *EMBO reports* **2**, 580-585, doi:10.1093/embo-reports/kve141 (2001).

198 Ghys, P. D. *et al.* The associations between cervicovaginal HIV shedding, sexually transmitted diseases and immunosuppression in female sex workers in Abidjan, Cote

d'Ivoire. *AIDS* **11**, F85-93 (1997).

199 Giacca, M. HIV-1 Tat, apoptosis and the mitochondria: a tubulin link? *Retrovirology* **2**, 7, doi:10.1186/1742-4690-2-7 (2005).

200 Gibbs, J. S. *et al.* Progression to AIDS in the absence of a gene for vpr or vpx. *Journal of virology* **69**, 2378-2383 (1995).

201 Gibbs, J. S., Regier, D. A. & Desrosiers, R. C. Construction and in vitro properties of SIVmac mutants with deletions in "nonessential" genes. *AIDS research and human retroviruses* **10**, 333-342 (1994).

202 Gilbert, M. T. *et al.* The emergence of HIV/AIDS in the Americas and beyond. *Proceedings of the National Academy of Sciences of the United States of America* **104**, 18566-18570, doi:10.1073/pnas.0705329104 (2007).

203 Gilbert, N., Lutz, S., Morrish, T. A. & Moran, J. V. Multiple fates of L1 retrotransposition intermediates in cultured human cells. *Molecular and cellular biology* **25**, 7780-7795, doi:10.1128/MCB.25.17.7780-7795.2005 (2005).

204 Goila-Gaur, R. *et al.* HIV-1 Vif promotes the formation of high molecular mass APOBEC3G complexes. *Virology* **372**, 136-146, doi:10.1016/j.virol.2007.10.017 (2008).

205 Goila-Gaur, R., Khan, M. A., Miyagi, E., Kao, S. & Strebel, K. Targeting APOBEC3A to the viral nucleoprotein complex confers antiviral activity. *Retrovirology* **4**, 61, doi:10.1186/1742-4690-4-61 (2007).

206 Goila-Gaur, R. & Strebel, K. HIV-1 Vif, APOBEC, and intrinsic immunity. *Retrovirology* **5**, 51, doi:10.1186/1742-4690-5-51 (2008).

207 Gooch, B. D. & Cullen, B. R. Functional domain organization of human APOBEC3G.

Virology **379**, 118-124, doi:10.1016/j.virol.2008.06.013 (2008).

208 Goto, T. *et al.* A novel membrane antigen selectively expressed on terminally differentiated human B cells. *Blood* **84**, 1922-1930 (1994).

209 Gotte, M., Rausch, J. W., Marchand, B., Sarafianos, S. & Le Grice, S. F. Reverse transcriptase in motion: conformational dynamics of enzyme-substrate interactions. *Biochimica et biophysica acta* **1804**, 1202-1212, doi:10.1016/j.bbapap.2009.07.020 (2010).

210 Goujon, C. *et al.* Characterization of simian immunodeficiency virus SIVSM/human immunodeficiency virus type 2 Vpx function in human myeloid cells. *Journal of virology* **82**, 12335-12345, doi:10.1128/JVI.01181-08 (2008).

211 Goujon, C. *et al.* SIVSM/HIV-2 Vpx proteins promote retroviral escape from a proteasome-dependent restriction pathway present in human dendritic cells. *Retrovirology* **4**, 2, doi:10.1186/1742-4690-4-2 (2007).

212 Goujon, C. *et al.* SIVSM/HIV-2 Vpx proteins promote retroviral escape from a proteasome-dependent restriction pathway present in human dendritic cells. *Retrovirology* **4**, 2, doi:10.1186/1742-4690-4-2 (2007).

213 Goymer, P. *et al.* Adaptive divergence in experimental populations of Pseudomonas fluorescens. II. Role of the GGDEF regulator WspR in evolution and development of the wrinkly spreader phenotype. *Genetics* **173**, 515-526, doi:10.1534/genetics.106.055863 (2006).

214 Gramberg, T., Sunseri, N. & Landau, N. R. Accessories to the crime: recent advances in HIV accessory protein biology. *Current HIV/AIDS reports* **6**, 36-42 (2009).

215 Granelli-Piperno, A., Golebiowska, A., Trumpfheller, C., Siegal, F. P. & Steinman, R. M. HIV-1-infected monocyte-derived dendritic cells do not undergo maturation but can elicit IL-10 production and T cell regulation. *Proceedings of the National Academy of Sciences of the United States of America* **101**, 7669-7674, doi:10.1073/pnas.0402431101 (2004).

216 Greenberg, M. E., Iafrate, A. J. & Skowronski, J. The SH3 domain-binding surface and an acidic motif in HIV-1 Nef regulate trafficking of class I MHC complexes. *The EMBO journal* **17**, 2777-2789, doi:10.1093/emboj/17.10.2777 (1998).

217 Greene, W. C. The brightening future of HIV therapeutics. *Nature immunology* **5**, 867-871, doi:10.1038/ni0904-867 (2004).

218 Grewe, B. & Uberla, K. The human immunodeficiency virus type 1 Rev protein: menage a trois during the early phase of the lentiviral replication cycle. *The Journal of general virology* **91**, 1893-1897, doi:10.1099/vir.0.022509-0 (2010).

219 Grice, A. L., Kerr, I. D. & Sansom, M. S. Ion channels formed by HIV-1 Vpu: a modelling and simulation study. *FEBS letters* **405**, 299-304 (1997).

220 Grzesiek, S. *et al.* Refined solution structure and backbone dynamics of HIV-1 Nef. *Protein science : a publication of the Protein Society* **6**, 1248-1263, doi:10.1002/pro.5560060613 (1997).

221 Guo, F., Cen, S., Niu, M., Saadatmand, J. & Kleiman, L. Inhibition of formula-primed reverse transcription by human APOBEC3G during human immunodeficiency virus type 1 replication. *Journal of virology* **80**, 11710-11722, doi:10.1128/JVI.01038-06 (2006).

222 Guo, F. *et al.* The interaction of APOBEC3G with human immunodeficiency virus type 1

nucleocapsid inhibits tRNA3Lys annealing to viral RNA. *Journal of virology* **81**, 11322-11331, doi:10.1128/JVI.00162-07 (2007).

223 Guo, F., Saadatmand, J., Niu, M. & Kleiman, L. Roles of Gag and NCp7 in facilitating tRNA(Lys)(3) Annealing to viral RNA in human immunodeficiency virus type 1. *Journal of virology* **83**, 8099-8107, doi:10.1128/JVI.00488-09 (2009).

224 Gupta, S., Boppana, R., Mishra, G. C., Saha, B. & Mitra, D. HIV-1 Tat suppresses gp120-specific T cell response in IL-10-dependent manner. *J Immunol* **180**, 79-88 (2008).

225 Gurtler, L. G. *et al.* A new subtype of human immunodeficiency virus type 1 (MVP-5180) from Cameroon. *Journal of virology* **68**, 1581-1585 (1994).

226 Guy, B. *et al.* HIV F/3' orf encodes a phosphorylated GTP-binding protein resembling an oncogene product. *Nature* **330**, 266-269, doi:10.1038/330266a0 (1987).

227 Habermann, A. *et al.* CD317/tetherin is enriched in the HIV-1 envelope and downregulated from the plasma membrane upon virus infection. *Journal of virology* **84**, 4646-4658, doi:10.1128/JVI.02421-09 (2010).

228 Hache, G., Liddament, M. T. & Harris, R. S. The retroviral hypermutation specificity of APOBEC3F and APOBEC3G is governed by the C-terminal DNA cytosine deaminase domain. *The Journal of biological chemistry* **280**, 10920-10924, doi:10.1074/jbc.M500382200 (2005).

229 Hache, G., Mansky, L. M. & Harris, R. S. Human APOBEC3 proteins, retrovirus restriction, and HIV drug resistance. *AIDS reviews* **8**, 148-157 (2006).

230 Hahn, B. H., Shaw, G. M., De Cock, K. M. & Sharp, P. M. AIDS as a zoonosis: scientific

and public health implications. *Science* **287**, 607-614 (2000).

231 Hamm, J. & Mattaj, I. W. Monomethylated cap structures facilitate RNA export from the nucleus. *Cell* **63**, 109-118 (1990).

232 Han, J. S. & Boeke, J. D. LINE-1 retrotransposons: modulators of quantity and quality of mammalian gene expression? *BioEssays : news and reviews in molecular, cellular and developmental biology* **27**, 775-784, doi:10.1002/bies.20257 (2005).

233 Harari, A., Ooms, M., Mulder, L. C. & Simon, V. Polymorphisms and splice variants influence the antiretroviral activity of human APOBEC3H. *Journal of virology* **83**, 295-303, doi:10.1128/JVI.01665-08 (2009).

234 Harjes, E. *et al.* An extended structure of the APOBEC3G catalytic domain suggests a unique holoenzyme model. *Journal of molecular biology* **389**, 819-832, doi:10.1016/j.jmb.2009.04.031 (2009).

235 Harmache, A. *et al.* Requirement of caprine arthritis encephalitis virus vif gene for in vivo replication. *Virology* **224**, 246-255, doi:10.1006/viro.1996.0526 (1996).

236 Harrich, D. & Hooker, B. Mechanistic aspects of HIV-1 reverse transcription initiation. *Reviews in medical virology* **12**, 31-45 (2002).

237 Harrich, D., Ulich, C. & Gaynor, R. B. A critical role for the TAR element in promoting efficient human immunodeficiency virus type 1 reverse transcription. *Journal of virology* **70**, 4017-4027 (1996).

238 Harris, R. S. *et al.* DNA deamination mediates innate immunity to retroviral infection. *Cell* **113**, 803-809 (2003).

239 Harris, R. S. & Liddament, M. T. Retroviral restriction by APOBEC proteins. *Nature*

reviews. Immunology **4**, 868-877, doi:10.1038/nri1489 (2004).

240 Harris, R. S., Petersen-Mahrt, S. K. & Neuberger, M. S. RNA editing enzyme APOBEC1 and some of its homologs can act as DNA mutators. *Molecular cell* **10**, 1247-1253 (2002).

241 Harris, R. S., Sheehy, A. M., Craig, H. M., Malim, M. H. & Neuberger, M. S. DNA deamination: not just a trigger for antibody diversification but also a mechanism for defense against retroviruses. *Nature immunology* **4**, 641-643, doi:10.1038/ni0703-641 (2003).

242 Harris, S. G. *et al.* Extract-specific heterogeneity in high-order complexes containing apolipoprotein B mRNA editing activity and RNA-binding proteins. *The Journal of biological chemistry* **268**, 7382-7392 (1993).

243 Hartley, C. L., Stevenson, M. & Callebert, J. A. The S-S-S connection. *NLN publications*, 207-210 (1990).

244 He, J. *et al.* Human immunodeficiency virus type 1 viral protein R (Vpr) arrests cells in the G2 phase of the cell cycle by inhibiting p34cdc2 activity. *Journal of virology* **69**, 6705-6711 (1995).

245 He, Y. J., McCall, C. M., Hu, J., Zeng, Y. & Xiong, Y. DDB1 functions as a linker to recruit receptor WD40 proteins to CUL4-ROC1 ubiquitin ligases. *Genes & development* **20**, 2949-2954, doi:10.1101/gad.1483206 (2006).

246 He, Z., Zhang, W., Chen, G., Xu, R. & Yu, X. F. Characterization of conserved motifs in HIV-1 Vif required for APOBEC3G and APOBEC3F interaction. *Journal of molecular biology* **381**, 1000-1011, doi:10.1016/j.jmb.2008.06.061 (2008).

247 Heeney, J. L., Dalgleish, A. G. & Weiss, R. A. Origins of HIV and the evolution of resistance to AIDS. *Science* **313**, 462-466, doi:10.1126/science.1123016 (2006).

248 Helseth, E., Olshevsky, U., Furman, C. & Sodroski, J. Human immunodeficiency virus type 1 gp120 envelope glycoprotein regions important for association with the gp41 transmembrane glycoprotein. *Journal of virology* **65**, 2119-2123 (1991).

249 Hemelaar, J. The origin and diversity of the HIV-1 pandemic. *Trends in molecular medicine*, doi:10.1016/j.molmed.2011.12.001 (2012).

250 Hemelaar, J., Gouws, E., Ghys, P. D. & Osmanov, S. Global and regional distribution of HIV-1 genetic subtypes and recombinants in 2004. *AIDS* **20**, W13-23, doi:10.1097/01.aids.0000247564.73009.bc (2006).

251 Henderson, B. R. & Percipalle, P. Interactions between HIV Rev and nuclear import and export factors: the Rev nuclear localisation signal mediates specific binding to human importin-beta. *Journal of molecular biology* **274**, 693-707, doi:10.1006/jmbi.1997.1420 (1997).

252 Henklein, P. *et al.* Synthesis and characterization of the hydrophilic C-terminal domain of the human immunodeficiency virus type 1-encoded virus protein U (Vpu). *Peptide research* **6**, 79-87 (1993).

253 Higa, L. A. *et al.* CUL4-DDB1 ubiquitin ligase interacts with multiple WD40-repeat proteins and regulates histone methylation. *Nature cell biology* **8**, 1277-1283, doi:10.1038/ncb1490 (2006).

254 Hill, M. S. *et al.* APOBEC3G expression is restricted to neurons in the brains of pigtailed macaques. *AIDS research and human retroviruses* **22**, 541-550,

doi:10.1089/aid.2006.22.541 (2006).

255 Hill, M. S. *et al.* APOBEC3G expression is restricted to epithelial cells of the proximal convoluted tubules and is not expressed in the glomeruli of macaques. *The journal of histochemistry and cytochemistry : official journal of the Histochemistry Society* **55**, 63-70, doi:10.1369/jhc.6A7054.2006 (2007).

256 Hill, M. S. *et al.* Modulation of the severe CD4+ T-cell loss caused by a pathogenic simian-human immunodeficiency virus by replacement of the subtype B vpu with the vpu from a subtype C HIV-1 clinical isolate. *Virology* **371**, 86-97, doi:10.1016/j.virol.2007.09.015 (2008).

257 Hill, M. S., Ruiz, A., Schmitt, K. & Stephens, E. B. Identification of amino acids within the second alpha helical domain of the human immunodeficiency virus type 1 Vpu that are critical for preventing CD4 cell surface expression. *Virology* **397**, 104-112, doi:10.1016/j.virol.2009.10.048 (2010).

258 Hirsch, I. *et al.* Differences in replication and cytopathogenicity of human immunodeficiency virus type 1 (HIV-1) are not determined by long terminal repeats (LTR). *Virology* **177**, 759-763 (1990).

259 Hirsch, V. M. *et al.* Vpx is required for dissemination and pathogenesis of SIV(SM) PBj: evidence of macrophage-dependent viral amplification. *Nature medicine* **4**, 1401-1408, doi:10.1038/3992 (1998).

260 Ho, D. D. *et al.* Rapid turnover of plasma virions and CD4 lymphocytes in HIV-1 infection. *Nature* **373**, 123-126, doi:10.1038/373123a0 (1995).

261 Hoffman, N. G., Seillier-Moiseiwitsch, F., Ahn, J., Walker, J. M. & Swanstrom, R.

Variability in the human immunodeficiency virus type 1 gp120 Env protein linked to phenotype-associated changes in the V3 loop. *Journal of virology* **76**, 3852-3864 (2002).

262 Hoffman, T. L. & Doms, R. W. HIV-1 envelope determinants for cell tropism and chemokine receptor use. *Molecular membrane biology* **16**, 57-65 (1999).

263 Hofmann-Lehmann, R. *et al.* Sensitive and robust one-tube real-time reverse transcriptase-polymerase chain reaction to quantify SIV RNA load: comparison of one- versus two-enzyme systems. *AIDS research and human retroviruses* **16**, 1247-1257, doi:10.1089/08892220050117014 (2000).

264 Holden, L. G. *et al.* Crystal structure of the anti-viral APOBEC3G catalytic domain and functional implications. *Nature* **456**, 121-124, doi:10.1038/nature07357 (2008).

265 Holmes, R. K., Koning, F. A., Bishop, K. N. & Malim, M. H. APOBEC3F can inhibit the accumulation of HIV-1 reverse transcription products in the absence of hypermutation. Comparisons with APOBEC3G. *The Journal of biological chemistry* **282**, 2587-2595, doi:10.1074/jbc.M607298200 (2007).

266 Holmes, R. K., Malim, M. H. & Bishop, K. N. APOBEC-mediated viral restriction: not simply editing? *Trends in biochemical sciences* **32**, 118-128, doi:10.1016/j.tibs.2007.01.004 (2007).

267 Hope, T. J., Huang, X. J., McDonald, D. & Parslow, T. G. Steroid-receptor fusion of the human immunodeficiency virus type 1 Rev transactivator: mapping cryptic functions of the arginine-rich motif. *Proceedings of the National Academy of Sciences of the United States of America* **87**, 7787-7791 (1990).

268 Hope, T. J., McDonald, D., Huang, X. J., Low, J. & Parslow, T. G. Mutational analysis of the human immunodeficiency virus type 1 Rev transactivator: essential residues near the amino terminus. *Journal of virology* **64**, 5360-5366 (1990).

269 Horton, R., Spearman, P. & Ratner, L. HIV-2 viral protein X association with the GAG p27 capsid protein. *Virology* **199**, 453-457, doi:10.1006/viro.1994.1144 (1994).

270 Hout, D. R. *et al.* A single amino acid substitution within the transmembrane domain of the human immunodeficiency virus type 1 Vpu protein renders simian-human immunodeficiency virus (SHIV(KU-1bMC33)) susceptible to rimantadine. *Virology* **348**, 449-461, doi:10.1016/j.virol.2005.12.025 (2006).

271 Hout, D. R. *et al.* Substitution of the transmembrane domain of Vpu in simian-human immunodeficiency virus (SHIVKU1bMC33) with that of M2 of influenza A results in a virus that is sensitive to inhibitors of the M2 ion channel and is pathogenic for pig-tailed macaques. *Virology* **344**, 541-559, doi:10.1016/j.virol.2005.08.022 (2006).

272 Hsu, K., Seharaseyon, J., Dong, P., Bour, S. & Marban, E. Mutual functional destruction of HIV-1 Vpu and host TASK-1 channel. *Molecular cell* **14**, 259-267 (2004).

273 Hua, J. & Cullen, B. R. Human immunodeficiency virus types 1 and 2 and simian immunodeficiency virus Nef use distinct but overlapping target sites for downregulation of cell surface CD4. *Journal of virology* **71**, 6742-6748 (1997).

274 Hulme, A. E., Bogerd, H. P., Cullen, B. R. & Moran, J. V. Selective inhibition of Alu retrotransposition by APOBEC3G. *Gene* **390**, 199-205, doi:10.1016/j.gene.2006.08.032 (2007).

275 Huthoff, H. & Malim, M. H. Identification of amino acid residues in APOBEC3G required

for regulation by human immunodeficiency virus type 1 Vif and Virion encapsidation. *Journal of virology* **81**, 3807-3815, doi:10.1128/JVI.02795-06 (2007).

276 Ichiyanagi, K., Nakajima, R., Kajikawa, M. & Okada, N. Novel retrotransposon analysis reveals multiple mobility pathways dictated by hosts. *Genome research* **17**, 33-41, doi:10.1101/gr.5542607 (2007).

277 Inoshima, Y. *et al.* Roles of the auxiliary genes and AP-1 binding site in the long terminal repeat of feline immunodeficiency virus in the early stage of infection in cats. *Journal of virology* **70**, 8518-8526 (1996).

278 Ishikawa, J. *et al.* Molecular cloning and chromosomal mapping of a bone marrow stromal cell surface gene, BST2, that may be involved in pre-B-cell growth. *Genomics* **26**, 527-534 (1995).

279 Ishikawa, K. *et al.* Improved detection of HIV-2 proviral DNA in dually seroreactive individuals by PCR. *AIDS* **12**, 1419-1425 (1998).

280 Iskow, R. C. *et al.* Natural mutagenesis of human genomes by endogenous retrotransposons. *Cell* **141**, 1253-1261, doi:10.1016/j.cell.2010.05.020 (2010).

281 Iwatani, Y. *et al.* Deaminase-independent inhibition of HIV-1 reverse transcription by APOBEC3G. *Nucleic acids research* **35**, 7096-7108, doi:10.1093/nar/gkm750 (2007).

282 Iwatani, Y., Takeuchi, H., Strebel, K. & Levin, J. G. Biochemical activities of highly purified, catalytically active human APOBEC3G: correlation with antiviral effect. *Journal of virology* **80**, 5992-6002, doi:10.1128/JVI.02680-05 (2006).

283 Jabbar, M. A. & Nayak, D. P. Intracellular interaction of human immunodeficiency virus type 1 (ARV-2) envelope glycoprotein gp160 with CD4 blocks the movement and

maturation of CD4 to the plasma membrane. *Journal of virology* **64**, 6297-6304 (1990).

284 Jacquot, G. *et al.* Localization of HIV-1 Vpr to the nuclear envelope: impact on Vpr functions and virus replication in macrophages. *Retrovirology* **4**, 84, doi:10.1186/1742-4690-4-84 (2007).

285 Jakobsen, M. R. *et al.* Transmission of HIV-1 drug-resistant variants: prevalence and effect on treatment outcome. *Clinical infectious diseases : an official publication of the Infectious Diseases Society of America* **50**, 566-573, doi:10.1086/650001 (2010).

286 Janardhan, A., Swigut, T., Hill, B., Myers, M. P. & Skowronski, J. HIV-1 Nef binds the DOCK2-ELMO1 complex to activate rac and inhibit lymphocyte chemotaxis. *PLoS biology* **2**, E6, doi:10.1371/journal.pbio.0020006 (2004).

287 Janini, M., Rogers, M., Birx, D. R. & McCutchan, F. E. Human immunodeficiency virus type 1 DNA sequences genetically damaged by hypermutation are often abundant in patient peripheral blood mononuclear cells and may be generated during near-simultaneous infection and activation of CD4(+) T cells. *Journal of virology* **75**, 7973-7986 (2001).

288 Jarmuz, A. *et al.* An anthropoid-specific locus of orphan C to U RNA-editing enzymes on chromosome 22. *Genomics* **79**, 285-296, doi:10.1006/geno.2002.6718 (2002).

289 Jarmuz, A. *et al.* An anthropoid-specific locus of orphan C to U RNA-editing enzymes on chromosome 22. *Genomics* **79**, 285-296, doi:10.1006/geno.2002.6718 (2002).

290 Jern, P., Russell, R. A., Pathak, V. K. & Coffin, J. M. Likely role of APOBEC3G-mediated G-to-A mutations in HIV-1 evolution and drug resistance. *PLoS pathogens* **5**, e1000367, doi:10.1371/journal.ppat.1000367 (2009).

291 Jin, J., Arias, E. E., Chen, J., Harper, J. W. & Walter, J. C. A family of diverse Cul4-Ddb1-interacting proteins includes Cdt2, which is required for S phase destruction of the replication factor Cdt1. *Molecular cell* **23**, 709-721, doi:10.1016/j.molcel.2006.08.010 (2006).

292 Joag, S. V. *et al.* Animal model of mucosally transmitted human immunodeficiency virus type 1 disease: intravaginal and oral deposition of simian/human immunodeficiency virus in macaques results in systemic infection, elimination of CD4+ T cells, and AIDS. *Journal of virology* **71**, 4016-4023 (1997).

293 Joag, S. V. *et al.* Characterization of the pathogenic KU-SHIV model of acquired immunodeficiency syndrome in macaques. *AIDS research and human retroviruses* **13**, 635-645 (1997).

294 Joag, S. V. *et al.* Chimeric SHIV that causes CD4+ T cell loss and AIDS in rhesus macaques. *Journal of medical primatology* **27**, 59-64 (1998).

295 Joag, S. V., Stephens, E. B., Adams, R. J., Foresman, L. & Narayan, O. Pathogenesis of SIVmac infection in Chinese and Indian rhesus macaques: effects of splenectomy on virus burden. *Virology* **200**, 436-446, doi:10.1006/viro.1994.1207 (1994).

296 Jonckheere, H., Anne, J. & De Clercq, E. The HIV-1 reverse transcription (RT) process as target for RT inhibitors. *Medicinal research reviews* **20**, 129-154 (2000).

297 Jonsson, S. R. *et al.* Evolutionarily conserved and non-conserved retrovirus restriction activities of artiodactyl APOBEC3F proteins. *Nucleic acids research* **34**, 5683-5694, doi:10.1093/nar/gkl721 (2006).

298 Jordan, A., Defechereux, P. & Verdin, E. The site of HIV-1 integration in the human

genome determines basal transcriptional activity and response to Tat transactivation. *The EMBO journal* **20**, 1726-1738, doi:10.1093/emboj/20.7.1726 (2001).

299 Jowett, J. B. *et al.* The human immunodeficiency virus type 1 vpr gene arrests infected T cells in the G2 + M phase of the cell cycle. *Journal of virology* **69**, 6304-6313 (1995).

300 Ju, S. M. *et al.* Extracellular HIV-1 Tat up-regulates expression of matrix metalloproteinase-9 via a MAPK-NF-kappaB dependent pathway in human astrocytes. *Experimental & molecular medicine* **41**, 86-93 (2009).

301 Jurka, J. Sequence patterns indicate an enzymatic involvement in integration of mammalian retroposons. *Proceedings of the National Academy of Sciences of the United States of America* **94**, 1872-1877 (1997).

302 Kahn, S. A. & Kirschner, B. S. Massive intestinal bleeding in a child with superior mesenteric artery aneurysm and gastrointestinal tuberculosis. *J Pediatr Gastroenterol Nutr* **43**, 256-259, doi:10.1097/01.mpg.0000221904.68781.03 (2006).

303 Kahn, S. E. *et al.* Glycemic durability of rosiglitazone, metformin, or glyburide monotherapy. *The New England journal of medicine* **355**, 2427-2443, doi:10.1056/NEJMoa066224 (2006).

304 Kahn, S. E., Hull, R. L. & Utzschneider, K. M. Mechanisms linking obesity to insulin resistance and type 2 diabetes. *Nature* **444**, 840-846, doi:10.1038/nature05482 (2006).

305 Kahn, S. E. *et al.* Obesity is a major determinant of the association of C-reactive protein levels and the metabolic syndrome in type 2 diabetes. *Diabetes* **55**, 2357-2364, doi:10.2337/db06-0116 (2006).

306 Kahn, S. M. Making technology familiar: orthodox Jews and infertility support, advice,

and inspiration. *Culture, medicine and psychiatry* **30**, 467-480, doi:10.1007/s11013-006-9029-8 (2006).

307 Kahn, S. R. Frequency and determinants of the postthrombotic syndrome after venous thromboembolism. *Curr Opin Pulm Med* **12**, 299-303, doi:10.1097/01.mcp.0000239543.40078.17 (2006).

308 Kahn, S. R. The post-thrombotic syndrome: progress and pitfalls. *Br J Haematol* **134**, 357-365, doi:10.1111/j.1365-2141.2006.06200.x (2006).

309 Kahn, S. R. Review: horse chestnut seed extract is effective for symptoms of chronic venous insufficiency. *ACP J Club* **145**, 20 (2006).

310 Kahn, S. R., Desmarais, S., Ducruet, T., Arsenault, L. & Ginsberg, J. S. Comparison of the Villalta and Ginsberg clinical scales to diagnose the post-thrombotic syndrome: correlation with patient-reported disease burden and venous valvular reflux. *J Thromb Haemost* **4**, 907-908, doi:10.1111/j.1538-7836.2006.01824.x (2006).

311 Kahn, S. R. *et al.* VEINES-QOL/Sym questionnaire was a reliable and valid disease-specific quality of life measure for deep venous thrombosis. *Journal of clinical epidemiology* **59**, 1049-1056, doi:10.1016/j.jclinepi.2005.10.016 (2006).

312 Kahn, S. R. *et al.* Multicenter evaluation of the use of venous thromboembolism prophylaxis in acutely ill medical patients in Canada. *Thromb Res* **119**, 145-155, doi:10.1016/j.thromres.2006.01.011 (2007).

313 Kahn, S. T., Flowers, C., Lechowicz, M. J., Hollenbach, K. & Johnstone, P. A. Value of PET restaging after chemotherapy for non-Hodgkin's lymphoma: implications for consolidation radiotherapy. *International journal of radiation oncology, biology, physics*

66, 961-965, doi:10.1016/j.ijrobp.2006.07.1365 (2006).

314 Kamura, T. *et al.* The Elongin BC complex interacts with the conserved SOCS-box motif present in members of the SOCS, ras, WD-40 repeat, and ankyrin repeat families. *Genes & development* **12**, 3872-3881 (1998).

315 Kao, S. *et al.* The human immunodeficiency virus type 1 Vif protein reduces intracellular expression and inhibits packaging of APOBEC3G (CEM15), a cellular inhibitor of virus infectivity. *Journal of virology* **77**, 11398-11407 (2003).

316 Kappes, J. C. *et al.* Intracellular transport and virion incorporation of vpx requires interaction with other virus type-specific components. *Virology* **193**, 222-233, doi:10.1006/viro.1993.1118 (1993).

317 Kar, A. K., Diaz-Griffero, F., Li, Y., Li, X. & Sodroski, J. Biochemical and biophysical characterization of a chimeric TRIM21-TRIM5alpha protein. *Journal of virology* **82**, 11669-11681, doi:10.1128/JVI.01559-08 (2008).

318 Karlsson, G. B. *et al.* Characterization of molecularly cloned simian-human immunodeficiency viruses causing rapid CD4+ lymphocyte depletion in rhesus monkeys. *Journal of virology* **71**, 4218-4225 (1997).

319 Kataropoulou, A. *et al.* Mutational analysis of the HIV-1 auxiliary protein Vif identifies independent domains important for the physical and functional interaction with HIV-1 reverse transcriptase. *Nucleic acids research* **37**, 3660-3669, doi:10.1093/nar/gkp226 (2009).

320 Kaul, M., Garden, G. A. & Lipton, S. A. Pathways to neuronal injury and apoptosis in HIV-associated dementia. *Nature* **410**, 988-994, doi:10.1038/35073667 (2001).

321 Kawamura, M., Sakai, H. & Adachi, A. Human immunodeficiency virus Vpx is required for the early phase of replication in peripheral blood mononuclear cells. *Microbiology and immunology* **38**, 871-878 (1994).

322 Kazazian, H. H., Jr. Mobile elements: drivers of genome evolution. *Science* **303**, 1626-1632, doi:10.1126/science.1089670 (2004).

323 Keckesova, Z., Ylinen, L. M. & Towers, G. J. The human and African green monkey TRIM5alpha genes encode Ref1 and Lv1 retroviral restriction factor activities. *Proceedings of the National Academy of Sciences of the United States of America* **101**, 10780-10785, doi:10.1073/pnas.0402474101 (2004).

324 Keele, B. F. *et al.* Chimpanzee reservoirs of pandemic and nonpandemic HIV-1. *Science* **313**, 523-526, doi:10.1126/science.1126531 (2006).

325 Kew, O. M., Sutter, R. W., de Gourville, E. M., Dowdle, W. R. & Pallansch, M. A. Vaccine-derived polioviruses and the endgame strategy for global polio eradication. *Annual review of microbiology* **59**, 587-635, doi:10.1146/annurev.micro.58.030603.123625 (2005).

326 Khan, M. A. *et al.* Encapsidation of APOBEC3G into HIV-1 virions involves lipid raft association and does not correlate with APOBEC3G oligomerization. *Retrovirology* **6**, 99, doi:10.1186/1742-4690-6-99 (2009).

327 Kidd, J. M., Newman, T. L., Tuzun, E., Kaul, R. & Eichler, E. E. Population stratification of a common APOBEC gene deletion polymorphism. *PLoS genetics* **3**, e63, doi:10.1371/journal.pgen.0030063 (2007).

328 Kijak, G. H. *et al.* Variable contexts and levels of hypermutation in HIV-1 proviral

genomes recovered from primary peripheral blood mononuclear cells. *Virology* **376**, 101-111, doi:10.1016/j.virol.2008.03.017 (2008).

329 Kilareski, E. M., Shah, S., Nonnemacher, M. R. & Wigdahl, B. Regulation of HIV-1 transcription in cells of the monocyte-macrophage lineage. *Retrovirology* **6**, 118, doi:10.1186/1742-4690-6-118 (2009).

330 Kim, E. Y. *et al.* Retroviral recombination in vivo: viral replication patterns and genetic structure of simian immunodeficiency virus (SIV) populations in rhesus macaques after simultaneous or sequential intravaginal inoculation with SIVmac239Deltavpx/Deltavpr and SIVmac239Deltanef. *Journal of virology* **79**, 4886-4895, doi:10.1128/JVI.79.8.4886-4895.2005 (2005).

331 Kirchhoff, F., Greenough, T. C., Brettler, D. B., Sullivan, J. L. & Desrosiers, R. C. Brief report: absence of intact nef sequences in a long-term survivor with nonprogressive HIV-1 infection. *The New England journal of medicine* **332**, 228-232, doi:10.1056/NEJM199501263320405 (1995).

332 Kirchhoff, F. *et al.* Nef proteins from simian immunodeficiency virus-infected chimpanzees interact with p21-activated kinase 2 and modulate cell surface expression of various human receptors. *Journal of virology* **78**, 6864-6874, doi:10.1128/JVI.78.13.6864-6874.2004 (2004).

333 Kobayashi, M., Takaori-Kondo, A., Miyauchi, Y., Iwai, K. & Uchiyama, T. Ubiquitination of APOBEC3G by an HIV-1 Vif-Cullin5-Elongin B-Elongin C complex is essential for Vif function. *The Journal of biological chemistry* **280**, 18573-18578, doi:10.1074/jbc.C500082200 (2005).

334 Kochendoerfer, G. G. *et al.* Functional characterization and NMR spectroscopy on full-length Vpu from HIV-1 prepared by total chemical synthesis. *Journal of the American Chemical Society* **126**, 2439-2446, doi:10.1021/ja038985i (2004).

335 Kock, J. & Blum, H. E. Hypermutation of hepatitis B virus genomes by APOBEC3G, APOBEC3C and APOBEC3H. *The Journal of general virology* **89**, 1184-1191, doi:10.1099/vir.0.83507-0 (2008).

336 Komatsu, A., Nagasaki, K., Fujimori, M., Amano, J. & Miki, Y. Identification of novel deletion polymorphisms in breast cancer. *International journal of oncology* **33**, 261-270 (2008).

337 Kondo, E., Mammano, F., Cohen, E. A. & Gottlinger, H. G. The p6gag domain of human immunodeficiency virus type 1 is sufficient for the incorporation of Vpr into heterologous viral particles. *Journal of virology* **69**, 2759-2764 (1995).

338 Koning, F. A. *et al.* Defining APOBEC3 expression patterns in human tissues and hematopoietic cell subsets. *Journal of virology* **83**, 9474-9485, doi:10.1128/JVI.01089-09 (2009).

339 Korin, Y. D. & Zack, J. A. Progression to the G1b phase of the cell cycle is required for completion of human immunodeficiency virus type 1 reverse transcription in T cells. *Journal of virology* **72**, 3161-3168 (1998).

340 Koulinska, I. N., Chaplin, B., Mwakagile, D., Essex, M. & Renjifo, B. Hypermutation of HIV type 1 genomes isolated from infants soon after vertical infection. *AIDS research and human retroviruses* **19**, 1115-1123, doi:10.1089/088922203771881211 (2003).

341 Kozak, S. L., Marin, M., Rose, K. M., Bystrom, C. & Kabat, D. The anti-HIV-1 editing

enzyme APOBEC3G binds HIV-1 RNA and messenger RNAs that shuttle between polysomes and stress granules. *The Journal of biological chemistry* **281**, 29105-29119, doi:10.1074/jbc.M601901200 (2006).

342 Kramer, M. S. *et al.* Intra- and interobserver agreement and statistical clustering of placental histopathologic features relevant to preterm birth. *Am J Obstet Gynecol* **195**, 1674-1679, doi:10.1016/j.ajog.2006.03.095 (2006).

343 Kreisberg, J. F., Yonemoto, W. & Greene, W. C. Endogenous factors enhance HIV infection of tissue naive CD4 T cells by stimulating high molecular mass APOBEC3G complex formation. *The Journal of experimental medicine* **203**, 865-870, doi:10.1084/jem.20051856 (2006).

344 Kriegs, J. O., Churakov, G., Jurka, J., Brosius, J. & Schmitz, J. Evolutionary history of 7SL RNA-derived SINEs in Supraprimates. *Trends in genetics : TIG* **23**, 158-161, doi:10.1016/j.tig.2007.02.002 (2007).

345 Kristbjornsdottir, H. B. *et al.* The vif gene of maedi-visna virus is essential for infectivity in vivo and in vitro. *Virology* **318**, 350-359, doi:10.1016/j.virol.2003.09.044 (2004).

346 Krudys, K. M., Kahn, S. E. & Vicini, P. Population approaches to estimate minimal model indexes of insulin sensitivity and glucose effectiveness using full and reduced sampling schedules. *Am J Physiol Endocrinol Metab* **291**, E716-723, doi:10.1152/ajpendo.00346.2005 (2006).

347 Kruger, J. & Fischer, W. B. Structural implications of mutations assessed by molecular dynamics: Vpu1-32 from HIV-1. *European biophysics journal : EBJ* **39**, 1069-1077, doi:10.1007/s00249-009-0487-0 (2010).

348 Kruger, J. & Fischer, W. B. Structural implications of mutations assessed by molecular dynamics: Vpu1-32 from HIV-1. *European biophysics journal : EBJ* **39**, 1069-1077, doi:10.1007/s00249-009-0487-0 (2010).

349 Kubota, S. *et al.* Functional similarity of HIV-I rev and HTLV-I rex proteins: identification of a new nucleolar-targeting signal in rev protein. *Biochemical and biophysical research communications* **162**, 963-970 (1989).

350 Kupzig, S. *et al.* Bst-2/HM1.24 is a raft-associated apical membrane protein with an unusual topology. *Traffic* **4**, 694-709 (2003).

351 Lander, E. S. *et al.* Initial sequencing and analysis of the human genome. *Nature* **409**, 860-921, doi:10.1038/35057062 (2001).

352 Landry, J. R., Medstrand, P. & Mager, D. L. Repetitive elements in the 5' untranslated region of a human zinc-finger gene modulate transcription and translation efficiency. *Genomics* **76**, 110-116, doi:10.1006/geno.2001.6604 (2001).

353 Lang, S. M. *et al.* Importance of vpr for infection of rhesus monkeys with simian immunodeficiency virus. *Journal of virology* **67**, 902-912 (1993).

354 Langelier, C. R. *et al.* Biochemical characterization of a recombinant TRIM5alpha protein that restricts human immunodeficiency virus type 1 replication. *Journal of virology* **82**, 11682-11694, doi:10.1128/JVI.01562-08 (2008).

355 Langley, C. L. *et al.* HIV-1, HIV-2, human papillomavirus infection and cervical neoplasia in high-risk African women. *AIDS* **10**, 413-417 (1996).

356 Langlois, M. A., Beale, R. C., Conticello, S. G. & Neuberger, M. S. Mutational comparison of the single-domained APOBEC3C and double-domained APOBEC3F/G

anti-retroviral cytidine deaminases provides insight into their DNA target site specificities. *Nucleic acids research* **33**, 1913-1923, doi:10.1093/nar/gki343 (2005).

357 LaRue, R. S. *et al.* The artiodactyl APOBEC3 innate immune repertoire shows evidence for a multi-functional domain organization that existed in the ancestor of placental mammals. *BMC molecular biology* **9**, 104, doi:10.1186/1471-2199-9-104 (2008).

358 Laurent-Crawford, A. G. & Hovanessian, A. G. Characterization of the Nef protein in HIV1-infected CEM cells. *Research in virology* **143**, 59-62 (1992).

359 Lavie, L., Maldener, E., Brouha, B., Meese, E. U. & Mayer, J. The human L1 promoter: variable transcription initiation sites and a major impact of upstream flanking sequence on promoter activity. *Genome research* **14**, 2253-2260, doi:10.1101/gr.2745804 (2004).

360 Le Rouzic, E. & Benichou, S. The Vpr protein from HIV-1: distinct roles along the viral life cycle. *Retrovirology* **2**, 11, doi:10.1186/1742-4690-2-11 (2005).

361 Le Tortorec, A. & Neil, S. J. Antagonism to and intracellular sequestration of human tetherin by the human immunodeficiency virus type 2 envelope glycoprotein. *Journal of virology* **83**, 11966-11978, doi:10.1128/JVI.01515-09 (2009).

362 Lecossier, D., Bouchonnet, F., Clavel, F. & Hance, A. J. Hypermutation of HIV-1 DNA in the absence of the Vif protein. *Science* **300**, 1112, doi:10.1126/science.1083338 (2003).

363 Lee, Y. N. & Bieniasz, P. D. Reconstitution of an infectious human endogenous retrovirus. *PLoS pathogens* **3**, e10, doi:10.1371/journal.ppat.0030010 (2007).

364 Li, J., Potash, M. J. & Volsky, D. J. Functional domains of APOBEC3G required for antiviral activity. *Journal of cellular biochemistry* **92**, 560-572, doi:10.1002/jcb.20082 (2004).

365 Li, J. C., Lee, D. C., Cheung, B. K. & Lau, A. S. Mechanisms for HIV Tat upregulation of IL-10 and other cytokine expression: kinase signaling and PKR-mediated immune response. *FEBS letters* **579**, 3055-3062, doi:10.1016/j.febslet.2005.04.060 (2005).

366 Li, L., Liang, D., Li, J. Y. & Zhao, R. Y. APOBEC3G-UBA2 fusion as a potential strategy for stable expression of APOBEC3G and inhibition of HIV-1 replication. *Retrovirology* **5**, 72, doi:10.1186/1742-4690-5-72 (2008).

367 Li, M. M., Wu, L. I. & Emerman, M. The range of human APOBEC3H sensitivity to lentiviral Vif proteins. *Journal of virology* **84**, 88-95, doi:10.1128/JVI.01344-09 (2010).

368 Li, X. Y., Guo, F., Zhang, L., Kleiman, L. & Cen, S. APOBEC3G inhibits DNA strand transfer during HIV-1 reverse transcription. *The Journal of biological chemistry* **282**, 32065-32074, doi:10.1074/jbc.M703423200 (2007).

369 Liao, G. Q. *et al.* [Maxilla reconstruction with the free iliac osteomuscular flap and simultaneous osseointegrated implant embeding]. *Zhonghua zheng xing wai ke za zhi = Zhonghua zhengxing waike zazhi = Chinese journal of plastic surgery* **20**, 457-460 (2004).

370 Liddament, M. T., Brown, W. L., Schumacher, A. J. & Harris, R. S. APOBEC3F properties and hypermutation preferences indicate activity against HIV-1 in vivo. *Current biology : CB* **14**, 1385-1391, doi:10.1016/j.cub.2004.06.050 (2004).

371 Lindwasser, O. W. *et al.* A diacidic motif in human immunodeficiency virus type 1 Nef is a novel determinant of binding to AP-2. *Journal of virology* **82**, 1166-1174, doi:10.1128/JVI.01874-07 (2008).

372 Liu, B., Yu, X., Luo, K., Yu, Y. & Yu, X. F. Influence of primate lentiviral Vif and

proteasome inhibitors on human immunodeficiency virus type 1 virion packaging of APOBEC3G. *Journal of virology* **78**, 2072-2081 (2004).

373 Liu, H. *et al.* Transvection mediated by the translocated cyclin D1 locus in mantle cell lymphoma. *The Journal of experimental medicine* **205**, 1843-1858, doi:10.1084/jem.20072102 (2008).

374 Liu, Z. Q. *et al.* Derivation and biological characterization of a molecular clone of SHIV(KU-2) that causes AIDS, neurological disease, and renal disease in rhesus macaques. *Virology* **260**, 295-307, doi:10.1006/viro.1999.9812 (1999).

375 Lockridge, K. M., Himathongkham, S., Sawai, E. T., Chienand, M. & Sparger, E. E. The feline immunodeficiency virus vif gene is required for productive infection of feline peripheral blood mononuclear cells and monocyte-derived macrophages. *Virology* **261**, 25-30, doi:10.1006/viro.1999.9831 (1999).

376 Lohman, B. L. *et al.* A partially attenuated simian immunodeficiency virus induces host immunity that correlates with resistance to pathogenic virus challenge. *Journal of virology* **68**, 7021-7029 (1994).

377 Lu, Y. L., Bennett, R. P., Wills, J. W., Gorelick, R. & Ratner, L. A leucine triplet repeat sequence (LXX)4 in p6gag is important for Vpr incorporation into human immunodeficiency virus type 1 particles. *Journal of virology* **69**, 6873-6879 (1995).

378 Luban, J. Cyclophilin A, TRIM5, and resistance to human immunodeficiency virus type 1 infection. *Journal of virology* **81**, 1054-1061, doi:10.1128/JVI.01519-06 (2007).

379 Lundquist, C. A., Tobiume, M., Zhou, J., Unutmaz, D. & Aiken, C. Nef-mediated downregulation of CD4 enhances human immunodeficiency virus type 1 replication in

primary T lymphocytes. *Journal of virology* **76**, 4625-4633 (2002).

380 Luo, K. *et al.* Amino-terminal region of the human immunodeficiency virus type 1 nucleocapsid is required for human APOBEC3G packaging. *Journal of virology* **78**, 11841-11852, doi:10.1128/JVI.78.21.11841-11852.2004 (2004).

381 Luo, K. *et al.* Cytidine deaminases APOBEC3G and APOBEC3F interact with human immunodeficiency virus type 1 integrase and inhibit proviral DNA formation. *Journal of virology* **81**, 7238-7248, doi:10.1128/JVI.02584-06 (2007).

382 Luo, K. *et al.* Primate lentiviral virion infectivity factors are substrate receptors that assemble with cullin 5-E3 ligase through a HCCH motif to suppress APOBEC3G. *Proceedings of the National Academy of Sciences of the United States of America* **102**, 11444-11449, doi:10.1073/pnas.0502440102 (2005).

383 Luo, T., Livingston, R. A. & Garcia, J. V. Infectivity enhancement by human immunodeficiency virus type 1 Nef is independent of its association with a cellular serine/threonine kinase. *Journal of virology* **71**, 9524-9530 (1997).

384 Ma, X. & Montaner, L. J. Proinflammatory response and IL-12 expression in HIV-1 infection. *Journal of leukocyte biology* **68**, 383-390 (2000).

385 Madani, N. & Kabat, D. An endogenous inhibitor of human immunodeficiency virus in human lymphocytes is overcome by the viral Vif protein. *Journal of virology* **72**, 10251-10255 (1998).

386 Madsen, P. *et al.* Psoriasis upregulated phorbolin-1 shares structural but not functional similarity to the mRNA-editing protein apobec-1. *The Journal of investigative dermatology* **113**, 162-169, doi:10.1046/j.1523-1747.1999.00682.x (1999).

387 Magnuson, D. S., Knudsen, B. E., Geiger, J. D., Brownstone, R. M. & Nath, A. Human immunodeficiency virus type 1 tat activates non-N-methyl-D-aspartate excitatory amino acid receptors and causes neurotoxicity. *Annals of neurology* **37**, 373-380, doi:10.1002/ana.410370314 (1995).

388 Mahalingam, S. *et al.* Functional analysis of the simian immunodeficiency virus Vpx protein: identification of packaging determinants and a novel nuclear targeting domain. *Journal of virology* **75**, 362-374, doi:10.1128/JVI.75.1.362-374.2001 (2001).

389 Mahieux, R. *et al.* Extensive editing of a small fraction of human T-cell leukemia virus type 1 genomes by four APOBEC3 cytidine deaminases. *The Journal of general virology* **86**, 2489-2494, doi:10.1099/vir.0.80973-0 (2005).

390 Mahlknecht, U., Dichamp, I., Varin, A., Van Lint, C. & Herbein, G. NF-kappaB-dependent control of HIV-1 transcription by the second coding exon of Tat in T cells. *Journal of leukocyte biology* **83**, 718-727, doi:10.1189/jlb.0607405 (2008).

391 Majumder, B. *et al.* Human immunodeficiency virus type 1 Vpr impairs dendritic cell maturation and T-cell activation: implications for viral immune escape. *Journal of virology* **79**, 7990-8003, doi:10.1128/JVI.79.13.7990-8003.2005 (2005).

392 Maksakova, I. A. *et al.* Retroviral elements and their hosts: insertional mutagenesis in the mouse germ line. *PLoS genetics* **2**, e2, doi:10.1371/journal.pgen.0020002 (2006).

393 Malim, M. H., Bohnlein, S., Hauber, J. & Cullen, B. R. Functional dissection of the HIV-1 Rev trans-activator--derivation of a trans-dominant repressor of Rev function. *Cell* **58**, 205-214 (1989).

394 Malim, M. H. & Cullen, B. R. HIV-1 structural gene expression requires the binding of

multiple Rev monomers to the viral RRE: implications for HIV-1 latency. *Cell* **65**, 241-248 (1991).

395 Malim, M. H., McCarn, D. F., Tiley, L. S. & Cullen, B. R. Mutational definition of the human immunodeficiency virus type 1 Rev activation domain. *Journal of virology* **65**, 4248-4254 (1991).

396 Mangasarian, A. *et al.* The HIV-1 Nef protein acts as a connector with sorting pathways in the Golgi and at the plasma membrane. *Immunity* **6**, 67-77 (1997).

397 Mangeat, B. *et al.* Broad antiretroviral defence by human APOBEC3G through lethal editing of nascent reverse transcripts. *Nature* **424**, 99-103, doi:10.1038/nature01709 (2003).

398 Mangeat, B., Turelli, P., Liao, S. & Trono, D. A single amino acid determinant governs the species-specific sensitivity of APOBEC3G to Vif action. *The Journal of biological chemistry* **279**, 14481-14483, doi:10.1074/jbc.C400060200 (2004).

399 Marcario, J. K. *et al.* Effect of morphine on the neuropathogenesis of SIVmac infection in Indian Rhesus Macaques. *Journal of neuroimmune pharmacology : the official journal of the Society on NeuroImmune Pharmacology* **3**, 12-25, doi:10.1007/s11481-007-9085-z (2008).

400 Marchand, C., Johnson, A. A., Semenova, E. & Pommier, Y. Mechanisms and inhibition of HIV integration. *Drug discovery today. Disease mechanisms* **3**, 253-260, doi:10.1016/j.ddmec.2006.05.004 (2006).

401 Margottin, F. *et al.* Interaction between the cytoplasmic domains of HIV-1 Vpu and CD4: role of Vpu residues involved in CD4 interaction and in vitro CD4 degradation. *Virology*

223, 381-386, doi:10.1006/viro.1996.0491 (1996).

402 Margottin, F. *et al.* A novel human WD protein, h-beta TrCp, that interacts with HIV-1 Vpu connects CD4 to the ER degradation pathway through an F-box motif. *Molecular cell* **1**, 565-574 (1998).

403 Mariani, R. *et al.* Species-specific exclusion of APOBEC3G from HIV-1 virions by Vif. *Cell* **114**, 21-31 (2003).

404 Marin, M., Rose, K. M., Kozak, S. L. & Kabat, D. HIV-1 Vif protein binds the editing enzyme APOBEC3G and induces its degradation. *Nature medicine* **9**, 1398-1403, doi:10.1038/nm946 (2003).

405 Marthas, M. L. *et al.* Immunization with a live, attenuated simian immunodeficiency virus (SIV) prevents early disease but not infection in rhesus macaques challenged with pathogenic SIV. *Journal of virology* **64**, 3694-3700 (1990).

406 Martin, S. J., Mazdai, G., Strain, J. J., Cotter, T. G. & Hannigan, B. M. Programmed cell death (apoptosis) in lymphoid and myeloid cell lines during zinc deficiency. *Clinical and experimental immunology* **83**, 338-343 (1991).

407 Martin, S. L., Branciforte, D., Keller, D. & Bain, D. L. Trimeric structure for an essential protein in L1 retrotransposition. *Proceedings of the National Academy of Sciences of the United States of America* **100**, 13815-13820, doi:10.1073/pnas.2336221100 (2003).

408 Martin, V. *et al.* History and evolution of HPAI viruses in southeast Asia. *Annals of the New York Academy of Sciences* **1081**, 153-162, doi:10.1196/annals.1373.017 (2006).

409 Masuyama, N. *et al.* HM1.24 is internalized from lipid rafts by clathrin-mediated endocytosis through interaction with alpha-adaptin. *The Journal of biological chemistry*

284, 15927-15941, doi:10.1074/jbc.M109.005124 (2009).

410 Mathias, S. L., Scott, A. F., Kazazian, H. H., Jr., Boeke, J. D. & Gabriel, A. Reverse transcriptase encoded by a human transposable element. *Science* **254**, 1808-1810 (1991).

411 Matsui, M., Warburton, R. J., Cogswell, P. C., Baldwin, A. S., Jr. & Frelinger, J. A. Effects of HIV-1 Tat on expression of HLA class I molecules. *Journal of acquired immune deficiency syndromes and human retrovirology : official publication of the International Retrovirology Association* **11**, 233-240 (1996).

412 Mattaj, I. W. & Englmeier, L. Nucleocytoplasmic transport: the soluble phase. *Annual review of biochemistry* **67**, 265-306, doi:10.1146/annurev.biochem.67.1.265 (1998).

413 Mayol, K., Munier, S., Beck, A., Verrier, B. & Guillon, C. Design and characterization of an HIV-1 Tat mutant: inactivation of viral and cellular functions but not antigenicity. *Vaccine* **25**, 6047-6060, doi:10.1016/j.vaccine.2007.05.048 (2007).

414 Mbisa, J. L. *et al.* Human immunodeficiency virus type 1 cDNAs produced in the presence of APOBEC3G exhibit defects in plus-strand DNA transfer and integration. *Journal of virology* **81**, 7099-7110, doi:10.1128/JVI.00272-07 (2007).

415 McCormick-Davis, C. *et al.* A molecular clone of simian-human immunodeficiency virus (DeltavpuSHIV(KU-1bMC33)) with a truncated, non-membrane-bound vpu results in rapid CD4(+) T cell loss and neuro-AIDS in pig-tailed macaques. *Virology* **272**, 112-126, doi:10.1006/viro.2000.0333 (2000).

416 McCormick-Davis, C., Dalton, S. B., Singh, D. K. & Stephens, E. B. Comparison of Vpu sequences from diverse geographical isolates of HIV type 1 identifies the presence of

highly variable domains, additional invariant amino acids, and a signature sequence motif common to subtype C isolates. *AIDS research and human retroviruses* **16**, 1089-1095, doi:10.1089/08892220050075363 (2000).

417 McCutchan, F. E. Global epidemiology of HIV. *Journal of medical virology* **78 Suppl 1**, S7-S12, doi:10.1002/jmv.20599 (2006).

418 McCutchan, F. E. *et al.* Subtype G and multiple forms of A/G intersubtype recombinant human immunodeficiency virus type 1 in Nigeria. *Virology* **254**, 226-234, doi:10.1006/viro.1998.9505 (1999).

419 Mehle, A., Goncalves, J., Santa-Marta, M., McPike, M. & Gabuzda, D. Phosphorylation of a novel SOCS-box regulates assembly of the HIV-1 Vif-Cul5 complex that promotes APOBEC3G degradation. *Genes & development* **18**, 2861-2866, doi:10.1101/gad.1249904 (2004).

420 Mehle, A. *et al.* Vif overcomes the innate antiviral activity of APOBEC3G by promoting its degradation in the ubiquitin-proteasome pathway. *The Journal of biological chemistry* **279**, 7792-7798, doi:10.1074/jbc.M313093200 (2004).

421 Mehle, A., Thomas, E. R., Rajendran, K. S. & Gabuzda, D. A zinc-binding region in Vif binds Cul5 and determines cullin selection. *The Journal of biological chemistry* **281**, 17259-17265, doi:10.1074/jbc.M602413200 (2006).

422 Mehle, A. *et al.* Identification of an APOBEC3G binding site in human immunodeficiency virus type 1 Vif and inhibitors of Vif-APOBEC3G binding. *Journal of virology* **81**, 13235-13241, doi:10.1128/JVI.00204-07 (2007).

423 Melo, F. & Feytmans, E. Assessing protein structures with a non-local atomic interaction

energy. *Journal of molecular biology* **277**, 1141-1152, doi:10.1006/jmbi.1998.1665 (1998).

424 Mermer, B., Felber, B. K., Campbell, M. & Pavlakis, G. N. Identification of trans-dominant HIV-1 rev protein mutants by direct transfer of bacterially produced proteins into human cells. *Nucleic acids research* **18**, 2037-2044 (1990).

425 Meyer, B. E., Meinkoth, J. L. & Malim, M. H. Nuclear transport of human immunodeficiency virus type 1, visna virus, and equine infectious anemia virus Rev proteins: identification of a family of transferable nuclear export signals. *Journal of virology* **70**, 2350-2359 (1996).

426 Michael, N. L. Host genetic influences on HIV-1 pathogenesis. *Current opinion in immunology* **11**, 466-474, doi:10.1016/S0952-7915(99)80078-8 (1999).

427 Migueles, S. A. *et al.* HIV-specific CD8+ T cell proliferation is coupled to perforin expression and is maintained in nonprogressors. *Nature immunology* **3**, 1061-1068, doi:10.1038/ni845 (2002).

428 Milich, L., Margolin, B. & Swanstrom, R. V3 loop of the human immunodeficiency virus type 1 Env protein: interpreting sequence variability. *Journal of virology* **67**, 5623-5634 (1993).

429 Miller, J. H., Presnyak, V. & Smith, H. C. The dimerization domain of HIV-1 viral infectivity factor Vif is required to block virion incorporation of APOBEC3G. *Retrovirology* **4**, 81, doi:10.1186/1742-4690-4-81 (2007).

430 Miller, M. A. *et al.* Alterations in cell membrane permeability by the lentivirus lytic peptide (LLP-1) of HIV-1 transmembrane protein. *Virology* **196**, 89-100,

doi:10.1006/viro.1993.1457 (1993).

431 Miller, M. D., Farnet, C. M. & Bushman, F. D. Human immunodeficiency virus type 1 preintegration complexes: studies of organization and composition. *Journal of virology* **71**, 5382-5390 (1997).

432 Miller, M. D., Warmerdam, M. T., Gaston, I., Greene, W. C. & Feinberg, M. B. The human immunodeficiency virus-1 nef gene product: a positive factor for viral infection and replication in primary lymphocytes and macrophages. *The Journal of experimental medicine* **179**, 101-113 (1994).

433 Mills, R. E., Bennett, E. A., Iskow, R. C. & Devine, S. E. Which transposable elements are active in the human genome? *Trends in genetics : TIG* **23**, 183-191, doi:10.1016/j.tig.2007.02.006 (2007).

434 Minagar, A. *et al.* HIV-associated dementia, Alzheimer's disease, multiple sclerosis, and schizophrenia: gene expression review. *Journal of the neurological sciences* **224**, 3-17, doi:10.1016/j.jns.2004.06.007 (2004).

435 Mirani, M. *et al.* HIV-1 protein Vpr suppresses IL-12 production from human monocytes by enhancing glucocorticoid action: potential implications of Vpr coactivator activity for the innate and cellular immunity deficits observed in HIV-1 infection. *J Immunol* **169**, 6361-6368 (2002).

436 Mitchell, R. S. *et al.* Vpu antagonizes BST-2-mediated restriction of HIV-1 release via beta-TrCP and endo-lysosomal trafficking. *PLoS pathogens* **5**, e1000450, doi:10.1371/journal.ppat.1000450 (2009).

437 Miyagi, E., Andrew, A. J., Kao, S. & Strebel, K. Vpu enhances HIV-1 virus release in the

absence of Bst-2 cell surface down-modulation and intracellular depletion. *Proceedings of the National Academy of Sciences of the United States of America* **106**, 2868-2873, doi:10.1073/pnas.0813223106 (2009).

438 Miyagi, E. *et al.* Stably expressed APOBEC3F has negligible antiviral activity. *Journal of virology* **84**, 11067-11075, doi:10.1128/JVI.01249-10 (2010).

439 Montavon, C. *et al.* Most env and gag subtype A HIV-1 viruses circulating in West and West Central Africa are similar to the prototype AG recombinant virus IBNG. *J Acquir Immune Defic Syndr* **23**, 363-374 (2000).

440 Moore, J. P. & Nara, P. L. The role of the V3 loop of gp120 in HIV infection. *AIDS* **5 Suppl 2**, S21-33 (1991).

441 Moran, J. V. *et al.* High frequency retrotransposition in cultured mammalian cells. *Cell* **87**, 917-927 (1996).

442 Morris, M. C., Depollier, J., Mery, J., Heitz, F. & Divita, G. A peptide carrier for the delivery of biologically active proteins into mammalian cells. *Nature biotechnology* **19**, 1173-1176, doi:10.1038/nbt1201-1173 (2001).

443 Muckenfuss, H. *et al.* APOBEC3 proteins inhibit human LINE-1 retrotransposition. *The Journal of biological chemistry* **281**, 22161-22172, doi:10.1074/jbc.M601716200 (2006).

444 Mulder, L. C., Harari, A. & Simon, V. Cytidine deamination induced HIV-1 drug resistance. *Proceedings of the National Academy of Sciences of the United States of America* **105**, 5501-5506, doi:10.1073/pnas.0710190105 (2008).

445 Muthumani, K. *et al.* HIV-1 Vpr and anti-inflammatory activity. *DNA and cell biology* **23**, 239-247, doi:10.1089/104454904773819824 (2004).

446 Nabatov, A. A. *et al.* Intrapatient alterations in the human immunodeficiency virus type 1 gp120 V1V2 and V3 regions differentially modulate coreceptor usage, virus inhibition by CC/CXC chemokines, soluble CD4, and the b12 and 2G12 monoclonal antibodies. *Journal of virology* **78**, 524-530 (2004).

447 Narayan, S. V. *et al.* Characterization of a neutralization-escape variant of SHIVKU-1, a virus that causes acquired immune deficiency syndrome in pig-tailed macaques. *Virology* **256**, 54-63, doi:10.1006/viro.1999.9605 (1999).

448 Narvaiza, I. *et al.* Deaminase-independent inhibition of parvoviruses by the APOBEC3A cytidine deaminase. *PLoS pathogens* **5**, e1000439, doi:10.1371/journal.ppat.1000439 (2009).

449 Nath, A., Conant, K., Chen, P., Scott, C. & Major, E. O. Transient exposure to HIV-1 Tat protein results in cytokine production in macrophages and astrocytes. A hit and run phenomenon. *The Journal of biological chemistry* **274**, 17098-17102 (1999).

450 Nathans, R. *et al.* Small-molecule inhibition of HIV-1 Vif. *Nature biotechnology* **26**, 1187-1192, doi:10.1038/nbt.1496 (2008).

451 Navarro, F. *et al.* Complementary function of the two catalytic domains of APOBEC3G. *Virology* **333**, 374-386, doi:10.1016/j.virol.2005.01.011 (2005).

452 Navarro, F. *et al.* Complementary function of the two catalytic domains of APOBEC3G. *Virology* **333**, 374-386, doi:10.1016/j.virol.2005.01.011 (2005).

453 Neer, E. J., Schmidt, C. J., Nambudripad, R. & Smith, T. F. The ancient regulatory-protein family of WD-repeat proteins. *Nature* **371**, 297-300, doi:10.1038/371297a0 (1994).

454 Neil, S. J., Eastman, S. W., Jouvenet, N. & Bieniasz, P. D. HIV-1 Vpu promotes release and prevents endocytosis of nascent retrovirus particles from the plasma membrane. *PLoS pathogens* **2**, e39, doi:10.1371/journal.ppat.0020039 (2006).

455 Neil, S. J., Zang, T. & Bieniasz, P. D. Tetherin inhibits retrovirus release and is antagonized by HIV-1 Vpu. *Nature* **451**, 425-430, doi:10.1038/nature06553 (2008).

456 Nekhai, S., Jerebtsova, M., Jackson, A. & Southerland, W. Regulation of HIV-1 transcription by protein phosphatase 1. *Current HIV research* **5**, 3-9 (2007).

457 Neville, M., Stutz, F., Lee, L., Davis, L. I. & Rosbash, M. The importin-beta family member Crm1p bridges the interaction between Rev and the nuclear pore complex during nuclear export. *Current biology : CB* **7**, 767-775 (1997).

458 Newman, E. N. *et al.* Antiviral function of APOBEC3G can be dissociated from cytidine deaminase activity. *Current biology : CB* **15**, 166-170, doi:10.1016/j.cub.2004.12.068 (2005).

459 Nguyen, D. H., Gummuluru, S. & Hu, J. Deamination-independent inhibition of hepatitis B virus reverse transcription by APOBEC3G. *Journal of virology* **81**, 4465-4472, doi:10.1128/JVI.02510-06 (2007).

460 Niederman, T. M. & Ratner, L. Functional analysis of HIV1 and SIV Nef proteins. *Research in virology* **143**, 43-46 (1992).

461 Niewiadomska, A. M. *et al.* Differential inhibition of long interspersed element 1 by APOBEC3 does not correlate with high-molecular-mass-complex formation or P-body association. *Journal of virology* **81**, 9577-9583, doi:10.1128/JVI.02800-06 (2007).

462 Nigg, E. A. Nucleocytoplasmic transport: signals, mechanisms and regulation. *Nature*

386, 779-787, doi:10.1038/386779a0 (1997).

463 Nisole, S., Lynch, C., Stoye, J. P. & Yap, M. W. A Trim5-cyclophilin A fusion protein found in owl monkey kidney cells can restrict HIV-1. *Proceedings of the National Academy of Sciences of the United States of America* **101**, 13324-13328, doi:10.1073/pnas.0404640101 (2004).

464 Nitahara-Kasahara, Y. *et al.* Novel nuclear import of Vpr promoted by importin alpha is crucial for human immunodeficiency virus type 1 replication in macrophages. *Journal of virology* **81**, 5284-5293, doi:10.1128/JVI.01928-06 (2007).

465 Noguchi, C. *et al.* Dual effect of APOBEC3G on Hepatitis B virus. *The Journal of general virology* **88**, 432-440, doi:10.1099/vir.0.82319-0 (2007).

466 Noguchi, C. *et al.* G to A hypermutation of hepatitis B virus. *Hepatology* **41**, 626-633, doi:10.1002/hep.20580 (2005).

467 Noviello, C. M., Benichou, S. & Guatelli, J. C. Cooperative binding of the class I major histocompatibility complex cytoplasmic domain and human immunodeficiency virus type 1 Nef to the endosomal AP-1 complex via its mu subunit. *Journal of virology* **82**, 1249-1258, doi:10.1128/JVI.00660-07 (2008).

468 O'Neill, E. *et al.* Dynamic evolution of the human immunodeficiency virus type 1 pathogenic factor, Nef. *Journal of virology* **80**, 1311-1320, doi:10.1128/JVI.80.3.1311-1320.2006 (2006).

469 Ogert, R. A. *et al.* N-linked glycosylation sites adjacent to and within the V1/V2 and the V3 loops of dualtropic human immunodeficiency virus type 1 isolate DH12 gp120 affect coreceptor usage and cellular tropism. *Journal of virology* **75**, 5998-6006,

doi:10.1128/JVI.75.13.5998-6006.2001 (2001).

470 OhAinle, M., Kerns, J. A., Li, M. M., Malik, H. S. & Emerman, M. Antiretroelement activity of APOBEC3H was lost twice in recent human evolution. *Cell host & microbe* **4**, 249-259, doi:10.1016/j.chom.2008.07.005 (2008).

471 OhAinle, M., Kerns, J. A., Malik, H. S. & Emerman, M. Adaptive evolution and antiviral activity of the conserved mammalian cytidine deaminase APOBEC3H. *Journal of virology* **80**, 3853-3862, doi:10.1128/JVI.80.8.3853-3862.2006 (2006).

472 Ohtomo, T. *et al.* Molecular cloning and characterization of a surface antigen preferentially overexpressed on multiple myeloma cells. *Biochemical and biophysical research communications* **258**, 583-591, doi:10.1006/bbrc.1999.0683 (1999).

473 Okeoma, C. M., Lovsin, N., Peterlin, B. M. & Ross, S. R. APOBEC3 inhibits mouse mammary tumour virus replication in vivo. *Nature* **445**, 927-930, doi:10.1038/nature05540 (2007).

474 Olsen, H. S., Cochrane, A. W., Dillon, P. J., Nalin, C. M. & Rosen, C. A. Interaction of the human immunodeficiency virus type 1 Rev protein with a structured region in env mRNA is dependent on multimer formation mediated through a basic stretch of amino acids. *Genes & development* **4**, 1357-1364 (1990).

475 Ooms, M., Majdak, S., Seibert, C. W., Harari, A. & Simon, V. The localization of APOBEC3H variants in HIV-1 virions determines their antiviral activity. *Journal of virology* **84**, 7961-7969, doi:10.1128/JVI.00754-10 (2010).

476 Op de Coul, E. L. *et al.* Using phylogenetic analysis to trace HIV-1 migration among western European injecting drug users seroconverting from 1984 to 1997. *AIDS* **15**,

257-266 (2001).

477 Opatrny, L., David, M., Kahn, S. R., Shrier, I. & Rey, E. Association between antiphospholipid antibodies and recurrent fetal loss in women without autoimmune disease: a metaanalysis. *The Journal of rheumatology* **33**, 2214-2221 (2006).

478 Opi, S. *et al.* Human immunodeficiency virus type 1 Vif inhibits packaging and antiviral activity of a degradation-resistant APOBEC3G variant. *Journal of virology* **81**, 8236-8246, doi:10.1128/JVI.02694-06 (2007).

479 Opi, S. *et al.* Monomeric APOBEC3G is catalytically active and has antiviral activity. *Journal of virology* **80**, 4673-4682, doi:10.1128/JVI.80.10.4673-4682.2006 (2006).

480 Osmanov, S., Pattou, C., Walker, N., Schwardlander, B. & Esparza, J. Estimated global distribution and regional spread of HIV-1 genetic subtypes in the year 2000. *J Acquir Immune Defic Syndr* **29**, 184-190 (2002).

481 Ostertag, E. M., Goodier, J. L., Zhang, Y. & Kazazian, H. H., Jr. SVA elements are nonautonomous retrotransposons that cause disease in humans. *American journal of human genetics* **73**, 1444-1451, doi:10.1086/380207 (2003).

482 Ostertag, E. M., Prak, E. T., DeBerardinis, R. J., Moran, J. V. & Kazazian, H. H., Jr. Determination of L1 retrotransposition kinetics in cultured cells. *Nucleic acids research* **28**, 1418-1423 (2000).

483 Ozato, K., Shin, D. M., Chang, T. H. & Morse, H. C., 3rd. TRIM family proteins and their emerging roles in innate immunity. *Nature reviews. Immunology* **8**, 849-860, doi:10.1038/nri2413 (2008).

484 Pagans, S. *et al.* SIRT1 regulates HIV transcription via Tat deacetylation. *PLoS biology*

3, e41, doi:10.1371/journal.pbio.0030041 (2005).

485 Pak, V., Heidecker, G., Pathak, V. K. & Derse, D. The role of amino-terminal sequences in cellular localization and antiviral activity of APOBEC3B. *Journal of virology* **85**, 8538-8547, doi:10.1128/JVI.02645-10 (2011).

486 Pantaleo, G. *et al.* HIV infection is active and progressive in lymphoid tissue during the clinically latent stage of disease. *Nature* **362**, 355-358, doi:10.1038/362355a0 (1993).

487 Paprotka, T. *et al.* Inhibition of xenotropic murine leukemia virus-related virus by APOBEC3 proteins and antiviral drugs. *Journal of virology* **84**, 5719-5729, doi:10.1128/JVI.00134-10 (2010).

488 Parazzini, F. *et al.* Number of sexual partners, condom use and risk of human immunodeficiency virus infection. *International journal of epidemiology* **24**, 1197-1203 (1995).

489 Pardieu, C. *et al.* The RING-CH ligase K5 antagonizes restriction of KSHV and HIV-1 particle release by mediating ubiquitin-dependent endosomal degradation of tetherin. *PLoS pathogens* **6**, e1000843, doi:10.1371/journal.ppat.1000843 (2010).

490 Park, S. H. *et al.* Three-dimensional structure of the channel-forming trans-membrane domain of virus protein "u" (Vpu) from HIV-1. *Journal of molecular biology* **333**, 409-424 (2003).

491 Paul, I., Cui, J. & Maynard, E. L. Zinc binding to the HCCH motif of HIV-1 virion infectivity factor induces a conformational change that mediates protein-protein interactions. *Proceedings of the National Academy of Sciences of the United States of America* **103**, 18475-18480, doi:10.1073/pnas.0604150103 (2006).

492 Paxton, W., Connor, R. I. & Landau, N. R. Incorporation of Vpr into human immunodeficiency virus type 1 virions: requirement for the p6 region of gag and mutational analysis. *Journal of virology* **67**, 7229-7237 (1993).

493 Peeters, M. The genetic variability of HIV-1 and its implications. *Transfusion clinique et biologique : journal de la Societe francaise de transfusion sanguine* **8**, 222-225 (2001).

494 Peeters, M. *et al.* Predominance of subtype A and G HIV type 1 in Nigeria, with geographical differences in their distribution. *AIDS research and human retroviruses* **16**, 315-325, doi:10.1089/088922200309197 (2000).

495 Peng, G. *et al.* Myeloid differentiation and susceptibility to HIV-1 are linked to APOBEC3 expression. *Blood* **110**, 393-400, doi:10.1182/blood-2006-10-051763 (2007).

496 Peng, G., Lei, K. J., Jin, W., Greenwell-Wild, T. & Wahl, S. M. Induction of APOBEC3 family proteins, a defensive maneuver underlying interferon-induced anti-HIV-1 activity. *The Journal of experimental medicine* **203**, 41-46, doi:10.1084/jem.20051512 (2006).

497 Perepelitsa-Belancio, V. & Deininger, P. RNA truncation by premature polyadenylation attenuates human mobile element activity. *Nature genetics* **35**, 363-366, doi:10.1038/ng1269 (2003).

498 Perez-Caballero, D. *et al.* Tetherin inhibits HIV-1 release by directly tethering virions to cells. *Cell* **139**, 499-511, doi:10.1016/j.cell.2009.08.039 (2009).

499 Perkovic, M. *et al.* Species-specific inhibition of APOBEC3C by the prototype foamy virus protein bet. *The Journal of biological chemistry* **284**, 5819-5826, doi:10.1074/jbc.M808853200 (2009).

500 Perron, M. J. *et al.* The human TRIM5alpha restriction factor mediates accelerated

uncoating of the N-tropic murine leukemia virus capsid. *Journal of virology* **81**, 2138-2148, doi:10.1128/JVI.02318-06 (2007).

501 Perron, M. J. *et al.* TRIM5alpha mediates the postentry block to N-tropic murine leukemia viruses in human cells. *Proceedings of the National Academy of Sciences of the United States of America* **101**, 11827-11832, doi:10.1073/pnas.0403364101 (2004).

502 Pery, E., Rajendran, K. S., Brazier, A. J. & Gabuzda, D. Regulation of APOBEC3 proteins by a novel YXXL motif in human immunodeficiency virus type 1 Vif and simian immunodeficiency virus SIVagm Vif. *Journal of virology* **83**, 2374-2381, doi:10.1128/JVI.01898-08 (2009).

503 Piantadosi, A., Humes, D., Chohan, B., McClelland, R. S. & Overbaugh, J. Analysis of the percentage of human immunodeficiency virus type 1 sequences that are hypermutated and markers of disease progression in a longitudinal cohort, including one individual with a partially defective Vif. *Journal of virology* **83**, 7805-7814, doi:10.1128/JVI.00280-09 (2009).

504 Piatak, M., Jr. *et al.* High levels of HIV-1 in plasma during all stages of infection determined by competitive PCR. *Science* **259**, 1749-1754 (1993).

505 Pillai, S. K., Wong, J. K. & Barbour, J. D. Turning up the volume on mutational pressure: is more of a good thing always better? (A case study of HIV-1 Vif and APOBEC3). *Retrovirology* **5**, 26, doi:10.1186/1742-4690-5-26 (2008).

506 Pion, M. *et al.* APOBEC3G/3F mediates intrinsic resistance of monocyte-derived dendritic cells to HIV-1 infection. *The Journal of experimental medicine* **203**, 2887-2893, doi:10.1084/jem.20061519 (2006).

507 Pizzato, M. *et al.* Dynamin 2 is required for the enhancement of HIV-1 infectivity by Nef. *Proceedings of the National Academy of Sciences of the United States of America* **104**, 6812-6817, doi:10.1073/pnas.0607622104 (2007).

508 Plantier, J. C. *et al.* A new human immunodeficiency virus derived from gorillas. *Nature medicine* **15**, 871-872, doi:10.1038/nm.2016 (2009).

509 Platt, E. J., Bilska, M., Kozak, S. L., Kabat, D. & Montefiori, D. C. Evidence that ecotropic murine leukemia virus contamination in TZM-bl cells does not affect the outcome of neutralizing antibody assays with human immunodeficiency virus type 1. *Journal of virology* **83**, 8289-8292, doi:10.1128/JVI.00709-09 (2009).

510 Poggi, A. & Zocchi, M. R. HIV-1 Tat triggers TGF-beta production and NK cell apoptosis that is prevented by pertussis toxin B. *Clinical & developmental immunology* **13**, 369-372, doi:10.1080/17402520600645712 (2006).

511 Pollard, V. W. & Malim, M. H. The HIV-1 Rev protein. *Annual review of microbiology* **52**, 491-532, doi:10.1146/annurev.micro.52.1.491 (1998).

512 Poulsen, A. G. *et al.* Prevalence of and mortality from human immunodeficiency virus type 2 in Bissau, West Africa. *Lancet* **1**, 827-831 (1989).

513 Prochnow, C., Bransteitter, R., Klein, M. G., Goodman, M. F. & Chen, X. S. The APOBEC-2 crystal structure and functional implications for the deaminase AID. *Nature* **445**, 447-451, doi:10.1038/nature05492 (2007).

514 Pulkkinen, K., Renkema, G. H., Kirchhoff, F. & Saksela, K. Nef associates with p21-activated kinase 2 in a p21-GTPase-dependent dynamic activation complex within lipid rafts. *Journal of virology* **78**, 12773-12780, doi:10.1128/JVI.78.23.12773-12780.2004

(2004).

515 Pumfery, A. *et al.* Chromatin remodeling and modification during HIV-1 Tat-activated transcription. *Current HIV research* **1**, 343-362 (2003).

516 Qi, M. & Aiken, C. Selective restriction of Nef-defective human immunodeficiency virus type 1 by a proteasome-dependent mechanism. *Journal of virology* **81**, 1534-1536, doi:10.1128/JVI.02099-06 (2007).

517 Qi, M. & Aiken, C. Nef enhances HIV-1 infectivity via association with the virus assembly complex. *Virology* **373**, 287-297, doi:10.1016/j.virol.2007.12.001 (2008).

518 Qiu, J. & Pintel, D. J. The adeno-associated virus type 2 Rep protein regulates RNA processing via interaction with the transcription template. *Molecular and cellular biology* **22**, 3639-3652 (2002).

519 Raghavan, R. *et al.* Neuropathogenesis of chimeric simian/human immunodeficiency virus infection in pig-tailed and rhesus macaques. *Brain Pathol* **7**, 851-861 (1997).

520 Rangel, H. R. *et al.* Deletion, insertion and stop codon mutations in vif genes of HIV-1 infecting slow progressor patients. *Journal of infection in developing countries* **3**, 531-538 (2009).

521 Rangwala, S. H. & Kazazian, H. H., Jr. The L1 retrotransposition assay: a retrospective and toolkit. *Methods* **49**, 219-226, doi:10.1016/j.ymeth.2009.04.012 (2009).

522 Rauch, S., Pulkkinen, K., Saksela, K. & Fackler, O. T. Human immunodeficiency virus type 1 Nef recruits the guanine exchange factor Vav1 via an unexpected interface into plasma membrane microdomains for association with p21-activated kinase 2 activity. *Journal of virology* **82**, 2918-2929, doi:10.1128/JVI.02185-07 (2008).

523 Re, F., Braaten, D., Franke, E. K. & Luban, J. Human immunodeficiency virus type 1 Vpr arrests the cell cycle in G2 by inhibiting the activation of p34cdc2-cyclin B. *Journal of virology* **69**, 6859-6864 (1995).

524 Reeves, J. D. & Doms, R. W. Human immunodeficiency virus type 2. *The Journal of general virology* **83**, 1253-1265 (2002).

525 Refsland, E. W. *et al.* Quantitative profiling of the full APOBEC3 mRNA repertoire in lymphocytes and tissues: implications for HIV-1 restriction. *Nucleic acids research* **38**, 4274-4284, doi:10.1093/nar/gkq174 (2010).

526 Renkema, G. H., Manninen, A., Mann, D. A., Harris, M. & Saksela, K. Identification of the Nef-associated kinase as p21-activated kinase 2. *Current biology : CB* **9**, 1407-1410 (1999).

527 Renkema, G. H., Manninen, A. & Saksela, K. Human immunodeficiency virus type 1 Nef selectively associates with a catalytically active subpopulation of p21-activated kinase 2 (PAK2) independently of PAK2 binding to Nck or beta-PIX. *Journal of virology* **75**, 2154-2160, doi:10.1128/JVI.75.5.2154-2160.2001 (2001).

528 Rey-Cuille, M. A. *et al.* Simian immunodeficiency virus replicates to high levels in sooty mangabeys without inducing disease. *Journal of virology* **72**, 3872-3886 (1998).

529 Richman, D. D. *et al.* The challenge of finding a cure for HIV infection. *Science* **323**, 1304-1307, doi:10.1126/science.1165706 (2009).

530 Rizzuto, C. D. *et al.* A conserved HIV gp120 glycoprotein structure involved in chemokine receptor binding. *Science* **280**, 1949-1953 (1998).

531 Robb, M. L. Failure of the Merck HIV vaccine: an uncertain step forward. *Lancet* **372**,

1857-1858, doi:10.1016/S0140-6736(08)61593-7 (2008).

532 Roberts, J. D., Bebenek, K. & Kunkel, T. A. The accuracy of reverse transcriptase from HIV-1. *Science* **242**, 1171-1173 (1988).

533 Robertson, D. L. *et al.* HIV-1 nomenclature proposal. *Science* **288**, 55-56 (2000).

534 Roeth, J. F. & Collins, K. L. Human immunodeficiency virus type 1 Nef: adapting to intracellular trafficking pathways. *Microbiology and molecular biology reviews : MMBR* **70**, 548-563, doi:10.1128/MMBR.00042-05 (2006).

535 Rogel, M. E., Wu, L. I. & Emerman, M. The human immunodeficiency virus type 1 vpr gene prevents cell proliferation during chronic infection. *Journal of virology* **69**, 882-888 (1995).

536 Rohr, O., Marban, C., Aunis, D. & Schaeffer, E. Regulation of HIV-1 gene transcription: from lymphocytes to microglial cells. *Journal of leukocyte biology* **74**, 736-749, doi:10.1189/jlb.0403180 (2003).

537 Rold, C. J. & Aiken, C. Proteasomal degradation of TRIM5alpha during retrovirus restriction. *PLoS pathogens* **4**, e1000074, doi:10.1371/journal.ppat.1000074 (2008).

538 Rollason, R., Korolchuk, V., Hamilton, C., Schu, P. & Banting, G. Clathrin-mediated endocytosis of a lipid-raft-associated protein is mediated through a dual tyrosine motif. *Journal of cell science* **120**, 3850-3858, doi:10.1242/jcs.003343 (2007).

539 Roques, P. *et al.* Phylogenetic characteristics of three new HIV-1 N strains and implications for the origin of group N. *AIDS* **18**, 1371-1381 (2004).

540 Roshal, M., Kim, B., Zhu, Y., Nghiem, P. & Planelles, V. Activation of the ATR-mediated DNA damage response by the HIV-1 viral protein R. *The Journal of biological chemistry*

278, 25879-25886, doi:10.1074/jbc.M303948200 (2003).

541 Rosler, C. *et al.* APOBEC-mediated interference with hepadnavirus production. *Hepatology* **42**, 301-309, doi:10.1002/hep.20801 (2005).

542 Rosler, C., Kock, J., Malim, M. H., Blum, H. E. & von Weizsacker, F. Comment on "Inhibition of hepatitis B virus replication by APOBEC3G". *Science* **305**, 1403; author reply 1403, doi:10.1126/science.1100464 (2004).

543 Ross, T. M., Bieniasz, P. D. & Cullen, B. R. Multiple residues contribute to the inability of murine CCR-5 to function as a coreceptor for macrophage-tropic human immunodeficiency virus type 1 isolates. *Journal of virology* **72**, 1918-1924 (1998).

544 Rossi, A. *et al.* Human immunodeficiency virus type 1 Tat prevents dephosphorylation of Sp1 by TCF-4 in astrocytes. *The Journal of general virology* **87**, 1613-1623, doi:10.1099/vir.0.81691-0 (2006).

545 Ruiz, A., Hill, M. S., Schmitt, K., Guatelli, J. & Stephens, E. B. Requirements of the membrane proximal tyrosine and dileucine-based sorting signals for efficient transport of the subtype C Vpu protein to the plasma membrane and in virus release. *Virology* **378**, 58-68, doi:10.1016/j.virol.2008.05.022 (2008).

546 Ruiz, A., Hill, M. S., Schmitt, K. & Stephens, E. B. Membrane raft association of the Vpu protein of human immunodeficiency virus type 1 correlates with enhanced virus release. *Virology* **408**, 89-102, doi:10.1016/j.virol.2010.08.031 (2010).

547 Ruiz, A. *et al.* BST-2 mediated restriction of simian-human immunodeficiency virus. *Virology* **406**, 312-321, doi:10.1016/j.virol.2010.07.021 (2010).

548 Russell, R. A., Moore, M. D., Hu, W. S. & Pathak, V. K. APOBEC3G induces a

hypermutation gradient: purifying selection at multiple steps during HIV-1 replication results in levels of G-to-A mutations that are high in DNA, intermediate in cellular viral RNA, and low in virion RNA. *Retrovirology* **6**, 16, doi:10.1186/1742-4690-6-16 (2009).

549 Russell, R. A. & Pathak, V. K. Identification of two distinct human immunodeficiency virus type 1 Vif determinants critical for interactions with human APOBEC3G and APOBEC3F. *Journal of virology* **81**, 8201-8210, doi:10.1128/JVI.00395-07 (2007).

550 Russell, R. A., Smith, J., Barr, R., Bhattacharyya, D. & Pathak, V. K. Distinct domains within APOBEC3G and APOBEC3F interact with separate regions of human immunodeficiency virus type 1 Vif. *Journal of virology* **83**, 1992-2003, doi:10.1128/JVI.01621-08 (2009).

551 Russell, R. A. *et al.* Foamy virus Bet proteins function as novel inhibitors of the APOBEC3 family of innate antiretroviral defense factors. *Journal of virology* **79**, 8724-8731, doi:10.1128/JVI.79.14.8724-8731.2005 (2005).

552 Sakai, H. *et al.* Cell-dependent requirement of human immunodeficiency virus type 1 Vif protein for maturation of virus particles. *Journal of virology* **67**, 1663-1666 (1993).

553 Sandefur, S., Smith, R. M., Varthakavi, V. & Spearman, P. Mapping and characterization of the N-terminal I domain of human immunodeficiency virus type 1 Pr55(Gag). *Journal of virology* **74**, 7238-7249 (2000).

554 Santiago, M. L. *et al.* SIVcpz in wild chimpanzees. *Science* **295**, 465, doi:10.1126/science.295.5554.465 (2002).

555 Sasada, A. *et al.* APOBEC3G targets human T-cell leukemia virus type 1. *Retrovirology* **2**, 32, doi:10.1186/1742-4690-2-32 (2005).

556 Sato, K. *et al.* Comparative study on the effect of human BST-2/Tetherin on HIV-1 release in cells of various species. *Retrovirology* **6**, 53, doi:10.1186/1742-4690-6-53 (2009).

557 Sawyer, S. L., Emerman, M. & Malik, H. S. Ancient adaptive evolution of the primate antiviral DNA-editing enzyme APOBEC3G. *PLoS biology* **2**, E275, doi:10.1371/journal.pbio.0020275 (2004).

558 Schafer, A., Bogerd, H. P. & Cullen, B. R. Specific packaging of APOBEC3G into HIV-1 virions is mediated by the nucleocapsid domain of the gag polyprotein precursor. *Virology* **328**, 163-168, doi:10.1016/j.virol.2004.08.006 (2004).

559 Schindler, M. *et al.* Vpu serine 52 dependent counteraction of tetherin is required for HIV-1 replication in macrophages, but not in ex vivo human lymphoid tissue. *Retrovirology* **7**, 1, doi:10.1186/1742-4690-7-1 (2010).

560 Schmitt, K. *et al.* Comparison of the replication and persistence of simian-human immunodeficiency viruses expressing Vif proteins with mutation of the SLQYLA or HCCH domains in macaques. *Virology* **404**, 187-203, doi:10.1016/j.virol.2010.04.017 (2010).

561 Schmitt, K. *et al.* Mutations in the highly conserved SLQYLA motif of Vif in a simian-human immunodeficiency virus result in a less pathogenic virus and are associated with G-to-A mutations in the viral genome. *Virology* **383**, 362-372, doi:10.1016/j.virol.2008.10.013 (2009).

562 Schrofelbauer, B., Chen, D. & Landau, N. R. A single amino acid of APOBEC3G controls its species-specific interaction with virion infectivity factor (Vif). *Proceedings of*

the National Academy of Sciences of the United States of America **101**, 3927-3932, doi:10.1073/pnas.0307132101 (2004).

563 Schrofelbauer, B., Senger, T., Manning, G. & Landau, N. R. Mutational alteration of human immunodeficiency virus type 1 Vif allows for functional interaction with nonhuman primate APOBEC3G. *Journal of virology* **80**, 5984-5991, doi:10.1128/JVI.00388-06 (2006).

564 Schrofelbauer, B., Yu, Q., Zeitlin, S. G. & Landau, N. R. Human immunodeficiency virus type 1 Vpr induces the degradation of the UNG and SMUG uracil-DNA glycosylases. *Journal of virology* **79**, 10978-10987, doi:10.1128/JVI.79.17.10978-10987.2005 (2005).

565 Schubert, U. *et al.* Identification of an ion channel activity of the Vpu transmembrane domain and its involvement in the regulation of virus release from HIV-1-infected cells. *FEBS letters* **398**, 12-18 (1996).

566 Schubert, U. *et al.* The human immunodeficiency virus type 1 encoded Vpu protein is phosphorylated by casein kinase-2 (CK-2) at positions Ser52 and Ser56 within a predicted alpha-helix-turn-alpha-helix-motif. *Journal of molecular biology* **236**, 16-25, doi:10.1006/jmbi.1994.1114 (1994).

567 Schumacher, A. J., Nissley, D. V. & Harris, R. S. APOBEC3G hypermutates genomic DNA and inhibits Ty1 retrotransposition in yeast. *Proceedings of the National Academy of Sciences of the United States of America* **102**, 9854-9859, doi:10.1073/pnas.0501694102 (2005).

568 Schwartz, O., Marechal, V., Le Gall, S., Lemonnier, F. & Heard, J. M. Endocytosis of major histocompatibility complex class I molecules is induced by the HIV-1 Nef protein.

Nature medicine **2**, 338-342 (1996).

569 Sebastian, S. & Luban, J. TRIM5alpha selectively binds a restriction-sensitive retroviral capsid. *Retrovirology* **2**, 40, doi:10.1186/1742-4690-2-40 (2005).

570 Selig, L. *et al.* Interaction with the p6 domain of the gag precursor mediates incorporation into virions of Vpr and Vpx proteins from primate lentiviruses. *Journal of virology* **73**, 592-600 (1999).

571 Shaikh, T. H., Roy, A. M., Kim, J., Batzer, M. A. & Deininger, P. L. cDNAs derived from primary and small cytoplasmic Alu (scAlu) transcripts. *Journal of molecular biology* **271**, 222-234, doi:10.1006/jmbi.1997.1161 (1997).

572 Shandilya, S. M. *et al.* Crystal structure of the APOBEC3G catalytic domain reveals potential oligomerization interfaces. *Structure* **18**, 28-38, doi:10.1016/j.str.2009.10.016 (2010).

573 Shao, Q., Wang, Y., Hildreth, J. E. & Liu, B. Polyubiquitination of APOBEC3G is essential for its degradation by HIV-1 Vif. *Journal of virology* **84**, 4840-4844, doi:10.1128/JVI.01911-09 (2010).

574 Shapshak, P. *et al.* Elevated expression of IFN-gamma in the HIV-1 infected brain. *Frontiers in bioscience : a journal and virtual library* **9**, 1073-1081 (2004).

575 Shapshak, P. *et al.* Editorial neuroAIDS review. *AIDS* **25**, 123-141, doi:10.1097/QAD.0b013e328340fd42 (2011).

576 Sharova, N. *et al.* Primate lentiviral Vpx commandeers DDB1 to counteract a macrophage restriction. *PLoS pathogens* **4**, e1000057, doi:10.1371/journal.ppat.1000057 (2008).

577 Sharp, P. M. *et al.* The origins of acquired immune deficiency syndrome viruses: where and when? *Philosophical transactions of the Royal Society of London. Series B, Biological sciences* **356**, 867-876, doi:10.1098/rstb.2001.0863 (2001).

578 Sheehy, A. M., Gaddis, N. C., Choi, J. D. & Malim, M. H. Isolation of a human gene that inhibits HIV-1 infection and is suppressed by the viral Vif protein. *Nature* **418**, 646-650, doi:10.1038/nature00939 (2002).

579 Sheehy, A. M., Gaddis, N. C. & Malim, M. H. The antiretroviral enzyme APOBEC3G is degraded by the proteasome in response to HIV-1 Vif. *Nature medicine* **9**, 1404-1407, doi:10.1038/nm945 (2003).

580 Sherman, M. P. *et al.* Nuclear export of Vpr is required for efficient replication of human immunodeficiency virus type 1 in tissue macrophages. *Journal of virology* **77**, 7582-7589 (2003).

581 Shi, J. & Aiken, C. Saturation of TRIM5 alpha-mediated restriction of HIV-1 infection depends on the stability of the incoming viral capsid. *Virology* **350**, 493-500, doi:10.1016/j.virol.2006.03.013 (2006).

582 Shibata, R. *et al.* Infection and pathogenicity of chimeric simian-human immunodeficiency viruses in macaques: determinants of high virus loads and CD4 cell killing. *The Journal of infectious diseases* **176**, 362-373 (1997).

583 Shimura, M. *et al.* Micronuclei formation and aneuploidy induced by Vpr, an accessory gene of human immunodeficiency virus type 1. *The FASEB journal : official publication of the Federation of American Societies for Experimental Biology* **13**, 621-637 (1999).

584 Shindo, K. *et al.* The enzymatic activity of CEM15/Apobec-3G is essential for the

regulation of the infectivity of HIV-1 virion but not a sole determinant of its antiviral activity. *The Journal of biological chemistry* **278**, 44412-44416, doi:10.1074/jbc.C300376200 (2003).

585 Simmons, A., Aluvihare, V. & McMichael, A. Nef triggers a transcriptional program in T cells imitating single-signal T cell activation and inducing HIV virulence mediators. *Immunity* **14**, 763-777 (2001).

586 Simon, F. *et al.* Identification of a new human immunodeficiency virus type 1 distinct from group M and group O. *Nature medicine* **4**, 1032-1037, doi:10.1038/2017 (1998).

587 Simon, J. H., Gaddis, N. C., Fouchier, R. A. & Malim, M. H. Evidence for a newly discovered cellular anti-HIV-1 phenotype. *Nature medicine* **4**, 1397-1400, doi:10.1038/3987 (1998).

588 Simon, J. H., Sheehy, A. M., Carpenter, E. A., Fouchier, R. A. & Malim, M. H. Mutational analysis of the human immunodeficiency virus type 1 Vif protein. *Journal of virology* **73**, 2675-2681 (1999).

589 Simon, V. *et al.* Natural variation in Vif: differential impact on APOBEC3G/3F and a potential role in HIV-1 diversification. *PLoS pathogens* **1**, e6, doi:10.1371/journal.ppat.0010006 (2005).

590 Singh, D. K. *et al.* The presence of the casein kinase II phosphorylation sites of Vpu enhances the CD4(+) T cell loss caused by the simian-human immunodeficiency virus SHIV(KU-lbMC33) in pig-tailed macaques. *Virology* **313**, 435-451 (2003).

591 Singh, R., Kaur, M. & Arora, D. Neurological complications in late-stage hospitalized patients with HIV disease. *Annals of Indian Academy of Neurology* **14**, 172-177,

doi:10.4103/0972-2327.85878 (2011).

592 Smed-Sorensen, A., Lore, K., Walther-Jallow, L., Andersson, J. & Spetz, A. L. HIV-1-infected dendritic cells up-regulate cell surface markers but fail to produce IL-12 p70 in response to CD40 ligand stimulation. *Blood* **104**, 2810-2817, doi:10.1182/blood-2003-07-2314 (2004).

593 Smith, J. L. & Pathak, V. K. Identification of specific determinants of human APOBEC3F, APOBEC3C, and APOBEC3DE and African green monkey APOBEC3F that interact with HIV-1 Vif. *Journal of virology* **84**, 12599-12608, doi:10.1128/JVI.01437-10 (2010).

594 Sobczak, K. & Krzyzosiak, W. J. Structural determinants of BRCA1 translational regulation. *The Journal of biological chemistry* **277**, 17349-17358, doi:10.1074/jbc.M109162200 (2002).

595 Song, L., Nath, A., Geiger, J. D., Moore, A. & Hochman, S. Human immunodeficiency virus type 1 Tat protein directly activates neuronal N-methyl-D-aspartate receptors at an allosteric zinc-sensitive site. *Journal of neurovirology* **9**, 399-403, doi:10.1080/13550280390201704 (2003).

596 Soros, V. B., Yonemoto, W. & Greene, W. C. Newly synthesized APOBEC3G is incorporated into HIV virions, inhibited by HIV RNA, and subsequently activated by RNase H. *PLoS pathogens* **3**, e15, doi:10.1371/journal.ppat.0030015 (2007).

597 Sova, P. & Volsky, D. J. Efficiency of viral DNA synthesis during infection of permissive and nonpermissive cells with vif-negative human immunodeficiency virus type 1. *Journal of virology* **67**, 6322-6326 (1993).

598 Sowden, M. P., Ballatori, N., Jensen, K. L., Reed, L. H. & Smith, H. C. The editosome for cytidine to uridine mRNA editing has a native complexity of 27S: identification of intracellular domains containing active and inactive editing factors. *Journal of cell science* **115**, 1027-1039 (2002).

599 Sparger, E. E. *et al.* Vaccination of rhesus macaques with a vif-deleted simian immunodeficiency virus proviral DNA vaccine. *Virology* **374**, 261-272, doi:10.1016/j.virol.2008.01.020 (2008).

600 Srinivas, S. K., Srinivas, R. V., Anantharamaiah, G. M., Segrest, J. P. & Compans, R. W. Membrane interactions of synthetic peptides corresponding to amphipathic helical segments of the human immunodeficiency virus type-1 envelope glycoprotein. *The Journal of biological chemistry* **267**, 7121-7127 (1992).

601 Srivastava, S. *et al.* Lentiviral Vpx accessory factor targets VprBP/DCAF1 substrate adaptor for cullin 4 E3 ubiquitin ligase to enable macrophage infection. *PLoS pathogens* **4**, e1000059, doi:10.1371/journal.ppat.1000059 (2008).

602 Stade, K., Ford, C. S., Guthrie, C. & Weis, K. Exportin 1 (Crm1p) is an essential nuclear export factor. *Cell* **90**, 1041-1050 (1997).

603 Stanley, B. J. *et al.* Structural insight into the human immunodeficiency virus Vif SOCS box and its role in human E3 ubiquitin ligase assembly. *Journal of virology* **82**, 8656-8663, doi:10.1128/JVI.00767-08 (2008).

604 Stauch, B. *et al.* Model structure of APOBEC3C reveals a binding pocket modulating ribonucleic acid interaction required for encapsidation. *Proceedings of the National Academy of Sciences of the United States of America* **106**, 12079-12084,

doi:10.1073/pnas.0900979106 (2009).

605 Stenglein, M. D., Burns, M. B., Li, M., Lengyel, J. & Harris, R. S. APOBEC3 proteins mediate the clearance of foreign DNA from human cells. *Nature structural & molecular biology* **17**, 222-229, doi:10.1038/nsmb.1744 (2010).

606 Stenglein, M. D. & Harris, R. S. APOBEC3B and APOBEC3F inhibit L1 retrotransposition by a DNA deamination-independent mechanism. *The Journal of biological chemistry* **281**, 16837-16841, doi:10.1074/jbc.M602367200 (2006).

607 Stephens, E. B. *et al.* Deletion of the vpu sequences prior to the env in a simian-human immunodeficiency virus results in enhanced Env precursor synthesis but is less pathogenic for pig-tailed macaques. *Virology* **293**, 252-261, doi:10.1006/viro.2001.1244 (2002).

608 Stephens, E. B., Tian, C., Dalton, S. B. & Gattone, V. H., 2nd. Simian-human immunodeficiency virus-associated nephropathy in macaques. *AIDS research and human retroviruses* **16**, 1295-1306, doi:10.1089/08892220050117050 (2000).

609 Sterjovski, J. *et al.* An altered and more efficient mechanism of CCR5 engagement contributes to macrophage tropism of CCR5-using HIV-1 envelopes. *Virology* **404**, 269-278, doi:10.1016/j.virol.2010.05.006 (2010).

610 Stettner, M. R. *et al.* SMAD proteins of oligodendroglial cells regulate transcription of JC virus early and late genes coordinately with the Tat protein of human immunodeficiency virus type 1. *The Journal of general virology* **90**, 2005-2014, doi:10.1099/vir.0.011072-0 (2009).

611 Stevenson, M. HIV-1 pathogenesis. *Nature medicine* **9**, 853-860, doi:10.1038/nm0703-

853 (2003).

612 Stevenson, M., Stanwick, T. L., Dempsey, M. P. & Lamonica, C. A. HIV-1 replication is controlled at the level of T cell activation and proviral integration. *The EMBO journal* **9**, 1551-1560 (1990).

613 Stopak, K., de Noronha, C., Yonemoto, W. & Greene, W. C. HIV-1 Vif blocks the antiviral activity of APOBEC3G by impairing both its translation and intracellular stability. *Molecular cell* **12**, 591-601 (2003).

614 Stopak, K. S., Chiu, Y. L., Kropp, J., Grant, R. M. & Greene, W. C. Distinct patterns of cytokine regulation of APOBEC3G expression and activity in primary lymphocytes, macrophages, and dendritic cells. *The Journal of biological chemistry* **282**, 3539-3546, doi:10.1074/jbc.M610138200 (2007).

615 Strebel, K. APOBEC3G & HTLV-1: inhibition without deamination. *Retrovirology* **2**, 37, doi:10.1186/1742-4690-2-37 (2005).

616 Strebel, K. *et al.* The HIV 'A' (sor) gene product is essential for virus infectivity. *Nature* **328**, 728-730, doi:10.1038/328728a0 (1987).

617 Strebel, K., Klimkait, T. & Martin, M. A. A novel gene of HIV-1, vpu, and its 16-kilodalton product. *Science* **241**, 1221-1223 (1988).

618 Strebel, K., Klimkait, T. & Martin, M. A. A novel gene of HIV-1, vpu, and its 16-kilodalton product. *Science* **241**, 1221-1223 (1988).

619 Stremlau, M. *et al.* The cytoplasmic body component TRIM5alpha restricts HIV-1 infection in Old World monkeys. *Nature* **427**, 848-853, doi:10.1038/nature02343 (2004).

620 Stremlau, M. *et al.* Specific recognition and accelerated uncoating of retroviral capsids

by the TRIM5alpha restriction factor. *Proceedings of the National Academy of Sciences of the United States of America* **103**, 5514-5519, doi:10.1073/pnas.0509996103 (2006).

621 Sui, Y. *et al.* Innate and adaptive immune correlates of vaccine and adjuvant-induced control of mucosal transmission of SIV in macaques. *Proceedings of the National Academy of Sciences of the United States of America* **107**, 9843-9848, doi:10.1073/pnas.0911932107 (2010).

622 Suspene, R. *et al.* Somatic hypermutation of human mitochondrial and nuclear DNA by APOBEC3 cytidine deaminases, a pathway for DNA catabolism. *Proceedings of the National Academy of Sciences of the United States of America* **108**, 4858-4863, doi:10.1073/pnas.1009687108 (2011).

623 Suspene, R. *et al.* Genetic editing of herpes simplex virus 1 and Epstein-Barr herpesvirus genomes by human APOBEC3 cytidine deaminases in culture and in vivo. *Journal of virology* **85**, 7594-7602, doi:10.1128/JVI.00290-11 (2011).

624 Suspene, R. *et al.* Extensive editing of both hepatitis B virus DNA strands by APOBEC3 cytidine deaminases in vitro and in vivo. *Proceedings of the National Academy of Sciences of the United States of America* **102**, 8321-8326, doi:10.1073/pnas.0408223102 (2005).

625 Suspene, R. *et al.* APOBEC3G is a single-stranded DNA cytidine deaminase and functions independently of HIV reverse transcriptase. *Nucleic acids research* **32**, 2421-2429, doi:10.1093/nar/gkh554 (2004).

626 Svarovskaia, E. S. *et al.* Human apolipoprotein B mRNA-editing enzyme-catalytic polypeptide-like 3G (APOBEC3G) is incorporated into HIV-1 virions through interactions

with viral and nonviral RNAs. *The Journal of biological chemistry* **279**, 35822-35828, doi:10.1074/jbc.M405761200 (2004).

627 Swanson, C. M. & Malim, M. H. SnapShot: HIV-1 proteins. *Cell* **133**, 742, 742 e741, doi:10.1016/j.cell.2008.05.005 (2008).

628 Swergold, G. D. Identification, characterization, and cell specificity of a human LINE-1 promoter. *Molecular and cellular biology* **10**, 6718-6729 (1990).

629 Szak, S. T. *et al.* Molecular archeology of L1 insertions in the human genome. *Genome biology* **3**, research0052 (2002).

630 Tagalakis, V. *et al.* Thrombophilia in short peripheral catheter thrombophlebitis. *Thromb Res* **119**, 587-592, doi:10.1016/j.thromres.2006.04.012 (2007).

631 Takeuchi, Y., McClure, M. O. & Pizzato, M. Identification of gammaretroviruses constitutively released from cell lines used for human immunodeficiency virus research. *Journal of virology* **82**, 12585-12588, doi:10.1128/JVI.01726-08 (2008).

632 Tang, C. H. *et al.* [Primary culture of human periodontal ligament fibroblasts by explants with enzymatic digestion]. *Zhonghua yi xue za zhi* **84**, 656-658 (2004).

633 Tang, J., Shen, Y. M., Zou, Z. L., Qiu, D. H. & Zheng, Y. H. Experimental study on pollutant movement in surf zone. *J Environ Sci (China)* **16**, 762-764 (2004).

634 Temin, H. M. Retrovirus variation and reverse transcription: abnormal strand transfers result in retrovirus genetic variation. *Proceedings of the National Academy of Sciences of the United States of America* **90**, 6900-6903 (1993).

635 Terwilliger, E. F., Cohen, E. A., Lu, Y. C., Sodroski, J. G. & Haseltine, W. A. Functional role of human immunodeficiency virus type 1 vpu. *Proceedings of the National Academy*

of Sciences of the United States of America **86**, 5163-5167 (1989).

636 Thielen, B. K. *et al.* Innate immune signaling induces high levels of TC-specific deaminase activity in primary monocyte-derived cells through expression of APOBEC3A isoforms. *The Journal of biological chemistry* **285**, 27753-27766, doi:10.1074/jbc.M110.102822 (2010).

637 Thippeshappa, R. *et al.* Vif substitution enables persistent infection of pig-tailed macaques by human immunodeficiency virus type 1. *Journal of virology* **85**, 3767-3779, doi:10.1128/JVI.02438-10 (2011).

638 Tian, C. *et al.* Differential requirement for conserved tryptophans in human immunodeficiency virus type 1 Vif for the selective suppression of APOBEC3G and APOBEC3F. *Journal of virology* **80**, 3112-3115, doi:10.1128/JVI.80.6.3112-3115.2006 (2006).

639 Tiganos, E. *et al.* Structural and functional analysis of the membrane-spanning domain of the human immunodeficiency virus type 1 Vpu protein. *Virology* **251**, 96-107, doi:10.1006/viro.1998.9368 (1998).

640 Tong, J. *et al.* Plasma pancreatic polypeptide levels are associated with differences in body fat distribution in human subjects. *Diabetologia* **50**, 439-442, doi:10.1007/s00125-006-0553-4 (2007).

641 Towers, G. J. The control of viral infection by tripartite motif proteins and cyclophilin A. *Retrovirology* **4**, 40, doi:10.1186/1742-4690-4-40 (2007).

642 Turelli, P., Mangeat, B., Jost, S., Vianin, S. & Trono, D. Inhibition of hepatitis B virus replication by APOBEC3G. *Science* **303**, 1829, doi:10.1126/science.1092066 (2004).

643 Turelli, P., Vianin, S. & Trono, D. The innate antiretroviral factor APOBEC3G does not affect human LINE-1 retrotransposition in a cell culture assay. *The Journal of biological chemistry* **279**, 43371-43373, doi:10.1074/jbc.C400334200 (2004).

644 Ueno, F. *et al.* Vpx and Vpr proteins of HIV-2 up-regulate the viral infectivity by a distinct mechanism in lymphocytic cells. *Microbes and infection / Institut Pasteur* **5**, 387-395 (2003).

645 Ulenga, N. K. *et al.* The level of APOBEC3G (hA3G)-related G-to-A mutations does not correlate with viral load in HIV type 1-infected individuals. *AIDS research and human retroviruses* **24**, 1285-1290, doi:10.1089/aid.2008.0072 (2008).

646 Utzschneider, K. M. & Kahn, S. E. Review: The role of insulin resistance in nonalcoholic fatty liver disease. *The Journal of clinical endocrinology and metabolism* **91**, 4753-4761, doi:10.1210/jc.2006-0587 (2006).

647 Vallari, A. *et al.* Confirmation of putative HIV-1 group P in Cameroon. *Journal of virology* **85**, 1403-1407, doi:10.1128/JVI.02005-10 (2011).

648 Van Damme, N. *et al.* The interferon-induced protein BST-2 restricts HIV-1 release and is downregulated from the cell surface by the viral Vpu protein. *Cell host & microbe* **3**, 245-252, doi:10.1016/j.chom.2008.03.001 (2008).

649 van Genugten, R. E. *et al.* Effects of sex and hormone replacement therapy use on the prevalence of isolated impaired fasting glucose and isolated impaired glucose tolerance in subjects with a family history of type 2 diabetes. *Diabetes* **55**, 3529-3535, doi:10.2337/db06-0577 (2006).

650 Van Heuverswyn, F. *et al.* Human immunodeficiency viruses: SIV infection in wild

gorillas. *Nature* **444**, 164, doi:10.1038/444164a (2006).

651 Varin, A. *et al.* Synthetic Vpr protein activates activator protein-1, c-Jun N-terminal kinase, and NF-kappaB and stimulates HIV-1 transcription in promonocytic cells and primary macrophages. *The Journal of biological chemistry* **280**, 42557-42567, doi:10.1074/jbc.M502211200 (2005).

652 Vartanian, J. P., Guetard, D., Henry, M. & Wain-Hobson, S. Evidence for editing of human papillomavirus DNA by APOBEC3 in benign and precancerous lesions. *Science* **320**, 230-233, doi:10.1126/science.1153201 (2008).

653 Vartanian, J. P., Meyerhans, A., Asjo, B. & Wain-Hobson, S. Selection, recombination, and G----A hypermutation of human immunodeficiency virus type 1 genomes. *Journal of virology* **65**, 1779-1788 (1991).

654 Vartanian, J. P., Meyerhans, A., Sala, M. & Wain-Hobson, S. G-->A hypermutation of the human immunodeficiency virus type 1 genome: evidence for dCTP pool imbalance during reverse transcription. *Proceedings of the National Academy of Sciences of the United States of America* **91**, 3092-3096 (1994).

655 Varthakavi, V., Smith, R. M., Bour, S. P., Strebel, K. & Spearman, P. Viral protein U counteracts a human host cell restriction that inhibits HIV-1 particle production. *Proceedings of the National Academy of Sciences of the United States of America* **100**, 15154-15159, doi:10.1073/pnas.2433165100 (2003).

656 Veazey, R. S. *et al.* Gastrointestinal tract as a major site of CD4+ T cell depletion and viral replication in SIV infection. *Science* **280**, 427-431 (1998).

657 Venkatesh, L. K. & Chinnadurai, G. Mutants in a conserved region near the carboxy-

terminus of HIV-1 Rev identify functionally important residues and exhibit a dominant negative phenotype. *Virology* **178**, 327-330 (1990).

658 Viberti, G. *et al.* A Diabetes Outcome Progression Trial (ADOPT): baseline characteristics of Type 2 diabetic patients in North America and Europe. *Diabetic medicine : a journal of the British Diabetic Association* **23**, 1289-1294, doi:10.1111/j.1464-5491.2006.02022.x (2006).

659 Virgen, C. A. & Hatziioannou, T. Antiretroviral activity and Vif sensitivity of rhesus macaque APOBEC3 proteins. *Journal of virology* **81**, 13932-13937, doi:10.1128/JVI.01760-07 (2007).

660 von Schwedler, U., Song, J., Aiken, C. & Trono, D. Vif is crucial for human immunodeficiency virus type 1 proviral DNA synthesis in infected cells. *Journal of virology* **67**, 4945-4955 (1993).

661 Voytas, D. & Ke, N. Detection and quantitation of radiolabeled proteins and DNA in gels and blots. *Current protocols in immunology / edited by John E. Coligan ... [et al.]* **Appendix 3**, Appendix 3J, doi:10.1002/0471142735.ima03js50 (2002).

662 Wade, J. *et al.* Enhanced CD4+ cellular apoptosis by CCR5-restricted HIV-1 envelope glycoprotein variants from patients with progressive HIV-1 infection. *Virology* **396**, 246-255, doi:10.1016/j.virol.2009.10.029 (2010).

663 Walker, B. D. *et al.* HIV-specific cytotoxic T lymphocytes in seropositive individuals. *Nature* **328**, 345-348, doi:10.1038/328345a0 (1987).

664 Walker, E. A. *et al.* Adherence to preventive medications: predictors and outcomes in the Diabetes Prevention Program. *Diabetes Care* **29**, 1997-2002, doi:10.2337/dc06-

0454 (2006).

665 Walker, R. C., Jr. *et al.* Identification of dominant negative human immunodeficiency virus type 1 Vif mutants that interfere with the functional inactivation of APOBEC3G by virus-encoded Vif. *Journal of virology* **84**, 5201-5211, doi:10.1128/JVI.02318-09 (2010).

666 Wang, F. *et al.* [Effect of 1-MCP on senescence and quality in cold-stored edible podded pea]. *Zhi wu sheng li yu fen zi sheng wu xue xue bao = Journal of plant physiology and molecular biology* **30**, 167-172 (2004).

667 Wang, H. *et al.* SVA elements: a hominid-specific retroposon family. *Journal of molecular biology* **354**, 994-1007, doi:10.1016/j.jmb.2005.09.085 (2005).

668 Wang, X. *et al.* Analysis of human APOBEC3H haplotypes and anti-human immunodeficiency virus type 1 activity. *Journal of virology* **85**, 3142-3152, doi:10.1128/JVI.02049-10 (2011).

669 Wang, X., Dolan, P. T., Dang, Y. & Zheng, Y. H. Biochemical differentiation of APOBEC3F and APOBEC3G proteins associated with HIV-1 life cycle. *The Journal of biological chemistry* **282**, 1585-1594, doi:10.1074/jbc.M610150200 (2007).

670 Watts, J. M. *et al.* Architecture and secondary structure of an entire HIV-1 RNA genome. *Nature* **460**, 711-716, doi:10.1038/nature08237 (2009).

671 Wedekind, J. E., Dance, G. S., Sowden, M. P. & Smith, H. C. Messenger RNA editing in mammals: new members of the APOBEC family seeking roles in the family business. *Trends in genetics : TIG* **19**, 207-216 (2003).

672 Wei, B. L. *et al.* Activation of p21-activated kinase 2 by human immunodeficiency virus type 1 Nef induces merlin phosphorylation. *Journal of virology* **79**, 14976-14980,

doi:10.1128/JVI.79.23.14976-14980.2005 (2005).

673 Wei, B. L. *et al.* Inhibition of lysosome and proteasome function enhances human immunodeficiency virus type 1 infection. *Journal of virology* **79**, 5705-5712, doi:10.1128/JVI.79.9.5705-5712.2005 (2005).

674 Wei, W. *et al.* Human L1 retrotransposition: cis preference versus trans complementation. *Molecular and cellular biology* **21**, 1429-1439, doi:10.1128/MCB.21.4.1429-1439.2001 (2001).

675 Wei, X. *et al.* Emergence of resistant human immunodeficiency virus type 1 in patients receiving fusion inhibitor (T-20) monotherapy. *Antimicrobial agents and chemotherapy* **46**, 1896-1905 (2002).

676 Wei, X. *et al.* Viral dynamics in human immunodeficiency virus type 1 infection. *Nature* **373**, 117-122, doi:10.1038/373117a0 (1995).

677 Weichselbraun, I., Farrington, G. K., Rusche, J. R., Bohnlein, E. & Hauber, J. Definition of the human immunodeficiency virus type 1 Rev and human T-cell leukemia virus type I Rex protein activation domain by functional exchange. *Journal of virology* **66**, 2583-2587 (1992).

678 Weiner, A. M., Deininger, P. L. & Efstratiadis, A. Nonviral retroposons: genes, pseudogenes, and transposable elements generated by the reverse flow of genetic information. *Annual review of biochemistry* **55**, 631-661, doi:10.1146/annurev.bi.55.070186.003215 (1986).

679 Weis, K. Importins and exportins: how to get in and out of the nucleus. *Trends in biochemical sciences* **23**, 185-189 (1998).

680 Wen, W., Meinkoth, J. L., Tsien, R. Y. & Taylor, S. S. Identification of a signal for rapid export of proteins from the nucleus. *Cell* **82**, 463-473 (1995).

681 Whitford, P. C. *et al.* An all-atom structure-based potential for proteins: bridging minimal models with all-atom empirical forcefields. *Proteins* **75**, 430-441, doi:10.1002/prot.22253 (2009).

682 Wichroski, M. J., Ichiyama, K. & Rana, T. M. Analysis of HIV-1 viral infectivity factor-mediated proteasome-dependent depletion of APOBEC3G: correlating function and subcellular localization. *The Journal of biological chemistry* **280**, 8387-8396, doi:10.1074/jbc.M408048200 (2005).

683 Wichroski, M. J., Robb, G. B. & Rana, T. M. Human retroviral host restriction factors APOBEC3G and APOBEC3F localize to mRNA processing bodies. *PLoS pathogens* **2**, e41, doi:10.1371/journal.ppat.0020041 (2006).

684 Wiegand, H. L., Doehle, B. P., Bogerd, H. P. & Cullen, B. R. A second human antiretroviral factor, APOBEC3F, is suppressed by the HIV-1 and HIV-2 Vif proteins. *The EMBO journal* **23**, 2451-2458, doi:10.1038/sj.emboj.7600246 (2004).

685 Wilkins, A. *et al.* The epidemiology of HIV infection in a rural area of Guinea-Bissau. *AIDS* **7**, 1119-1122 (1993).

686 Williams, A. P., Burke, M., Vayda, E. & Stevenson, M. The reproduction of physician autonomy in Ontario medical group practice. *Health services management research : an official journal of the Association of University Programs in Health Administration / HSMC, AUPHA* **3**, 87-97 (1990).

687 Williams, S. A. *et al.* NF-kappaB p50 promotes HIV latency through HDAC recruitment

and repression of transcriptional initiation. *The EMBO journal* **25**, 139-149, doi:10.1038/sj.emboj.7600900 (2006).

688 Wissing, S., Montano, M., Garcia-Perez, J. L., Moran, J. V. & Greene, W. C. Endogenous APOBEC3B restricts LINE-1 retrotransposition in transformed cells and human embryonic stem cells. *The Journal of biological chemistry* **286**, 36427-36437, doi:10.1074/jbc.M111.251058 (2011).

689 Wittlich, M., Koenig, B. W., Stoldt, M., Schmidt, H. & Willbold, D. NMR structural characterization of HIV-1 virus protein U cytoplasmic domain in the presence of dodecylphosphatidylcholine micelles. *The FEBS journal* **276**, 6560-6575, doi:10.1111/j.1742-4658.2009.07363.x (2009).

690 Wolfrum, N. *et al.* Impact of viral accessory proteins of SIVsmmPBj on early steps of infection of quiescent cells. *Virology* **364**, 330-341, doi:10.1016/j.virol.2007.03.008 (2007).

691 Wonderlich, E. R., Williams, M. & Collins, K. L. The tyrosine binding pocket in the adaptor protein 1 (AP-1) mu1 subunit is necessary for Nef to recruit AP-1 to the major histocompatibility complex class I cytoplasmic tail. *The Journal of biological chemistry* **283**, 3011-3022, doi:10.1074/jbc.M707760200 (2008).

692 Wong, K. *et al.* HIV-1 Tat interactions with p300 and PCAF transcriptional coactivators inhibit histone acetylation and neurotrophin signaling through CREB. *The Journal of biological chemistry* **280**, 9390-9399, doi:10.1074/jbc.M408643200 (2005).

693 Wray, V. *et al.* Solution structure of the hydrophilic region of HIV-1 encoded virus protein U (Vpu) by CD and 1H NMR spectroscopy. *International journal of peptide and protein*

research **45**, 35-43 (1995).

694 Wu, X., Anderson, J. L., Campbell, E. M., Joseph, A. M. & Hope, T. J. Proteasome inhibitors uncouple rhesus TRIM5alpha restriction of HIV-1 reverse transcription and infection. *Proceedings of the National Academy of Sciences of the United States of America* **103**, 7465-7470, doi:10.1073/pnas.0510483103 (2006).

695 Wu, X. G., Shen, Y. M., Zheng, Y. H. & Yang, Z. F. Numerical model of flow and pollutant transportation in non-orthogonal curvilinear coordinates. *J Environ Sci (China)* **16**, 293-296 (2004).

696 Wyand, M. S., Manson, K. H., Garcia-Moll, M., Montefiori, D. & Desrosiers, R. C. Vaccine protection by a triple deletion mutant of simian immunodeficiency virus. *Journal of virology* **70**, 3724-3733 (1996).

697 Wyatt, R. *et al.* Relationship of the human immunodeficiency virus type 1 gp120 third variable loop to a component of the CD4 binding site in the fourth conserved region. *Journal of virology* **66**, 6997-7004 (1992).

698 Xiao, X., Li, J. & Samulski, R. J. Production of high-titer recombinant adeno-associated virus vectors in the absence of helper adenovirus. *Journal of virology* **72**, 2224-2232 (1998).

699 Xiao, Z., Ehrlich, E., Luo, K., Xiong, Y. & Yu, X. F. Zinc chelation inhibits HIV Vif activity and liberates antiviral function of the cytidine deaminase APOBEC3G. *The FASEB journal : official publication of the Federation of American Societies for Experimental Biology* **21**, 217-222, doi:10.1096/fj.06-6773com (2007).

700 Xiao, Z. *et al.* Assembly of HIV-1 Vif-Cul5 E3 ubiquitin ligase through a novel zinc-

binding domain-stabilized hydrophobic interface in Vif. *Virology* **349**, 290-299, doi:10.1016/j.virol.2006.02.002 (2006).

701 Xiao, Z. *et al.* Characterization of a novel Cullin5 binding domain in HIV-1 Vif. *Journal of molecular biology* **373**, 541-550, doi:10.1016/j.jmb.2007.07.029 (2007).

702 Xie, K. *et al.* The structure of a yeast RNA-editing deaminase provides insight into the fold and function of activation-induced deaminase and APOBEC-1. *Proceedings of the National Academy of Sciences of the United States of America* **101**, 8114-8119, doi:10.1073/pnas.0400493101 (2004).

703 Xu, H. *et al.* A single amino acid substitution in human APOBEC3G antiretroviral enzyme confers resistance to HIV-1 virion infectivity factor-induced depletion. *Proceedings of the National Academy of Sciences of the United States of America* **101**, 5652-5657, doi:10.1073/pnas.0400830101 (2004).

704 Yamaguchi, J., Devare, S. G. & Brennan, C. A. Identification of a new HIV-2 subtype based on phylogenetic analysis of full-length genomic sequence. *AIDS research and human retroviruses* **16**, 925-930, doi:10.1089/08892220050042864 (2000).

705 Yamanaka, S. *et al.* Apolipoprotein B mRNA-editing protein induces hepatocellular carcinoma and dysplasia in transgenic animals. *Proceedings of the National Academy of Sciences of the United States of America* **92**, 8483-8487 (1995).

706 Yamashita, T., Kamada, K., Hatcho, K., Adachi, A. & Nomaguchi, M. Identification of amino acid residues in HIV-1 Vif critical for binding and exclusion of APOBEC3G/F. *Microbes and infection / Institut Pasteur* **10**, 1142-1149, doi:10.1016/j.micinf.2008.06.003 (2008).

707 Yang, B., Chen, K., Zhang, C., Huang, S. & Zhang, H. Virion-associated uracil DNA glycosylase-2 and apurinic/apyrimidinic endonuclease are involved in the degradation of APOBEC3G-edited nascent HIV-1 DNA. *The Journal of biological chemistry* **282**, 11667-11675, doi:10.1074/jbc.M606864200 (2007).

708 Yang, B. *et al.* Potent suppression of viral infectivity by the peptides that inhibit multimerization of human immunodeficiency virus type 1 (HIV-1) Vif proteins. *The Journal of biological chemistry* **278**, 6596-6602, doi:10.1074/jbc.M210164200 (2003).

709 Yang, S., Sun, Y. & Zhang, H. The multimerization of human immunodeficiency virus type I Vif protein: a requirement for Vif function in the viral life cycle. *The Journal of biological chemistry* **276**, 4889-4893, doi:10.1074/jbc.M004895200 (2001).

710 Yang, Y., Guo, F., Cen, S. & Kleiman, L. Inhibition of initiation of reverse transcription in HIV-1 by human APOBEC3F. *Virology* **365**, 92-100, doi:10.1016/j.virol.2007.03.022 (2007).

711 Yap, M. W., Nisole, S., Lynch, C. & Stoye, J. P. Trim5alpha protein restricts both HIV-1 and murine leukemia virus. *Proceedings of the National Academy of Sciences of the United States of America* **101**, 10786-10791, doi:10.1073/pnas.0402876101 (2004).

712 Yedavalli, V. S., Benkirane, M. & Jeang, K. T. Tat and trans-activation-responsive (TAR) RNA-independent induction of HIV-1 long terminal repeat by human and murine cyclin T1 requires Sp1. *The Journal of biological chemistry* **278**, 6404-6410, doi:10.1074/jbc.M209162200 (2003).

713 Yu, Q. *et al.* APOBEC3B and APOBEC3C are potent inhibitors of simian immunodeficiency virus replication. *The Journal of biological chemistry* **279**, 53379-

53386, doi:10.1074/jbc.M408802200 (2004).

714 Yu, Q. *et al.* Single-strand specificity of APOBEC3G accounts for minus-strand deamination of the HIV genome. *Nature structural & molecular biology* **11**, 435-442, doi:10.1038/nsmb758 (2004).

715 Yu, X. *et al.* Induction of APOBEC3G ubiquitination and degradation by an HIV-1 Vif-Cul5-SCF complex. *Science* **302**, 1056-1060, doi:10.1126/science.1089591 (2003).

716 Yu, X. F., Yu, Q. C., Essex, M. & Lee, T. H. The vpx gene of simian immunodeficiency virus facilitates efficient viral replication in fresh lymphocytes and macrophage. *Journal of virology* **65**, 5088-5091 (1991).

717 Yu, Y., Xiao, Z., Ehrlich, E. S., Yu, X. & Yu, X. F. Selective assembly of HIV-1 Vif-Cul5-ElonginB-ElonginC E3 ubiquitin ligase complex through a novel SOCS box and upstream cysteines. *Genes & development* **18**, 2867-2872, doi:10.1101/gad.1250204 (2004).

718 Zack, J. A. *et al.* HIV-1 entry into quiescent primary lymphocytes: molecular analysis reveals a labile, latent viral structure. *Cell* **61**, 213-222 (1990).

719 Zapp, M. L., Hope, T. J., Parslow, T. G. & Green, M. R. Oligomerization and RNA binding domains of the type 1 human immunodeficiency virus Rev protein: a dual function for an arginine-rich binding motif. *Proceedings of the National Academy of Sciences of the United States of America* **88**, 7734-7738 (1991).

720 Zauli, G. *et al.* HIV-1 Tat protein down-regulates CREB transcription factor expression in PC12 neuronal cells through a phosphatidylinositol 3-kinase/AKT/cyclic nucleoside phosphodiesterase pathway. *The FASEB journal : official publication of the Federation*

of American Societies for Experimental Biology **15**, 483-491, doi:10.1096/fj.00-0354com (2001).

721 Zennou, V. & Bieniasz, P. D. Comparative analysis of the antiretroviral activity of APOBEC3G and APOBEC3F from primates. *Virology* **349**, 31-40, doi:10.1016/j.virol.2005.12.035 (2006).

722 Zennou, V., Perez-Caballero, D., Gottlinger, H. & Bieniasz, P. D. APOBEC3G incorporation into human immunodeficiency virus type 1 particles. *Journal of virology* **78**, 12058-12061, doi:10.1128/JVI.78.21.12058-12061.2004 (2004).

723 Zennou, V. *et al.* HIV-1 genome nuclear import is mediated by a central DNA flap. *Cell* **101**, 173-185, doi:10.1016/S0092-8674(00)80828-4 (2000).

724 Zhang, H. *et al.* The cytidine deaminase CEM15 induces hypermutation in newly synthesized HIV-1 DNA. *Nature* **424**, 94-98, doi:10.1038/nature01707 (2003).

725 Zhang, K. L. *et al.* Model structure of human APOBEC3G. *PloS one* **2**, e378, doi:10.1371/journal.pone.0000378 (2007).

726 Zhang, W. *et al.* Conserved and non-conserved features of HIV-1 and SIVagm Vif mediated suppression of APOBEC3 cytidine deaminases. *Cellular microbiology* **10**, 1662-1675, doi:10.1111/j.1462-5822.2008.01157.x (2008).

727 Zhang, W. *et al.* Cytidine deaminase APOBEC3B interacts with heterogeneous nuclear ribonucleoprotein K and suppresses hepatitis B virus expression. *Cellular microbiology* **10**, 112-121, doi:10.1111/j.1462-5822.2007.01020.x (2008).

728 Zheng, L., Yang, Y. D., Lu, G. C. & Salvato, M. S. Extracellular HIV Tat and Tat cysteine rich peptide increase CCR5 expression in monocytes. *Journal of Zhejiang University.*

Science. B **6**, 668-672, doi:10.1631/jzus.2005.B0668 (2005).

729 Zheng, S., Strzalka, J., Jones, D. H., Opella, S. J. & Blasie, J. K. Comparative structural studies of Vpu peptides in phospholipid monolayers by x-ray scattering. *Biophysical journal* **84**, 2393-2415, doi:10.1016/S0006-3495(03)75045-0 (2003).

730 Zheng, Y. H. *et al.* Human APOBEC3F is another host factor that blocks human immunodeficiency virus type 1 replication. *Journal of virology* **78**, 6073-6076, doi:10.1128/JVI.78.11.6073-6076.2004 (2004).

731 Zheng, Y. H. & Peterlin, B. M. Intracellular immunity to HIV-1: newly defined retroviral battles inside infected cells. *Retrovirology* **2**, 25, doi:10.1186/1742-4690-2-25 (2005).

732 Zhou, M. *et al.* The Tat/TAR-dependent phosphorylation of RNA polymerase II C-terminal domain stimulates cotranscriptional capping of HIV-1 mRNA. *Proceedings of the National Academy of Sciences of the United States of America* **100**, 12666-12671, doi:10.1073/pnas.1835726100 (2003).

733 Zhu, H. J., Liang, Y. X., Zhou, J. C. & Zheng, Y. H. [Effects of bkdAB interruption on avermectin biosynthesis]. *Sheng wu gong cheng xue bao = Chinese journal of biotechnology* **20**, 269-273 (2004).

734 Zimmerman, E. S. *et al.* Human immunodeficiency virus type 1 Vpr induces DNA replication stress in vitro and in vivo. *Journal of virology* **80**, 10407-10418, doi:10.1128/JVI.01212-06 (2006).

735 Zingler, N. *et al.* Analysis of 5' junctions of human LINE-1 and Alu retrotransposons suggests an alternative model for 5'-end attachment requiring microhomology-mediated end-joining. *Genome research* **15**, 780-789, doi:10.1101/gr.3421505 (2005).

736 Zink, M. C. & Clements, J. E. A novel simian immunodeficiency virus model that provides insight into mechanisms of human immunodeficiency virus central nervous system disease. *Journal of neurovirology* **8 Suppl 2**, 42-48, doi:10.1080/13550280290101076 (2002).

XI. Apendix

Schmitt, K., Guo, K., Algaier, M., Ruiz, A., Cheng, F., Qiu, J., Silke, W., Santiago, M.L., Stephens, E.B. (2011). Differential virus restriction patterns of rhesus macaque and human APOBEC3A: implications for lentivirus evolution. Virology, 419(1): 24-42.

Ruiz, A., Hill, M.S., **Schmitt, K.,** Stephens, E.B. (2010). Membrane raft association of the Vpu protein of human immunodeficiency virus type 1 correlates with enhanced virus release. Virology, 408(1): 89-102.

Ruiz, A., Lau, G., Mitchell, R.S., Hill, M.S., **Schmitt, K.,** Guatelli, J.C., Stephens, E.B. (2010). BST-2 mediated restriction of simian-human immunodeficiency virus. Virology, 406(2): 312-321.

Schmitt, K., Hill, S., Hill, S., Zhenqian, L., Ruiz, R., Culley, N., Pinson, D.M., Stephens, E.B., (2010). Comparison of the replication and persistence of simian-human immunodeficiency viruses expressing Vif proteins with mutation of the SLQYLA or HCCH domains in macaques. Virology, 404(2): 187-203.

Hill S, Ruiz, A., **Schmitt, K.,** Stephens, E.B., (2010). Identification of amino acids within the second alpha helical domain of the human immunodeficiency virus type 1 Vpu that are critical for preventing CD4 cell surface expression. Virology, 397(1): 104-12.

Schmitt, K., Hill, S., Culley, N., Pinson, D.M., Wong, S.W., Stephens, EB., (2009). Mutations in the highly conserved SLQYLA motif of Vif in simian-human immunodeficiency virus results in a less pathogenic virus and are associated with G-to-A mutations in the viral genome. Virology, 383(2): 362-72.

Ruiz, A., Hill, S., **Schmitt, K.,** Guatelli, J., Stephens, E.B., (2008). Requirements of the membrane proximal tyrosine and dileucine based sorting signals for efficient transport of the subtype C Vpu protein to the plasma membrane. Virology, 378(1): 86-97